Radioligand binding and reporter gene assays for histamine H_3 and H_4 receptor species orthologs

Dissertation

Zur Erlangung des Doktorgrades der Naturwissenschaften (Dr. rer. nat.)

der Fakultät für Chemie und Pharmazie

der Universität Regensburg

vorgelegt von

Uwe Nordemann

aus Ohrte

2013

Die vorliegende Arbeit entstand in der Zeit von Januar 2009 bis März 2013 unter der Leitung von Herrn Prof. Dr. A. Buschauer und Herrn Prof. Dr. G. Bernhardt am Institut für Pharmazie der Naturwissenschaftlichen Fakultät IV – Cheimie und Pharmazie – der Universität Regensburg.

Das Promotionsgesuch wurde eingereicht im März 2013

Tag der mündlichen Prüfung: 04. April 2013

Prüfungsausschuss:

Prof. Dr. D. Horinek	(Vorsitzender)
Prof. Dr. A. Buschauer	(Erstgutachter)
Prof. Dr. G. Bernhardt	(Zweitgutachter)
Prof. Dr. J. Wegener	(Drittprüfer)

für meine Eltern

„Man sollte alles so einfach wie möglich sehen - aber auch nicht einfacher.“

Albert Einstein, 1879 - 1955

Danksagungen

An dieser Stelle möchte ich mich bedanken bei:

Herrn Prof. Dr. A. Buschauer für die Gelegenheit, an diesem interessanten Projekt arbeiten zu dürfen, für seine wissenschaftlichen Anregungen und seine konstruktive Kritik bei der Durchsicht der Arbeit,

Herrn Prof. Dr. G. Bernhardt für seine fachliche Anleitung, seine Anregungen bei experimentellen Problemen und seine konstruktive Kritik bei der Durchsicht der Arbeit,

Herrn Prof. Dr. R. Seifert (Institut für Pharmakologie, Medizinische Hochschule Hannover) für die Bereitstellung der Vektoren pcDNA3.1(+)-SF-rH_3R-His_6 und pcDNA3.1(+)-SF-rH_4R-His_6 sowie diverser Histamin Rezeptor Liganden,

Herrn Prof. Dr. H. Stark (Institut für Pharmazeutische Chemie, Goethe Universität Frankfurt am Main) für die Bereitstellung der H_4 Rezeptor Liganden ST-1006 und ST-1012,

Herrn Dr. D. Schnell für die Bereitstellung der HEK293-SF-hH_3R-His_6 und HEK293-SF-hH_4R-His_6 Zellen sowie der Vektoren pcDNA3.1(+)-SF-hH_3R-His_6 und pGEM-SF-mH_4R-His_6,

Herrn Dr. P. Igel für die Bereitstellung des Radioliganden [^{3}H]UR-PI294 und der Histamin Rezeptor Liganden UR-PI294 und UR-PI376 sowie für seine kompetente Hilfe bei experimentellen Problemen und pharmakologischen Fragestellungen,

Herrn Dr. J. Mosandl für seine Hilfe beim Erlernen der Zellkultur und des Radioliganden-bindungsassays sowie beim theoretischen Einarbeiten in das Thema,

Herrn Dr. P. Höcherl und Dr. M. Kühnle für die wertvollen Ratschläge bei der Durchführung der Transfektionen und die Hilfe beim Zytotoxizitätsassay,

Herrn Dr. R. Geyer für die Bereitstellung der Cyanoguanidine und diverser anderer H_4R Liganden,

Frau B. Wenzl für ihre tatkräftige Unterstützung in der Zellkultur und der guten Zusammenarbeit während des Biochemie Praktikums,

Frau M. Beer-Krön für ihre tatkräftige Unterstützung in der Zellkultur und die vielen Süßigkeiten im Büro,

Herrn P. Richthammer für seine Hilfsbereitschaft und Kompetenz bei allen technischen Problemen und seine stets norddeutsche Begrüßung,

Frau U. Hasselmann und Frau K. Reindl für ihre freundliche Unterstützung bei allen organisatorischen Dingen,

Herrn Dr. M. Keller, T. Holzammer und D. Wifling für die vielen fachlichen Gespräche,

meinen aktuellen und ehemaligen Bürokollegen Frau M. Kaske, N. Kagermeier, Herrn M. Rothenhöfer, S. Huber und J. Felixberger für die angenehme und amüsante Atmosphäre und die gute Zusammenarbeit,

Frau S. Dukorn und allen anderen Forschungspraktikanten / -innen für ihre engagierte Mitarbeit im Labor,

allen ehemaligen und aktuellen Doktoranden / innen, Diplomanden / -innen und Masteranden / -innen für eine tolle Zeit am und außerhalb des Lehrstuhls,

allen aktuellen und ehemaligen Mitarbeitern des Lehrstuhls für eine sehr gute Kollegialität, Arbeitsatmosphäre und Zusammenarbeit,

der Deutschen Forschungsgemeinschaft für die finanzielle Förderung im Rahmen des Graduiertenkollegs 760 sowie der EU für die Unterstützung im Rahmen des COST Projektes BM0806,

und insbesondere meinen Eltern, meinen Geschwistern und natürlich meiner Freundin Doris für ihren Rückhalt, ihre Unterstützung und Hilfe in jeglicher Art und Weise.

Poster presentations

Nordemann U.; Schnell D.; Bernhardt G.; Seifert R.; Buschauer A.: *Reporter gene assay for the investigation of human, murine and rat histamine H_4 receptor ligands*. 6th Summer School Medicinal Chemistry, Regensburg, Germany, September 26 – 28, 2012

Geyer R.; Nordemann U.; Baumeister P.; Bernhardt G.; Buschauer A.: *trans-(+)-(1S,3S)-UR-RG98: Synthesis, absolute configuration and pharmacological characterization of a highly potent and selective histamine H_4 receptor agonist*. EFMC-ISMC 2012, 22nd International Symposium on Medicinal Chemistry, Berlin, Germany, September 02 – 06, 2012

Nordemann U.; Schnell D.; Bernhardt G.; Seifert R.; Buschauer A.: *Gene reporter assay for the investigation of human and murine histamine H_4 receptor ligands*. Joint meeting of the Austrian and German Pharmaceutical Societies, Innsbruck, Austria, September 20 – 23, 2011

Baumeister P.; Nordemann U.; Buschauer A.: *2-Arylbenzimidazoles as potent human H_4 receptor agonists*. Frontiers in Medicinal Chemistry, Saarbrücken, Germany, March 20 – 23, 2011

Nordemann U.; Mosandl J.; Schnell D.; Bernhardt G.; Buschauer A.: *Development of cell-based binding and functional assays for the human histamine H_3 and H_4 receptor*. 5th Summer School Medicinal Chemistry, Regensburg, Germany, September 13 – 15, 2010

Erdmann D.; Mosandl J.; Nordemann U.; Bernhardt G.; Wolfbeis O.S.; Seifert R.; Buschauer A.: *Pharmacological activity and selectivity of fluorescent histamine H_3 receptor ligands*. Annual meeting of the German Pharmaceutical Society, Jena, Germany, September 28 – October 1, 2009

Contents

Abbreviations

5(4)MH	5(4)-methylhistamine
aa	amino acid
Å	Ångström
AC	adenylyl cyclase
AMP	adenosine monophosphate
ATP	adenosine 5'-triphosphate
β_1-AR, β_2-AR	β-adrenergic receptor subtypes
BSA	bovine serum albumin
B_{max}	maximal specific binding of a ligand
bp	base pair(s)
$[Ca^{2+}]_i$	intracellular calcium concentration
cAMP	cyclic-adenosine 3',5'-monophosphate
cDNA	copy-DNA
CAM	constitutively active mutant (of a receptor)
CHO cells	chinese hamster ovary cells
CIP	ciproxifan
CLOB	clobenpropit
CLOZ	clozapine
CNS	central nervous system
CON	conessine
CRE	cAMP response element
CREB	cAMP response element binding protein
CTCM	cubic ternary complex model
DAG	diacylglycerol
DAO	diamine oxidase
DMEM	Dulbecco's modified eagle medium
DMSO	dimethylsulfoxide
DNA	deoxyribonucleic acid
dpm	decays per minute
DSMZ	Deutsche Sammlung von Mikroorganismen und Zellkulturen
DTT	dithiothreitol
EC_{50}	agonist concentration which induces 50% of the maximum effect
ECL	extracellular loop
EDTA	ethylenediaminetetraacetic acid (Ca^{2+}-chelator)
E.coli	*Escherichia coli*
EGTA	ethyleneglycol-O,O'-bis(2-aminoethyl)-N,N,N',N'-tetraacetic acid (Ca^{2+}-chelator)
ERK	extracellular signal-regulated kinase
ETCM	extended ternary complex model
F	FLAG epitope
FCS	fetal calf serum
FLAG	octapeptide epitope for the labeling of proteins (mostly DYKDDDDK)
FLIPR	fluorescence imaging plate reader
G418	geneticin
GDP	guanosine diphosphate
GF/C	a glass fiber filter
Gly-Gly	glycyl-glycine
GPCR	G-protein coupled receptor
GRAFS	glutamate, rhodopsin, adhesion, frizzled/taste2, secretin receptor families (GPCR classification system)

GRK	G-protein coupled receptor kinase
GTP	guanosine triphosphate
h	hour(s) or human (in context with a receptor name)
HA	histamine
H_1R, H_2R, H_3R, H_4R	histamine receptor subtypes
HEK293T cells	human embryonic kidney cells containing the large T antigen from SV40 virus
His_6	hexahistidine tag for the labeling and purification of proteins
HSA	human serum albumin
IBMX	3-isobutyl-1-methyl-xanthine
IC_{50}	antagonist concentration which suppresses 50 % of an agonist induced effect (functional assay) or ligand concentration which inhibits specific binding of a labeled ligand by 50 % (binding assay)
ICER	inducible cAMP early repressor
ICL	intracellular loop
IME	imetit
IMMEP	immepip
IMMET	immethridine
IODO	iodophenpropit
IP_3	inosithol-1,4,5-trisphosphate
K_B	dissociation constant (functional assay)
K_D	dissociation constant (saturation binding assay)
K_i	dissociation constant (competition binding assay)
LB	Luria bertani broth (for *E. coli* culture)
m	mouse (in context with a receptor name)
MAPK	mitogen-activated protein kinase
min	minute(s)
NAMH	N^{α}-methylhistamine
n.d.	not determined
PBS	phosphate buffered saline
PDE	phosphodiesterase
pEC_{50}	negative decade logarithm of EC_{50}
PEI	polyethyleneimine
P_i	inorganic phosphate
PP_i	pyrophosphate
PIP_2	phosphatitylinositolbisphosphate
PKA	protein kinase A
PKC	protein kinase C
pK_i	negative decade logarithm of K_i
PLCβ	phospholipase Cβ
PRO	proxyfan
qi5-HA	chimeric $G\alpha_q$ proteins which incorporate a hemagglutinin epitope
RAMH	(R)-α-methylhistamine
RGS	regulators of G-protein signaling
RLU	relative luminescence units
rpm	revolutions per minute
S	cleavable signal peptide from influenza hemagglutinin
s	second(s)
SAMH	(S)-α-methylhistamine
SEM	standard error of the mean
Sf9	Spodoptera frugiperda (an insect cell line)
SOC	salt optimized + carbon broth (for transformation of *E. coli*)

SRE	serum response element
TAE	tris-acetate-EDTA-buffer
TCM	ternary complex model
THIO	thioperamide
TM	transmembrane domain
Tris	tris(hydroxymethyl)aminomethane

Chapter 1

General introduction

1.1 G-protein coupled receptors (GPCRs)

1.1.1 GPCRs as drug target

In the human genome, G-protein-coupled receptors (GPCRs) constitute the largest superfamily of membrane-bound receptors that transmit a wide variety of signals across the cell membrane. GPCRs respond to a broad range of extracellular messenger such as biogenic amines, purines, lipids, peptides and proteins, odorants, pheromones, tastants, ions and even photons (Jacoby *et al.*, 2006). Approximately 800 genes encoding functional GPCRs have been identified in the human genome, and more than 50 % of these receptors are related to olfaction and taste (Gloriam *et al.*, 2007). Roughly 130 of the remaining GPCRs that could present drug targets are so-called orphans, “proteins having similarity to receptors but whose endogenous ligands have not yet been conclusively identified” (Sharman *et al.*, 2013). More than 50 GPCRs are targeted by approved drugs (Overington *et al.*, 2006), which present 30 - 40 % of all marketed drugs (Stevens *et al.*, 2013), emphasizing the current value for the treatment of human diseases and the prospects for the development of GPCR ligands as future drugs as well.

1.1.2 Structure and classification

The common architecture of a GPCR includes an extracellular N-terminus, seven α-helices spanning the plasma membrane and arranged in a counter-clockwise manner (TM1 – TM7), alternating intracellular (ICL1 –ICL3) and extracellular loops (ECL1 – ECL3) that interlink the seven transmembrane bundle and an intracellular C-terminus (see **Figure 1.1**). The transmembrane (TM) domains share the highest degree of sequence conservation, whereas the intracellular and extracellular domains display distinct variability in size and complexity. The extracellular and the transmembrane regions are involved in ligand binding, whereas the intracellular region is important for signal transduction. The classical way of signaling results from coupling to heterotrimeric G-proteins. However, G-protein coupling was not found for every GPCR and alternative signaling pathways involving interactions with various proteins have been described (Ritter and Hall, 2009). Therefore, the term “seven TM receptor” for this superfamily seems to be technically more correct, but the GPCR terminology is more common (Fredriksson *et al.*, 2003).

An important overview of the GPCR superfamily based on their ligands or sequence similarity gives the widely used A – F classification system (Kolakowski, 1994). The GPCRs are divided into six families, of which three families (families A, B, C) comprise the majority of known human receptors. This system is also used by the International Union of

Pharmacology, Committee on Receptor Nomenclature and Classification (NC-IUPHAR) (Foord *et al.*, 2005). The complete sequencing of the human genome has enabled a detailed analysis of the GPCR phylogeny. Fredriksson and co-workers divided the human GPCRs into five families termed glutamate, rhodopsin, adhesion, frizzled/taste2 and secretin (shortened to the acronym GRAFS) (Fredriksson *et al.*, 2003). The principle difference between the GRAFS system and the former classification system is the further division of family B into the secretin and adhesion family and the reclassification of the taste receptors into two subgroups, one within the glutamate group and one together with the frizzled/taste2 group.

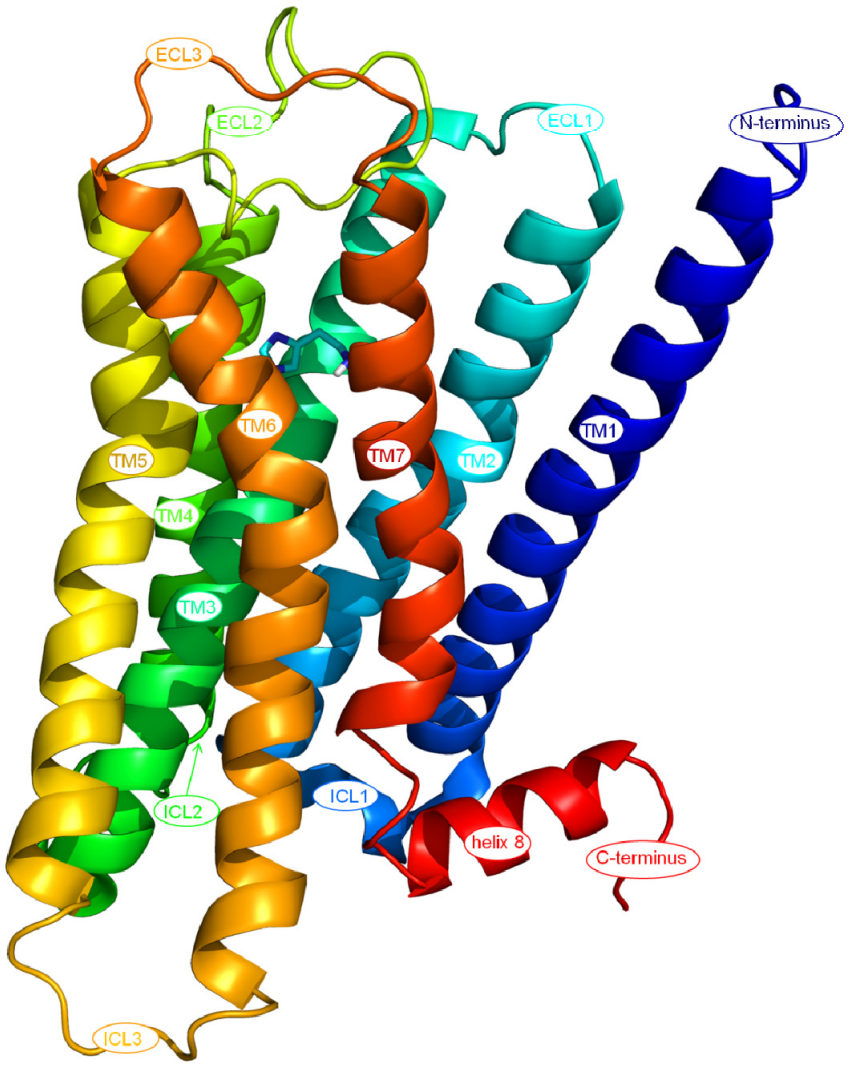

Figure 1.1: Model of the active state of the human histamine H_4R in complex with the endogenous agonist histamine. The homology model is based on the recently published active state of the β_2-adrenergic receptor (AR) (Rasmussen *et al.*, 2011a) (provided by (Wifling, 2012)).

The rhodopsin family (class A) contains about 670 full length human receptor proteins and is thus by far the largest family of GPCRs. Members of this family bind a wide variety of ligands such as peptides, small molecules like amines and purines or odorants in the case of olfactory receptors. Therefore, it is not surprising that this family represents the largest number of receptors that are targeted by clinically used drugs. Among the most widely prescribed classes of drugs are, for instance, “beta blockers” that antagonize the action of endogenous catecholamines on β-adrenergic receptors (β-ARs) and are used for the treatment of hypertension, coronary heart disease and cardiac arrhythmia. The rhodopsin family is characterized by several highly conserved structural motifs in the TM region such as the NSxxNPxxY in TM7 or the D(E)-R-Y(F) at the border between TM3 and IL2. The binding pocket for small molecule ligands is formed by the transmembrane spanning α-helices and therefore located within the seven TM bundle (Fredriksson *et al.*, 2003; Jacoby *et al.*, 2006).

The secretin family (class B) is a small family with only 15 members that bind rather large peptide hormones such as secretin, calcitonin and parathyroid hormone. The name of this family originates from the first discovered receptor of this family, the secretin receptor from rat (Ishihara *et al.*, 1991). Binding occurs at the proximal region and the juxtamembrane region of the N-terminus, the extracellular loops and the upper parts of the TM helices. Six conserved disulfide-bonded cysteine residues are found in a glycosylated extracellular amino-terminal tail in almost all receptors of the secretin receptor family (Jacoby et al., 2006; Lagerström and Schiöth, 2008).

The adhesion family (class B) is the second largest receptor family in humans with 33 members, of which the majority is orphan (Civelli *et al.*, 2013). The family name is derived from the long and diverse N-terminus which contains motifs that are likely to participate in cell adhesion (Fredriksson *et al.*, 2003).

The glutamate receptor family (class C) comprises 22 receptor proteins including the metabotropic glutamate receptors, the γ-aminobutyric acid type B receptors, the calcium sensing receptor and the sweet/umami taste receptors. The ligand binding site is located in the N-terminal domain where two lobes of the region form a cavity in which glutamate binds, the so called “Venus fly trap” (Kunishima *et al.*, 2000). In addition to drugs that bind to the glutamate binding domain, e.g. baclofen (McLean, 1993), there are also allosteric modulators that bind within the TM region such as cinacalcet (Iqbal *et al.*, 2003).

The frizzled/taste2 receptor family in humans consists of ten frizzled receptors and 25 functional bitter taste receptors. The frizzled receptors are involved in cell development and proliferation. The name frizzled is related to the curled and twisted glycoprotein ligand (Wnt) of a receptor cloned from *D. melanogaster* (Fredriksson *et al*., 2003) (for reviews see Luttrell et al. (Luttrell, 2008) and Davies et al. (Davies *et al.*, 2011)).

1.1.3 Advances in X-ray crystallography for GPCRs

To better understand how GPCRs work at a molecular level, high resolution crystal structures are very helpful. So far, the structures of 18 different class A GPCRs have been published, alone 14 of them in the last three years (Venkatakrishnan *et al.*, 2013). This required technical challenges to be overcome such as the production of large quantities (> 200 mg) of functional protein or the stabilization of the flexible ICL3 to increase the polar surface area potential for crystal contacts (Kobilka and Schertler, 2008). The latter has been resolved for the human (h) β_2-AR structure by crystallizing the receptor in complex with an antibody fragment that bound to a structural epitope at the cytoplasmic base of TM5 and TM6 (Rasmussen *et al.*, 2007) and by insertion of the enzyme T4-lysozyme into ICL3 of the receptor (Cherezov *et al.*, 2007). In another approach, first used for the structure determination of the turkey β_1AR, the receptor was stabilized by a number of point mutations (Warne *et al.*, 2008).

The first three-dimensional structure of a GPCR was obtained from bovine rhodopsin containing the covalently bound inverse agonist 11-cis retinal (Palczewski *et al.*, 2000). Interestingly, only bovine rhodopsin has successfully been crystallized from its native source, with intact sequence and without artificial stabilization. A comparison with non-rhodopsin structures revealed some structural differences. For instance, the ECL2 of rhodopsin forms a β-sheet lid that covers the bound 11cis-retinal and protects this from hydrolysis. In contrast, the ECL2 of the β_1-AR and β_2-AR forms a short helix that enables an open binding pocket (Kobilka and Schertler, 2008; Rosenbaum *et al.*, 2009). A ionic interaction between R135 (part of the highly conserved D(E)-R-Y(F) motif) of TM3 and E247 of TM6 in rhodopsin, the so called “ionic lock”, has been supposed to help hold the receptor in an inactive conformation (Hofmann *et al.*, 2009). However, this ionic lock has not been observed in several other structures that bind antagonists. It is a matter of speculation that the ionic lock is lacking due to the presence of the antibody fragment or T4-lysozyme fusions that could have altered the receptor structure or due to the fact that the ligands are not in all cases full inverse agonists, since the ionic lock can only be observed in the full ground state conformation (Congreve *et al.*, 2011) (for further recent reviews see Salon et al. (Salon *et al.*, 2011) and Hanson et al. (Hanson and Stevens, 2009).

The first crystal structures of GPCRs represented inactive receptor conformations, since they were obtained in complex with antagonists or inverse agonists, respectively. To learn how binding of an agonist does activate a receptor, the crystal structure of an active receptor conformation was needed. This was first accomplished for opsin, the ligand-free form of rhodopsin (Park *et al.*, 2008; Scheerer *et al.*, 2008), but proved to be difficult for other GPCRs, since the interaction with a G-protein is essential to stabilize the active state of the receptor. Rasmussen and co-workers reached this milestone in GPCR research by

crystallization of the agonist-bound active-state β_2-AR in complex with a nanobody as a replacement of the G-protein (Rasmussen *et al.*, 2011a) and, more importantly, by the crystallization of the active state ternary complex consisting of the agonist-occupied monomeric β_2-AR and the nucleotide-free Gs heterotrimer (Rasmussen *et al.*, 2011b). Both structures consistently show that the largest difference between the inactive and active structures is a 11 - 14 Å outward movement of TM6. In complex with a G-protein, the active state of the β_2-AR is stabilized by interactions of ICL2, TM5 and TM6 with the Ras-like GTPase domain of the Gαs subunit (GαsRas). Surprisingly, there is no interaction with the Gβγ subunit. Of particular interest is also a large movement of the α-helical domain of Gαs relative to GαsRas in the nucleotide-free β_2-AR-Gs complex. The guanidine nucleotide binding pocket is formed by the interface of these two domains and stabilized by binding of guanosine triphosphate (GTP) or guanosine diphosphate (GDP) (see **Figure 1.2**). As the release of GDP is an essential step in the G-protein cycle (see section 1.1.4.1), it will be of particular interest to determine the functional significance of this large movement in future studies (Rasmussen *et al.*, 2011b).

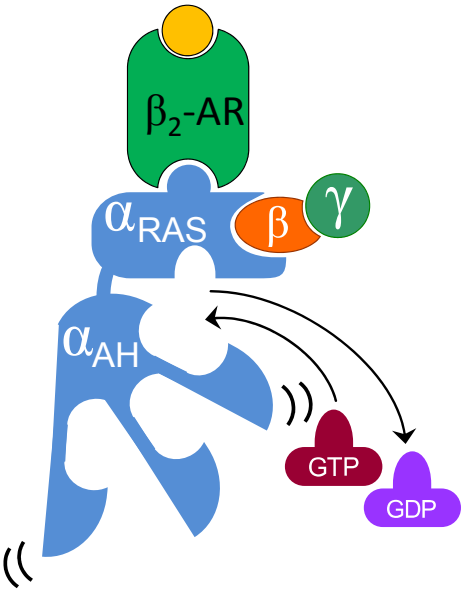

Figure 1.2: Illustration of the agonist (A) bound, nucleotide-free β_2-AR-Gs-protein complex. The $G\alpha_s$ subunit is formed by the Ras domain (αRas) and the α-helical domain (αAH), which are both involved in nucleotide binding. In the nucleotide–free state, the αAH domain has a variable position relative the αRas domain (modified from (Rasmussen *et al.*, 2011b)).

Additional insights are expected from efforts to determine the structures of GPCRs in complex with other signaling proteins to characterize the role of protein dynamics in receptor function (Granier and Kobilka, 2012) (for a recent review see Venkatakrishnan et al. (Venkatakrishnan *et al.*, 2013)).

1.1.4 Signal transduction

1.1.4.1 G-protein mediated signal transduction

The G-protein cycle is the “classical mode” of GPCR-mediated intracellular signaling. Agonist binding to extracellular or transmembrane domains of a GPCR promotes conformational changes that initiate coupling of intracellular receptor domains to heterotrimeric G-protein. This agonist-receptor-G-protein complex, termed as ternary complex, triggers a G-protein conformational change that catalyzes exchange of GTP for GDP on the Gα subunit. Subsequently, the activated heterotrimeric G-protein dissociates into Gα-GTP and Gβγ subunits, which then regulate the activity of intracellular effector proteins. The intrinsic GTPase activity of the GTP-bound Gα subunit terminates the signal by hydrolysis of GTP to GDP, i. e. the cycle is completed through the returning of the G-protein to the inactive heterotrimeric state (see **Figure 1.3**).

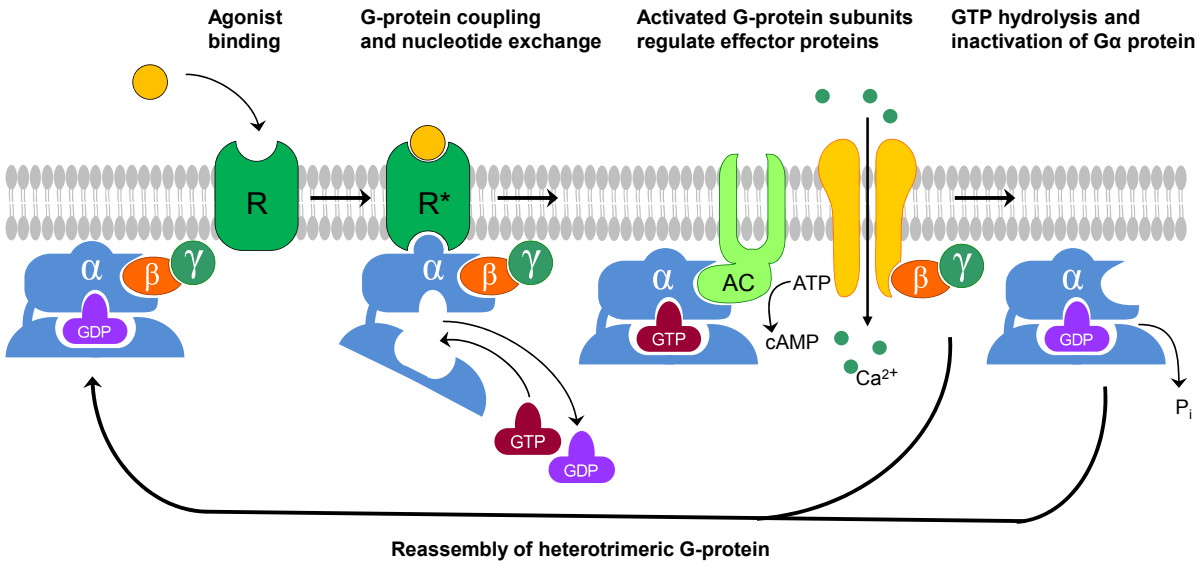

Figure 1.3: Activation of a heterotrimeric G-protein by interaction with an agonist-occupied GPCR. The activated receptor is represented by R*, whereas the inactive type is named R. The dissociated subunits regulate their respective effector proteins such as the adenylyl cyclase (AC) and calcium channels. Further details are described in the text (modified from (Rasmussen *et al.*, 2011b)).

The currently known 16 genes encoding for mammalian Gα subunits are divided into four subfamilies ($G\alpha_s$, $G\alpha_{i/o}$, $G\alpha_{q11}$ and $G\alpha_{q12/13}$) based on sequence homology (Cabrera-Vera *et al.*, 2003). The best characterized G-protein-regulated enzyme is the adenylyl cyclase, which forms the second messenger cyclic-adenosine 3’,5’-monophosphate (cAMP) from adenosine triphosphate (ATP). cAMP is a ubiquitous second messenger in cells activating numerous cellular pathways such as the cAMP dependent protein kinase A (PKA). All of the nine

mammalian membrane bound ACs are stimulated by $G\alpha_s$, whereas only some can be inhibited by activated $G\alpha_{i/o}$ (Hanoune and Defer, 2001; Pavan *et al.*, 2009). Members of the $G\alpha_{q11}$ family activate the phospholipases Cβ 1-3 (PLCβ), which catalyze the hydrolysis of phosphatidylinositol 4,5-bisphosphate (PIP_2) to 1,2-diacylglycerol (DAG) and inositol-1,4,5-trisphosphate (IP_3). The latter second messenger controls calcium efflux from the endoplasmic reticulum. DAG and the released calcium control the activity of several protein kinase C (PKC) isoforms, which in turn activate a number of other proteins by phosphorylation. The main effector system activated by the $G\alpha_{12/13}$ subfamily is the guanine nucleotide exchange factor RhoGEF, which triggers the GDP/GTP exchange on the small molecular weight G-protein Rho (Birnbaumer, 2007; Cabrera-Vera *et al.*, 2003).

In addition to the Gα subunits, five different Gβ subunits and 12 different Gγ subunits have been identified (Luttrell, 2008). The Gβγ heterodimer, originally thought to primarily facilitate signal termination and membrane attachment by binding to the Gα subunits, also activates several effector proteins such as the the PLCβ 2 and 3 (usually in combination with $G\alpha_{i/o}$ coupled GPCRs), GPCR kinases or potassium and calcium channels (Cabrera-Vera *et al.*, 2003).

The complexity of G-protein signaling is demonstrated by the fact that GPCRs can couple to multiple G-proteins and activate multiple signaling pathways (Eason *et al.*, 1992; Galandrin and Bouvier, 2006). Additionally, a fine tuning of the signaling through a complex of regulatory events occurs that has impact on the cellular responsiveness. Receptor-G-protein coupling is directly impaired by phosphorylation of specific residues within the intracellular domains of the receptor through second messenger dependent protein kinases like PKA and PKC (heterologous desensitization). Agonist-occupied GPCRs are phosphorylated by G-protein-coupled receptor kinases (GRKs) resulting in β-arrestin binding and subsequent desensitization (homologous desensitization) and internalization into clathrin-coated pits (see section 1.1.4.2) (Luttrell and Gesty-Palmer, 2010). Gα subunit activity is modulated by direct binding of regulators of G-protein signaling proteins (RGS proteins), which accelerate the GTP hydrolysis of Gα-GTP and thus the termination of signaling (Hepler, 2003). Second messengers are enzymatically inactivated by cAMP phosohodiesterases (PDE), phosphatidylinositol phosphatases and diacylglycerol kinases (Luttrell, 2008). More regulatory mechanisms are summarized and reviewed by Luttrell et al. (Luttrell, 2008).

1.1.4.2 β-Arrestin dependent signaling

There are four known mammalian arrestins. Arrestin1 (rod arrestin) and -4 (cone arrestin) are expressed in the retina and exist primarily to regulate photoreceptor function. The two non-visual arrestins, arrestin 2 and -3 (also referred to as β-arrestin 1 and -2) are found in most tissue types and were originally identified as mediators of GPCR desensitization (Luttrell and

Gesty-Palmer, 2010). All four arrestins bind directly to activated GRK-phosphorylated GPCRs and block the receptor-G-protein interaction. Next to desensitization, non-visual β-arrestins have additional functions that are not shared with visual arrestins. Receptor-bound β-arrestin also serves as an adaptor linking the receptor to the clathrin-dependent endocytosis machinery. Once internalized the receptor can return back to the plasma membrane via recycling endosomes (resensitization) or be directed to lysosomes and degraded (down-regulation) (Gurevich and Gurevich, 2006).

Within the past decade, it has been discovered that β-arrestins not only serve as adaptors in the context of GPCR desensitization and internalization, but also as multifunctional adaptor proteins that link GPCRs to several effector proteins such as mitogen-activated protein kinases (MAPKs), Src family kinases and nuclear factor-κB (Rajagopal *et al.*, 2010). This led to a paradigm shift in GPCR signal transduction (DeWire *et al.*, 2007; Miller and Lefkowitz, 2001; Perry and Lefkowitz, 2002). As β-arrestin binding terminates G-protein signaling, both pathways should be temporally discrete. In fact, the well characterized extracellular signal-regulated kinase (ERK) cascade showed that the beginning of β-arrestin ERK1/2 activation coincides with the decreasing of G-protein signaling and still persists when the receptor is internalized (see **Figure 1.4**) (Ahn *et al.*, 2004; Luttrell and Gesty-Palmer, 2010).

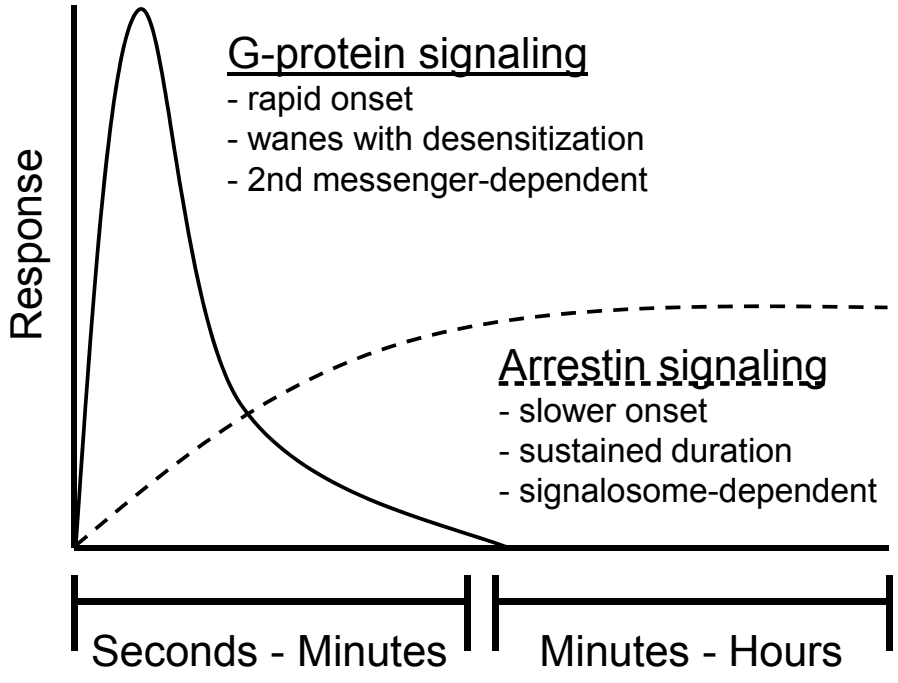

Figure 1.4: Comparison of the time course of G-protein- with β-arrestin mediated signaling. Unlike G-protein signaling through second messenger, β-arrestin dependent signals originate within stoichiometric complexes of receptors, β-arrestins, and effectors, often termed as signalosomes (modified from (Luttrell and Gesty-Palmer, 2010).

1.1.4.3 Models of GPCR signaling, ligand classification and functional selectivity

Early efforts to describe the functional effects of drugs on isolated tissues were based on the assumption that binding of a ligand to a receptor follows the law of mass action according to the Langmuir adsorption isotherm (Clark, 1937; Clark, 1933). This “classical model” of receptor function was successively modified due to constantly new experimental evidences in receptor pharmacology. For instance, Ariens introduced a proportionality factor termed intrinsic activity (also referred to as α) to the binding function in order to characterize the degree of receptor stimulation for different drugs (Ariens, 1954). α = 1 indicates agonists that induce the maximal response, α = 0.5 describes agonists that reach only half of the maximal response and an intrinsic activity of zero indicates no agonism. In the so called “two-state model”, which was originally formulated to describe ion channels (Del Castillo and Katz, 1957), it is assumed that the receptor could persist in a inactive conformation (R) and change in complex with an agonist (L) into an active conformation (LR*) that triggers signaling (Leff, 1995). The “two-state-model” was also helpful to explain experimental findings relating to constitutive activity in the late 1980s (Kenakin, 2009). High receptor density in genetically engineered cells uncovered the existence of a constitutively active receptor population (Costa and Herz, 1989). It was supposed that receptors could exist in a spontaneously active state (R*), just like ion channels can open without agonist binding (Kenakin, 2009).

Observations of two affinity forms of the β-AR receptor (Lefkowitz *et al.*, 1976; Maguire *et al.*, 1976) led to the assumption that the receptor interacts with other unknown membrane-bound proteins, which later turned out to be G-proteins, leading to the agonist promoted formation of a high-affinity ternary complex (LRT). This model is termed the “ternary complex model” (TCM) and was first described by DeLean and colleagues (see **Figure 1.5** A) (De Lean *et al.*, 1980). Interestingly, although the existence of the heterotrimeric G-protein as a cellular signaling component was already known at that time (Rodbell *et al.*, 1971; Ross and Gilman, 1977), the link to the role as transducer protein (T) for receptor signaling was identified later (Gilman, 1987).

The discovery of a constitutively active β_2-AR mutant resulted in the modification of the TCM, which is called “extended ternary complex model” (ETCM) (Samama *et al.*, 1993). According to this model, ligands are divided into five classes. The inactive receptors (R_i) can adopt either spontaneously or in complex with an agonist the active conformation (R_a or LR_a), which then can induce signaling by forming a complex with the G-protein (R_aT or LR_aT) (see **Figure 1.5** B). Contrary, inverse agonists stabilize the inactive receptor state and prevent signaling. Partial agonists and partial inverse agonists also shift the equilibrium to the particular active or inactive conformation, but to a minor extent compared to full (inverse) agonists. Neutral antagonists do not prefer a receptor conformation and leave the basal activity unchanged.

From a thermodynamicalpoint of view, the ETCM is incomplete due to the missing interaction between the inactive receptor (ligand bound and unbound) and G-protein. The “cubic ternary complex model” accommodates this possibility and thus increases the number of states compared to the ETCM (Weiss *et al.*, 1996) (see **Figure 1.5** C).

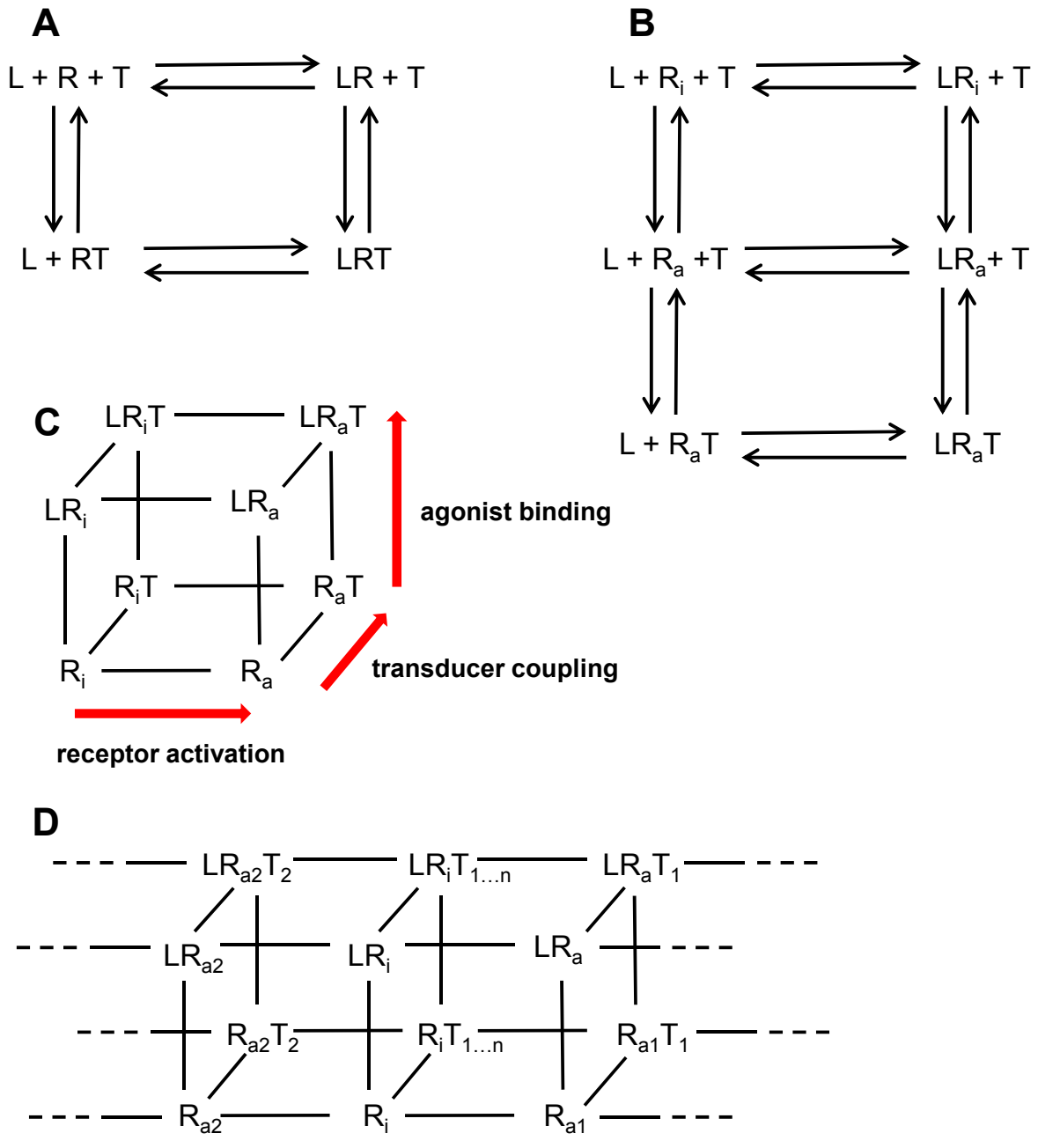

Figure 1.5: Models of GPCR signaling: Ternary complex model (**A**), extended ternary complex model (**B**), cubic ternary complex model (**C**), multiple signaling-component model (**D**). Further details are described in the text. Abbreviations are: L: ligand, R: receptor, T: transducer (e.g. G-protein or β-arrestin), R_a: active receptor conformation, R_i: inactive receptor conformation (modified from (Rajagopal *et al.*, 2010).

Nowadays, it is assumed that GPCRs can adopt multiple conformations including more than one active state (Kenakin, 2007; Kobilka and Deupi, 2007). This assumption accounts for ligands that preferentially activate one possible downstream pathway over another (e.g. either G-protein or β-arrestin) in contrast to the endogenous ligand, which is considered to be neutral. These ligands are termed as biased agonists and would be expected to elicit a conformational change that can only stimulate G-protein signaling without β-arrestin recruitment, or vice versa. These type of effects has received various names, which include "stimulus trafficking", "biased agonism", "collateral efficacy" or generally accepted "functional selectivity (Kenakin, 2007). In fact, several biophysical studies on the β_2-AR (Kahsai *et al.*, 2011; Swaminath *et al.*, 2004) and on the α_2-adrenergic receptor (Zurn *et al.*, 2009) demonstrated that binding of functionally different ligands results in distinct conformations. Moreover, very recently for the β_2-AR (Liu *et al.*, 2012) and for the vasopressin type 2 receptor (Rahmeh *et al.*, 2012) it was shown that the functional β-arrestin outcome depends on movement of TM7 and helix 8, whereas conformational changes in TM6 are associated with G-protein activation (cf. section 1.1.3). Therefore, an additional state(s) for receptor activation is required (R_{a1}, R_{a2},…) as well as additional ternary complexes which comprise also other transducers of signaling than G-proteins such as β-arrestin (T_1, T_2,…) (**Figure 1.5** D). Considering ligands that bind at allosteric sites and thereby affect receptor activity, further complexity is added to the "multi-state model" for receptor activation. The model includes the presence of biased ligands, which are useful as pharmacological tools to improve the understanding of protein dynamics in GPCR function and, most importantly, as more efficient and economical therapeutics that maximize beneficial effects and minimize side effects (Rajagopal *et al.*, 2010).

1.2 Histamine and the histamine receptor family

1.2.1 The biogenic amine histamine

About a hundred years ago, the discovery of histamine and the first description of its biological action were carried out by Sir Henry Dale owing to its ability to constrict the guinea pig ileum and its potent vasodepressor action (Dale and Laidlaw, 1910). Subsequently, additional histamine effects such as the induction of a shock-like syndrome, when injected into animal (Dale and Laidlaw, 1919), the stimulation of acid secretion from the stomach of dogs (Popielski, 1920) or the classic "triple response" to histamine consisting of a red spot (vasodilatation), a wheal (increased permeability) and flare (axon reflex) (Lewis and Grant, 1924) were reported. Nowadays, histamine is considered to be a ubiquitous and multifunctional biogenic amine which is involved in various physiological and

pathophysiological situations. Histamine holds a key position in a number of brain functions including sleep-waking cycle, emotion or learning, it is involved in secretion of pituitary hormones, regulation of gastrointestinal and circulatory functions, inflammatory reactions and modulation of immune response (Dy and Schneider, 2004).

Histamine is formed in the body from L-histidine by the action of the enzyme histidine decarboxylase (HDC). In the hematopoietic system, mast cells (Riley and West, 1952) and basophils (Falcone *et al.*, 2006) store histamine in cytosolic granules, and can release the mediator in large amounts during degranulation in response to various immunological and non-immunological stimuli (Dy and Schneider, 2004). Histamine is also produced by enterochromaffin-like cells in the stomach (Prinz *et al.*, 2003) and histaminergic neurons in the tuberomamillary nucleus (Haas *et al.*, 2008). After liberation into the extracellular space, histamine is metabolized rapidly. The two main catabolic pathways are methylation by histamine N-methyltransferase (HNMT) to form N^{T}-methylhistamine and deamination by the diamine oxidase (DAO) to form imidazole-4-acetaldehyd (Beaven, 1982). Both products are further metabolized by xanthin oxidase and DAO or ribosyltransferase as shown in **Figure 1.6**.

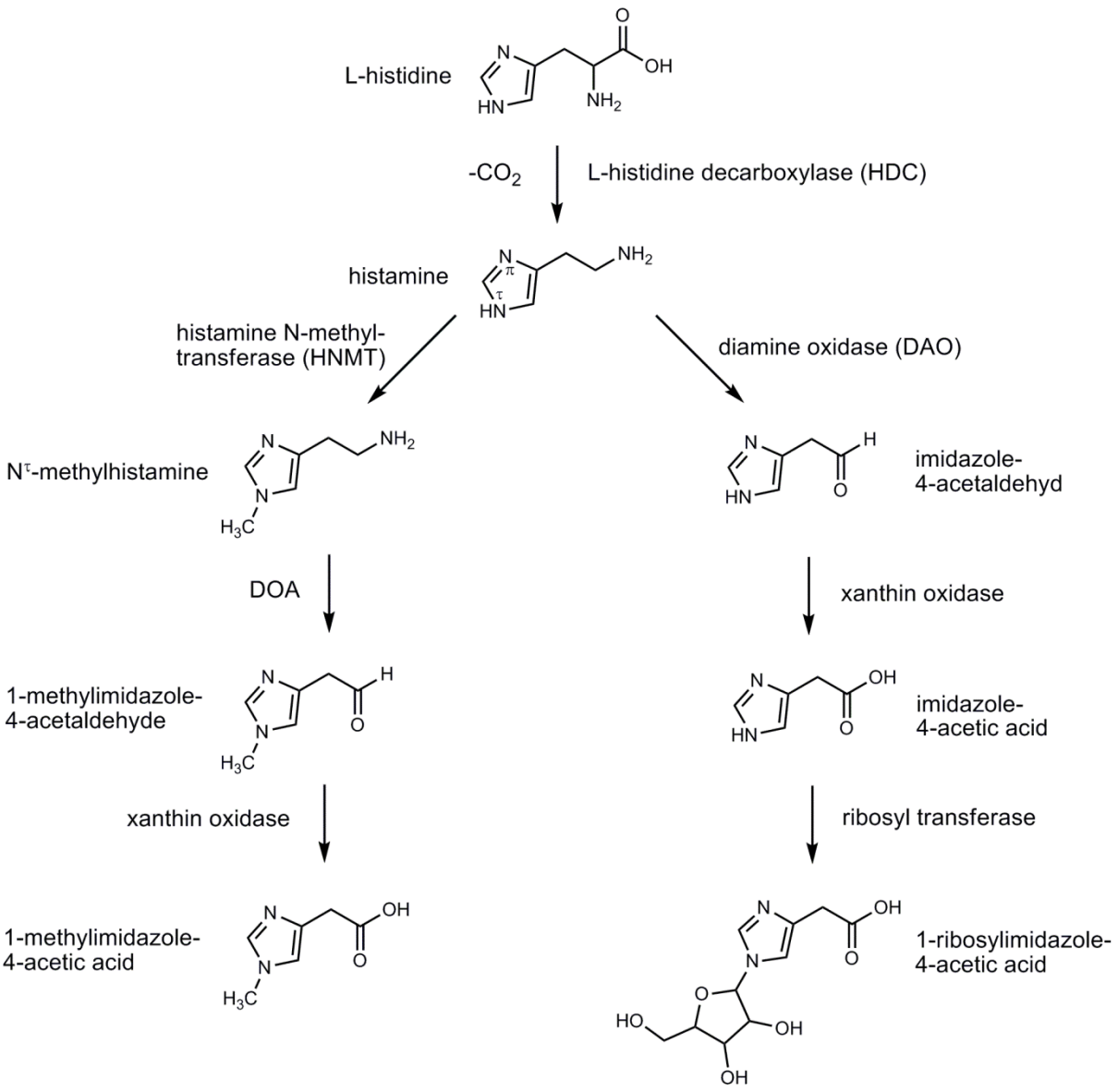

Figure 1.6: Biosynthesis and metabolism of histamine.

Histamine can be protonated at the strongly basic amino group in the side chain (pKa_2 = 9.4) and at the imidazole ring (pKa_1 = 5.8) to form a dication. Under physiological conditions (pH 7.4), however, the monocation predominates and is thus supposed to be the biologically active species. The monocation exists in an equilibrium mixture of two possible tautomeric forms, the N^{π}-H tautomer and the N^{τ}-H tautomer. In aqueous solution, about 80 % of histamine monocation is in the N^{τ}-H form (Ganellin *et al.*, 1973) (see **Figure 1.7**).

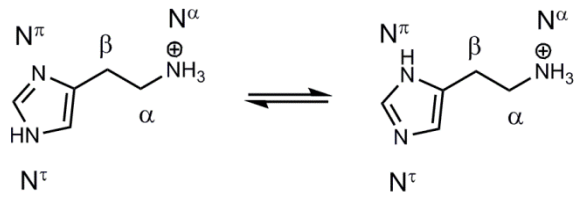

Figure 1.7: Tautomerism of histamine in the monocationic form.

1.2.2 Histamine receptors and their ligands

Histamine exerts its biological effects via four receptor subtypes, namely the H_1R, H_2R, H_3R and H_4R, belonging all to class A (rhodopsin-like family) of GPCRs (Foord *et al.*, 2005) (cf. section 1.1.2). The H_3R and H_4R displayed the highest overall sequence homology of about 40 % (58 % in the TM regions) (Hough, 2001). The sequence similarity between the H_1R and H_2R is rather low (about 28 % identity) (De Backer *et al.*, 1993). The comparison of the $H_{1/2}Rs$ with the $H_{3/4}Rs$ also yields a relatively low average sequence homology of about 20 % (Leurs *et al.*, 2009; Lovenberg *et al.*, 1999).

1.2.2.1 The histamine H_1 receptor

The term H_1R was introduced by Ash and Schild in the year 1966 after it was evident that two distinct receptors are involved in histamine response (Ash and Schild, 1966). Thus, the first antihistamines such as the adrenolytic benzodioxan, piperoxan (933F) (see **Figure 1.8**), which blocked the histamine effect in the guinea pig ileum (Ungar *et al.*, 1937), are also referred to as H_1R antagonists. The H_1R was first cloned in 1993 and the corresponding receptor protein consists of 487 amino acids (De Backer *et al.*, 1993). The H_1R predominantly couples to $G\alpha_{q/11}$ proteins upon agonist stimulation, leading to the release of calcium as described in section 1.1.4.1. Moreover, the activated H_1R expressed in HEK293 cells can increase the cAMP level as described recently (Esbenshade *et al.*, 2003). The H_1R is expressed in airway and vascular smooth muscle cells, neurons, endothelial and epithelial cells as well as hematopoietic cells (Dy and Schneider, 2004). H_1Rs are involved in the pathophysiological process of allergy and inflammatory reactions. Histamine induces via the H_1R, for instance, vasodilatation, bronchoconstriction, increased vascular permeability, pain and itching upon insect stings (Bongers *et al.*, 2010). Accordingly, H_1R antagonists have been successfully used for the treatment of allergic disorders such as hay fever, allergic rhinitis and urticaria (Parsons and Ganellin, 2006). Side effects, especially sedation, due to occupancy of H_1R in the central nervous system (CNS) were characteristic of the first

generation of H_1R antagonists such as mepyramine (Pyrilamine®) or diphenhydramine (Dolestan®) (see **Figure 1.8**). However, for instance, diphenhydramine 8-chlortheophyllinate (Dramamine®) is approved as antiemetic for the treatment of travel sickness. More polar compounds that penetrate poorly into the CNS, like cetirizine (Zyrtec®) or fexofenadine (Telfast®) (see **Figure 1.8**), have been developed to prevent CNS side effects. These compounds belong to the "non-sedating" second generation of H_1R antagonist and are blockbuster drugs for the treatment of allergic disorders (Hill *et al.*, 1997).

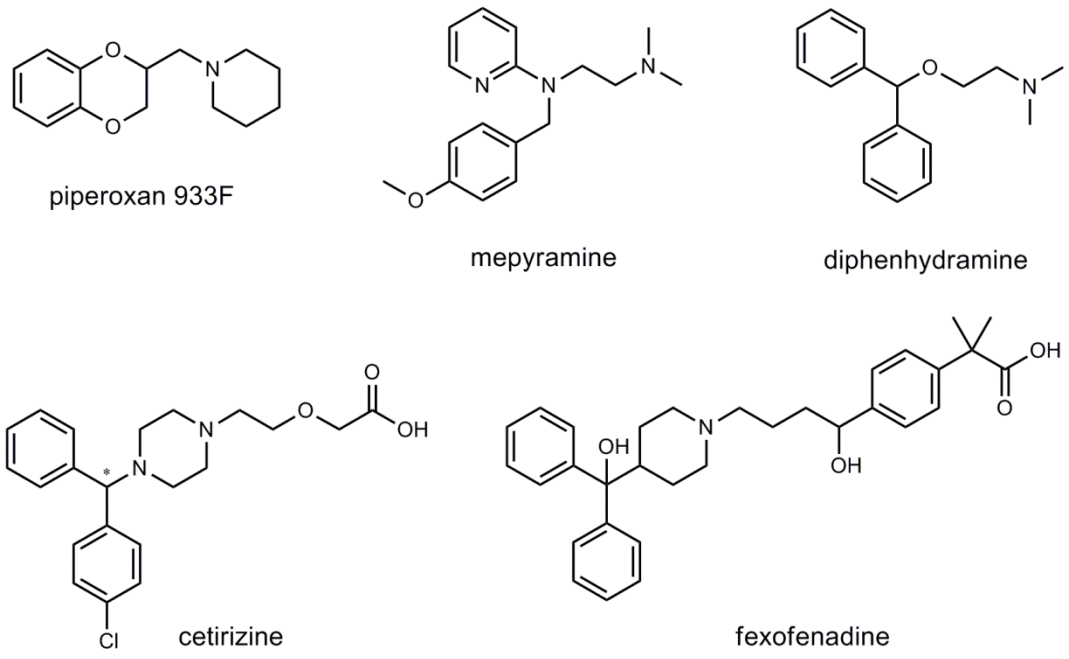

Figure 1.8: Structures of selected H_1R antagonists.

H_1R agonists do not have the same clinical prospects as H_1R antagonist and are thus not readily available. The only clinically used H_1R agonist is the centrally acting betahistine (Aequamen®) (see **Figure 1.9**), which can be orally administered for the treatment of Menière's disease (Barak, 2008). Selective H_1R agonists have been developed as well, and represent interesting pharmacological tools. Substitution in the 2-position of the imidazole ring of histamine presents a valuable method to obtain selective H_1R agonists such as 2-(3-bromophenyl)histamine and 2-[3-(trifluoromethyl)phenyl]histamine (Leschke *et al.*, 1995) (see **Figure 1.9**). More recently, Schunack and colleagues developed a new class of highly potent and selective H_1R agonists which are characterized by a 3,3-diphenylpropyl substituent and named histaprodifens (Elz *et al.*, 2000a; Elz *et al.*, 2000b). The dimerisation of histaprodifen with histamine resulted in the even more potent suprahistaprodifen (Menghin *et al.*, 2003) (see **Figure 1.9**).

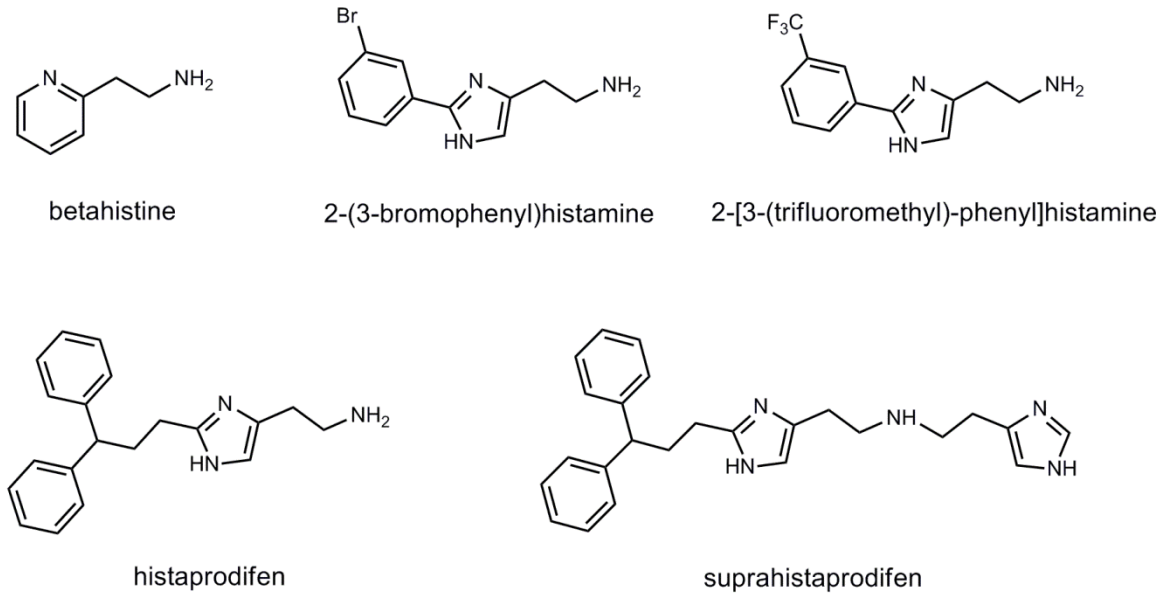

Figure 1.9: Structures of selected H_1R agonists.

1.2.2.2 The histamine H_2 receptor

The existence of a second histamine receptor subtype was confirmed by the discovery of the first selective H_2R antagonist burimamide, which blocked the action of histamine on H_2R containing tissues such as the histamine-induced gastric acid secretion and the chronotropic effect on the heart (Black *et al.*, 1972). About 20 years after the first pharmacological characterization, the copy-DNA (cDNA) of the canine and subsequently of the human H_2R were cloned by Gantz and coworkers (Gantz *et al.*, 1991a; Gantz *et al.*, 1991b). The H_2R primarily couples to the $G\alpha_s$ family of G-proteins, leading to activation of AC (cf. section 1.1.4.1) (Gantz *et al.*, 1991a; Johnson *et al.*, 1979; Klein and Levey, 1971). Depending on the used cell system, the H_2R may additionally trigger calcium signaling by coupling to the $G\alpha_{q/11}$ G-protein (cf. section 1.1.4.1) (Esbenshade *et al.*, 2003; Mitsuhashi *et al.*, 1989; Wang *et al.*, 1996). H_2Rs were found in numerous peripheral tissues and cells such as gastric parietal cells, heart, airways, uterus and vascular smooth muscle cells, hematopoietic cells (neutrophils, eosinophils, monocytes, dendritic cells, T and B lymphocytes) and in the brain (Baumer and Rossbach, 2010; Dove *et al.*, 2004; Hill *et al.*, 1997). The first marketed H_2R antagonist cimetidine (Tagamet®) (see **Figure 1.10**) has revolutionized the treatment of peptic ulcer and gastro-oesophageal reflux disease (Parsons and Ganellin, 2006). Following the success of cimetidine, several other H_2R antagonists were developed and launched onto the market like ranitidine (Zantac®) and famotidine (Pepdul®), which, unlike cimetidine, do not affect cytochrome P450 enzymes in the liver (Hill *et al.*, 1997; Parsons and Ganellin, 2006) (see **Figure 1.10**). In addition to the therapeutically used drugs, selective H_2R antagonists with high affinity such as tiotidine (see **Figure 1.10**) and iodoaminopotentidine

were successfully applied as pharmacological tools (Gajtkowski *et al.*, 1983; Hirschfeld *et al.*, 1992).

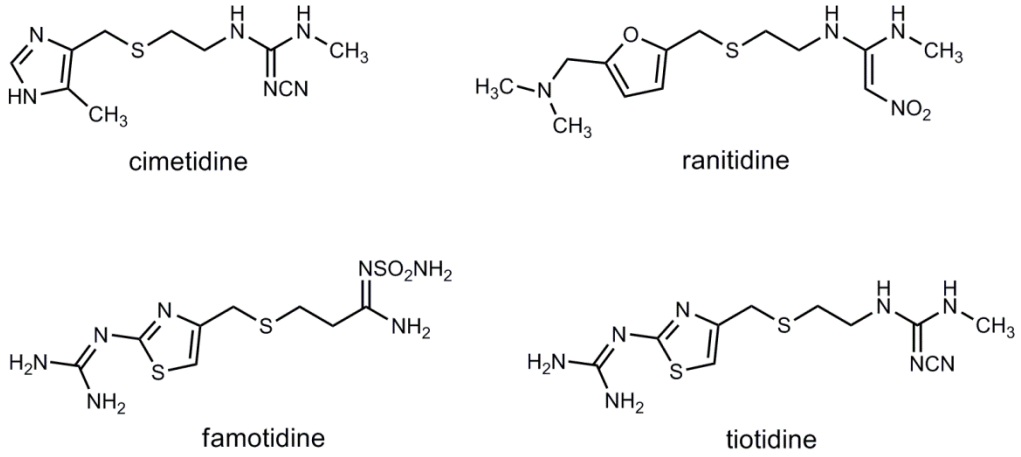

Figure 1.10: Structures of selected H_2R antagonists.

Dimaprit was one of the first available relatively selective H_2R agonist (Durant *et al.*, 1977) (see **Figure 1.11**). Highly potent and selective guanidine-type H_2R agonists like impromidine (Durant *et al.*, 1978; Durant *et al.*, 1985) and arpromidine (Buschauer, 1989) (see **Figure 1.11**) have been developed (Timmerman, 1992), which, however, showed poor oral bioavailability (Dove *et al.*, 2004). In order to obtain agonists with an improved pharmacokinetic profile, the basicity was reduced by replacement of the guanidine group with an acylguanidine moiety, resulting in N^G-acetylated imidazolylpropylguanidines such as UR-AK24 (Ghorai *et al.*, 2008) (see **Figure 1.11**). A further bioisosteric replacement of the imidazole ring with a 2-amino-4-methylthiazol-5-yl moiety led to agonists such as UR-PG278 (see **Figure 1.11**) with substantially improved H_2R selectivity compared to the other H_xRs (Kraus *et al.*, 2009). Recently, the application of the bivalent ligand approach to acylguanidines yielded UR-AK459 (see **Figure 1.11**), which is highly selective and 4000 times more potent than histamine at the guinea pig right atrium (Birnkammer *et al.*, 2012). Although Baumann and co-workers demonstrated in a clinical trial with impromidine about 30 years ago that the combined vasodilator and inotropic action may be an effective treatment of severe catecholamine-insensitive congestive heart failure (Baumann *et al.*, 1984), H_2R agonists are still not used therapeutically. Nevertheless, they are important as pharmacological tools to study the (patho)physiological role of the H_2R.

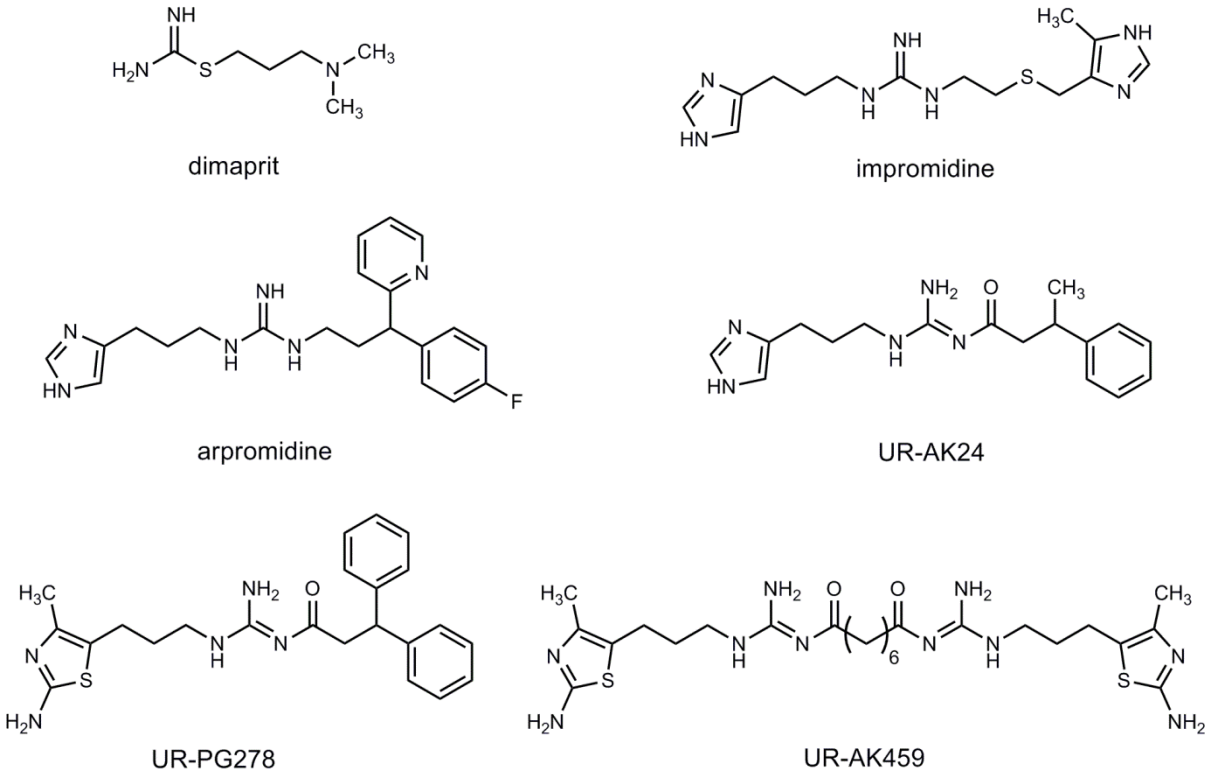

Figure 1.11: Structure of selected H_2R agonists.

1.2.2.3 The histamine H_3 receptor

A third histamine receptor subtype was first described in a pharmacological approach by Arrang and colleagues in 1983, who found that histamine inhibits its own synthesis and release in rat cerebral cortical slices via presynaptic feedback mechanisms. Due to the fact that neither H_1R nor H_2R activity of histaminergic ligands correlated with these inhibitory effects, a novel subtype of histamine receptor was proposed (Arrang *et al.*, 1983). The discovery of the agonist (R)-α-methylhistamine and the competitive antagonist thioperamide as selective pharmacological tools for the H_3R confirmed its existence and enabled a detailed pharmacological characterization (Arrang *et al.*, 1987). The molecular architecture of the H_3R was unknown until Lovenberg and co-workers succeeded in the cloning of the receptor cDNA in 1999 by performing homology searches of expressed sequence tag database (Lovenberg *et al.*, 1999). This confirmed that the H_3R belongs, like the H_1R and H_2R, to the large super-family of GPCRs. The elucidation of the genomic organization led also to the discovery of at least 20 hH_3R isoforms of which, however, the full length 445 (aa) sequence seems to encode the functionally dominant and abundantly expressed isoform (Berlin *et al.*, 2011). The physiological significance of most of the other isoforms is unknown and needs to be further investigated. H_3R signaling is mediated through $G\alpha_{i/o}$ proteins leading to inhibition of AC (cf. section 1.1.4.1) (Clark and Hill, 1996). Moreover, the H_3R mediates the activation of

phospholipase A_2 (PLA_2), MAPKs, phosphatidyl inositol-3 kinase, inhibition of the Na^+/H^+ exchanger and modulation of intracellular calcium (Bongers *et al.*, 2007). The H_3R is mainly expressed in the central nervous system where the highest densities of H_3Rs were found in the basal ganglia, hippocampus and cortical areas (Martinez-Mir *et al.*, 1990). In the peripheral nervous system, H_3Rs are located, for instance, in the gastrointestinal tract, the airways and the cardiovascular system (Wijtmans *et al.*, 2007). The H_3R acts as presynaptic autoreceptor to regulate the release of histamine and as heteroreceptor on non-histaminergic neurons, regulating the release of several other important neurotransmitters such as acetylcholine, norepinephrine, dopamine and serotonin (Gemkow *et al.*, 2009). The position at the crossroad of neurotransmission suggests a broad range of therapeutic indications including cognitive disorders, sleep disorders, pain and obesity. Consequently the H_3R has become an attractive drug target for both academic research groups and pharmaceutical companies (Leurs *et al.*, 2005). Antagonists for the H_3R currently undergo clinical evaluation for the treatment of Alzheimer`s diseases, schizophrenia, attention deficit hyperactivity disorder, dementia, epilepsy, narcolepsy, obesity and neuropathic pain (Berlin *et al.*, 2011; Gemkow *et al.*, 2009; Leurs *et al.*, 2011; Sander *et al.*, 2008). Recently, pitolisant (formerly known as BF2.649) (see **Figure 1.2**) has been introduced as the first H_3R inverse agonist/ antagonist in the clinics for the treatment of narcolepsy (Schwartz, 2011). The starting point for the design of the first potent H_3R antagonists such as thioperamide (Arrang *et al.*, 1987) and clobenpropit (van der Goot *et al.*, 1992) was the structure of the endogenous ligand, histamine, so that these compounds have an imidazole ring in common (see **Figure 1.12**). As imidazole containing H_3R antagonists exhibit insufficient drug-likeness due to the risk of CYP interactions, poor brain penetration and species-dependent differences (Sander *et al.*, 2008), several pharmaceutical companies developed non-imidazole H_3R antagonists such as pitolisant and JNJ 5207852 (Barbier *et al.*, 2004), containing other nitrogen heterocycles (see **Figure 1.12**).

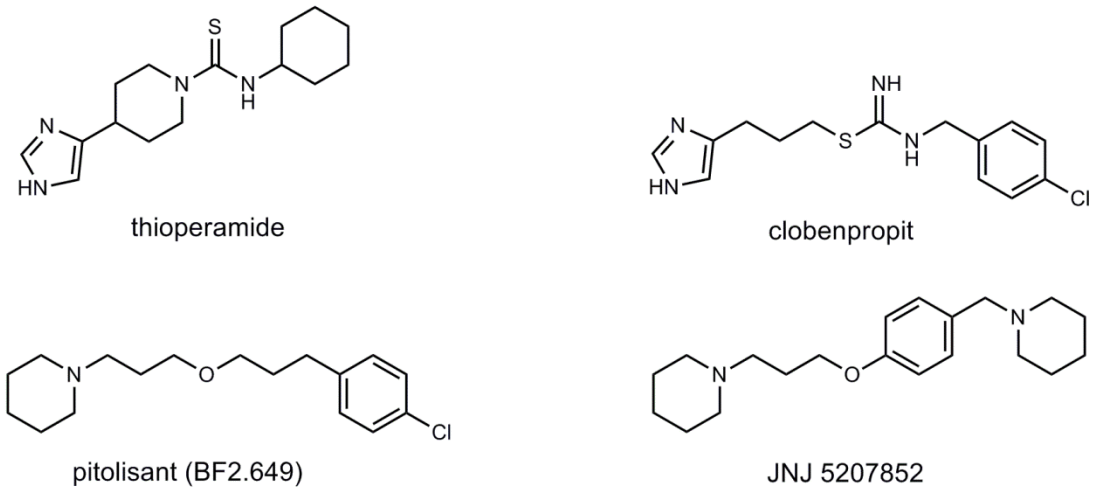

Figure 1.12: Structures of selected H_3R antagonists.

Due to negative neurotransmitter modulation, beneficial effects of H_3R agonists are expected at pathological conditions caused by elevated neurotransmitter levels. Thus, H_3R agonists also have a variety of potential therapeutic application including inflammation, migraine, asthma, insomnia, pain, ulcer, hypertension, immunological regulation and ischemic arrhythmias (Berlin *et al.*, 2011). Contrary to H_3R antagonists, the imidazole moiety in H_3R agonists seems to be essential to maintain agonistic activity (Leurs *et al.*, 2005). Structures of H_3R agonists closely resemble to histamine and contain only minor modifications in the imidazole side chain as, for example, in (R)-α-methylhistamine, N^{α}-methylhistamine, imetit and immepip (see **Figure 1.13**). Major drawbacks of these compounds are missing selectivity over the newly identified H_4R and limited utilization *in vivo* due to low oral bioavailability and rapid metabolism. In the case of (R)-α-methylhistamine the latter problem was overcome by applying an azomethine prodrug concept to (R)-α-methylhistamine resulting in BP 2-94 (Krause *et al.*, 1995) (see **Figure 1.13**), which shows improved oral bioavailability and pharmacokinetic properties (Rouleau *et al.*, 1997). To enhance selectivity over the H_4R, new potent H_3R agonists such as immethridine and methimmepip have been developed (Kitbunnadaj *et al.*, 2004) (see **Figure 1.13**).

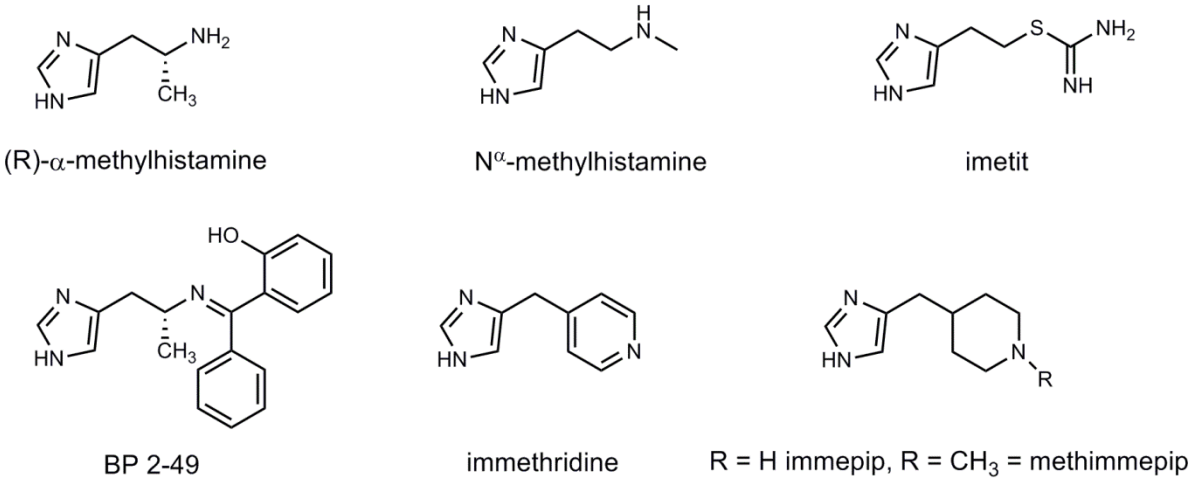

Figure 1.13: Structure of selected H_3R agonists.

1.2.2.4 The histamine H_4 receptor

Early examples of H_4 receptor signaling can be found in literature from the time in which the existence of the receptor was still unknown. In 1975 Clark and his co-workers observed histamine induced chemotaxis of human eosinophils that was not inhibited by H_1 or H_2 receptor antagonists (Clark *et al.*, 1975). Two decades later, Raible and his colleagues identified pertussis toxin-sensitive cytosolic calcium increase in eosinophils by histamine, which was blocked by H_3R antagonists. Furthermore, known H_3R agonists (R-α-methylhistamine and N^{α}-methylhistamine) could trigger calcium increase, but the potencies were much lower than the potency of histamine. This led to the assumption that a fourth histamine receptor subtype is present on eosinophils (Raible *et al.*, 1994). On the basis of high sequence homology with the H_3R, several research groups independently identified the H_4R sequence in the human genome at the beginning of the new century (Liu *et al.*, 2001; Morse *et al.*, 2001; Nakamura *et al.*, 2000; Nguyen *et al.*, 2001; Oda *et al.*, 2000; Zhu *et al.*, 2001). The human H_4R gene encodes for a 390 amino acid protein and contains, like the H_3R, three exons and two introns. So far, only two non-signaling H_4R isoforms have been identified, which are supposed to act as negative regulatory elements on full length receptor functionality (vanRijn *et al.*, 2008). The H_4R inhibits adenylyl cyclase via activation of $G\alpha_{i/o}$ proteins (cf. section 1.1.4.1) (Leurs *et al.*, 2009). Additionally, stimulation of the H_4R leads to pertussis-toxin sensitive activation of MAPK pathway (Morse *et al.*, 2001) and calcium mobilization (Hofstra *et al.*, 2003). Very recently, also hH_4R mediated β-arrestin activation has been reported for several H_4R ligands (Nijmeijer *et al.*, 2012). The H_4R is predominantly expressed in cells of hematopoietic origin including neutrophils, mast cells, eosinophils, basophils, dendritic cells, monocytes and T cells. Furthermore, the H_4R has been identified on nerves from the nasal mucosa, in the enteric and, as with the other histamine receptors,

in the central nervous system (Leurs *et al.*, 2009). Concerns regarding the specificity of antibodies, which were used for the analysis of expression and localization of the H_4R, have emerged recently and are currently under discussion (Beermann *et al.*, 2012b; Gutzmer *et al.*, 2012; Neumann *et al.*, 2012; Seifert *et al.*, 2013). Although the (patho)physiological role of the H_4R is still not fully understood, the involvement in chemotaxis and cytokine release in cells of the immune system suggest that the H_4R plays an important pro-inflammatory role in various diseases including allergic asthma, allergic rhinitis, pruritis and inflammatory pain (Leurs *et al.*, 2011; Walter *et al.*, 2011; Zampeli and Tiligada, 2009). Accordingly, H_4R antagonists have the potential for the treatment of the aforementioned diseases. Due to overlapping function of the H_4R in immunological responses with the H_1R (cf. section 1.2.2.1), dual H_1R/H_4R antagonists may offer additional benefit over monotherapy, particularly in the treatment of allergic reactions (Deml *et al.*, 2009; Thurmond *et al.*, 2008). Recent findings suggest that histamine is also an important modulator of biological processes such as cell proliferation, senescence and apoptosis via the H_4R in malignant cells. Therefore, the H_4R is considered as new drug target in the pharmacotherapy of cancer (Medina and Rivera, 2010).

In the search for novel H_4R antagonists or inverse agonists, the imidazole-containing H_3R inverse agonist thioperamide has been identified as equipotent H_4R inverse agonist and is until now a frequently used reference compound (Lim *et al.*, 2005) (cf. **Figure 1.12**). However, the potential of H_4R antagonists in the treatment of inflammatory diseases stimulated the search for selective H_4R ligands. A high-throughput screening campaign resulted in the early identification of the indole carboxamide JNJ 7777120 (see **Figure 1.14**) as selective H_4R antagonist (Jablonowski *et al.*, 2003). JNJ 7777120 is reported as equipotent at the human, mouse and rat H_4R (Thurmond *et al.*, 2004), and served as standard antagonist for the investigation of the biological function of the H_4R in animal models (Beermann *et al.*, 2012a; Cowden *et al.*, 2010; Deml *et al.*, 2009; Dunford *et al.*, 2006; Morgan *et al.*, 2007; Rossbach *et al.*, 2009a; Rossbach *et al.*, 2009b; Zampeli *et al.*, 2009). However, *in vivo* results of JNJ 7777120 must be interpreted with caution in view of partial agonistic activity at mouse and rat H_4Rs, which have only low constitutive activity, in a GTPase assay (Schnell *et al.*, 2011) and agonist-like beta-arrestin recruitment to the hH_4R (Nijmeijer *et al.*, 2012; Rosethorne and Charlton, 2011; Seifert *et al.*, 2011). Meanwhile, other highly selective and potent H_4R antagonists such as quinazolines (Smits *et al.*, 2008) and 2-aminopyrimidines (Cowart *et al.*, 2008; Mowbray *et al.*, 2011) have been developed (see **Figure 1.14**).

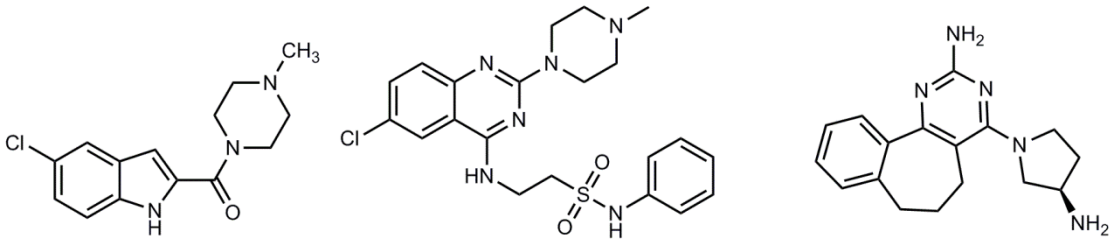

Figure 1.14: Structures of selected H_4R antagonists.

To further investigate the pathophysiological role of the H_4R, selective agonists are of particular interest as pharmacological tools. Considering the high degree of sequence homology with the H_3R, it is not surprising that the H_4R is activated by numerous compounds which were originally designed as H_3R agonists, and, consequently, contain an imidazole ring, for instance (R)-α-methylhistamine, N^{α}-methylhistamine and imetit (cf. **Figure 1.13**). The first ligand with improved selective H_4R activation is OUP-16, a chiral tetrahydrofuran analog which was derived from imifuramine (Hashimoto *et al.*, 2003). Thereafter, various compounds originally developed as H_2R agonist, for example (4)5-methylhistamine (Lim *et al.*, 2005) and the dimaprit analog VUF 8430 (Lim *et al.*, 2006), turned out to be H_4R agonists with about 100- and 30-fold selectivity over the other HxR subtypes, respectively. Similarly, N^{G}-acetylated imidazolylpropylguanidine-type H_2R agonists such as UR-AK24 (cf. **Figure 1.11**) were found to be more potent at the hH_3R and hH_4R. Modification of the N^{G}-acyl groups in UR-AK24 resulted in potent nearly full H_4R agonists such as UR-PI294, which possess improved selectivity over the hH_1R and hH_2R, but show residual activity at the hH_3R (Igel *et al.*, 2009b). Tritium labeling of the N^{G}-propionyl group in UR-PI294 yielded a novel high affinity radioligand for the H_3R and H_4R (c.f. chapter 3 and 5) (Igel *et al.*, 2009c). Aiming at improved selectivity for the H_4R, the acylguanidine moiety was replaced by a non-basic cyanoguanidine group. Further structural optimization provided highly potent and selective cyanoguanidine-type H_4R agonists such as UR-PI376 and trans-(+)-(1S,3S)-UR-RG98 (Geyer, 2011; Igel *et al.*, 2009a) (see **Figure 1.15**). Other recently reported structural classes comprising selective H_4R agonists are oxime analogs of JNJ 7777120 (Yu *et al.*, 2010) and 2-arylbenzimidazoles (Lee-Dutra *et al.*, 2006). Of importance are the oxime-type compounds, especially owing to their applicability as pharmacological tools for investigating the H_4R in rodent animal models. Other H_4R agonists (and antagonists) are often unsuitable due to species-dependent discrepancies, including potencies, receptor selectivities and even opposite qualities of action (Esbenshade *et al.*, 2003; Igel *et al.*, 2010; Strasser *et al.*, 2013).

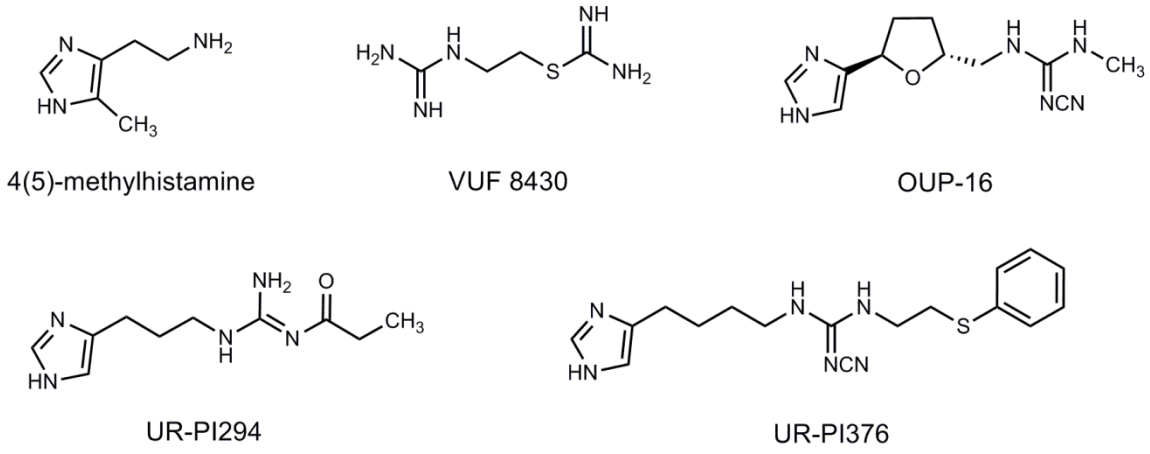

Figure 1.15: Structure of selected H_4R agonists.

1.3 References

Ahn, S.; Shenoy, S. K.; Wei, H.; Lefkowitz, R. J. Differential kinetic and spatial patterns of beta-arrestin and G protein-mediated ERK activation by the angiotensin II receptor. *J. Biol. Chem.* ***2004,*** 279, 35518-25.

Ariens, E. J. Affinity and intrinsic activity in the theory of competitive inhibition. I. Problems and theory. *Arch. Int. Pharmacodyn. Ther.* ***1954,*** 99, 32-49.

Arrang, J. M.; Garbarg, M.; Lancelot, J. C.; Lecomte, J. M.; Pollard, H.; Robba, M.; Schunack, W.; Schwartz, J. C. Highly potent and selective ligands for histamine H_3-receptors. *Nature* ***1987,*** 327, 117-23.

Arrang, J. M.; Garbarg, M.; Schwartz, J. C. Auto-inhibition of brain histamine release mediated by a novel class (H_3) of histamine receptor. *Nature* ***1983,*** 302, 832-7.

Ash, A. S.; Schild, H. O. Receptors mediating some actions of histamine. *Br. J. Pharmacol. Chemother.* ***1966,*** 27, 427-39.

Barak, N. Betahistine: what's new on the agenda? *Expert. Opin. Investig. Drugs* ***2008,*** 17, 795-804.

Barbier, A. J.; Berridge, C.; Dugovic, C.; Laposky, A. D.; Wilson, S. J.; Boggs, J.; Aluisio, L.; Lord, B.; Mazur, C.; Pudiak, C. M. and others. Acute wake-promoting actions of JNJ-5207852, a novel, diamine-based H_3 antagonist. *Br. J. Pharmacol.* ***2004,*** 143, 649-61.

Baumann, G.; Permanetter, B.; Wirtzfeld, A. Possible value of H_2-receptor agonists for treatment of catecholamine-insensitive congestive heart failure. *Pharmacol. Ther.* ***1984,*** 24, 165-77.

Baumer, W.; Rossbach, K. [Histamine as an immunomodulator]. *J. Dtsch. Dermatol. Ges.* ***2010,*** 8, 495-504.

Beaven, M. A. 1982. Factors regulating availability of histamine and tissue receptors. In: Ganellin CR, Parsons ME, editors. Pharmacology of histamine receptors. Bristol: Wright. p 103-145.

Beermann, S.; Glage, S.; Jonigk, D.; Seifert, R.; Neumann, D. Opposite effects of mepyramine on JNJ 7777120-induced amelioration of experimentally induced asthma in mice in sensitization and provocation. *PLoS One* ***2012a,*** 7, e30285.

Beermann, S.; Seifert, R.; Neumann, D. Commercially available antibodies against human and murine histamine H(4)-receptor lack specificity. *Naunyn-Schmiedeberg's Arch. Pharmacol.* ***2012b,*** 385, 125-35.

Berlin, M.; Boyce, C. W.; Ruiz Mde, L. Histamine H_3 receptor as a drug discovery target. *J. Med. Chem.* ***2011,*** 54, 26-53.

Birnbaumer, L. Expansion of signal transduction by G proteins. The second 15 years or so: from 3 to 16 alpha subunits plus betagamma dimers. *Biochim. Biophys. Acta* ***2007,*** 1768, 772-93.

Birnkammer, T.; Spickenreither, A.; Brunskole, I.; Lopuch, M.; Kagermeier, N.; Bernhardt, G.; Dove, S.; Seifert, R.; Elz, S.; Buschauer, A. The bivalent ligand approach leads to highly potent and selective acylguanidine-type histamine H(2) receptor agonists. *J. Med. Chem.* ***2012,*** 55, 1147-60.

Black, J. W.; Duncan, W. A.; Durant, C. J.; Ganellin, C. R.; Parsons, E. M. Definition and antagonism of histamine H 2 -receptors. *Nature* ***1972,*** 236, 385-90.

Bongers, G.; Bakker, R. A.; Leurs, R. Molecular aspects of the histamine H_3 receptor. *Biochem. Pharmacol.* ***2007,*** 73, 1195-204.

Bongers, G.; de Esch, I.; Leurs, R. Molecular pharmacology of the four histamine receptors. *Adv. Exp. Med. Biol.* ***2010,*** 709, 11-9.

Buschauer, A. Synthesis and in Vitro Pharmacology of Arpromidine and Related Phenyl(pyridylalkyl)guanidines, a Potential New Class of Positive Inotropic Drugs. *J. Med. Chem.* ***1989,*** 32, 1963-1970.

Cabrera-Vera, T. M.; Vanhauwe, J.; Thomas, T. O.; Medkova, M.; Preininger, A.; Mazzoni, M. R.; Hamm, H. E. Insights into G protein structure, function, and regulation. *Endocr. Rev.* ***2003,*** 24, 765-81.

Cherezov, V.; Rosenbaum, D. M.; Hanson, M. A.; Rasmussen, S. G.; Thian, F. S.; Kobilka, T. S.; Choi, H. J.; Kuhn, P.; Weis, W. I.; Kobilka, B. K. and others. High-resolution crystal structure of an engineered human beta2-adrenergic G protein-coupled receptor. *Science* ***2007,*** 318, 1258-65.

Civelli, O.; Reinscheid, R. K.; Zhang, Y.; Wang, Z.; Fredriksson, R.; Schioth, H. B. G protein-coupled receptor deorphanizations. *Annu. Rev. Pharmacool. Toxicol.* ***2013,*** 53, 127-46.

Clark, A. J. 1937. General pharmacology. In: Heffter A, editor. Handbuch der experimentellen Pharmakologie, Ergänzungswerk Band 4. Berlin: Springer. p 165-176.

Clark, A. J. 1933. The mode of action of drugs on cells. London: Edward Arnold.

Clark, E. A.; Hill, S. J. Sensitivity of histamine H_3 receptor agonist-stimulated [^{35}S]GTP γ[S] binding to pertussis toxin. *Eur. J. Pharmacol.* ***1996,*** 296, 223-225.

Clark, R. A.; Gallin, J. I.; Kaplan, A. P. The selective eosinophil chemotactic activity of histamine. *J. Exp. Med.* ***1975,*** 142, 1462-76.

Congreve, M.; Langmead, C. J.; Mason, J. S.; Marshall, F. H. Progress in structure based drug design for G protein-coupled receptors. *J. Med. Chem.* ***2011,*** 54, 4283-311.

Costa, T.; Herz, A. Antagonists with negative intrinsic activity at delta opioid receptors coupled to GTP-binding proteins. *Proc. Natl. Acad. Sci. U. S. A.* ***1989,*** 86, 7321-5.

Cowart, M. D.; Altenbach, R. J.; Liu, H.; Hsieh, G. C.; Drizin, I.; Milicic, I.; Miller, T. R.; Witte, D. G.; Wishart, N.; Fix-Stenzel, S. R. and others. Rotationally Constrained 2,4-Diamino-5,6-disubstituted Pyrimidines: A New Class of Histamine H_4 Receptor Antagonists with Improved Druglikeness and in Vivo Efficacy in Pain and Inflammation Models. *J. Med. Chem.* ***2008,*** 51, 6547-6557.

Cowden, J. M.; Riley, J. P.; Ma, J. Y.; Thurmond, R. L.; Dunford, P. J. Histamine H_4 receptor antagonism diminishes existing airway inflammation and dysfunction via modulation of Th2 cytokines. *Respir. Res.* ***2010,*** 11, 86.

Dale, H. H.; Laidlaw, P. P. Histamine shock. *J. Physiol.* ***1919,*** 52, 355-90.

Dale, H. H.; Laidlaw, P. P. The physiological action of beta-iminazolylethylamine. *J. Physiol.* ***1910,*** 41, 318-44.

Davies, M. N.; Gloriam, D. E.; Secker, A.; Freitas, A. A.; Timmis, J.; Flower, D. R. Present perspectives on the automated classification of the G-protein coupled receptors (GPCRs) at the protein sequence level. *Curr. Top. Med. Chem.* ***2011,*** 11, 1994-2009.

De Backer, M. D.; Gommeren, W.; Moereels, H.; Nobels, G.; Van Gompel, P.; Leysen, J. E.; Luyten, W. H. Genomic cloning, heterologous expression and pharmacological characterization of a human histamine H_1 receptor. *Biochem. Biophys. Res. Commun.* ***1993,*** 197, 1601-8.

De Lean, A.; Stadel, J. M.; Lefkowitz, R. J. A ternary complex model explains the agonist-specific binding properties of the adenylate cyclase-coupled beta-adrenergic receptor. *J. Biol. Chem.* ***1980,*** 255, 7108-17.

Del Castillo, J.; Katz, B. Interaction at end-plate receptors between different choline derivatives. *Proc. R. Soc. Lond. B. Biol. Sci.* ***1957,*** 146, 369-81.

Deml, K. F.; Beermann, S.; Neumann, D.; Strasser, A.; Seifert, R. Interactions of histamine H_1-receptor agonists and antagonists with the human histamine H_4-receptor. *Mol. Pharmacol.* ***2009,*** 76, 1019-30.

DeWire, S. M.; Ahn, S.; Lefkowitz, R. J.; Shenoy, S. K. Beta-arrestins and cell signaling. *Annu. Rev. Physiol.* ***2007,*** 69, 483-510.

Dove, S.; Elz, S.; Seifert, R.; Buschauer, A. Structure-Activity Relationsships of Histamine H_2 Receptor Ligands. *Mini. Rev. Med. Chem.* ***2004,*** 4, 941-954.

Dunford, P. J.; O'Donnell, N.; Riley, J. P.; Williams, K. N.; Karlsson, L.; Thurmond, R. L. The histamine H_4 receptor mediates allergic airway inflammation by regulating the activation of CD4+ T cells. *J. Immunol.* ***2006,*** 176, 7062-70.

Durant, G. J.; Duncan, W. A.; Ganellin, C. R.; Parsons, M. E.; Blakemore, R. C.; Rasmussen, A. C. Impromidine (SK&F 92676) is a very potent and specific agonist for histamine H_2 receptors. *Nature* ***1978,*** 276, 403-5.

Durant, G. J.; Ganellin, C. R.; Hills, D. W.; Miles, P. D.; Parsons, M. E.; Pepper, E. S.; White, G. R. The Histamine H_2 Receptor Agonist Impromidine: Synthesis and Structure-Activity Considerations. *J. Med. Chem.* ***1985,*** 28, 1414-1422.

Durant, G. J.; Ganellin, C. R.; Parsons, M. E. Dimaprit, (S-[3-(N,N-dimethylamino)propyl]isothiourea). A highly specific histamine H_2-receptor agonist. Part 2. Structure-activity considerations. *Agents Actions* ***1977,*** 7, 39-43.

Dy, M.; Schneider, E. Histamine-cytokine connection in immunity and hematopoiesis. *Cytokine Growth Factor Rev.* ***2004,*** 15, 393-410.

Eason, M. G.; Kurose, H.; Holt, B. D.; Raymond, J. R.; Liggett, S. B. Simultaneous coupling of alpha 2-adrenergic receptors to two G-proteins with opposing effects. Subtype-selective coupling of alpha 2C10, alpha 2C4, and alpha 2C2 adrenergic receptors to Gi and Gs. *J. Biol. Chem.* ***1992,*** 267, 15795-801.

Elz, S.; Kramer, K.; Leschke, C.; Schunack, W. Ring-substituted histaprodifen analogues as partial agonists for histamine H(1) receptors: synthesis and structure-activity relationships. *Eur. J. Med. Chem.* ***2000a,*** 35, 41-52.

Elz, S.; Kramer, K.; Pertz, H. H.; Detert, H.; ter Laak, A. M.; Kuhne, R.; Schunack, W. Histaprodifens: synthesis, pharmacological in vitro evaluation, and molecular

modeling of a new class of highly active and selective histamine H(1)-receptor agonists. *J. Med. Chem.* ***2000b,*** 43, 1071-84.

Esbenshade, T. A.; Kang, C. H.; Krueger, K. M.; Miller, T. R.; Witte, D. G.; Roch, J. M.; Masters, J. N.; Hancock, A. A. Differential activation of dual signaling responses by human H_1 and H_2 histamine receptors. *J. Recept. Signal Transduct. Res.* ***2003,*** 23, 17-31.

Falcone, F. H.; Zillikens, D.; Gibbs, B. F. The 21st century renaissance of the basophil? Current insights into its role in allergic responses and innate immunity. *Exp. Dermatol.* ***2006,*** 15, 855-64.

Foord, S. M.; Bonner, T. I.; Neubig, R. R.; Rosser, E. M.; Pin, J. P.; Davenport, A. P.; Spedding, M.; Harmar, A. J. International Union of Pharmacology. XLVI. G protein-coupled receptor list. *Pharmacol. Rev.* ***2005,*** 57, 279-88.

Fredriksson, R.; Lagerstrom, M. C.; Lundin, L. G.; Schioth, H. B. The G-protein-coupled receptors in the human genome form five main families. Phylogenetic analysis, paralogon groups, and fingerprints. *Mol. Pharmacol.* ***2003,*** 63, 1256-72.

Gajtkowski, G. A.; Norris, D. B.; Rising, T. J.; Wood, T. P. Specific binding of 3H-tiotidine to histamine H_2 receptors in guinea pig cerebral cortex. *Nature* ***1983,*** 304, 65-7.

Galandrin, S.; Bouvier, M. Distinct signaling profiles of beta1 and beta2 adrenergic receptor ligands toward adenylyl cyclase and mitogen-activated protein kinase reveals the pluridimensionality of efficacy. *Mol. Pharmacol.* ***2006,*** 70, 1575-84.

Ganellin, C. R.; Pepper, E. S.; Port, G. N.; Richards, W. G. Conformation of histamine derivatives. 1. Application of molecular orbital calculations and nuclear magnetic resonance spectroscopy. *J. Med. Chem.* ***1973,*** 16, 610-6.

Gantz, I.; Munzert, G.; Tashiro, T.; Schaffer, M.; Wang, L.; DelValle, J.; Yamada, T. Molecular cloning of the human histamine H_2 receptor. *Biochem. Biophys. Res. Commun.* ***1991a,*** 178, 1386-92.

Gantz, I.; Schaffer, M.; DelValle, J.; Logsdon, C.; Campbell, V.; Uhler, M.; Yamada, T. Molecular cloning of a gene encoding the histamine H_2 receptor. *Proc. Natl. Acad. Sci. U. S. A.* ***1991b,*** 88, 429-33.

Gemkow, M. J.; Davenport, A. J.; Harich, S.; Ellenbroek, B. A.; Cesura, A.; Hallett, D. The histamine H_3 receptor as a therapeutic drug target for CNS disorders. *Drug Discov Today* ***2009,*** 14, 509-15.

Geyer, R. Hetarylalkyl(aryl)cyanoguanidines as histamine H_4 receptor ligands: Synthesis, chiral separation, pharmacological characterization, structure-activity and -selectivity relationships. PhD thesis, University of Regensburg, Regensburg, 2011.

Ghorai, P.; Kraus, A.; Keller, M.; Gotte, C.; Igel, P.; Schneider, E.; Schnell, D.; Bernhardt, G.; Dove, S.; Zabel, M. and others. Acylguanidines as bioisosteres of guanidines: NG-acylated imidazolylpropylguanidines, a new class of histamine H_2 receptor agonists. *J. Med. Chem.* ***2008,*** 51, 7193-204.

Gilman, A. G. G proteins: transducers of receptor-generated signals. *Annu. Rev. Biochem* ***1987,*** 56, 615-49.

Gloriam, D. E.; Fredriksson, R.; Schioth, H. B. The G protein-coupled receptor subset of the rat genome. *BMC Genomics* ***2007,*** 8, 338.

Granier, S.; Kobilka, B. A new era of GPCR structural and chemical biology. *Nat. Chem. Biol.* ***2012,*** 8, 670-3.

Gurevich, V. V.; Gurevich, E. V. The structural basis of arrestin-mediated regulation of G-protein-coupled receptors. *Pharmacol. Ther.* ***2006,*** 110, 465-502.

Gutzmer, R.; Werfel, T.; Baumer, W.; Kietzmann, M.; Chazot, P. L.; Leurs, R. Well characterized antihistamine 4 receptor antibodies contribute to current knowledge of the expression and biology of the human and murine histamine 4 receptor. *Naunyn-Schmiedeberg's Arch. Pharmacol.* ***2012,*** 385, 853-4; author reply 855-60.

Haas, H. L.; Sergeeva, O. A.; Selbach, O. Histamine in the nervous system. *Physiol. Rev.* ***2008,*** 88, 1183-241.

Hanoune, J.; Defer, N. Regulation and role of adenylyl cyclase isoforms. *Annu. Rev. Pharmacool. Toxicol.* ***2001,*** 41, 145-74.

Hanson, M. A.; Stevens, R. C. Discovery of new GPCR biology: one receptor structure at a time. *Structure* ***2009,*** 17, 8-14.

Hashimoto, T.; Harusawa, S.; Araki, L.; Zuiderveld, O. P.; Smit, M. J.; Imazu, T.; Takashima, S.; Yamamoto, Y.; Sakamoto, Y.; Kurihara, T. and others. A Selective Human H_4-Receptor Agonist: (-)-2-Cyano-1-methyl-3-{(2*R*,5*R*)-5-[1*H*-imidazol-4(5)-yl]tetrahydrofuran-2-yl}methylguanidine. *J. Med. Chem.* ***2003,*** 46, 3162-3165.

Hepler, J. R. RGS protein and G protein interactions: a little help from their friends. *Mol. Pharmacol.* ***2003,*** 64, 547-9.

Hill, S. J.; Ganellin, C. R.; Timmerman, H.; Schwartz, J. C.; Shankley, N. P.; Young, J. M.; Schunack, W.; Levi, R.; Haas, H. L. International Union of Pharmacology. XIII. Classification of histamine receptors. *Pharmacol. Rev.* ***1997,*** 49, 253-78.

Hirschfeld, J.; Buschauer, A.; Elz, S.; Schunack, W.; Ruat, M.; Traiffort, E.; Schwartz, J. C. Iodoaminopotentidine and related compounds: a new class of ligands with high affinity and selectivity for the histamine H_2 receptor. *J. Med. Chem.* ***1992,*** 35, 2231-8.

Hofmann, K. P.; Scheerer, P.; Hildebrand, P. W.; Choe, H. W.; Park, J. H.; Heck, M.; Ernst, O. P. A G protein-coupled receptor at work: the rhodopsin model. *Trends Biochem. Sci.* ***2009,*** 34, 540-52.

Hofstra, C. L.; Desai, P. J.; Thurmond, R. L.; Fung-Leung, W.-P. Histamine H_4 Receptor Mediates Chemotaxis and Calcium Mobilization of Mast Cells. *J. Pharmacol. Exp. Ther.* ***2003,*** 305, 1212-1221.

Hough, L. B. Genomics meets histamine receptors: new subtypes, new receptors. *Mol. Pharmacol.* ***2001,*** 59, 415-9.

Igel, P.; Dove, S.; Buschauer, A. Histamine H_4 receptor agonists. *Bioorg. Med. Chem. Lett.* ***2010,*** 20, 7191-9.

Igel, P.; Geyer, R.; Strasser, A.; Dove, S.; Seifert, R.; Buschauer, A. Synthesis and structure-activity relationships of cyanoguanidine-type and structurally related histamine H_4 receptor agonists. *J. Med. Chem.* ***2009a,*** 52, 6297-313.

Igel, P.; Schneider, E.; Schnell, D.; Elz, S.; Seifert, R.; Buschauer, A. N(G)-acylated imidazolylpropylguanidines as potent histamine H_4 receptor agonists: selectivity by variation of the N(G)-substituent. *J. Med. Chem.* ***2009b,*** 52, 2623-7.

Igel, P.; Schnell, D.; Bernhardt, G.; Seifert, R.; Buschauer, A. Tritium-labeled N(1)-[3-(1H-imidazol-4-yl)propyl]-N(2)-propionylguanidine ([(3)H]UR-PI294), a high-affinity histamine H(3) and H(4) receptor radioligand. *ChemMedChem* ***2009c,*** 4, 225-31.

Iqbal, J.; Zaidi, M.; Schneider, A. E. Cinacalcet hydrochloride (Amgen). *IDrugs* ***2003,*** 6, 587-92.

Ishihara, T.; Nakamura, S.; Kaziro, Y.; Takahashi, T.; Takahashi, K.; Nagata, S. Molecular cloning and expression of a cDNA encoding the secretin receptor. *EMBO J.* ***1991,*** 10, 1635-41.

Jablonowski, J. A.; Grice, C. A.; Chai, W.; Dvorak, C. A.; Venable, J. D.; Kwok, A. K.; Ly, K. S.; Wei, J.; Baker, S. M.; Desai, P. J. and others. The first potent and selective non-imidazole human histamine H_4 receptor antagonists. *J. Med. Chem.* ***2003,*** 46, 3957-60.

Jacoby, E.; Bouhelal, R.; Gerspacher, M.; Seuwen, K. The 7 TM G-protein-coupled receptor target family. *ChemMedChem* ***2006,*** 1, 761-82.

Johnson, C. L.; Weinstein, H.; Green, J. P. Studies on histamine H_2 receptors coupled to cardiac adenylate cyclase. Blockade by H_2 and H_1 receptor antagonists. *Mol. Pharmacol.* ***1979,*** 16, 417-28.

Kahsai, A. W.; Xiao, K.; Rajagopal, S.; Ahn, S.; Shukla, A. K.; Sun, J.; Oas, T. G.; Lefkowitz, R. J. Multiple ligand-specific conformations of the beta2-adrenergic receptor. *Nat. Chem. Biol.* ***2011,*** 7, 692-700.

Kenakin, T. Functional selectivity through protean and biased agonism: who steers the ship? *Mol. Pharmacol.* ***2007,*** 72, 1393-401.

Kenakin, T. P. 2009. A pharmacology primer : theory, applications, and methods. Amsterdam ; Boston: Academic Press/Elsevier. xix, 389 p. p.

Kitbunnadaj, R.; Zuiderveld, O. P.; Christophe, B.; Hulscher, S.; Menge, W. M.; Gelens, E.; Snip, E.; Bakker, R. A.; Celanire, S.; Gillard, M. and others. Identification of 4-(1H-imidazol-4(5)-ylmethyl)pyridine (immethridine) as a novel, potent, and highly selective histamine H(3) receptor agonist. *J. Med. Chem.* ***2004,*** 47, 2414-7.

Klein, I.; Levey, G. S. Activation of myocardial adenyl cyclase by histamine in guinea pig, cat, and human heart. *J. Clin. Invest.* ***1971,*** 50, 1012-5.

Kobilka, B.; Schertler, G. F. New G-protein-coupled receptor crystal structures: insights and limitations. *Trends Pharmacol. Sci.* ***2008,*** 29, 79-83.

Kobilka, B. K.; Deupi, X. Conformational complexity of G-protein-coupled receptors. *Trends Pharmacol. Sci.* ***2007,*** 28, 397-406.

Kolakowski, L. F., Jr. GCRDb: a G-protein-coupled receptor database. *Recept. Channels* ***1994,*** 2, 1-7.

Kraus, A.; Ghorai, P.; Birnkammer, T.; Schnell, D.; Elz, S.; Seifert, R.; Dove, S.; Bernhardt, G.; Buschauer, A. N(G)-acylated aminothiazolylpropylguanidines as potent and selective histamine H(2) receptor agonists. *ChemMedChem* ***2009,*** 4, 232-40.

Krause, M.; Rouleau, A.; Stark, H.; Luger, P.; Lipp, R.; Garbarg, M.; Schwart, J. C.; Schunack, W. Synthesis, X-ray crystallography, and pharmacokinetics of novel

azomethine prodrugs of (R)-alpha-methylhistamine: highly potent and selective histamine H_3 receptor agonists. *J. Med. Chem.* ***1995,*** 38, 4070-9.

Kunishima, N.; Shimada, Y.; Tsuji, Y.; Sato, T.; Yamamoto, M.; Kumasaka, T.; Nakanishi, S.; Jingami, H.; Morikawa, K. Structural basis of glutamate recognition by a dimeric metabotropic glutamate receptor. *Nature* ***2000,*** 407, 971-7.

Lagerström, M. C.; Schiöth, H. B. Structural diversity of G protein-coupled receptors and significance for drug discovery. *Nat. Rev. Drug Discov.* ***2008,*** 7, 339-357.

Lee-Dutra, A.; Arienti, K. L.; Buzard, D. J.; Hack, M. D.; Khatuya, H.; Desai, P. J.; Nguyen, S.; Thurmond, R. L.; Karlsson, L.; Edwards, J. P. and others. Identification of 2-arylbenzimidazoles as potent human histamine H_4 receptor ligands. *Bioorg. Med. Chem. Lett.* ***2006,*** 16, 6043-6048.

Leff, P. The two-state model of receptor activation. *Trends Pharmacol. Sci.* ***1995,*** 16, 89-97.

Lefkowitz, R. J.; Mullikin, D.; Caron, M. G. Regulation of beta-adrenergic receptors by guanyl-5'-yl imidodiphosphate and other purine nucleotides. *J. Biol. Chem.* ***1976,*** 251, 4686-92.

Leschke, C.; Elz, S.; Garbarg, M.; Schunack, W. Synthesis and histamine H_1 receptor agonist activity of a series of 2-phenylhistamines, 2-heteroarylhistamines, and analogues. *J. Med. Chem.* ***1995,*** 38, 1287-94.

Leurs, R.; Bakker, R. A.; Timmerman, H.; de Esch, I. J. The histamine H_3 receptor: from gene cloning to H_3 receptor drugs. *Nat. Rev. Drug Discov.* ***2005,*** 4, 107-20.

Leurs, R.; Chazot, P. L.; Shenton, F. C.; Lim, H. D.; de Esch, I. J. Molecular and biochemical pharmacology of the histamine H_4 receptor. *Br. J. Pharmacol.* ***2009,*** 157, 14-23.

Leurs, R.; Vischer, H. F.; Wijtmans, M.; de Esch, I. J. En route to new blockbuster anti-histamines: surveying the offspring of the expanding histamine receptor family. *Trends Pharmacol. Sci.* ***2011,*** 32, 250-7.

Lewis, T.; Grant, R. T. Vascular reactions of the skin to injury. Part II. *Heart* ***1924,*** 11, 209-265.

Lim, H. D.; Smits, R. A.; Bakker, R. A.; van Dam, C. M.; de Esch, I. J.; Leurs, R. Discovery of S-(2-guanidylethyl)-isothiourea (VUF 8430) as a potent nonimidazole histamine H_4 receptor agonist. *J. Med. Chem.* ***2006,*** 49, 6650-1.

Lim, H. D.; van Rijn, R. M.; Ling, P.; Bakker, R. A.; Thurmond, R. L.; Leurs, R. Evaluation of histamine H_1-, H_2-, and H_3-receptor ligands at the human histamine H_4 receptor: identification of 4-methylhistamine as the first potent and selective H_4 receptor agonist. *J. Pharmacol. Exp. Ther.* ***2005,*** 314, 1310-21.

Liu, C.; Ma, X.; Jiang, X.; Wilson, S. J.; Hofstra, C. L.; Blevitt, J.; Pyati, J.; Li, X.; Chai, W.; Carruthers, N. and others. Cloning and pharmacological characterization of a fourth histamine receptor (H(4)) expressed in bone marrow. *Mol. Pharmacol.* ***2001,*** 59, 420-6.

Liu, J. J.; Horst, R.; Katritch, V.; Stevens, R. C.; Wuthrich, K. Biased signaling pathways in beta2-adrenergic receptor characterized by 19F-NMR. *Science* ***2012,*** 335, 1106-10.

Lovenberg, T. W.; Roland, B. L.; Wilson, S. J.; Jiang, X.; Pyati, J.; Huvar, A.; Jackson, M. R.; Erlander, M. G. Cloning and functional expression of the human histamine H_3 receptor. *Mol. Pharmacol.* ***1999,*** 55, 1101-7.

Luttrell, L. M. Reviews in molecular biology and biotechnology: transmembrane signaling by G protein-coupled receptors. *Mol. Biotechnol.* ***2008,*** 39, 239-64.

Luttrell, L. M.; Gesty-Palmer, D. Beyond desensitization: physiological relevance of arrestin-dependent signaling. *Pharmacol. Rev.* ***2010,*** 62, 305-30.

Maguire, M. E.; Van Arsdale, P. M.; Gilman, A. G. An agonist-specific effect of guanine nucleotides on binding to the beta adrenergic receptor. *Mol. Pharmacol.* ***1976,*** 12, 335-9.

Martinez-Mir, M. I.; Pollard, H.; Moreau, J.; Arrang, J. M.; Ruat, M.; Traiffort, E.; Schwartz, J. C.; Palacios, J. M. Three histamine receptors (H_1, H_2 and H_3) visualized in the brain of human and non-human primates. *Brain Res.* ***1990,*** 526, 322-7.

McLean, B. N. Intrathecal baclofen in severe spasticity. *Br. J. Hosp. Med.* ***1993,*** 49, 262-7.

Medina, V. A.; Rivera, E. S. Histamine receptors and cancer pharmacology. *Br. J. Pharmacol.* ***2010,*** 161, 755-67.

Menghin, S.; Pertz, H. H.; Kramer, K.; Seifert, R.; Schunack, W.; Elz, S. N(alpha)-imidazolylalkyl and pyridylalkyl derivatives of histaprodifen: synthesis and in vitro evaluation of highly potent histamine H(1)-receptor agonists. *J. Med. Chem.* ***2003,*** 46, 5458-70.

Miller, W. E.; Lefkowitz, R. J. Expanding roles for beta-arrestins as scaffolds and adapters in GPCR signaling and trafficking. *Curr. Opin. Cell Biol.* ***2001,*** 13, 139-45.

Mitsuhashi, M.; Mitsuhashi, T.; Payan, D. G. Multiple signaling pathways of histamine H_2 receptors. Identification of an H_2 receptor-dependent Ca2+ mobilization pathway in human HL-60 promyelocytic leukemia cells. *J. Biol. Chem.* ***1989,*** 264, 18356-62.

Morgan, R. K.; McAllister, B.; Cross, L.; Green, D. S.; Kornfeld, H.; Center, D. M.; Cruikshank, W. W. Histamine 4 receptor activation induces recruitment of FoxP3+ T cells and inhibits allergic asthma in a murine model. *J. Immunol.* ***2007,*** 178, 8081-9.

Morse, K. L.; Behan, J.; Laz, T. M.; West, R. E., Jr.; Greenfeder, S. A.; Anthes, J. C.; Umland, S.; Wan, Y.; Hipkin, R. W.; Gonsiorek, W. and others. Cloning and Characterization of a Novel Human Histamine Receptor. *J. Pharmacol. Exp. Ther.* ***2001,*** 296, 1058-1066.

Mowbray, C. E.; Bell, A. S.; Clarke, N. P.; Collins, M.; Jones, R. M.; Lane, C. A.; Liu, W. L.; Newman, S. D.; Paradowski, M.; Schenck, E. J. and others. Challenges of drug discovery in novel target space. The discovery and evaluation of PF-3893787: a novel histamine H_4 receptor antagonist. *Bioorg. Med. Chem. Lett.* ***2011,*** 21, 6596-602.

Nakamura, T.; Itadani, H.; Hidaka, Y.; Ohta, M.; Tanaka, K. Molecular cloning and characterization of a new human histamine receptor, HH_4R. *Biochem. Biophys. Res. Commun.* ***2000,*** 279, 615-20.

Neumann, D.; Beermann, S.; Magel, L.; Jonigk, D.; Weber-Steffens, D.; Mannel, D.; Seifert, R. Problems associated with the use of commercial and non-commercial antibodies against the histamine H-4 receptor. *Naunyn-Schmiedeberg's Arch. Pharmacol.* ***2012,*** 385, 855-860.

Nguyen, T.; Shapiro, D. A.; George, S. R.; Setola, V.; Lee, D. K.; Cheng, R.; Rauser, L.; Lee, S. P.; Lynch, K. R.; Roth, B. L. and others. Discovery of a Novel Member of the Histamine Receptor Family. *Mol. Pharmacol.* ***2001,*** 59, 427-433.

Nijmeijer, S.; Vischer, H. F.; Rosethorne, E. M.; Charlton, S. J.; Leurs, R. Analysis of Multiple Histamine H_4 Receptor Compound Classes Uncovers Galphai and beta-Arrestin2 Biased Ligands. *Mol. Pharmacol.* ***2012***.

Oda, T.; Morikawa, N.; Saito, Y.; Masuho, Y.; Matsumoto, S. Molecular cloning and characterization of a novel type of histamine receptor preferentially expressed in leukocytes. *J. Biol. Chem.* ***2000,*** 275, 36781-6.

Overington, J. P.; Al-Lazikani, B.; Hopkins, A. L. How many drug targets are there? *Nat. Rev. Drug Discov.* ***2006,*** 5, 993-6.

Palczewski, K.; Kumasaka, T.; Hori, T.; Behnke, C. A.; Motoshima, H.; Fox, B. A.; Le Trong, I.; Teller, D. C.; Okada, T.; Stenkamp, R. E. and others. Crystal structure of rhodopsin: A G protein-coupled receptor. *Science* ***2000,*** 289, 739-45.

Park, J. H.; Scheerer, P.; Hofmann, K. P.; Choe, H. W.; Ernst, O. P. Crystal structure of the ligand-free G-protein-coupled receptor opsin. *Nature* ***2008,*** 454, 183-7.

Parsons, M. E.; Ganellin, C. R. Histamine and its receptors. *Br. J. Pharmacol.* ***2006,*** 147 Suppl 1, S127-35.

Pavan, B.; Biondi, C.; Dalpiaz, A. Adenylyl cyclases as innovative therapeutic goals. *Drug Discov. Today* ***2009,*** 14, 982-91.

Perry, S. J.; Lefkowitz, R. J. Arresting developments in heptahelical receptor signaling and regulation. *Trends Cell Biol.* ***2002,*** 12, 130-8.

Popielski, L. β-Imidazolyläthylamin und die Organextrakte 1. Teil: β-Imidazolyläthylamin als mächtiger Erreger der Magendrüsen. *Pfluegers Arch./Eur. J. Physiol.* ***1920,*** 178, 214-236.

Prinz, C.; Zanner, R.; Gratzl, M. Physiology of gastric enterochromaffin-like cells. *Annu. Rev. Physiol.* ***2003,*** 65, 371-82.

Rahmeh, R.; Damian, M.; Cottet, M.; Orcel, H.; Mendre, C.; Durroux, T.; Sharma, K. S.; Durand, G.; Pucci, B.; Trinquet, E. and others. Structural insights into biased G protein-coupled receptor signaling revealed by fluorescence spectroscopy. *Proc. Natl. Acad. Sci. U. S. A.* ***2012,*** 109, 6733-8.

Raible, D. G.; Lenahan, T.; Fayvilevich, Y.; Kosinski, R.; Schulman, E. S. Pharmacologic characterization of a novel histamine receptor on human eosinophils. *Am. J. Respir. Crit. Care Med.* ***1994,*** 149, 1506-11.

Rajagopal, S.; Rajagopal, K.; Lefkowitz, R. J. Teaching old receptors new tricks: biasing seven-transmembrane receptors. *Nat. Rev. Drug Discov.* ***2010,*** 9, 373-86.

Rasmussen, S. G.; Choi, H. J.; Fung, J. J.; Pardon, E.; Casarosa, P.; Chae, P. S.; Devree, B. T.; Rosenbaum, D. M.; Thian, F. S.; Kobilka, T. S. and others. Structure of a nanobody-stabilized active state of the beta(2) adrenoceptor. *Nature* ***2011a,*** 469, 175-80.

Rasmussen, S. G.; Choi, H. J.; Rosenbaum, D. M.; Kobilka, T. S.; Thian, F. S.; Edwards, P. C.; Burghammer, M.; Ratnala, V. R.; Sanishvili, R.; Fischetti, R. F. and others. Crystal

structure of the human beta2 adrenergic G-protein-coupled receptor. *Nature* ***2007,*** 450, 383-7.

Rasmussen, S. G.; DeVree, B. T.; Zou, Y.; Kruse, A. C.; Chung, K. Y.; Kobilka, T. S.; Thian, F. S.; Chae, P. S.; Pardon, E.; Calinski, D. and others. Crystal structure of the beta2 adrenergic receptor-Gs protein complex. *Nature* ***2011b,*** 477, 549-55.

Riley, J. F.; West, G. B. Histamine in tissue mast cells. *J. Physiol.* ***1952,*** 117, 72P-73P.

Ritter, S. L.; Hall, R. A. Fine-tuning of GPCR activity by receptor-interacting proteins. *Nat. Rev. Mol. Cell Biol.* ***2009,*** 10, 819-30.

Rodbell, M.; Birnbaumer, L.; Pohl, S. L.; Krans, H. M. The glucagon-sensitive adenyl cyclase system in plasma membranes of rat liver. V. An obligatory role of guanylnucleotides in glucagon action. *J. Biol. Chem.* ***1971,*** 246, 1877-82.

Rosenbaum, D. M.; Rasmussen, S. G.; Kobilka, B. K. The structure and function of G-protein-coupled receptors. *Nature* ***2009,*** 459, 356-63.

Rosethorne, E. M.; Charlton, S. J. Agonist-biased signaling at the histamine H_4 receptor: JNJ7777120 recruits beta-arrestin without activating G proteins. *Mol. Pharmacol.* ***2011,*** 79, 749-57.

Ross, E. M.; Gilman, A. G. Resolution of some components of adenylate cyclase necessary for catalytic activity. *J. Biol. Chem.* ***1977,*** 252, 6966-9.

Rossbach, K.; Stark, H.; Sander, K.; Leurs, R.; Kietzmann, M.; Baumer, W. The histamine H receptor as a new target for treatment of canine inflammatory skin diseases. *Vet. Dermatol.* ***2009a,*** 20, 555-61.

Rossbach, K.; Wendorff, S.; Sander, K.; Stark, H.; Gutzmer, R.; Werfel, T.; Kietzmann, M.; Baumer, W. Histamine H_4 receptor antagonism reduces hapten-induced scratching behaviour but not inflammation. *Exp. Dermatol.* ***2009b,*** 18, 57-63.

Rouleau, A.; Garbarg, M.; Ligneau, X.; Mantion, C.; Lavie, P.; Advenier, C.; Lecomte, J. M.; Krause, M.; Stark, H.; Schunack, W. and others. Bioavailability, antinociceptive and antiinflammatory properties of BP 2-94, a histamine H_3 receptor agonist prodrug. *J. Pharmacol. Exp. Ther.* ***1997,*** 281, 1085-94.

Salon, J. A.; Lodowski, D. T.; Palczewski, K. The significance of G protein-coupled receptor crystallography for drug discovery. *Pharmacol. Rev.* ***2011,*** 63, 901-37.

Samama, P.; Cotecchia, S.; Costa, T.; Lefkowitz, R. J. A mutation-induced activated state of the beta 2-adrenergic receptor. Extending the ternary complex model. *J. Biol. Chem.* ***1993,*** 268, 4625-36.

Sander, K.; Kottke, T.; Stark, H. Histamine H_3 receptor antagonists go to clinics. *Biol. Pharm. Bull.* ***2008,*** 31, 2163-81.

Scheerer, P.; Park, J. H.; Hildebrand, P. W.; Kim, Y. J.; Krauss, N.; Choe, H. W.; Hofmann, K. P.; Ernst, O. P. Crystal structure of opsin in its G-protein-interacting conformation. *Nature* ***2008,*** 455, 497-502.

Schnell, D.; Brunskole, I.; Ladova, K.; Schneider, E. H.; Igel, P.; Dove, S.; Buschauer, A.; Seifert, R. Expression and functional properties of canine, rat, and murine histamine H(4) receptors in Sf9 insect cells. *Naunyn-Schmiedeberg's Arch. Pharmacol.* ***2011,*** 383, 457-70.

Schwartz, J. C. The histamine H_3 receptor: from discovery to clinical trials with pitolisant. *Br. J. Pharmacol.* ***2011,*** 163, 713-21.

Seifert, R.; Schneider, E. H.; Dove, S.; Brunskole, I.; Neumann, D.; Strasser, A.; Buschauer, A. Paradoxical stimulatory effects of the "standard" histamine H_4-receptor antagonist JNJ7777120: The H_4-receptor joins the club of 7TM receptors exhibiting functional selectivity. *Mol. Pharmacol.* ***2011***.

Seifert, R.; Strasser, A.; Schneider, E. H.; Neumann, D.; Dove, S.; Buschauer, A. Molecular and cellular analysis of human histamine receptor subtypes. *Trends Pharmacol. Sci.* ***2013,*** 34, 33-58.

Sharman, J. L.; Benson, H. E.; Pawson, A. J.; Lukito, V.; Mpamhanga, C. P.; Bombail, V.; Davenport, A. P.; Peters, J. A.; Spedding, M.; Harmar, A. J. IUPHAR-DB: updated database content and new features. *Nucleic Acids Res.* ***2013,*** 41, D1083-8.

Smits, R. A.; Esch, I. J. P. d.; Zuiderveld, O. P.; Broeker, J.; Sansuk, K.; Guaita, E.; Coruzzi, G.; Adami, M.; Haaksma, E.; Leurs, R. Discovery of Quinazolines as Histamine H_4 Receptor Inverse Agonists Using a Scaffold Hopping Approach. *J. Med. Chem.* ***2008,*** 51, 7855-7865.

Stevens, R. C.; Cherezov, V.; Katritch, V.; Abagyan, R.; Kuhn, P.; Rosen, H.; Wuthrich, K. The GPCR Network: a large-scale collaboration to determine human GPCR structure and function. *Nature reviews. Drug discovery* ***2013,*** 12, 25-34.

Strasser, A.; Wittmann, H. J.; Buschauer, A.; Schneider, E. H.; Seifert, R. Species-dependent activities of G-protein-coupled receptor ligands: lessons from histamine receptor orthologs. *Trends Pharmacol. Sci.* ***2013,*** 34, 13-32.

Swaminath, G.; Xiang, Y.; Lee, T. W.; Steenhuis, J.; Parnot, C.; Kobilka, B. K. Sequential binding of agonists to the beta2 adrenoceptor. Kinetic evidence for intermediate conformational states. *J. Biol. Chem.* ***2004,*** 279, 686-91.

Thurmond, R. L.; Desai, P. J.; Dunford, P. J.; Fung-Leung, W. P.; Hofstra, C. L.; Jiang, W.; Nguyen, S.; Riley, J. P.; Sun, S.; Williams, K. N. and others. A potent and selective histamine H_4 receptor antagonist with anti-inflammatory properties. *J. Pharmacol. Exp. Ther.* ***2004,*** 309, 404-13.

Thurmond, R. L.; Gelfand, E. W.; Dunford, P. J. The role of histamine H_1 and H_4 receptors in allergic inflammation: the search for new antihistamines. *Nat. Rev. Drug Discov.* ***2008,*** 7, 41-53.

Timmerman, H. Routes to Histamine H_2-Agonists. *Quant. Struct.-Act. Relat.* ***1992,*** 11, 219-223.

Ungar, G.; Parrot, J. L.; Bovet, D. Inhibition of the effects of histamine on isolated guinea-pig intestine by various sympathicomimetic and sympathicolytic substances. *C. R. Seances Soc. Biol. Ses Fil.* ***1937,*** 124, 445-6.

van der Goot, H.; Schepers, M. J. P.; Sterk, G. J.; Timmerman, H. Isothiourea analogues of histamine as potent agonists or antagonists of the histamine H_3-receptor. *Eur. J. Med. Chem.* ***1992,*** 27, 511-517.

vanRijn, R. M.; vanMarle, A.; Chazot, P. L.; Langemeijer, E.; Qin, Y.; Shenton, F. C.; Lim, H. D.; Zuiderveld, O. P.; Sansuk, K.; Dy, M. and others. Cloning and characterization of dominant negative splice variants of the human histamine H_4 receptor. *Biochem. J.* ***2008,*** 414, 121-131.

Venkatakrishnan, A. J.; Deupi, X.; Lebon, G.; Tate, C. G.; Schertler, G. F.; Babu, M. M. Molecular signatures of G-protein-coupled receptors. *Nature* ***2013,*** 494, 185-94.

Walter, M.; Kottke, T.; Stark, H. The histamine H(4) receptor: targeting inflammatory disorders. *Eur. J. Pharmacol.* ***2011,*** 668, 1-5.

Wang, L.; Gantz, I.; DelValle, J. Histamine H_2 receptor activates adenylate cyclase and PLC via separate GTP-dependent pathways. *Am. J. Physiol.* ***1996,*** 271, G613-20.

Warne, T.; Serrano-Vega, M. J.; Baker, J. G.; Moukhametzianov, R.; Edwards, P. C.; Henderson, R.; Leslie, A. G.; Tate, C. G.; Schertler, G. F. Structure of a beta1-adrenergic G-protein-coupled receptor. *Nature* ***2008,*** 454, 486-91.

Weiss, J. M.; Morgan, P. H.; Lutz, M. W.; Kenakin, T. P. The cubic ternary complex receptor-occupancy model. III. resurrecting efficacy. *J. Theor. Biol.* ***1996,*** 181, 381-97.

Wifling, D. 2012. Personal communication. University of Regensburg, Regensburg, Germany.

Wijtmans, M.; Leurs, R.; de Esch, I. Histamine H_3 receptor ligands break ground in a remarkable plethora of therapeutic areas. *Expert. Opin. Investig. Drugs* ***2007,*** 16, 967-85.

Yu, F.; Wolin, R. L.; Wei, J.; Desai, P. J.; McGovern, P. M.; Dunford, P. J.; Karlsson, L.; Thurmond, R. L. Pharmacological characterization of oxime agonists of the histamine H_4 receptor. *J. Receptor Ligand Channel Res.* ***2010,*** 3, 37-49.

Zampeli, E.; Thurmond, R. L.; Tiligada, E. The histamine H_4 receptor antagonist JNJ7777120 induces increases in the histamine content of the rat conjunctiva. *Inflammation Res.* ***2009,*** 58, 285-91.

Zampeli, E.; Tiligada, E. The role of histamine H_4 receptor in immune and inflammatory disorders. *Br. J. Pharmacol.* ***2009,*** 157, 24-33.

Zhu, Y.; Michalovich, D.; Wu, H.-L.; Tan, K. B.; Dytko, G. M.; Mannan, I. J.; Boyce, R.; Alston, J.; Tierney, L. A.; Li, X. and others. Cloning, Expression, and Pharmacological Characterization of a Novel Human Histamine Receptor. *Mol. Pharmacol.* ***2001,*** 59, 434-441.

Zurn, A.; Zabel, U.; Vilardaga, J. P.; Schindelin, H.; Lohse, M. J.; Hoffmann, C. Fluorescence resonance energy transfer analysis of alpha 2a-adrenergic receptor activation reveals distinct agonist-specific conformational changes. *Mol. Pharmacol.* ***2009,*** 75, 534-41.

Chapter 2

Scope and objectives

The discovery of histamine H_3 and H_4 receptors has stimulated the evaluation of these GPCRs as potential drug targets for the treatment of a variety of diseases. This includes the identification and characterization of new compounds in terms of affinity, potency, quality of action (agonism or antagonism) and receptor subtype selectivity, preferably by simple, fast and robust binding and functional assays. Since translational animal models are indispensable for the investigations on the (patho)physiological role of the respective receptor of interest and for preclinical studies of potential clinical candidates, additionally, there is a great need for *in vitro* models to identify pharmacological differences between H_3 and H_4 receptor species orthologs at an early stage of drug discovery and development.

This thesis aims at the development of binding and functional assays for the hH_4R, mH_4R, rH_4R, hH_3R and rH_3R. It is planned to establish radioligand binding assays using whole HEK293T cells for the determination of ligand affinities. Therefore, HEK293T cells are to be genetically engineered by the respective receptor cDNA to achieve stable expression of the receptor proteins.

For the development of functional assays, the receptor expressing cells will be stably co-transfected with a luciferase reporter gene, the transcription of which is under control of a cAMP responsive element (CRE). This ought to enable the quantification of the inhibitory effect on forskolin-stimulated adenylyl cyclase in response to H_3R and H_4R activation, since both receptors are coupling to $G\alpha_{i/o}$ proteins. The resulting luminescence signal should be detected by a luminescence plate reader, making the assay amenable to the 96-well format.

Furthermore, HEK293T cells which only express the CRE-directed luciferase reporter gene will be established. These engineered cells will enable the identification of ligand-induced off-target effects in control experiments and the use as “cellular building blocks” for the co-transfection with further H_3R and H_4R species orthologs.

For validation of the assays, a large panel of known H_3R and H_4R ligands including agonists, inverse agonists and antagonist will be investigated at optimized assay conditions and compared with data reported in literature.

Chapter 3

Development of radioligand binding assays for human and mouse histamine H_4 receptors

3.1 Radioligand binding assay for the human histamine H_4 receptor

3.1.1 Introduction

Since the cloning of the fourth histamine receptor (H_4R) one decade ago by several research groups (Liu *et al.*, 2001a; Morse *et al.*, 2001; Nguyen *et al.*, 2001; Oda *et al.*, 2000; Zhu *et al.*, 2001), various binding assays were established using [^{3}H]histamine and disrupted cellular preparations such as cell membranes or homogenates of hH_4R expressing SK-NMC cells (Kitbunnadaj *et al.*, 2004; Lim *et al.*, 2005; Liu *et al.*, 2001a), HEK293 cells (Morse *et al.*, 2001; Nguyen *et al.*, 2001) or Sf9 insect cells (Schneider and Seifert, 2009; Schnell *et al.*, 2011).

The present work focused on radioligand binding assays using whole HEK293T cells, which were stably transfected with the hH_4R (HEK293-SF-hH_4R-His_6). By performing receptor binding assays with intact cells, the receptor can be examined in a native environment, which is the most obvious advantage. So, for example, the gradients of pH or other ions that normally exist across the membrane remain intact as well as receptor associated components such as G-proteins, nucleotides and other modulators persist in their natural cytosolic environment (Bylund and Toews, 1993). Additionally, a whole cell binding assay allows a more direct comparison of binding properties with functional cell-based data (Bylund and Toews, 1993). What may be detrimental in the use of whole cells is the difficulty to control the assay conditions on the cytosolic side. The influence of the pH value, ion or especially GTP concentrations on the binding property cannot be investigated (Bylund and Toews, 1993). The HEK293T cell line is a widely used expression system for recombinant proteins. Furthermore, HEK293T cells are particular suitable for the expression of histamine receptors due to the lack of endogenous histamine receptor proteins (Mosandl, 2009).
As radioactive tracer, the recently described high affinity histamine H_3 and H_4 receptor radioligand [^{3}H]UR-PI294 (Igel *et al.*, 2009c) was selected. Compared to the standard H_4R radioligand [^{3}H]histamine, [^{3}H]UR-PI294 exhibits a high specific activity (78.5 Ci/mmol), which is required for an adequate signal, in particular, when the receptor density is low. However, it must be considered that the binding of [^{3}H]UR-PI294, which acts, like [^{3}H]histamine, as an agonist at the hH_4R, could be influenced by G-protein coupling (Kenakin, 2009; Lazareno, 2001), preference of only a portion of the receptor population (the high affinity state for GPCRs) (Bylund and Toews, 1993) or internalization.
In conventional radiochemical assays, separation of bound from free radioligand is required. Standard procedures for this purpose in the case of whole cells are filtration and, less commonly, centrifugation. Compared to centrifugation, the filtration method, which was used

in this study, is of advantage due to faster and more efficient separation und thus lower nonspecific binding. However, the filtration is not suitable for low-affinity, rapidly dissociating radioligands with a dissociation constant (K_D-value) > 10^{-8} M (Lazareno, 2001), since in the required washing step specifically bound radioligand could be flushed away.

For the purpose of validation, a set of imidazoles and non-imidazoles, comprising agonists, inverse agonists and antagonists, was investigated in competition binding assays using HEK293-SF-hH_4R-His_6 cells. The tested substances included several compounds which were originally designed as H_3R ligands and identified as H_4R ligands after the discovery of the fourth histamine receptor. Affinity to both receptor subtypes is not surprising due to the high sequence homology of the H_4R with the H_3R (cf. section 1.2.2).

3.1.2 Materials and Methods

3.1.2.1 Cell culture

HEK293T cells (DSMZ, Braunschweig, Germany) were cultured in Dulbecco's Modified Eagle Medium (DMEM) (Sigma, Munich, Germany) containing L-glutamine, 4500 mg/L glucose, 3.7 g/L $NaHCO_3$ (Merck, Darmstadt, Germany), 110 mg/L sodium pyruvate (Serva, Heidelberg, Germany) and 10 % fetal calf serum (FCS) (Biochrom, Berlin, Germany). The HEK293T cells, stably expressing the FLAG epitope (F)- hexahistidine (His_6)-tagged human H_4 receptor (HEK293-SF-hH_4R-His_6; S stands for the cleavable signal peptide from influenza hemagglutinin), were kindly provided by Dr. David Schnell (Department of Pharmacology and Toxicology, University of Regensburg, Germany) and cultured in the above-mentioned medium with the addition of 600 µg/mL Geneticin (G418) (Biochrom). Cells were maintained at 37 °C and 5 % CO_2 in water saturated atmosphere in 75-cm^2 culture flasks (Sarstedt, Nümbrecht, Germany) and diluted twice a week 1:10 with fresh medium after 0.05 % trypsin / 0.02 % EDTA treatment. The tenfold concentrate of trypsin / EDTA (PAA, Pasching, Austria) was diluted with phosphate buffered saline (PBS) (KCL 2.7 mM; KH_2PO_4 1.5 mM; NaCL 137 mM; Na_2HPO_4 5.6 mM; NaH_2PO_4 1.1 mM in Millipore water, pH 7.4; all chemicals were from Merck, Darmstadt, Germany) and sterile filtered before use.

3.1.2.2 Chemosensitivity assay

In order to determine the sensitivity of HEK293T cells to G418, a chemosensitivity assay was performed as described previously (Bernhardt *et al.*, 1992). Cells were seeded into flat-bottomed 96-well plates (Greiner, Frickenhausen, Germany) at a density of 10 – 15 cells per microscope-field (320-fold magnification). After 48 h of incubation the medium was replaced by fresh medium containing various concentrations of G418. Wells without G418 served as control. At various time points the growth was stopped by fixation with glutardialdehyde (Merck). Subsequently, the cells were covered with PBS and the plates were stored at 4 °C. After simultaneous staining of the plates with an aqueous 0.02 % crystal violet solution (Serva), the excess of dye was removed by rinsing the plates three times with water. The amount of cell-bound crystal violet was determined by the addition of 70 % ethanol to the dried plates, followed by shaking for 2 -3 h and measurement of the absorbance at 580 nm using a GENios Pro™ microplate reader (Tecan, Salzburg, Austria).

The effect of G418 on HEK293T cells were expressed as corrected T/C values according to

$$\frac{T}{C}corr(\%) = \frac{T-C_0}{C-C_0} \cdot 100 \qquad \text{(equation 1),}$$

where T is the mean absorbance of the treated cells, C the mean absorbance of the controls and C_0 the mean absorbance at the time when G418 was added (t = 0).
If the absorbance of treated cells was less than the absorbance at t = 0 (cytocidal drug effect), the extend of killed cells was calculated as

$$cytocidal\ effect\ (\%) = \frac{T-C_0}{C_0} \cdot 100 \qquad \text{(equation 2).}$$

3.1.2.3 H_4 receptor ligands

For the validation of the binding assay, a set of imidazole-containing and non-imidazole reference ligands were used. Histamine (HA) (**1**) was purchased from Alfa Aesar (Karlsruhe, Germany). (R)-α-Methylhistamine (RAMH) (**2**), (S)-α-methylhistamine (SAMH) (**3**), N^{α}-methyl-histamine (NAMH) (**4**), 5(4)-methylhistamine (5(4)MH) (**5**), immepip (IMMEP) (**6**), VUF 5681 (**7**), immethridine (IMMET) (**8**), imetit (IME) (**9**), clobenpropit (CLOB) (**10**), iodophenpropit (IODO) (**11**), proxyfan (PRO) (**13**), ciproxifan (CIP) (**14**), clozapine (CLOZ) (**18**) and conessine (CON) (**22**) were from Tocris Bioscience (Ellisville, USA). Thioperamide (THIO) (**12**), UR-PI294 (**15**), UR-PI376 (**16**), trans-(+)-(1S,3S)-UR-RG98 (**17**), JNJ 7777120 (**19**), VUF 8430 (**20**) and JNJ 5207852 (**21**) were synthesized in our laboratory. Chemical structures of ligands are depicted in **Figure 3.1**. Except for **16**, **17** and **18** all stock solutions (10 mM) were prepared in Millipore water. Stock solution of **18** was made in 20 mM HCl. Stock solutions of **17** and **18** were prepared in 50 % DMSO. The dilution series of the water dissolved ligands and **18** were prepared in Millipore water. The dilution series of **16** and **17** were made in 10 % DMSO.

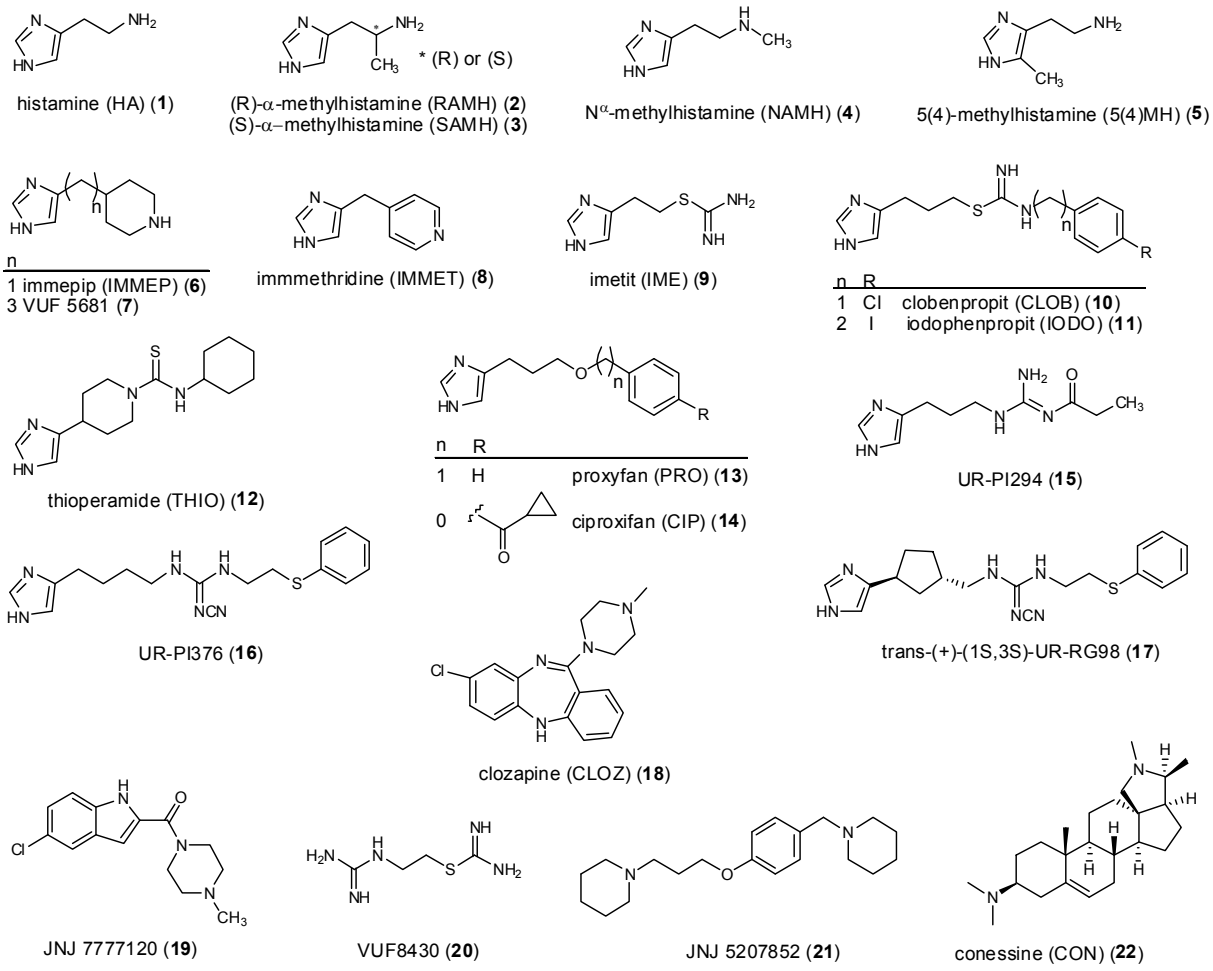

Figure 3.1: Structures of the examined ligands.

3.1.2.4 Whole cell radioligand binding assay

With some modifications, the radioligand binding assay was performed as described previously (Mosandl, 2009). HEK293-SF-hH_4R-His_6 cells were seeded into 175-cm^2 culture flasks until they reached 80 – 100 % confluency. After trypsinization, the cells were detached with Leibovitz's L-15 medium without phenol red (Invitrogen, Karlsruhe, Germany) including 1 % FCS and centrifuged for 10 min at 300 g. The supernatant was discarded and the cells were re-suspended in the aforementioned medium. After counting the cells in a hemocytometer, the cell density was adjusted to 2-3·10^6 cells/mL.

As radioactive tracer [^{3}H]UR-PI294 was used, which was synthesized in our laboratory (see **Figure 3.2**) (Igel *et al.*, 2009c). For saturation binding experiments 160 µL of the aforementioned cell suspension was added into each cavity of a flat-bottomed 96-well plate (Greiner). To the wells, which were intended for the determination of specific binding, 20 µL of Millipore water were added, whereas 20 µL of an aqueous solution containing 100 µM of thioperamide (**12**) was added to the wells for the determination of non-specific binding. Samples were completed by addition of 20 µL of the respective [^{3}H]UR-PI294 solution. All

added solutions were tenfold concentrated compared to the final concentration. Samples were incubated under light protection and slight shaking for 90 min prior to harvesting. Cell-bound radioactivity was separated from free radioactivity by filtration through a GF/C (Skatron Instruments, Sterling, USA) glass fiber filter pretreated with 0.3 % (v/v) polyethyleneimine (Sigma) solution and washed once with PBS (4 °C) using a Combi Cell Harvester 11025 (Skatron). Filter discs (with adhering cells) were punched out and transferred into 6 mL mini-vials (Sarstedt). Every vial was filled with 3 mL Rotiszint® eco plus (Carl Roth, Karlsruhe, Germany), shaken and incubated overnight. On the next day, radioactivity was determined by liquid scintillation counting using a LS 6500 Liquid Scintillation Counter (Beckman Coulter, Krefeld, Germany). Dpm (decays per minute) values of total and non-specific binding were processed with GraphPad Prism® 5.04 (GraphPad Software, San Diego (CA), USA). Specific binding was calculated by subtraction of non-specific binding from the respective values for total binding. Values for total, non-specific and specific binding were plotted against the concentration of [^{3}H]UR-PI294 and analyzed by nonlinear regression (GraphPad Prism®). The K_D value (molar concentration of a radioligand required to occupy 50 % of the receptor population) of [^{3}H]UR-PI294 is presented as the mean value ± SEM (standard error of the mean) of three independent experiments performed in triplicate.

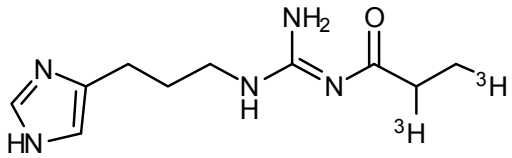

[^{3}H]UR-PI294

Figure 3.2: Structure of the radioligand [^{3}H]UR-PI294.

For competition binding assays, either 20 µL of a tenfold concentrated feed solution of the ligand of interest or 20 µL of the solvent (total binding) and 20 µL of a 50 nM [^{3}H]UR-PI294 solution were added to 160 µL of cell suspension. The following procedure was identical to that of the saturation binding experiments. Dpm values were converted to percentage values at which the total binding was set at 100 % and non-specific binding at 0 %. The percentage values were analyzed by nonlinear regression and best fitted to sigmoidal curve (GraphPad Prism®).

IC_{50} values (molar concentration required to inhibit the radioligand binding by half) were converted to K_i values according to the Cheng-Prusoff equation

$$K_i = \frac{IC_{50} \cdot K_D}{(K_D + [L])}$$ (equation 3),

where [L] represents the concentration of [^{3}H]UR-PI294 used in the competition binding assay (Cheng and Prusoff, 1973). Ligand binding affinity is presented as mean pK_i (negative decadic logarithm of the K_i value) value ± SEM from at least three independent experiments performed in duplicate.

3.1.3 Results and discussion

3.1.3.1 Effect of Geneticin (G418) on HEK293T cells

HEK293T cells have been extensively used as an expression tool for various recombinant proteins such as GPCRs. In literature the concentration of the antibiotic G418 used for the selection of transfected HEK293 cells range from 200 µg/mL (Lamb *et al.*, 2001) to 1000 µg/mL (Shyu *et al.*, 1999). To ensure that the concentration of G418 is sufficient for selection, the sensitivity of HEK293T wild type cells was determined in a crystal violet chemosensitivity assay (see **Figure 3.3**). G418 exhibited a cytotoxic effect, i.e. the cells recovered after a first initial damage, at the two lowest concentrations 50 µg/mL and 100 µg/mL. The effect at concentrations between 300 µg/mL and 1000 µg/mL was cytocidal and almost identical. The cells died after an incubation period of three days at these concentrations. Therefore, a concentration of 600 µg/mL was chosen to maintain the selection pressure during the cultivation of transfected HEK293T cells.

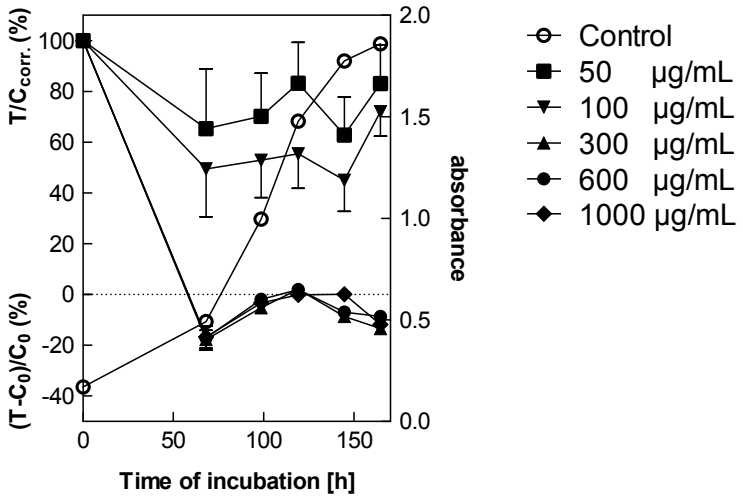

Figure 3.3: Effect of G418 on proliferating HEK293T cells. Crystal violet assay (mean values ± SD (n=16)).

3.1.3.2 Saturation binding assay

The radioligand [^{3}H]UR-PI294 bound specifically and in a saturable manner to HEK293-SF-hH_4R-His_6 cells. The non-specific binding, determined in the presence of thioperamide (**12**) (10 µM), was low (see **Figure 3.4** A). The determined K_D value of 7.5 ± 1.8 nM was in good agreement with data obtained in binding experiments using a membrane preparation of Sf9 insect cells expressing the hH_4R (Igel *et al.*, 2009c). The corresponding Scatchard plot

analysis of the specific binding isotherm showed a linear correlation within the investigated concentration range indicating that the radioligand binds to a single binding site (see **Figure 3.4** B).

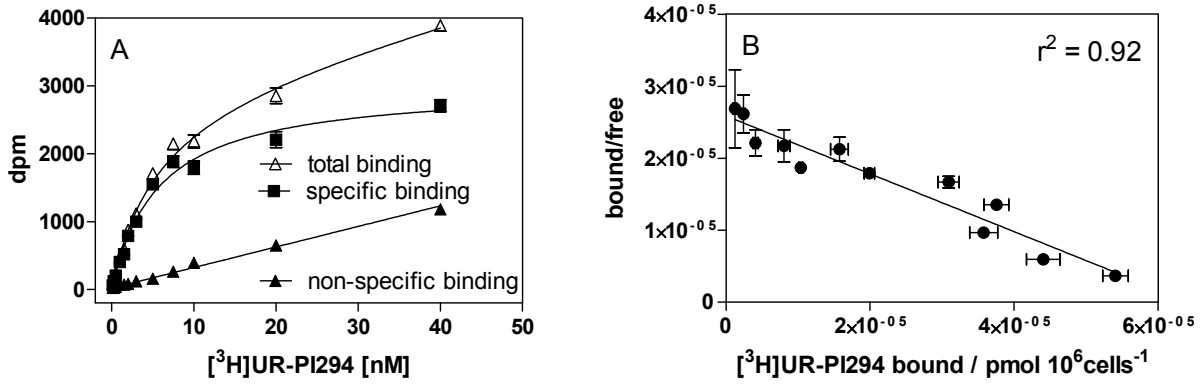

Figure 3.4: Representative [^{3}H]UR-PI294 saturation binding experiment, performed in triplicate, using HEK293-SF-hH_4R-His_6 cells. Non-specific binding was determined in the presence of 10 µM of thioperamide. Saturation binding curve, best fitted by nonlinear regression to a one-site model (A). Corresponding Scatchard plot of saturation binding data, best fitted by linear regression (B).

3.1.3.3 Competition binding assay

In competition binding experiments a set of imidazole containing and non-imidazole H_4R ligands were investigated for their ability to inhibit specific binding of 5 nM [^{3}H]UR-PI294 in HEK293-SF-hH_4R-His_6 cells. The obtained pK_i values were compared with affinities reported from competition binding experiment using [^{3}H]histamine or [^{3}H]UR-PI294 and either membrane preparations or cell homogenates of hH_4R expressing cells. The results are summarized in **Table 3.1** and compared with data from literature.

Histamine (**1**) and its methylated analogs (R)-α-methylhistamine (**2**), (S)-α-methylhistamine (**3**), N^{α}-methylhistamine (**4**) and 5(4)-methylhistamine (**5**) displaced [^{3}H]UR-PI294 on HEK293-SF-hH_4R-His_6 cells in a concentration-dependent manner (see **Figure 3.5**). The introduction of a methyl group led to a decreased affinity at the hH_4R, since histamine (**1**) (pK_i value 7.22 ± 0.04) achieved a higher affinity than its analogs. Although the pK_i values of **1**-**5** were lower than described in literature, the rank order was identical to the reported order (**1** > **5** > **4** > **2** > **3**) (see **Figure 3.8**), and the recently reported stereoselectivity of the hH_4R for (R)-α-methylhistamine (**2**) (pK_i = 5.75 ± 0.07) over (S)-α-methylhistamine (**3**) (pK_i = 4.92 ± 0.15) could be confirmed (Lim *et al.*, 2005).

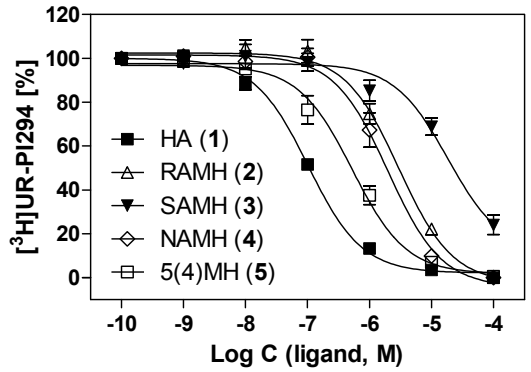

Figure 3.5: Displacement of [^{3}H]UR-PI294 by HA (**1**), RAMH (**2**), SAMH (**3**), NAMH (**4**) and 5(4)MH (**5**) on HEK293-SF-hH_4R-His_6 cells. Reaction mixtures contained 5 nM [^{3}H]UR-PI294 and ligand concentrations indicated on the abscissa. Data were analyzed by nonlinear regression and best fittet to one-site (monophasic) competition curves. Data points are the mean of at least four independent experiments performed in duplicate.

Immepip (**6**) and its pyridine analog immethridine (**8**) inhibited specific binding of [^{3}H]UR-PI294 with acceptable pK_i values of 7.32 ± 0.11 and 6.90 ± 0.07, respectively (see **Figure 3.6**). Interestingly, the extension of the spacer length by two carbon atoms between the imidazole and the piperidine ring in immepip (**6**), led to a significantly reduced affinity at the hH_4R as shown by VUF 5681 (**7**) (see **Figure 3.6**). Lower affinity of VUF 5681 (**7**) compared to immepip (**6**) was determined at the hH_3R as recently reported (Kitbunnadaj *et al.*, 2005). While the affinity of immepip (**6**) was marginally lower than reported, the affinities of its analogs VUF 5681 (**7**) and immethridine (**8**) were in good correlation with reported data.

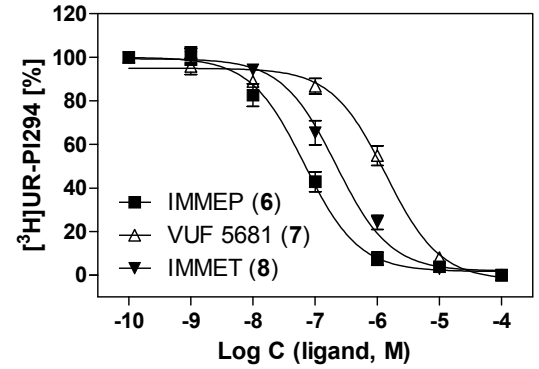

Figure 3.6: Inhibition of [^{3}H]UR-PI294 binding by IMMEP (**6**), VUF 5681 (**7**) and IMMET (**8**) on HEK293-SF-hH_4R-His_6 cells. Reaction mixtures contained 5 nM [^{3}H]UR-PI294 and ligand concentrations indicated on the abscissa. Data were analyzed by nonlinear regression and best fittet to one-site (monophasic) competition curves. Data points are the mean of at least three independent experiments performed in duplicate.

Imetit (**9**), the isothiourea analog of histamine (**1**), displayed a pK_i value of 7.57 ± 0.12 at the hH_4R. Clobenpropit (**10**) and iodophenpropit (**11**), which have an increased spacer length and a large lipophilic moiety in the side chain compared to imetit (**9**), exhibited considerable, but slightly lower affinities than imetit (**9**) at the hH_4R. Although the pK_i values were lower than described in literature, again, the rank order was in agreement with the reported order (**9** > **10** > **11**) (see **Figure 3.8**). The pK_i value of the $H_3/_4$R inverse agonist thioperamide (**12**) (pK_i = 6.68 ± 0.13) was in accordance to binding data described in literature. Further investigated ligands were proxyfan (**13**) and ciproxifan (**14**). The affinity of proxyfan (**13**) was only moderate and clearly lower than determined in competition binding assays using [^{3}H]histamine on SK-N-MC/hH_4R cell homogenates (see **Table 3.1** and (Lim *et al.*, 2005)). In

contrast, the affinity of ciproxifan (**14**) was low, but in good agreement with binding data determined in the aforementioned assay system (see **Table 3.1** and (Zhao *et al.*, 2008)). The recently described N^G-acylated imidazolylpropylguanidine UR-PI294 (**15** (Igel *et al.*, 2009b), the cyanoguanidines UR-PI376 (**16**) and trans-(+)-(1S,3S)-UR-RG98 (**17**) (Geyer, 2011; Igel *et al.*, 2009a) as well as the non-imidazoles clozapine (**18**), JNJ 7777120 (**19**) and VUF 8430 (**20**) inhibited specific binding of [^{3}H]UR-PI294 on HEK293-SF-hH_4R-His_6 cells (see **Figure 3.7**). The pK_i of UR-PI294 (**15**) (8.28 ± 0.07) was in good agreement with the pK_D value of its tritiated analog (cf. section 3.1.3.2). The cyanoguanidine UR-PI376 (**16**) and its cyclopentyl analog trans-(+)-(1S,3S)-UR-RG98 (**17**) exhibited comparable affinity at the hH_4R in competition binding assays (pK_i = 7.10 ± 0.04 and pK_i = 7.29 ± 0.05, respectively). Whereas the affinity of UR-PI376 (**16**) corresponded well to data determined in competition binding experiments using [^{3}H]histamine on Sf9 insect cell membranes expressing the hH_4R, the pK_i value of trans-(+)-(1S,3S)-UR-RG98 (**17**) was slightly lower (see **Table 3.1**).

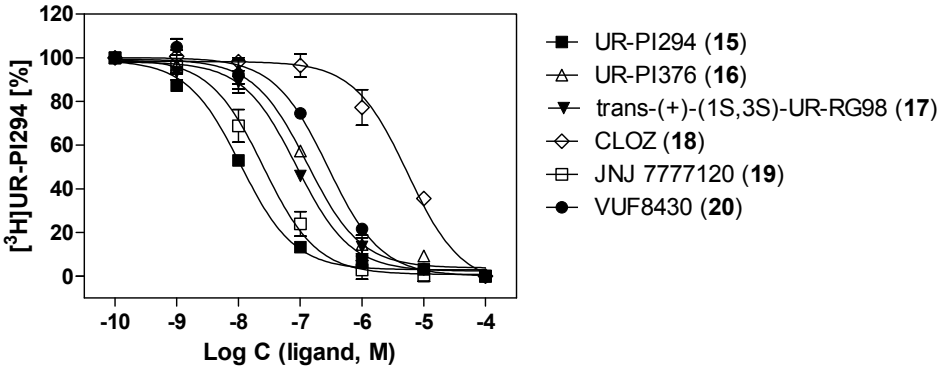

Figure 3.7: Inhibition of [^{3}H]UR-PI294 binding by UR-PI294 (**15**), UR-PI376 (**16**), trans-(+)-(1S,3S)-UR-RG98 (**17**), CLOZ (**18**), JNJ 7777120 (**19**) and VUF 8430 (**20**) on HEK293-SF-hH_4R-His_6 cells. Reaction mixtures contained 5 nM [^{3}H]UR-PI294 and ligand concentrations indicated on the abscissa. Data were analyzed by nonlinear regression and best fitted to one-site (monophasic) competition curves. Data points are the mean of at least three independent experiments performed in duplicate.

The antipsychotic drug clozapine (**18**) revealed only low affinity at the hH_4R, whereas the selective H_4R antagonist JNJ 7777120 (**19**) bound with high affinity (pK_i = 7.80 ± 0.16). With a pK_i value of 6.78 ± 0.04, the dimaprit analog VUF8430 (**20**) reached moderate affinity at the hH_4R. Whereas the affinity of JNJ 7777120 (**19**) was in good agreement with the reported data, the pK_i-values of clozapine (**18**) and VUF8430 (**20**) were lower than described in literature (see **Table 3.1**). JNJ 5207852 (**21**) and the alkaloid conessine (**22**) were not able to inhibit specific binding of [^{3}H]UR-PI294 to the hH_4R. Both compounds, **21** and **22**, were described as selective H_3R ligands (see **Table 3.1**).

Table 3.1: pK_i values of reference H_4R ligands determined in competitive binding experiments, using [^{3}H]UR-PI294 and HEK293-SF-hH_4R-His_6 cells, in comparison to pK_i values reported in literature.

Ligand	**hH_4R**		
	pK_i	N	pK_i
	HEK293-SF-hH_4R-His_6		Reported
Histamine (**1**)	7.22 ± 0.04	10	7.6-8.1[e, j, l, m, p, r]
(R)-α-Methylhistamine (**2**)	5.75 ± 0.07	6	6.5-6.8[f, j, l, m, r]
(S)-α-Methylhistamine (**3**)	4.92 ± 0.15	4	5.4-5.5[j, m]
N^{α}-Methylhistamine (**4**)	5.94 ± 0.09	6	6.5-7.6[j, m, r]
5(4)-Methylhistamine (**5**)	6.56 ± 0.14	4	7.3-7.7[j, o]
Immepip (**6**)	7.32 ± 0.11	5	7.7-8.2[i, j, l, r]
VUF 5681 (**7**)	6.20 ± 0.03	3	6.2[g]
Immethridine (**8**)	6.90 ± 0.07	3	6.6[h, j]
Imetit (**9**)	7.57 ± 0.12	3	7.8-8.6[j, l, m, r]
Clobenpropit (**10**)	7.28 ± 0.13	3	7.7-8.1[e, j, l, m]
Iodophenpropit (**11**)	7.11 ± 0.05	3	7.7-7.9[j, r]
Thioperamide (**12**)	6.68 ± 0.13	4	6.3-7.6[e, f, j, l, m, p, r]
Proxyfan (**13**)	6.58 ± 0.15	3	7.3[j]
Ciproxifan (**14**)	5.60 ± 0.04	3	5.7[q]
UR-PI294 (**15**)	8.28 ± 0.07	3	7.8[o]
UR-PI376 (**16**)	7.10 ± 0.04	3	7.1-7.2[d, o]
trans(+)UR-RG98 (**17**)	7.29 ± 0.05	3	7.7[c]
Clozapine (**18**)	5.50 ± 0.04	3	5.9-6.7[a, j, l, r]
JNJ 7777120 (**19**)	7.80 ± 0.16	5	7.5-8.4[c, d, h, l]
VUF 8430 (**20**)	6.78 ± 0.04	3	7.5[k]
JNJ 5207852 (**21**)	< 4	1	< 5[b]
Conessine (**22**)	< 4	1	< 5[q]

Mean values ± SEM. N: number of independent experiments performed in duplicate. Reference data taken from: [^{3}H]histamine binding on Sf9 cell membranes [a] (Appl *et al.*, 2011), [d] (Igel *et al.*, 2009a), [o] (Schnell *et al.*, 2011); [b] (Barbier *et al.*, 2004); [^{3}H]UR-PI294 binding on Sf9 cell membranes [c] (Geyer, 2011), [e] (Igel *et al.*, 2009c); [^{3}H]histamine binding on SK-N-MC cell membranes [f] (Jablonowski *et al.*, 2003), [l] (Liu *et al.*, 2001a); [^{3}H]histamine binding on SK-N-MC cell homogenates [g] (Kitbunnadaj *et al.*, 2003), [h] (Kitbunnadaj *et al.*, 2004), [l] (Kitbunnadaj *et al.*, 2005), [j] (Lim *et al.*, 2005), [k] (Lim *et al.*, 2006); [^{3}H]histamine binding on HEK293 cell membranes [m] (Morse *et al.*, 2001), [p] (van Rijn *et al.*, 2006); [q] (Zhao *et al.*, 2008); [^{3}H]histamine binding on Cos-1 cell membranes [r] (Zhu *et al.*, 2001).

In summary, using whole HEK293-SF-hH_4R-His_6 cells and [^{3}H]UR-PI294 as radioligand, binding data of H_4R ligands could be determined in a highly reproducible manner. However, two tendencies were noticeable. Firstly, most pK_i values of H_4R agonists (**1**–**6**, **9**-**11**, **13**, **17**, **18**, **20**) were slightly to considerably lower, whereas all pK_i values of antagonists (**7**, **12**, **14**,

19) were in agreement with or in the same range as those described in literature as shown in **Figure 3.8** (see section 4.1.3.8 and (Lim *et al.*, 2005) for the classification, whether a ligand is an agonist or antagonist at the hH_4R). Only the H_4R partial agonists immethridine (**8**), UR-PI294 (**15**) and UR-PI376 (**16**) (intrinsic activities 0.5, 0.93 and 0.93) (Igel *et al.*, 2009a; Igel *et al.*, 2009b; Lim *et al.*, 2005) showed equal or higher affinities in the whole cell radioligand binding assay. Secondly, the rank order of agonist affinity was in accordance with the reported affinities (see **Figure 3.8**) and the order of potency (cf. section 4.1.3.8); this is essential with respect to the pharmacological characterization of H_4R agonists.

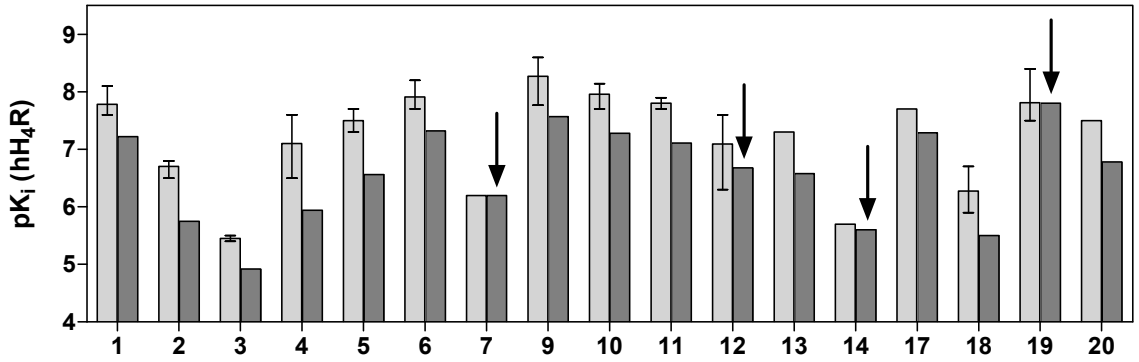

Figure 3.8: Affinities of the examined H_4R ligands **1**-**7**, **9**-**14**, **17**-**20** in whole cells (dark gray bars) and reported data from broken cell preparations (light gray bars). Data are the mean values according to table 3.1. Additionally, the span coverd by reported pK_i values is given ("error bars"). Black arrows indicate H_4R antagonists for which the affinity was comparable to reported data.

A possible explanation for these tendencies could be the so called GTP-shift (Kenakin, 2009; Lazareno, 2001). In brief, the binding of an agonist to a GPCR is described by a two stage binding reaction, represented as

$$[A] + [R] \underset{k_{-1}}{\overset{k_1}{\rightleftarrows}} [AR] + [G] \underset{k_{-2}}{\overset{k_2}{\rightleftarrows}} [ARG] \qquad \text{(equation 4).}$$

The agonist [A] binds to the receptor [R] with k_1. The agonist-receptor complex [AR] binds subsequently due to the activation of the receptor to the G-protein [G] with the constant k_2 and forms the ternary complex [ARG], consisting of agonist, receptor and G-protein (cf. section 1.1.4.3). The formation of the ternary complex will drive the equilibrium to the right, i.e., the concentration of [AR] complex will be shifted in favor of [ARG]. Hence, all in all more agonist binds to the receptor and the observed affinity will be higher than in the absence of G-protein. Especially in assay systems allowing for accumulation of the ternary complex, high affinity binding can be observed. One crucial factor is the concentration of GTP (or GTPγS).

In the presence of a high GTP concentration, as in whole cells, the formation of the ternary complex is followed promptly by the hydrolysis of GTP and the dissociation of the heterotrimeric G-protein into α- and βγ subunits (i.e. the ternary complex cannot accumulate). Since in broken-cell preparations, such as membranes or cell homogenates, the GTP concentration is low, the ternary complex can accumulate and two stage binding is observed. Due to the fact that in the referenced literature invariably broken-cell preparations were used to study H_4R ligands, the GTP shift could be the reason for lower agonist affinities in whole cell radioligand binding assays.

In contrast, for binding studies using membranes of Sf9 insect cells, co-expressing the hH_4R + $G\alpha_{i2}$ +$G\beta_{1\gamma2}$, a GTPγS resistant high affinity agonist binding hH_4R state was assumed, since the presence of 10 µM GTPγS did not alter the K_D value of [^{3}H]histamine (Schneider *et al.*, 2009). However, on the one hand, the K_D value of [^{3}H]histamine was not determined in this study, and, on the other hand, the influence of GTPγS on the affinity of agonists in competition binding experiments was not investigated with Sf9 cell membranes (Schneider *et al.*, 2009). Therefore, comparison of the results with data from the literature, obtained under different conditions, is impossible.

3.2 Radioligand binding assay for the mouse histamine H_4 receptor

3.2.1 Introduction

After cloning of the mouse (m) H_4R, it became clear that the human and mouse H_4R only share 68 % the amino acid sequence (Liu *et al.*, 2001b), which causes substantial differences with respect to affinities (Lim *et al.*, 2010; Liu *et al.*, 2001b; Neumann *et al.*, 2010; Schnell *et al.*, 2011), potencies and efficacies of the pharmacological tools (Liu *et al.*, 2001b; Schnell *et al.*, 2011). Affinities were determined in binding assays using [^{3}H]histamine on membrane preparations of HEK293T (Lim et al., 2010) or SK-NM-C cells (Liu et al., 2001b) expressing the mH_4R. By contrast, no specific-binding of [^{3}H]histamine was found on Sf9 cell membranes expressing the mH_4R (Schnell et al., 2011).

To evaluate species-dependent discrepancies regarding affinities of the pharmacological tools in a whole-cell radioligand binding assay, HEK293T cells were stably transfected with the mH_4R. For this purpose the FLAG epitope (F)- and hexahistidine (His_6)-tagged mH_4R cDNA was subcloned into a mammalian expression vector, pcDNA3.1(+). The commercially available pcDNA3.1(+) vector (Invitrogen, Karlsruhe, Germany) contains an ampicillin resistance for the propagation of DNA in bacteria and a resistance gene against G418 for the selection of the transfected cells. Furthermore, the SV40 origin in the pcDNA3.1(+) vector together with the SV40 Large T-antigen in HEK293T cells allows episomal replication of the plasmid, which in turn leads to a amplification of the plasmid and extended temporal expression of the mH_4R (DuBridge *et al.*, 1987; Mahon, 2011; Pear *et al.*, 1993). Stable transfection is preferred compared to transient transfection. Once a stable cell line is generated, ideally, a defined, constant quantity of the recombinant protein is expressed over a long period of time, affording reproducible results.

The affinity of the standard mH_4R radioligand [^{3}H]histamine as well as of the putative mH_4R ligand [^{3}H]UR-PI294 were determined in saturation binding assay using HEK293-SF-mH_4R-His_6 cells. Thereupon, the most suitable radioligand was chosen to evaluate the feasibility of performing competition binding experiments on the mH_4R.

For validation of the competition binding assay, a selection of standard H_4R ligands was investigated for the ability to inhibit specific binding of the radioligand. Due to the need for ligands as pharmacological tools for the mH_4R, the enantiomers of the imidazolylcyclopentylmethylcyanoguanidines UR-RG94 and UR-RG98 were additionally investigated in competition binding experiments.

3.2.2 Materials and methods

3.2.2.1 Subcloning of the pcDNA3.1(+)SF-mH$_4$R-His$_6$ vector

The FLAG epitope (F)- and hexahistidine (His$_6$)-tagged mH$_4$R cDNA cloned in pGEM-3Z (Schnell *et al.*, 2011) was subcloned into a mammalian expression vector, pcDNA3.1(+) (including the tagged hH$_3$R, was kindly provided by Dr. Schnell, University of Regensburg, Germany) , at *Hind*III and *Xba*I restriction sites.

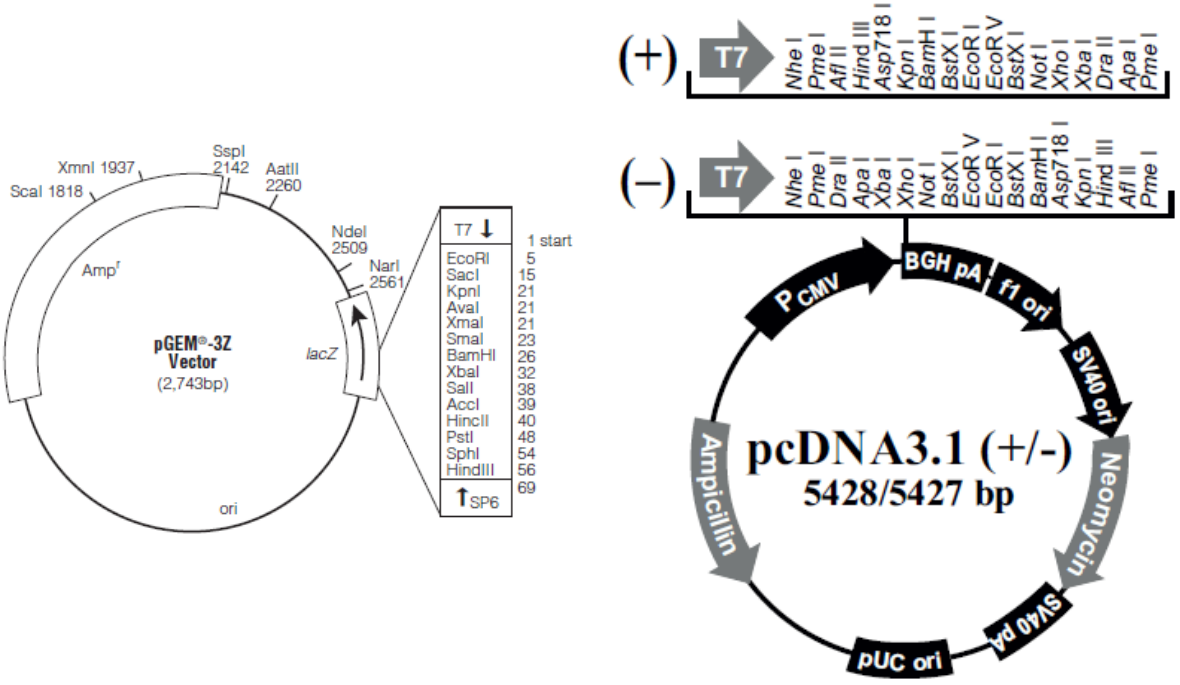

Figure 3.9: Vector maps of pGEM-3Z and pcDNA3.1 (+/-) vectors (adopted from manuals provided by Promega (Mannheim, Germany) and Invitrogen, respectively).

3.2.2.1.1 Restriction enzyme digestion

The double digestion with *Hind*III (Fermentas GmbH, St. Leon-Rot, Germany) and *Xba*I (Fermentas) for a preparative agarose gel electrophoresis was performed in the reaction buffer Tango^{TM} (Fermentas) with 2-fold excess of *Hind*III at 37 °C (recommendations of the manufacturer) for 3 h. The final volume of the enzyme restrictions digestion was 50 µL of Millipore water containing 5 µL of the 10x reaction buffer, 4 µL of the *Hind*III stock solution (10 U/µL), 2 µL of the *Xba*I (10 U/µL) stock solution and 3500 – 7000 ng of DNA. For the agarose gel electrophoresis 10 µL of the 6x gel loading buffer (Peqlab, Erlangen, Germany) were added to each sample to yield a final volume of 60 µL.

The restriction analysis at the *Hind*III and *Xba*I restrictions sites was performed with the enzymes *Hind*III-HF™ (New England Biolabs, Ipswich Massachusetts, USA) and *Xba*I (New England Biolabs) in the reaction buffer NEBuffer 4 with BSA (New England Biolabs) at 37 °C for 90 min. The final volume was 15 µL of Millipore water containing 1.5 µL of the 10x reaction buffer, 1 µL of *Hind*III-HF™ stock solution (20 U/µL), 1 µL of the *Xba*I stock solution (20 U/µL) (only for the double digestion) and 600 – 800 ng of DNA. For agarose gel electrophoresis 10 µL of the digestion, 3 µL of the 6x gel loading dye (New England Biolabs) and 5 µL of Millipore water were mixed to a final volume of 18 µL.

3.2.2.1.2 Agarose gel electrophoresis, gel extraction and determination of DNA concentration

For the preparation of the agarose gels 0.5 g of agarose (pegGOLD Universal-Agarose, Peqlab) were dissolved in 50 mL TAE buffer containing 40 mM tris-acetate (tris was from Pro-Lab, Hamburg, Germany; conc. acetic acid was from Merck) and 1 mM EDTA (Titriplex III; Merck) under heating and continuous stirring. 2 µL of an aqueous ethidium bromide solution (10 mg/mL; Janssen Chimica, Beerse, Belgium) were added and the warm agarose solution was poured into the gel chamber of the perfectBlue™ Mini S gel system (Peqlab). A comb served as placeholder for the wells. Prior to electrophoresis, the gel was covered with TAE buffer and the comb was carefully removed. The above mentioned digestion samples (see section 3.2.2.1.1) as well as 15 µL of the MassRuler™ DNA ladder mix (Fermentas), ready to use or 6 µL of 1kb DNA Ladder (New England Biolabs) were added into the wells of the gel.

The preparative gel electrophoresis (150 V) was stopped after a period of 45 min and the analytical gel electrophoresis (90 V) after 75 min. The gels were analyzed by transillumination at 254 nm (Gel Doc 2000; Bio-Rad Laboratories, Munich) using the Quantity one software (Bio-Rad Laboratories).

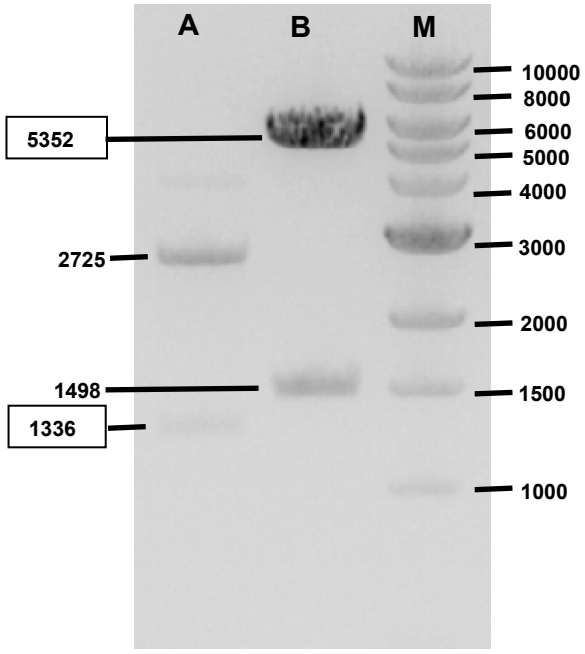

Figure 3.10: Restriction analysis at *Hind*III and *Xba*I restriction sites. Digestion of pGEM-3Z-SF-mH_4R-His_6 (A). Digestion of pcDNA3.1(+)-SF-hH_3R-His_6 (B). 1 kb DNA Ladder (New England Biolabs) (M).

The DNA bands of the SF-mH_4R-His_6 (1336 bp) (see **Figure 3.10**, lane A (very weak)) insert consisting of the cleavable signal peptide from influenza hemagglutinin (S), the FLAG epitope (F)- and hexahistidine (His_6)-tagged mH_4R as well as the empty and linearized pcDNA3.1(+) vector (5352 bp) (see **Figure 3.10**, lane B) were extracted from the agarose gel using the QIAquick Gel Extraction Kit (QIAGEN, Hilden, Germany) according to the manufactures protocol. The DNA was finally eluted with 50 µL of the buffer provided.
The DNA concentration of a 1:20 dilution was determined with the BioPhotometer plus (Eppendorf, Hamburg, Germany) and the samples were stored at -20 °C until the ligation.

3.2.2.1.3 Ligation of DNA fragments

50 ng of the digested pcDNA3.1(+) vector, 62.4 ng of the digested SF-mH_4R-His_6 insert (5-fold excess over the vector with regard to molar amounts) from section 3.2.2.1.2 and 2µL of a 10x T4-DNA- ligase buffer stock solution (New England Biolabs) were filled up with Millipore water to 19.5 µL. After heating for 5 min at 45 °C, 1 µL of T4-DNA-Ligase (6 Weiss U/µL) (New England Biolabs) was added, and the completed sample was incubated at 15 °C overnight. On the next day, the ligase was inactivated by heating the sample for 10 min at 65 °C. The sample was stored at -20 °C until transformation of competent bacteria.

3.2.2.1.4 Preparation of media and agar plates

For the preparation of LB medium, 10 g of bacto tryptone (Difco, Detroit, USA), 5 g of yeast extract (Roth) and 10 g of NaCl (Merck) were added to 800 mL of Millipore water. After

dissolving of the ingredients, the pH value was adjusted to 7.5 with NaOH solution (1 M) (Merck). The solution was filled up to 1000 mL with Millipore water and sterilized by autoclaving for 20 min at 121 °C. Selective LB medium was made by adding a sterile thousand-fold concentrated ampicillin (Sigma) solution (100 mg/mL).

For the preparation of selective agar plates, 15 g of agar (Roth) were dissolved in 1 L LB medium under constant heating and stirring. After autoclaving, the solution was allowed to cool down to approx. 60 °C, before ampicillin was added, and plates were casted (approx. 20 mL per plate). After cooling, selective plates were stored at 4 °C for 3 to 4 weeks.

SOC medium was prepared by addition of 20 g bacto tryptone, 5 g of yeast extract, 0.5 g of NaCl, 2.5 mL of KCl (Merck) (1M), 10 mL $MgCl_2$ (Merck) (1M) to 900 mL of Millipore water. After adjustment of the pH value to 7.0 with NaOH (1 M), the solution was filled up to 1000 mL with Millipore water and autoclaved. Finally, 20 mL of glucose (Merck) (1 M) were added under sterile conditions.

3.2.2.1.5 Transformation of competent *E. coli*

Competent *E. coli* (TOP10 strain) cells were prepared according to a recently described method and stored at -80 °C (Mosandl, 2009). An aliquot of competent bacteria was carefully thawed and kept on ice for 10 min. For chemical transformation, 1 µL of the ligation reaction mixture (corresponds to approx. 2 ng of plasmid vector which was applied for ligation, see section 3.2.2.1.3) was added to 100 µL of the competent bacterial suspension prior to the incubation on ice for 30 min. Then, the suspension was heat-shocked at 42 °C for 90 s and cooled on ice for another 3 min. 900 µL of pre-warmed SOC medium were added, and the bacteria were incubated at 37 °C for 1 h under slight shaking (150 rpm).

To ensure a sufficient quantity of colonies on the selective agar plates, the bacterial suspension was plated in two densities. For a low density, 100 µL of the suspension were streaked onto a pre-warmed selective agar plate. For a high bacterial density the residual 800 µl were centrifuged for 5 min at 3000 rpm. Thereafter, 800 µL of the supernatant were discarded, and the bacterial pellet was re-suspended in the residual volume of 100 µL. The concentrated suspension was streaked on a pre-warmed selective agar plate. The plates were incubated overnight at 37 °C and stored at 4 °C up to 4 weeks.

3.2.2.1.6 Preparation of glycerol cultures and plasmid DNA (Maxi-Prep)

Some colonies were picked, and 5 mL of the selective LB medium containing ampicillin (100 µg/mL) were inoculated with the bacteria in each case. The bacteria were incubated at 37 °C overnight under slight shaking (150 rpm). On the next day, 700 µL of the overnight cultures were transferred into a 1.5 mL reaction vessel (Eppendorf) containing 300 µL of a 50 % (v/v) glycerol solution. After a brief mixing, the glycerol culture was stored at -80 ° C.

One overnight culture was chosen in order to prepare the start culture for large scale preparation of plasmid DNA (Maxi-Prep). 200 µL of the overnight culture were added to 100 mL of selective LB medium, and the bacteria were allowed to grow overnight at 37 °C and 150 rpm. The following steps were performed using the Qiagen Plasmid Purification kit (Qiagen) according to the manufacturer's instructions. The determination of DNA concentration was performed as described in section 3.2.2.1.2.

3.2.2.1.7 Restriction analysis and sequencing of pcDNA3.1(+)SF-mH$_4$R-His$_6$

The linearization of pcDNA3.1(+)SF-mH$_4$R-His$_6$ with the restriction enzyme *Hind*III resulted in the expected band with a length of 6688 bp (see **Figure 3.11**, lane A). The double digestion at *Hind*III and *Xba*I restriction sites gave two fragments with a length of 5352 and 1336 bp, respectively (see **Figure 3.11**, lane B), which corresponds to the pcDNA3.1(+) vector (5352 bp), lacking an insert (cf. **Figure 3.10**, lane B) and the SF-mH$_4$R-His$_6$ insert (1336 bp, very weak) (cf. **Figure 3.10**, lane A).

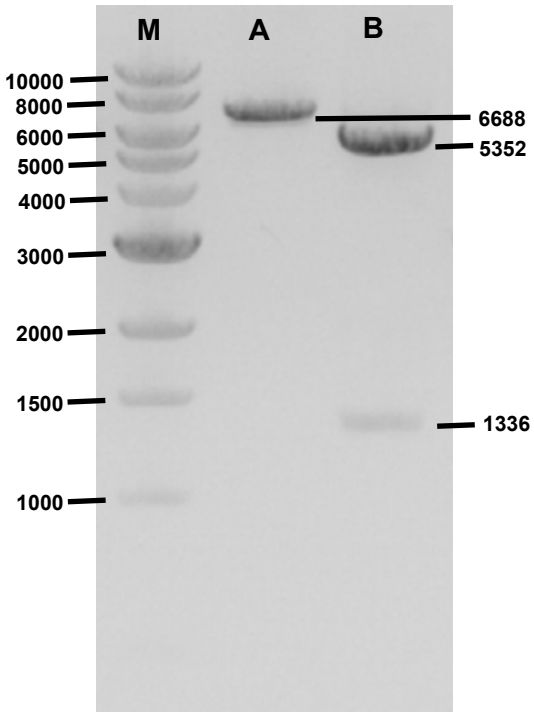

Figure 3.11: Restriction analysis of pcDNA3.1(+)SF-mH$_4$R-His$_6$. Linearized vector at *Hind*III restriction site (A). Double digestion with *Hind*III and *Xba*I (B). 1kb DNA Ladder (New England Biolabs) (M).

The sequencing of the pcDNA3.1(+)SF-mH$_4$R-His$_6$ vector (performed by Entelechon, Bad Abbach, Germany) confirmed correctness of the mammalian shuttle vector.

3.2.2.2 Stable transfection of HEK293T cells with the pcDNA3.1(+)SF-mH$_4$R-His$_6$ vector

HEK293T cells were cultured as described in section 3.1.2.1. One day before transfection, cells were detached with 5 mL of DMEM +10 % FCS from a densely grown 75-cm^2 culture flask. The cell suspension was seeded dropwise at different densities into the cavities of a 24-well-plate (Becton Dickinson, Heidelberg, Germany), so that 8 (2 vertical rows) wells contained the same number of cells. Approx. 500 µL DEMEM + 10 % FCS was added, and the cells were evenly distributed in the wells by gentle shaking. The next day, two rows with a confluency of 60 – 70 % were selected for transfection. The medium was carefully removed by suction and replaced by 475 µL of fresh DEMEM +10 % FCS. A few hours later, 100 µL of the transfection complex containing 2 µg of DNA and either 4 µL (ratio: 4:2) or 6 µL (ratio: 6:2) of FuGene®HD (Roche Diagnostics GmbH, Mannheim, Germany) transfection reagent were prepared according to the manufactures protocol. 25 µL of the transfection complexes were each added to the wells, and the cells were incubated for 48 h. After short trypsinization, 4 wells (of ratio 4:2 and 6:2, respectively) were pooled in a 25-cm^2 culture flask (Sarstedt) with DMEM + 10 % FCS. For selection, the medium was replaced after 24 h by DMEM + 10 % FCS containing 800 µg/mL G418. After another 72 h, the medium was again replaced by DMEM + 10 % FCS containing 600 µg/mL G418. At that time, the stable transfectants (HEK293-SF-mH$_4$R-His$_6$, 4:2 and 6:2 batches) had formed colonies in the selective medium, the extent of receptor expression was determined in a radioligand binding assay.

3.2.2.3 Whole cell radioligand binding assay

The preparation of the HEK293-SF-mH$_4$R-His$_6$ cells, the separation of bound from free radioligand and the data processing were performed as described in section 3.1.2.4. For selection of the transfectant with the higher expression level, specific binding of 50 nM [^{3}H]UR-PI294 and 100 nM [^{3}H]histamine (specific activity of 14.2 Ci/mmol; Perkin Elmer, Rodgau, Germany) was determined. For the determination of non-specific binding thioperamide (**12**) (100 µM) was used.

In saturation binding assays with [^{3}H]UR-PI294 and [^{3}H]histamine, non-specific binding was determined in the presence of JNJ 7777120 (**19**) at a final concentration of 10 µM. The K_D value of [^{3}H]UR-PI294 was calculated as means of two independent experiments performed in triplicate. In competition binding assays 50 nM [^{3}H]UR-PI294 were used. The determined K_i values are given in **Table 3.3** and **Table 3.4**. To save radioligand in saturation and competition binding experiments with [^{3}H]UR-PI294, 50 % and 75 %, respectively, were

replaced by the unlabeled form, UR-PI294 (**15**). The dilution was feasible due to a high specific activity of [^{3}H]UR-PI294 (78.5 Ci/mmol) (synthesized in our laboratory).

3.2.2.4 Imidazolylcyclopentylmethylcyanoguanidines UR-RG94 and UR-RG98

The three stereoisomers of the (S,S)-configured phenylthioethyl-substituted cyanoguanidine UR-RG98 (cf. **Figure 3.1**, compound no. **17**) and the stereoisomers of the methyl-substituted cyanoguanidine UR-RG94 were investigated for the ability to inhibit specific binding of [^{3}H]UR-PI294 at the mH_4R. Trans-(-)-(1R,3R)-UR-RG98 (**23**), cis-(-)-(1S,3R)-UR-RG98 (**24**), cis-(+)-(1R,3S)-UR-RG98 (**25**), trans-(-)-(1R,3R)-UR-RG94 (**26**), trans-(+)-(1S,3S)-UR-RG94 (**27**), cis-(-)-(1S,3R)-UR-RG94 (**28**) and cis-(+)-(1R,3S)-UR-RG94 (**29**) were synthesized in our laboratory as described recently (Geyer, 2011). Chemical structures of the stereoisomers **23-29** are depicted in **Figure 3.12**. All stock solutions (10 mM) were made in 50 % DMSO. The dilution series were prepared in 10 % DMSO.

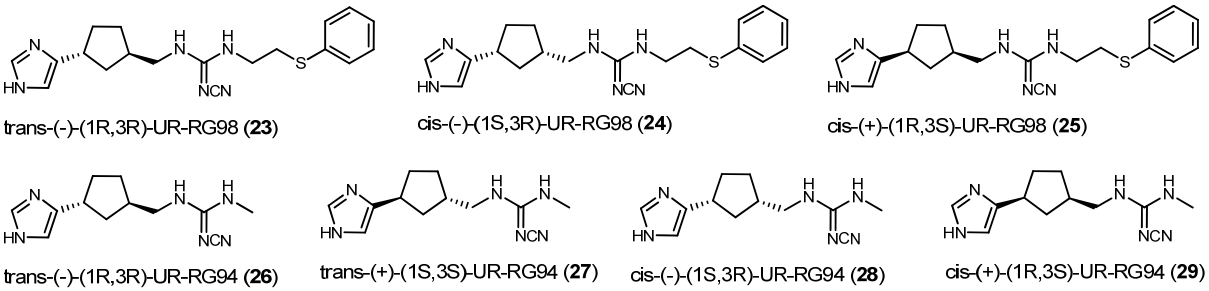

Figure 3.12: Structures of the stereoisomers of UR-RG98 (**23-25**, (S,S)-configured stereoisomer **17**: cf. Figure 3.1) and UR-RG94 (**26-29**). The designation includes the relative and absolute configuration, the sign of optical rotation and the lab code according to Geyer (Geyer, 2011).

3.2.3 Results and discussion

3.2.3.1 Selection of the transfected cells

HEK293T cells were stably transfected with the pcDNA3.1(+)-SF-mH_4R-His_6 vector with two different ratios of transfection reagent volumes (µL) to DNA amount (µg), namely 4:2 and 6:2. For selection, the total-, non-specific- and the resulting specific binding of 50 nM [^{3}H]UR-PI294 and 100 nM [^{3}H]histamine were determined (see **Figure 3.13**). Although the total binding of 50 nM [^{3}H]UR-PI294 was nearly identical in the two transfection batches, the 6:2 cells revealed a distinctly higher specific binding compared to the 4:2 cells (78 % vs. 43 %, relating to the total binding) as shown in **Figure 3.13** A, B. Similarly, the specific binding of 100 nM [^{3}H]histamine was clearly higher in the 6:2 than in the 4:2 batch (see **Figure 3.13** C, D). Moreover, the extent of specific binding (72 %) was in good agreement with the specific binding determined with [^{3}H]UR-PI294 (**Figure 3.13** B, D). In conclusion, the HEK293-SF-mH_4R-His_6 6:2 cells were used for further radioligand binding studies.

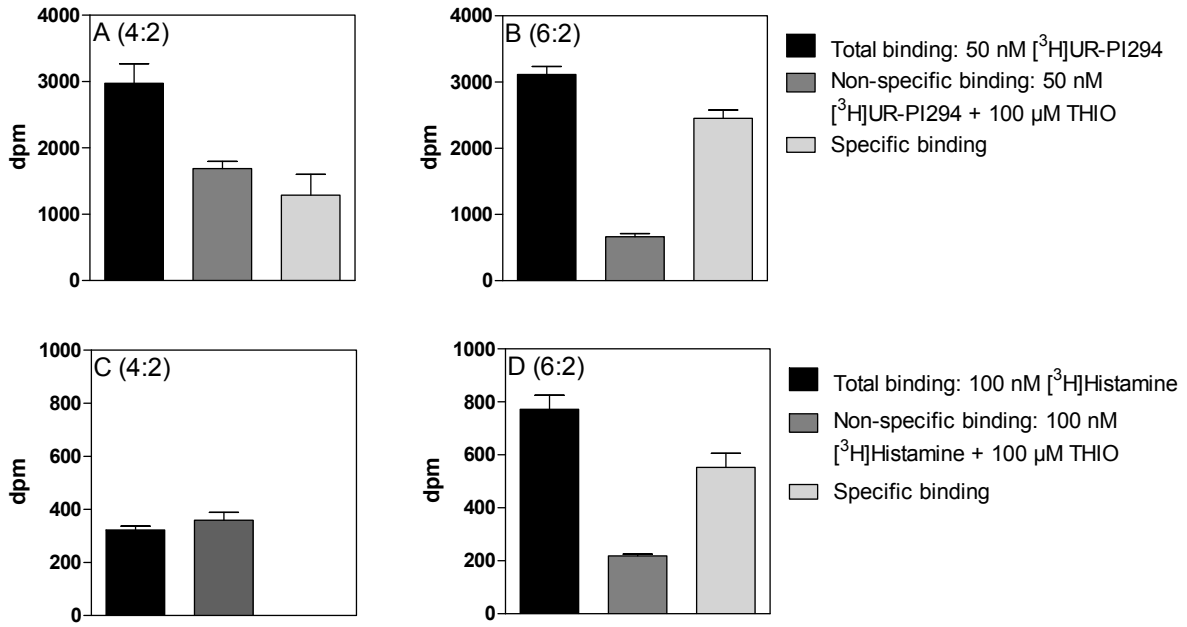

Figure 3.13: Selection of the HEK293-SF-mH_4R-His_6 transfection batches pertaining to specific binding of radioligands**.** Total-, non-specific-, and specific binding of 50 nM [^{3}H]UR-PI294 referring to the 4:2 batch (A) and the 6:2 batch (B). Total-, non-specific-, and specific binding of 100 nM [^{3}H]histamine referring to the 4:2 batch (C) (the specific binding was negative, therefore it was assumed to be zero) and the 6:2 batch (D). Non-specific binding was obtained in the presence of 100 µM of thioperamide (**12**). Shown are the mean values ± SEM. Each experiment was performed in triplicate.

3.2.3.2 Saturation binding assays

The binding of [^{3}H]UR-PI294 was specific and saturable up to a concentration of 125 nM as shown for two independent saturation binding experiments in **Figure 3.14**. Since in initial saturation binding experiments the values for the non-specific binding strongly fluctuated using thioperamide (**12**) (data not shown), non specific binding was determined in the presence of JNJ 7777120 (**19**) (10 µM). The non-imidazole **19**, which exhibited high affinity at the mH_4R (Lim *et al.*, 2010), was capable to keep non-specific binding sufficiently low (see **Figure 3.14**). [^{3}H]UR-PI294 bound to the mH_4R with a ten-fold lower affinity (K_D = 75 ± 9 nM) than to the hH_4R (see **Table 3.2**). This result was not unexpected, as previous studies revealed also a decrease in affinity for H_4R ligands at the mH_4R compared to the hH_4R (Lim *et al.*, 2010; Lim *et al.*, 2008; Liu *et al.*, 2001b; Schnell *et al.*, 2011).

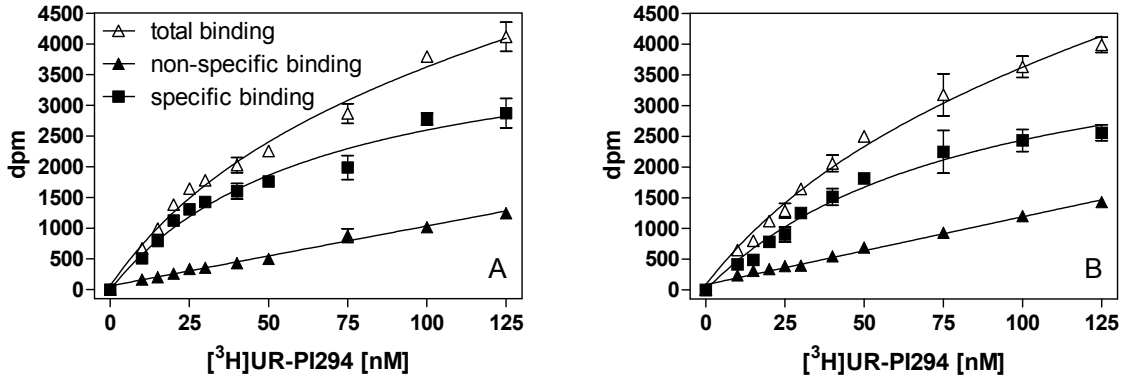

Figure 3.14: Representative [^{3}H]UR-PI294 saturation binding experiments using HEK293-SF-mH_4R-His_6 cells, each performed in triplicate (A and B). Non-specific binding was determined in the presence of 10 µM of JNJ 7777120 (**19**). Saturation binding curves, best fitted by non-linear regression to a one-site model.

Contrary to Sf9 insect cell membranes expressing the mH_4R (Schnell *et al.*, 2011), specific binding of [^{3}H]histamine was detected on HEK293-SF-mH_4R-His_6 cells (see **Figure 3.15**). However, although the non-specific binding in the presence of JNJ 7777120 (**19**) (10 µM) seemed to be sufficiently low, the binding of [^{3}H]histamine was apparently not saturable up to a concentration of 125 nM (see **Figure 3.15**).

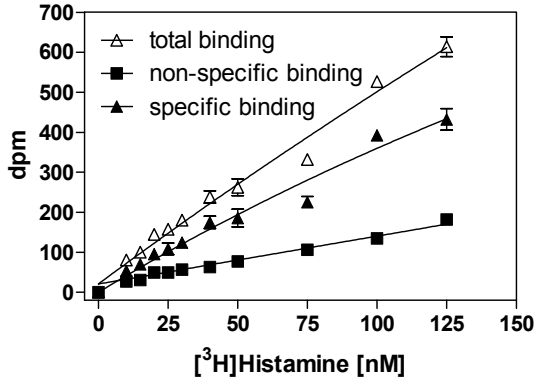

Figure 3.15: Representative non-saturable binding of [^{3}H]histamine to HEK293-SF-mH$_4$R-His$_6$ cells. Non-specific binding was determined in the presence of 10 µM of JNJ 7777120 (**19**).

Table 3.2: Results from saturation binding experiments with [^{3}H]UR-PI294 at the mH$_4$R and hH$_4$R, using HEK293-SF-m/hH$_4$R-His$_6$ cells, in comparison with data reported in literature.

Radioligand	**mH$_4$R**			**hH$_4$R**		
	K_D [nM]		K_D [nM]	K_D [nM]		K_D [nM]
	HEK293-SF-mH$_4$R-His$_6$	N	reported	HEK293-SF-hH$_4$R-His$_6$	N	reported
[^{3}H]UR-PI294	75 ± 9	2	-	7.5 ± 1.8	3	5.1[a]
[^{3}H]Histamine	n.d.	2	42-75[b,c]	-	-	9-18[b–f]

Mean values ± SEM. N: number of independent experiments performed in duplicate; n.d.: not determinable. Reference data taken from: [^{3}H]UR-PI294 binding on Sf9 cell membranes expressing the hH$_4$R-RGS19 fusion protein [a] (Igel *et al.*, 2009c); [^{3}H]histamine binding on HEK293T cell membranes expressing the human and mouse H$_4$R, respectively [b] (Lim *et al.*, 2010); [^{3}H]histamine binding on SK-N-MC cell membranes stably expressing the human and mouse H$_4$R, respectively [c] (Liu *et al.*, 2001b); [^{3}H]histamine binding on HEK293 cell membranes expressing the hH$_4$R [d] (Morse *et al.*, 2001); [^{3}H]histamine binding on Sf9 cell membranes expressing the hH$_4$R-RGS19 fusion protein [e] (Schnell *et al.*, 2011); [^{3}H]histamine binding on Cos-1 cell membranes transiently expressing the hH$_4$R [f] (Zhu *et al.*, 2001).

In summary, [^{3}H]UR-PI294 revealed considerably lower affinity to the mH$_4$R compared to the hH$_4$R (see **Table 3.2**), limiting the explanatory power of binding studies. Since the specific binding of [^{3}H]histamine to HEK293-SF-mH$_4$R-His$_6$ cells was not saturable, [^{3}H]UR-PI294 was chosen to perform competition binding studies at the mH$_4$R.

3.2.3.3 Competition binding assay

The mH$_4$R affinities of selected standard H$_4$R ligands (**1**, **5**, **10**, **12**, **18**–**20**; cf. **Figure 3.1**) were determined in competition binding experiments. For this purpose, HEK293-SFmH$_4$R-His$_6$ cells were co-incubated with 50 nM of [^{3}H]UR-PI294 and increasing ligand concentrations. For comparison, the determined pK_i values and reported data from

competition binding experiments using [^{3}H]histamine and homogenates of mH_4R expressing SK-N-MC cells (Lim *et al.*, 2010; Liu *et al.*, 2001b) are summarized in **Table 3.3**.

All tested H_4R standard ligands were able to inhibit specific binding of [^{3}H]UR-PI294 on HEK293-SF-mH_4R-His_6 cells in a concentration dependent manner (**Figure 3.16**, competition curves of compound 5-(4)-methylhistamine (**5**) and clozapine (**18**) are not shown). The pK_i value of histamine (**1**) was in good accordance with the reported binding data. Interestingly, histamine (**1**) showed only a slight decrease in affinity at the mH_4R compared to the hH_4R (cf. **Table 3.1**). The determined affinity of 5-(4)-methylhistamine (**5**) was considerably lower than reported (see **Table 3.3**) and by one order of magnitude lower compared to the K_i value at the hH_4R (cf. **Table 3.1**). Clobenpropit (**10**) displayed good affinity at the mH_4R (pK_i = 7.10 ± 0.06), which was comparable with reported data. Furthermore, clobenpropit (**10**) bound with nearly the same affinity to both the mH_4R and the hH_4R (hH_4R: pK_i = 7.28 ± 0.13). Thioperamide (**12**) showed only moderate binding at the mH_4R (pK_i = 5.84 ± 0.32), whereas the reported affinity was about two orders of magnitude higher. The obvious low affinity of thioperamide (**12**) at the mH_4R could be the reason why the use of **12** for the non-specific binding in section 3.2.3.2 failed. Clozapine (**18**) showed, as at the hH_4R, also only moderate affinity at the mH_4R (pK_i = 5.18 ± 0.14), which was consistent with the reported affinity (see **Table 3.3**). JNJ 7777120 (**19**) displayed the highest affinity of all investigated ligands (pK_i = 7.40 ± 0.14) at the mH_4R, and the decrease in affinity compared to the hH_4R was very low (cf. **Table 3.1**). The pK_i value at the mH_4R reported by Lim et al. is even by one order of magnitude higher (Lim et al., 2010). VUF 8430 (**20**) bound only with a moderate affinity to the mH_4R (pK_i = 5.89 ± 0.14) and, similar to JNJ 7777120 (**19**), the affinity described in literature was significantly higher (see **Table 3.3**).

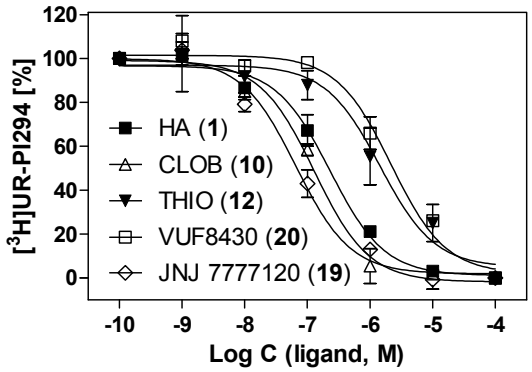

Figure 3.16: Inhibition of [^{3}H]UR-PI294 binding by HA (**1**), CLOB (**10**), THIO (**12**), JNJ 7777120 (**19**) and VUF 8430 (**20**) on HEK293-SF-mH_4R-His_6 cells. Reaction mixtures contained 50 nM [^{3}H]UR-PI294 and ligand concentrations indicated on the abscissa. Data were analyzed by nonlinear regression and best fitted to one-site (monophasic) competition curves. Data points are the mean of at least two independent experiments performed in duplicate.

Table 3.3: pK_i values of reference H_4R ligands determined in competitive binding experiments, using HEK293-SF-mH_4R-His_6 cells and [^{3}H]UR-PI294, in comparison to pK_i values reported in literature.

Ligand	**mH_4R**		
	pK_i		pK_i
	HEK293-SFmH_4R-His_6	N	Reported
Histamine (**1**)	6.89 ± 0.14	2	7.1-7.4[a, b]
5(4)-Methylhistamine (**5**)	5.49 ± 0.46	2	6.8[a]
Clobenpropit (**10**)	7.10 ± 0.06	2	7.3-7.8[a, b]
Thioperamide (**12**)	5.84 ± 0.32	3	7.6[a, b]
Clozapine (**18**)	5.18 ± 0.14	2	5.5[a, b]
JNJ 7777120 (**19**)	7.40 ± 0.14	3	8.4[a]
VUF 8430 (**20**)	5.89 ± 0.14	2	6.7[a]

Mean values ± SEM. N: number of independent experiments performed in duplicate. Data taken from: [^{3}H]histamine binding on HEK293T cell membranes [a] (Lim *et al.*, 2010); [^{3}H]histamine binding on SK-N-MC cell membranes [b] (Liu *et al.*, 2001b).

Additionally, UR-PI294 (**15**), UR-PI376 (**16**) and the stereoisomers of UR-RG98 (**17**, **23** -**25**) as well as of UR-RG94 (**26**-**29**) (cf. **Figure 3.1** and **Figure 3.12**) were investigated in displacement studies using [^{3}H]UR-PI294 and HEK293-SF-hH_4R-His_6 cells. The results are summarized in **Table 3.4**.

UR-PI294 (**15**), UR-PI376 (**16**) and trans-(+)-(1S,3S)-UR-RG98) (**17**) displaced [^{3}H]UR-PI294 from the mH_4R, however, with lower pK_i values in comparison to the hH_4R (see **Figure 3.17**, cf. **Table 3.1**). UR-PI294 (**15**) revealed a ten-fold lower affinity at the mH_4R (pK_i = 7.23 ± 0.08), which was consistent with the K_D value of [^{3}H]UR-PI294 at the mH_4R (cf. **Table 3.2**). UR-PI376 (**16**) showed a decreased affinity at the mH_4R (pK_i = 6.54 ± 0.13) compared to the hH_4R (pK_i = 7.10 ± 0.04); this was expected due to the results from steady state [^{33}P]GTPase assay using Sf9 insect cell membranes either expressing the hH_4R or the mH_4R (Schnell *et al.*, 2011). A marked difference between the human and mouse H_4R orthologs was observed for trans-(+)-(1S,3S)-UR-RG98) (**17**), which bound to the mH_4R with a ten-fold lower affinity (cf. **Table 3.1**). Interestingly, the pK_i value (5.94 ± 0.35) of trans-(-)-(1R,3R)-UR-RG98 (**23**) at the mH_4R was the same as that reported for the hH_4R (Geyer, 2011). cis-(-)-(1S,3R)-UR-RG98 (**24**) and cis-(+)-(1R,3S)-UR-RG98 (**25**) (see **Figure 3.17**) displayed the same affinity at the mH_4R, whereas the hH_4R was found to prefer **25** as recently reported (Geyer, 2011). Among the methyl-substituted cyanoguandines **26-29**, cis-(+)-(1R,3S)-UR-RG94 (**29**) had the highest affinity (pK_i = 6.43 ± 0.02), whereas cis-(-)-(1S,3R)-UR-RG94 (**28**) showed no noteworthy binding at the mH_4R (see **Table 3.4**). The mH_4R affinities of trans-(-)-(1R,3R)-UR-RG94 (**26**) as well as of trans-(+)-(1S,3S)-UR-RG94 (**27**) were very low (pK_i = 5.15 ± 0.00 and pK_i = 4.57 ± 0.53, respectively). The affinity of **27** at the mH_4R was about two orders of magnitude lower compared to the hH_4R (Geyer, 2011).

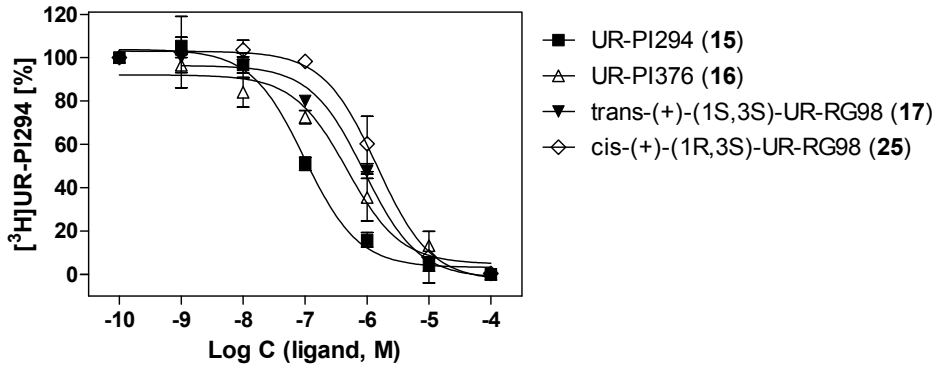

Figure 3.17: Inhibition of [^{3}H]UR-PI294 binding by UR-PI294 (**15**), UR-PI376 (**16**), trans-(+)-(1S,3S)-UR-RG98 (**17**) and cis-(+)-(1R,3S)-UR-RG98 (**25**) in HEK293-SF-mH_4R-His_6 cells. Reaction mixtures contained 50 nM [^{3}H]UR-PI294 and ligand concentrations indicated on the abscissa. Data were analyzed by nonlinear regression and best fitted to one-site (monophasic) competition curves. Data points are the mean of at least two independent experiments, each performed in duplicate.

Table 3.4: pK_i values of guanidine-type H_4R ligands determined in competitive binding experiments using HEK293-SF-mH_4R-His_6 cells and [^{3}H]UR-PI294 as radioligand.

Ligand	**mH_4R**	
	pK_i	N
	HEK293-SF-mH_4R-His_6	
UR-PI294 (**15**)	7.23 ± 0.08	2
UR-PI376 (**16**)	6.54 ± 0.13	2
trans-(+)-(1S,3S)-UR-RG98 (**17**)	6.27 ± 0.05	2
trans-(-)-(1R,3R)- UR-RG98 (**23**)	5.94 ± 0.35	2
cis-(-)-(1S,3R)-UR-RG98 (**24**)	6.07 ± 0.08	2
cis-(+)-(1R,3S)-UR-RG98 (**25**)	6.02 ± 0.27	2
trans-(-)-(1R,3R)-UR-RG94 (**26**)	5.15 ± 0.00	1
trans-(+)-(1S,3S)-UR-RG94 (**27**)	4.57 ± 0.53	3
cis-(-)-(1S,3R)-UR-RG94 (**28**)	< 4	3
cis-(+)-(1R,3S)-UR-RG94 (**29**)	6.43 ± 0.02	2

Mean values ± SEM. N: number of independent experiments performed in duplicate.

3.3 Summary and Conclusion

Stably transfected HEK293T cells are appropriate as expression tool for the human and mouse H_4 receptor. By the treatment with 600 µg/mL of G418, HEK293-SF-h/mH_4R-His_6 cells expressed a defined and constant quantity of the recombinant protein for a long period of time.

[^{3}H]UR-PI294 bound with high affinity to the HEK293-SF-hH_4R-his_6 cells. In competition binding assays the affinity of standard H_4R ligands was determined in a highly reproducible manner. However, not least by the investigation of a high number of diverse ligands, it was shown that the pK_i values of almost every agonist at the hH_4R was lower than reported in broken cell test systems, whereas the pK_i values of every antagonist was either identical or in the same range as the reported data. The discrepancies between agonistic binding data may be caused by the so called GTP-shift, which can arise in intact cells due to high GTP concentration, contrary to broken cell preparations.

After stable transfection of HEK293T cells with the tagged mH_4R, specific binding of [^{3}H]histamine as well as of [^{3}H]UR-PI294 was detected in saturation binding experiments. However, binding of [^{3}H]histamine appeared to be not saturable and [^{3}H]UR-PI294 revealed a substantial decrease in affinity compared to the hH_4R. Affinities of H_4R ligands at the mH_4R were determined by competition binding studies using whole HEK293-SF-mH_4R-His_6 cells and [^{3}H]UR-PI294. However, although [^{3}H]UR-PI294 exhibited high specific activity, the determination and interpretation of binding data proved to be difficult due to the relatively high K_D value of 75 nM. This became obvious from comparison with the very reliable data from competition binding assays at the hH_4R, which bind [^{3}H]UR-PI294 with 10-fold higher affinity. A possible explanation could be a removal of specifically bound radioligand during the washing step, which can occur with low affine radioligands in the used filtration method (Lazareno, 2001). Furthermore, the need to apply 10-fold more radioligand in competition binding assays at the mH_4R compared to the hH_4R increases costs and the amount of radioactive waste. Nevertheless, the established binding assay at the mH_4R with [^{3}H]UR-PI294 will be useful in the search for new pharmacological tools with higher affinity for the mH_4R.

3.4 References

Appl, H.; Holzammer, T.; Dove, S.; Haen, E.; Strasser, A.; Seifert, R. Interactions of recombinant human histamine H(1)R, H(2)R, H(3)R, and H(4)R receptors with 34 antidepressants and antipsychotics. *Naunyn-Schmiedeberg's Arch. Pharmacol.* ***2011,*** 385, 145-70.

Barbier, A. J.; Berridge, C.; Dugovic, C.; Laposky, A. D.; Wilson, S. J.; Boggs, J.; Aluisio, L.; Lord, B.; Mazur, C.; Pudiak, C. M. and others. Acute wake-promoting actions of JNJ-5207852, a novel, diamine-based H_3 antagonist. *Br. J. Pharmacol.* ***2004,*** 143, 649-61.

Bernhardt, G.; Reile, H.; Birnbock, H.; Spruss, T.; Schonenberger, H. Standardized kinetic microassay to quantify differential chemosensitivity on the basis of proliferative activity. *J. Cancer Res. Clin. Oncol.* ***1992,*** 118, 35-43.

Bylund, D. B.; Toews, M. L. Radioligand binding methods: practical guide and tips. *Am. J. Physiol.* ***1993,*** 265, L421-9.

Cheng, Y.; Prusoff, W. H. Relationship between the inhibition constant (K1) and the concentration of inhibitor which causes 50 per cent inhibition (I50) of an enzymatic reaction. *Biochem. Pharmacol.* ***1973,*** 22, 3099-108.

DuBridge, R. B.; Tang, P.; Hsia, H. C.; Leong, P. M.; Miller, J. H.; Calos, M. P. Analysis of mutation in human cells by using an Epstein-Barr virus shuttle system. *Mol. Cell. Biol.* ***1987,*** 7, 379-87.

Geyer, R. Hetarylalkyl(aryl)cyanoguanidines as histamine H_4 receptor ligands: Synthesis, chiral separation, pharmacological characterization, structure-activity and -selectivity relationships. PhD thesis, University of Regensburg, Regensburg, 2011.

Igel, P.; Geyer, R.; Strasser, A.; Dove, S.; Seifert, R.; Buschauer, A. Synthesis and structure-activity relationships of cyanoguanidine-type and structurally related histamine H_4 receptor agonists. *J. Med. Chem.* ***2009a,*** 52, 6297-313.

Igel, P.; Schneider, E.; Schnell, D.; Elz, S.; Seifert, R.; Buschauer, A. N(G)-acylated imidazolylpropylguanidines as potent histamine H_4 receptor agonists: selectivity by variation of the N(G)-substituent. *J. Med. Chem.* ***2009b,*** 52, 2623-7.

Igel, P.; Schnell, D.; Bernhardt, G.; Seifert, R.; Buschauer, A. Tritium-labeled N(1)-[3-(1H-imidazol-4-yl)propyl]-N(2)-propionylguanidine ([(3)H]UR-PI294), a high-affinity histamine H(3) and H(4) receptor radioligand. *ChemMedChem* ***2009c,*** 4, 225-31.

Jablonowski, J. A.; Grice, C. A.; Chai, W.; Dvorak, C. A.; Venable, J. D.; Kwok, A. K.; Ly, K. S.; Wei, J.; Baker, S. M.; Desai, P. J. and others. The first potent and selective non-imidazole human histamine H_4 receptor antagonists. *J. Med. Chem.* ***2003,*** 46, 3957-60.

Kenakin, T. P. 2009. A pharmacology primer : theory, applications, and methods. Amsterdam ; Boston: Academic Press/Elsevier. xix, 389 p. p.

Kitbunnadaj, R.; Hoffmann, M.; Fratantoni, S. A.; Bongers, G.; Bakker, R. A.; Wieland, K.; Jilali, A. e.; De Esch, I. J. P.; Menge, W. M. P. B.; Timmerman, H. and others. New high affinity H_3 receptor agonists without a basic side chain. *Biorg. Med. Chem.* ***2005,*** 13, 6309-6323.

Kitbunnadaj, R.; Zuiderveld, O. P.; Christophe, B.; Hulscher, S.; Menge, W. M.; Gelens, E.; Snip, E.; Bakker, R. A.; Celanire, S.; Gillard, M. and others. Identification of 4-(1H-imidazol-4(5)-ylmethyl)pyridine (immethridine) as a novel, potent, and highly selective histamine H(3) receptor agonist. *J. Med. Chem.* ***2004,*** 47, 2414-7.

Kitbunnadaj, R.; Zuiderveld, O. P.; De Esch, I. J.; Vollinga, R. C.; Bakker, R.; Lutz, M.; Spek, A. L.; Cavoy, E.; Deltent, M. F.; Menge, W. M. and others. Synthesis and structure-activity relationships of conformationally constrained histamine H(3) receptor agonists. *J. Med. Chem.* ***2003,*** 46, 5445-57.

Lamb, M. E.; De Weerd, W. F.; Leeb-Lundberg, L. M. Agonist-promoted trafficking of human bradykinin receptors: arrestin- and dynamin-independent sequestration of the B2 receptor and bradykinin in HEK293 cells. *Biochem. J.* ***2001,*** 355, 741-50.

Lazareno, S. Quantification of receptor interactions using binding methods. *J. Recept. Signal Transduct. Res.* ***2001,*** 21, 139-165.

Lim, H. D.; de Graaf, C.; Jiang, W.; Sadek, P.; McGovern, P. M.; Istyastono, E. P.; Bakker, R. A.; de Esch, I. J.; Thurmond, R. L.; Leurs, R. Molecular determinants of ligand binding to H_4R species variants. *Mol. Pharmacol.* ***2010,*** 77, 734-43.

Lim, H. D.; Jongejan, A.; Bakker, R. A.; Haaksma, E.; de Esch, I. J.; Leurs, R. Phenylalanine 169 in the second extracellular loop of the human histamine H_4 receptor is responsible for the difference in agonist binding between human and mouse H_4 receptors. *J. Pharmacol. Exp. Ther.* ***2008,*** 327, 88-96.

Lim, H. D.; Smits, R. A.; Bakker, R. A.; van Dam, C. M.; de Esch, I. J.; Leurs, R. Discovery of S-(2-guanidylethyl)-isothiourea (VUF 8430) as a potent nonimidazole histamine H_4 receptor agonist. *J. Med. Chem.* ***2006,*** 49, 6650-1.

Lim, H. D.; van Rijn, R. M.; Ling, P.; Bakker, R. A.; Thurmond, R. L.; Leurs, R. Evaluation of histamine H_1-, H_2-, and H_3-receptor ligands at the human histamine H_4 receptor: identification of 4-methylhistamine as the first potent and selective H_4 receptor agonist. *J. Pharmacol. Exp. Ther.* ***2005,*** 314, 1310-21.

Liu, C.; Ma, X.; Jiang, X.; Wilson, S. J.; Hofstra, C. L.; Blevitt, J.; Pyati, J.; Li, X.; Chai, W.; Carruthers, N. and others. Cloning and pharmacological characterization of a fourth histamine receptor (H(4)) expressed in bone marrow. *Mol. Pharmacol.* ***2001a,*** 59, 420-6.

Liu, C.; Wilson, S. J.; Kuei, C.; Lovenberg, T. W. Comparison of human, mouse, rat, and guinea pig histamine H_4 receptors reveals substantial pharmacological species variation. *J. Pharmacol. Exp. Ther.* ***2001b,*** 299, 121-30.

Mahon, M. J. Vectors bicistronically linking a gene of interest to the SV40 large T antigen in combination with the SV40 origin of replication enhance transient protein expression and luciferase reporter activity. *BioTechniques* ***2011,*** 51, 119-28.

Morse, K. L.; Behan, J.; Laz, T. M.; West, R. E., Jr.; Greenfeder, S. A.; Anthes, J. C.; Umland, S.; Wan, Y.; Hipkin, R. W.; Gonsiorek, W. and others. Cloning and Characterization of a Novel Human Histamine Receptor. *J. Pharmacol. Exp. Ther.* ***2001,*** 296, 1058-1066.

Mosandl, J. Radiochemical and luminescence-based binding and functional assays for human histamine receptors using genetically engineered cells. PhD thesis, University of Regensburg, Regensburg, Germany, 2009.

Neumann, D.; Beermann, S.; Seifert, R. Does the Histamine H(4) Receptor Have a Pro- or Anti-Inflammatory Role in Murine Bronchial Asthma? *Pharmacology* ***2010,*** 85, 217-223.

Nguyen, T.; Shapiro, D. A.; George, S. R.; Setola, V.; Lee, D. K.; Cheng, R.; Rauser, L.; Lee, S. P.; Lynch, K. R.; Roth, B. L. and others. Discovery of a Novel Member of the Histamine Receptor Family. *Mol. Pharmacol.* ***2001,*** 59, 427-433.

Oda, T.; Morikawa, N.; Saito, Y.; Masuho, Y.; Matsumoto, S. Molecular Cloning and Characterization of a Novel Type of Histamine Receptor Preferentially Expressed in Leukocytes. *J. Biol. Chem.* ***2000,*** 275, 36781-36786.

Pear, W. S.; Nolan, G. P.; Scott, M. L.; Baltimore, D. Production of high-titer helper-free retroviruses by transient transfection. *Proc. Natl. Acad. Sci. U. S. A.* ***1993,*** 90, 8392-6.

Schneider, E. H.; Schnell, D.; Papa, D.; Seifert, R. High constitutive activity and a G-protein-independent high-affinity state of the human histamine H(4)-receptor. *Biochemistry* ***2009,*** 48, 1424-38.

Schneider, E. H.; Seifert, R. Histamine H(4) receptor-RGS fusion proteins expressed in Sf9 insect cells: a sensitive and reliable approach for the functional characterization of histamine H(4) receptor ligands. *Biochem. Pharmacol.* ***2009,*** 78, 607-16.

Schnell, D.; Brunskole, I.; Ladova, K.; Schneider, E. H.; Igel, P.; Dove, S.; Buschauer, A.; Seifert, R. Expression and functional properties of canine, rat, and murine histamine H(4) receptors in Sf9 insect cells. *Naunyn-Schmiedeberg's Arch. Pharmacol.* ***2011,*** 383, 457-70.

Shyu, J. F.; Zhang, Z.; Hernandez-Lagunas, L.; Camerino, C.; Chen, Y.; Inoue, D.; Baron, R.; Horne, W. C. Protein kinase C antagonizes pertussis-toxin-sensitive coupling of the calcitonin receptor to adenylyl cyclase. *Eur. J. Biochem.* ***1999,*** 262, 95-101.

van Rijn, R. M.; Chazot, P. L.; Shenton, F. C.; Sansuk, K.; Bakker, R. A.; Leurs, R. Oligomerization of Recombinant and Endogenously Expressed Human Histamine H_4 Receptors. *Mol. Pharmacol.* ***2006,*** 70, 604-615.

Zhao, C.; Sun, M.; Bennani, Y. L.; Gopalakrishnan, S. M.; Witte, D. G.; Miller, T. R.; Krueger, K. M.; Browman, K. E.; Thiffault, C.; Wetter, J. and others. The alkaloid conessine and analogues as potent histamine H_3 receptor antagonists. *J. Med. Chem.* ***2008,*** 51, 5423-30.

Zhu, Y.; Michalovich, D.; Wu, H.-L.; Tan, K. B.; Dytko, G. M.; Mannan, I. J.; Boyce, R.; Alston, J.; Tierney, L. A.; Li, X. and others. Cloning, Expression, and Pharmacological Characterization of a Novel Human Histamine Receptor. *Mol. Pharmacol.* ***2001,*** 59, 434-441.

Chapter 4

Development of luminescence based reporter gene assays for the human, mouse and rat histamine H_4 receptor

4.1 Development of a reporter gene assay for the human histamine H_4 receptor

4.1.1 Introduction

A reporter gene assay provides a highly sensitive, reliable and convenient method for the measurement of functional response to $G\alpha_s$, $G\alpha_{i/o}$ and $G\alpha_q$ coupled GPCRs (Tang *et al.*, 2004). Reporter gene assays are based on the modulation of transcriptions factors by GPCR-signaling. The binding of these factors to regulatory elements in the promoter region of a target gene causes an enhanced or repressed transcription rate of the gene. In the genetically engineered cells, used for a reporter gene assay, the transcription of the reporter gene is under control of a promoter capable of binding a specified transcription factor. The choice of the promoter is determined by the GPCR signaling pathway of interest (for detailed information on promoters and their suitability for the different signaling pathways see (Hill *et al.*, 2001). For instance, the reporter gene encoding for luciferase is very often used, as the enzymatic activity of the gene product can be conveniently assayed in the cell lysate.

The H_4R is coupling to $G\alpha_{i/o}$ G-proteins which mediate inhibition of the adenylyl cyclase (AC), resulting in a decrease in cAMP formation. Therefore, in case of the H_4R, the cAMP response element (CRE) has been used as the preferred promoter, for instance, to control β-galactosidase gene transcription in SK-NM-C cells expressing the H_4R (Lim *et al.*, 2005; Liu *et al.*, 2001a; Liu *et al.*, 2001b). In order to detect a negative regulation of the AC, the reporter gene assay must be performed in the presence of the diterpene forskolin (see **Figure 4.1**), a direct stimulator of the AC (Seamon *et al.*, 1981), to raise the cAMP level.

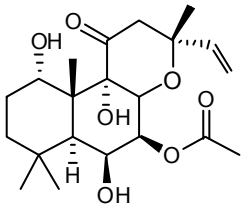

Figure 4.1: Chemical structure of the diterpene forskolin.

A scheme showing the H_4R signaling pathway monitored by a CRE-linked reporter gene is given in **Figure 4.2** A. Agonist activation of the H_4R decreases forskolin stimulated luciferase activity, reflecting the inhibitory quality of the $G\alpha_{i/o}$ protein. Inverse agonists shift the constitutively active receptors to an inactive conformation, which results in a lowering of the (constitutive) inhibition of the AC and, subsequently, in an increased forskolin stimulated luciferase activity. Since antagonists do not change the receptor state, the luciferase activity remains at the level of forskolin stimulation (see **Figure 4.2** B).

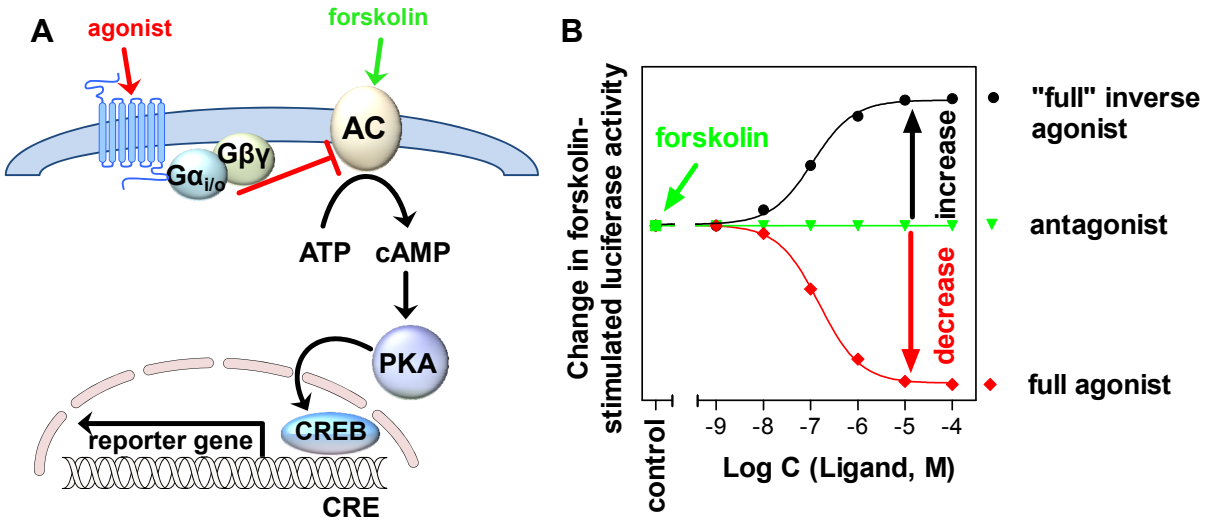

Figure 4.2: Schematic illustration of a CRE-controlled reporter gene assay. The adenylyl cyclase (AC) is directly stimulated by forskolin to allow for the quantification of $G\alpha_{i/o}$-mediated response. The AC produces cAMP, which activates protein kinase A (PKA). The catalytic subunit of PKA gets into the nucleus and phosphorylates a CRE binding protein (CREB), enabling this protein to bind to CRE in the promoter of the reporter gene and to induce transcription (A). Activation of the $G_{i/o}$ coupled H_4R by agonists results in inhibition of the AC and thus in a decreased transcription, whereas increased transcription refers to inverse agonism. Forskolin-induced luciferase activity in cells in the absence of H_4R ligands serves as control (B).

Furthermore, two luciferase reporter gene assays in HEK293 cells were described, where the luciferase is under the control of a multiple response element (MRE)/ CRE (Zhu *et al.*, 2001) or of a serum response element (SRE) (Jiang *et al.*, 2008; Yu *et al.*, 2010). In case of the latter, the H_4R was co-expresssed along with the chimeric Gα-protein qi5-HA in order to redirect the H_4R signaling to the $G\alpha_q$-mediated mitogen-activated protein (MAP) kinase pathway, which in turn can activate the SRE. Additionally, the co-expression with the chimeric Gα-protein qi5-HA re-directed the H_4R to an intracellular calcium response, which can be measured using the fluorimetric imaging plate reader (FLIPR^{TM}) (Liu *et al.*, 2001b; Morse *et al.*, 2001; Strakhova *et al.*, 2009; Zhu *et al.*, 2001). More proximal functional assays for the H_4R are the steady-state [^{33}P]GTPase activity (Igel *et al.*, 2009b; Schneider and Seifert, 2009) and the [^{35}S]GTPγS assay binding assay (Geyer and Buschauer, 2011; Morse *et al.*, 2001; Sander *et al.*, 2009) on membrane preparations of Sf9 insect cells co-expressing the H_4R with the G-protein $G\alpha_{i2}$ and $G\beta_1\gamma_2$ subunits. Furthermore, functional assays including chemotaxis and changes of cellular calcium levels in human eosinophils, endogenously expressing the hH_4R, were described (Buckland *et al.*, 2003; Ling *et al.*, 2004; O'Reilly *et al.*, 2002; Reher *et al.*, 2012). However, these assays are hampered by poor availability and an elaborate preparation of the human eosinophils (Reher *et al.*, 2012). Another study used mouse mast cells, endogenously expressing the H_4R, for the detection of H_4R mediated chemotaxis and calcium mobilization (Hofstra *et al.*, 2003).

The aim of this work was to develop a CRE-directed luciferase reporter gene assay in HEK293T cells, stably expressing the hH_4R. As a distal readout, reporter gene assays are characterized by signal amplification between ligand binding and transcription. This may lead to increased agonist efficacy (George *et al.*, 1997). Therefore, the reporter gene assay was validated by evaluating a set of H_4R ligands (cf. section 3.1.2.3). The determined potencies and efficacies were, if possible, compared with results from a CRE-driven β-galactosidase reporter gene assay in SK-N-MC/hH_4R cells (Lim *et al.*, 2005) and with results from the (more proximal) functional assays on Sf9 cell membranes (Schnell *et al.*, 2011; Wifling, 2012). For the determination of possible non-H_4R mediated ligand effects, HEK293T reporter gene cells were established, which stably express the CRE-directed luciferase reporter gene, but are devoid of the recombinant GPCR. This enables control experiments which may be necessary to exclude interferences with the signaling cascade caused by factors other than the GPCR of interest. For example, explicit evidence for an endogenous β_2-adrenergic receptor in HEK293T cells, which was additionally active in a MRE (multiple response element)/CRE-directed luciferase reporter gene assay, was reported recently (Fitzgerald *et al.*, 1999; Zhu *et al.*, 2001). Furthermore, the engineered cells can be used as "building blocks", since they are suitable for the transfection with every $G\alpha_i$ coupled GPCR of interest. This can lead to a tremendous saving of time in the development of the reporter gene assay as well as to improved comparability of functional data. Moreover, binding and reporter gene assays can be performed on the same cellular system.

The concentration of forskolin used for pre-stimulation depends on the cell type (Williams, 2004) and should correspond to the EC_{50} value of forskolin in the assay system (Rodrigues and McLoughlin, 2009). Therefore, the potency of forskolin was determined to optimize assay sensitivity. Furthermore, the use of the phosphodiesterase (PDE) inhibitor 3-isobutyl-1-methylxanthine (IBMX) for stabilizing the cAMP level was evaluated. Due to the protracted gene transcription, incubation periods of at least 4 - 6 h are required (Hill *et al.*, 2001). However, this raises the risk of agonist mediated receptor desensitization, which can lead to a decrease in agonist potencies (Hill *et al.*, 2001): Therefore, the time course of the luciferase reporter gene transcription was determined to find the minimum incubation period required for appropriate signal strength. The luciferase enzyme from the American firefly *Photinus pyralis* catalyzes in a multistep reaction the formation of oxyluciferin from the natural substrate D-Luciferin, accompanied by emission of yellow/green light (560 nm) (see **Figure 4.3**). After injection of the substrate light is emitted, the intensity of which decreases during several seconds and reaches a plateau. The luciferase reaction is highly efficient, achieving high quantum yields for bioluminescence and a high signal-to-noise ratio, since cells or cell lysates normally do not emit interfering light (Bronstein *et al.*, 1994; Shinde *et al.*, 2006).

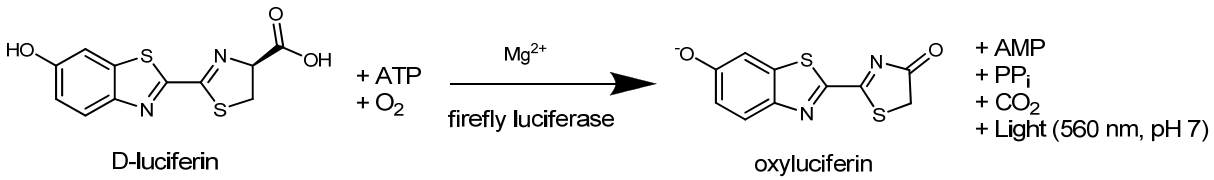

Figure 4.3: Conversion of D-luciferin by firefly luciferase to oxyluciferin (according to (Shinde *et al.*, 2006)).

In order to increase the throughput, the reporter gene assay was adapted to the 96-well format. Furthermore, all used buffers and solutions were self-made to keep the costs down.

4.1.2 Materials and Methods

4.1.2.1 Chemosensitivity assay

To determine the sensitivity of HEK293-SF-hH$_4$R-His$_6$ cells to hygromycin B (A.G. Scientific, San Diego, USA) in the presence of 600 µg/mL of G418, a chemosensitivity assay was performed as described in section 3.1.2.2.

4.1.2.2 Preparation of the pGL4.29[luc2P/CRE/Hygro] vector (Maxi-Prep) and sequencing

The pGL4.29[luc2P/CRE/Hygro] vector (see **Figure 4.4**) was purchased from Promega, Mannheim, Germany. The preparation of media and agar plates was performed as described in section 3.2.2.1.4. The transformation of competent *E. coli* was carried out according to section 3.2.2.1.5. For glycerol culture and large scale preparation of plasmid DNA (Maxi-Prep) cf. section 3.2.2.1.6. The determination of DNA concentration was performed as described in section 3.2.2.1.2. The sequencing (performed by Entelechon) of the DNA obtained from large scale preparation confirmed the identity of pGL4.29[luc2P/CRE/Hygro].

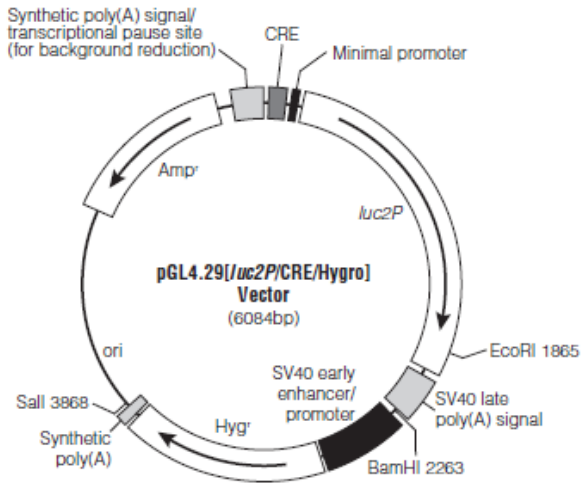

Figure 4.4: Map of pGL4.29[luc2P/CRE/Hygro] vector (adopted from the manual provided by Promega). The luc2P gene, which encodes the luciferase, is under control of CRE. The hygromycin resistance (Hyg) enables the stable expression in mammalian cells, whereas ampicillin resistance (Amp) enables selection of transformed competent bacteria.

4.1.2.3 Stable transfection of HEK293-SF-hH$_4$R-His$_6$ cells with the pGL4.29[luc2P/CRE/Hygro] vector

HEK293-SF-hH$_4$R-His$_6$ cells were cultured as described in section 3.1.2.1. The transfection was performed according to section 3.2.2.2. For an initial selection of the 4:2 and 6:2 transfection mixture, the medium was replaced by DMEM containing 10 % FCS, 600 µg/mL

of G418 and 100 µg/mL of hygromycin B. After 72 h, the HEK293-SF-hH_4R-His_6-CRE-Luc cells were passaged and then maintained in DMEM containing 10 % FCS, 600 µg/mL of G418 and 200 µg/mL of hygromycin B.

4.1.2.4 Stable transfection of HEK293T cells with the vector pGL4.29[luc2P/CRE/Hygro]

Culture of HEK293T cells cf. section 3.1.2.1. The transfection was performed as described in section 3.2.2.2 with the exception that the ratios of transfection reagent (µL) to DNA amount (µg) were 6:2 and 8:2. The transfectants were selected and maintained in DMEM containing 10 % FCS, 600 µg/mL of G418 and 200 µg/mL of hygromycin B.

4.1.2.5 Luciferase reporter gene assay in the 24-well format

The reporter gene assay was performed with some modifications as described recently (Mosandl, 2009). Approx. 0.5 – 1.0 · 10^5 HEK293-SF-hH_4R-His_6-CRE-Luc cells were seeded per cavity of a 24-well plate in DMEM supplemented with 10 % FCS and selection antibiotics (600 µg/mL of G418 and 200 µg/mL of hygromycin B). The cells were grown to 100 % confluency within 4 - 5 days at 5 % CO_2 and 37 °C in a water saturated atmosphere. In order to start the assay, the medium was carefully removed by suction and replaced by 495 µL of fresh medium (same composition as described above) including histaminergic ligands. To determine the response to forskolin, medium without histaminergic ligands, containing 5 µL of a hundred-fold concentrated forskolin (Sigma) solution, prepared in 50 % (v/v) DMSO, was added for pre-stimulation of the AC. Forskolin-free wells served for the determination of the basal luciferase expression. After 5 h of incubation under the above mentioned culture conditions, the medium was removed again, and the cells were washed once with 500 µL of PBS. 100 µL of lysis buffer (Biotium, Hayward, USA) were added to each well, and the cells were lysed for 30 min under constant shaking (150 rpm). For the preparation of luminescence measurements, 20 µL of the lysate were transferred into luminometer tubes, and the luminometer Lumat LB 9501(Berthold Technologies, Bad Wildbad, Germany) was primed with a D-luciferin potassium salt (Synchem, Felsberg, Germany) solution (0.2 mg/mL) in luciferase assay buffer (Biotium). Light emission was induced by successive injection of 100 µL of the D-luciferin solution into each luminometer tubes. The luminescence signal was measured for 10 s and expressed as relative light units [RLU]. For analysis, the basal RLUs were subtracted from each value and finally normalized to total protein content, which was quantified by Bradford's protein assay. For this purpose 5 µL of the lysate were diluted with 95 µL of Millipore water directly in a cuvette. The sample was finalized by adding 1 mL of the 1:5 diluted Protein Assay Dye reagent Concentrate (Bio-Rad Laboratories) into the cuvette.

After mixing and incubating for 10 min, absorbance at 595 nm was determined by VIS spectroscopy. The protein amounts were calculated by means of a linear calibration curve determined with HSA (Behringwerke, Marburg, Germany). Finally, the data were analyzed by nonlinear regression and best fitted to sigmoidal concentration response curve. Each experiment was performed in triplicate.

4.1.2.6 Luciferase reporter gene assay in the 96-well format

4.1.2.6.1 Preparation of stock solutions, dilution series and buffers

Forskolin stock solution was prepared in 100 % DMSO. All forskolin dilutions were freshly made in DMEM supplemented with 10 % FCS and either 1 % DMSO or 10 % DMSO. Dilution series of compounds **1**–**15** and **18**–**20** were prepared in DMEM supplemented with 10 % FCS, whereas dilution series of **16**, **17** and **23**–**29** contained additionally 10 % DMSO.

The lysis buffer was prepared as recently described (Memminger, 2009) and stored at 4 °C (see **Table 4.1**). The luciferase assay buffer was made as shown in **Table 4.2** and stored at 4 °C (Ma *et al.*, 1998). Tricine (N-[2-hydroxy-1,1-bis(hydroxymethyl)ethyl]glycine), EGTA (ethyleneglycoltetraacetic acid), Gly-Gly (Glycyl-glycine), ATP (adenosin 5'-triphosphate disodium salt) and DTT (dithiotreitol) were from Sigma. Glycerol 87 %, $MgSO_4 \cdot 7H_2O$ and KH_2PO_4 were from Merck. Triton™ X-100 was from Serva. All stock solutions for the buffers were prepared in Millipore water, except for the D-Luciferin stock solution, which was made in 25 mM tricine (pH7.8) and 10 mM DTT.

Table 4.1: Composition and preparation of the lysis buffer.

Ingredient	Stock concentration	Stock solution	Final concentration
Tricine	250 mM (pH 7.8)[b]	10 mL	25 mM
Glycerol	87 % (v/v)[a]	11.15 mL	10 % (v/v)
EGTA	0.1 M (pH 7.8)[b]	2 mL	2 mM
Triton™ X-100	100 %[a]	1 mL	1 % (v/v)
$MgSO_4 \cdot 7H_2O$	0.5 M[b]	1 mL	5 mM
H_2O		to final 100 mL	
Added directly before use to give a volume of 10 mL:			
DTT	1 M[c]	10 µL	1 mM

Storage temperature: [a] RT; [b] 4 - 8 °C; [c] -20 °C.

Table 4.2: Composition and preparation of the luciferase assay buffer.

Ingredient	Stock concentration	Stock solution	Final concentration
Gly-Gly	1 M[a]	12.5 mL	25 mM
$MgSO_4 \cdot 7H_2O$	1 M[a]	7.5 mL	15 mM
KH_2PO_4	1 M (pH 7.8)[a]	7.5 mL	15 mM
EGTA	0.1 M (pH7.8)[a]	20 mL	4 mM
H_2O		to final 500 mL	
	Added directly before use to 10 mL:		
ATP	100 mM[b]	200 µL	2 mM
DTT	1 M[b]	20 µL	2 mM
D-Luciferin	10 mg/mL[1, c]	200 µL	0.2 mg/mL

[1] Stock solution was prepared in 25 mM of tricine (pH7.8) and 10 mM of DTT.
Storage temperature: [a] 4 – 8 °C; [b] -20 °C; [c] -80 °C.

4.1.2.6.2 Preparation of the cells

A suspension of reporter gene cells (HEK293-SF-hH_4R-His_6-CRE-Luc or HEK293-CRE-Luc) in DEMEM + 10 % FCS (devoid of selection antibiotics) with a density of approx. $1.2 \cdot 10^6$ cells/mL was prepared in a crystallization dish. In order to keep a homogenous distribution of the cells, the cell suspension was continuously stirred. 160 µL or 180 µL of the suspension were seeded per well on a flat-bottomed 96-well plate (Greiner). The cells were allowed to adhere during the following 17 h at 37 °C, 5 % CO_2 and water saturated atmosphere.

4.1.2.6.3 Determination of hH_4R ligand activity

20 µL of a H_4R ligand solution and 20 µL of a forskolin solution (4 µM, 1 % DMSO) were successively added to 160 µL of cell culture medium per well (c.f. section 4.1.2.6.2) to a final volume of 200 µL. For assays performed in the agonist mode, only forskolin was added, whereas in the antagonist mode the forskolin solution was supplemented with 1 µM of histamine (**1**). All added solutions were diluted 1:10 within the assay. The cells were incubated for 5 h at 37 °C, 5 % CO_2 and water saturated atmosphere. After measuring of the luminescence values (cf. section 4.1.2.6.7), the basal luciferase activity was subtracted from each value by Microsoft ® Office Excel 2007 before the data were transferred to GraphPad Prism® 5.04. EC_{50} values (molar concentration of agonist causing 50 % of the maximal response) and IC_{50} values (molar concentration required to reduce the agonist response by half) were analyzed by nonlinear regression and best fitted to sigmoidal concentration-response curves in GraphPad Prism® 5.04. IC_{50} values were converted to K_B values (dissociation constant of the antagonist-receptor complex) using the Cheng-Prussoff equation (Cheng and Prusoff, 1973) (see equation 3 in section 3.1.2.4). The intrinsic activity

of ligands was referred to the maximal response to histamine (**1**), defined as α = 1 (full agonist). Agonist potencies were represented as pEC_{50} values (negative decadic logarithm of the EC_{50} value) and antagonist affinities were given as pK_B values (negative decadic logarithm of the K_B value). Measured RLUs were converted to percental values referred to the span between the maximum effect induced by forskolin and the residual luciferase activity in the presence of histamine at the highest tested concentration. All presented data are mean values ± SEM of N independent experiments performed in triplicate.

4.1.2.6.4 Determination of non-H_4R-mediated ligand effects

The procedure was the same as described in section 4.1.2.6.3, but "reporter gene cells" devoid of H_4R, i. e. HEK293-CRE-Luc cells, were used. All RLUs were referred to the luciferase activity at 1 µM forskolin, which was used for pre-stimulation and set at 100 %. If non-H_4R mediated effects were detected, the corresponding ligand concentrations were excluded from EC_{50} calculations.

4.1.2.6.5 Determination of the optimal forskolin concentration

20 µL of a tenfold concentrated forskolin solution (containing 10 % DMSO) were added to 180 µL of cell culture medium per well (c.f. section 4.1.2.6.2). The cells were incubated for 5 h at 37 °C and 5 % CO_2 in a water saturated atmosphere. Forskolin was investigated at concentrations up to 10 µM to determine the EC_{50} value. For measurement of luminescence cf. 4.1.2.6.7, for data processing and EC_{50} calculation cf. section 4.1.2.6.3. On a percental scale, basal luciferase expression was defined as 0 % and the maximum forskolin effect at 10 µM as 100 %. EC_{50} values are mean values of N independent experiments performed in triplicate.

4.1.2.6.6 Monitoring the time course of luciferase expression

20 µL of a forskolin solution (100 µM, 1% DMSO) were added to 180 µL of cell culture medium per well (c.f. section 4.1.2.6.2). The luciferase expression was stopped and luminescence was measured (cf. 4.1.2.6.7) after 0.0, 0.5, 1.0, 2.0, 3.0, 5.0, 8.0 and 24 h. The basal luciferase activity was subtracted from each signal, and the obtained values were plotted against the time.

4.1.2.6.7 Measurement of luminescence with a microplate reader

After incubation, the medium was discarded, the cells were washed once with 100 µL of PBS and lysed in 40 µL of lysis buffer under shaking (180 rpm) for 45 – 60 min. For luminescence measurement, 20 µL of each lysate was transferred into a white flat-bottomed 96-well plate (Greiner) and the GENios Pro™ microplate reader (Tecan, Salzburg, Austria) was primed with the luciferase assay buffer. Light emission was induced by the injection of 80 µL of the luciferase assay buffer into each well. RLUs were measured for 10 s.

4.1.2.7 Aminopyrimidines

ST-1006 (**30**) and ST-10012 (**31**) were kindly provided by Prof. Dr. Holger Stark (Institute of Pharmacy and Medicinal Chemistry, Johann Wolfgang Goethe University, Frankfurt am Main, Germany). Functional activities of the aminopyrimidines were investigated in the luciferase reporter gene assay. The stock solutions (10 mM) were made in 50 % DMSO. The solution series were prepared in DMEM supplemented with 10 % FCS and 10 % DMSO.

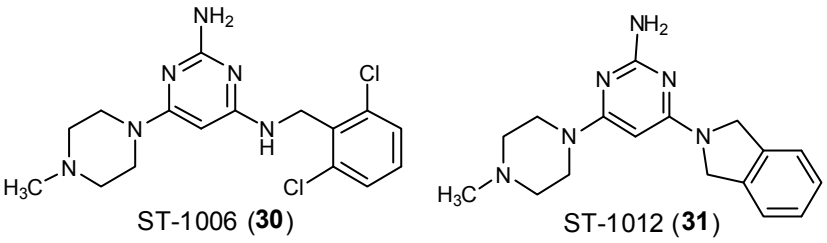

ST-1006 (**30**) ST-1012 (**31**)

Figure 4.5: Chemical structures of ST-1006 and ST-1012.

4.1.3 Results and discussion

4.1.3.1 Effect of hygromycin B on HEK293-SF-hH$_4$R-His$_6$ cells

The pGL4.29[luc2P/CRE/Hygro] vector contains a resistance gene for hygromycin to allow for the selection of the transfected HEK293-SF-hH$_4$R-His$_6$ cells. In literature, the concentration of hygromycin B used for selection ranges from 100 µg/mL (Werthmann *et al.*, 2012) to 500 µg/mL (Eishingdrelo *et al.*, 2011). In order to find the sufficient concentration of hygromycin B, a chemosensitivity assay was performed with HEK293-SF-hH$_4$R-His$_6$ cells. In addition to different concentrations of hygromycin B, the cells (including control) were permanently exposed to 600 µg/mL of G418 (see **Figure 4.6**). At 10 µg/mL of hygromycin B the cells recovered completely after initial impairement (cytotoxic effect). A concentration of 50 µg/mL was also insufficient for selection, since the cells started to grow again after five days. However, the cells were fatally damaged at concentrations of 100 µg/mL to 400 µg/mL of hygromycin B after two days of incubation (cytocidal effect). Since the cytocidal effect at 200 µg/mL and 400 µg/mL was almost equal and clearly higher than at 100 µg/mL, a concentration of 200 µg/mL of hygromycin B was chosen for the selection of the transfected HEK293-SF-hH$_4$R-His$_6$ cells.

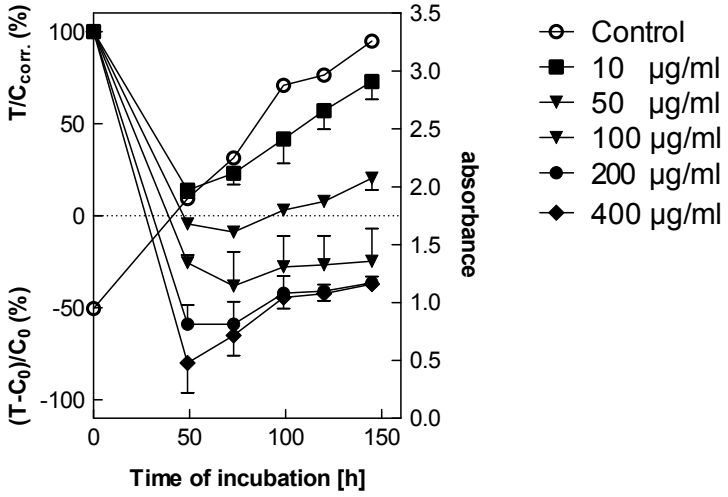

Figure 4.6: Cytotoxic effect of hygromycin B on proliferating HEK293-SF-hH$_4$R-His$_6$ cells in the presence of 600 µg/mL of G418. Crystal violet assay (mean values ± SD (n = 16)).

4.1.3.2 Testing and selection of the HEK293-SF-hH$_4$R-His$_6$-CRE-Luc cells

After transfection of the HEK293-SF-hH$_4$R-His$_6$ cells with pGL4.29[luc2P/CRE/Hygro], the transfectants (4:2 and 6:2 transfection batches) were evaluated regarding luciferase expression upon forskolin stimulation. As shown in **Figure 4.7**, forskolin activated AC and thus luciferase expression in HEK293-SF-hH$_4$R-His$_6$-CRE-Luc cells in a concentration dependent manner, i.e. the gene expression was under the control of the CRE. A difference between the two transfection batches was already observed at this time, since the maximum expression at 10 µM of forskolin at a DNA to fugene ratio of 6:2 was about five times higher than for the 4:2 batch.

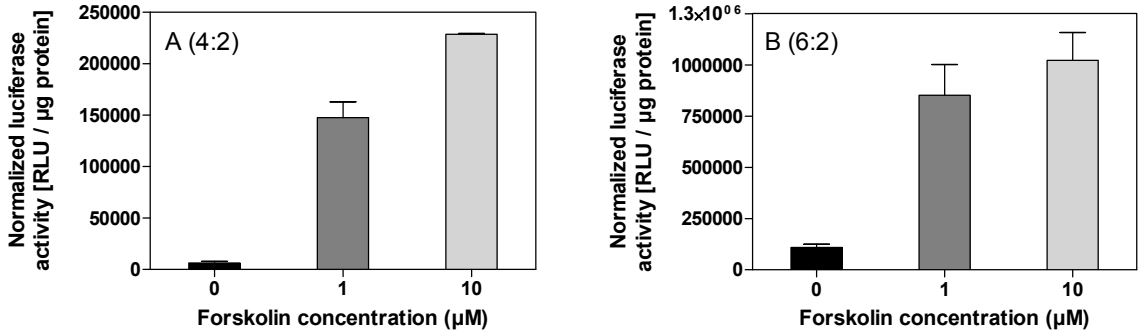

Figure 4.7: Stimulation of the luciferase expression by forskolin activated adenylyl cyclase in HEK293-SF-hH$_4$R-His$_6$-CRE-Luc cells performed in 24-well format. 4:2 transfection batch (A). 6:2 transfection batch (B).

The next step was to test, if the activated AC was influenced by the G$\alpha_{i/o}$ coupled hH$_4$R. For this purpose the cells were co-incubated with 100 nM of forskolin and either 100 µM of the endogenous full agonist histamine (**1**) or 100 µM of the inverse agonist thioperamide (**12**). Both transfection batches resulted in cellular systems enabling the detection of distinct hH$_4$R mediated effects (see **Figure 4.8**). In the presence of histamine (**1**), the forskolin-induced stimulation of the AC was counteracted by hH$_4$R-mediated G$\alpha_{i/o}$ activation and, thus, the transcription of the reporter gene was almost completely inhibited. By contrast, thioperamide (**12**) reduced the portion of constitutively active hH$_4$Rs, resulting an additional stimulation of the AC and in an increased reporter gene expression. The pronounced forskolin effect in the 6:2 cells became obvious again. In the present experiment the normalized 6:2 RLU values were about ten times higher compared to the 4:2 approach. Therefore, the 6:2 cells were preferred to perform the reporter gene assay with the hH$_4$R.

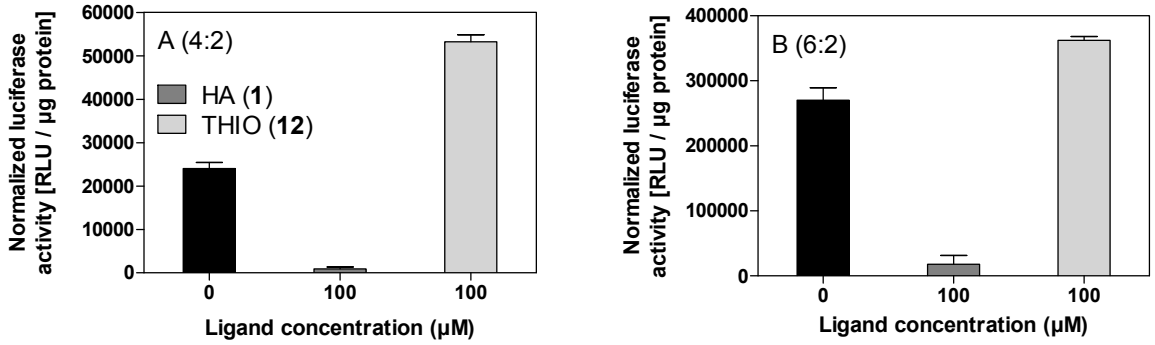

Figure 4.8: $G\alpha_{i/o}$-mediated hH_4R response in the 4:2 transfection batch (A) and 6:2 transfection batch (B). Effects of the agonist histamine (HA, **1**) and the inverse agonist thioperamide (THIO, **12**) upon pre-stimulation by 100 nM of forskolin in HEK293-SF-hH_4R-His_6-CRE-Luc cells.

4.1.3.3 Adaptation of the luciferase reporter gene assay to the 96-well format

To keep the costs of the luciferase reporter gene assay down, all buffers and solution were home-made as described in section 4.1.2.6.1. The use of Triton™ X100 in the lysis buffer offered the advantage that the detergent increased the intensity and duration of the firefly luciferase-catalyzed reaction above the critical micelle concentration. The micelles are thought to sequester or separate the oxyluciferin product (cf. **Figure 4.3**), which otherwise inhibits the luciferase activity (Kricka and De Luca, 1982; Williams *et al.*, 1989).

In order to increase the throughput, the luciferase reporter gene assay was adapted to the 96-well format. Firstly, to avoid a complete replacement of the medium at the beginning of the reporter gene assay (cf. section 4.1.2.5), the volume of the cell suspension was reduced to 160 µL and 180 µL. By addition of 20 µL of a tenfold feed solution (of forskolin and H_4R ligands) each sample was finally filled up to 200 µL and the feed solution was diluted 1:10 within the assay. Secondly, the need for normalization based on the protein content was evaluated. Usually, the protein determination according to Bradford was performed in single cuvettes, which promised no high throughput. Additionally, there was a serious interference of the detergent Triton™ X-100 in the lysis buffer with Bradford's protein assay in the microplate format (data not shown). Potencies and intrinsic activities of histamine (**1**) and thioperamide (**12**) were determined with and without normalization to the total protein content of HEK293-hH_4R-His_6-CRE-Luc cells (see **Figure 4.9**). The cells were seeded two days prior the assay in a 96-well plate. The comparison of the normalized with the non-normalized pEC_{50} and α values showed no significant differences. The curves presenting the data as percental values were almost completely superimposable (see **Figure 4.9**). Therefore, the normalization of the luminescence values was omitted in subsequent reporter gene assays. However, in order to prevent noteworthy differences in cell number, the incubation of the

cells in the 96-well plate before the assay was shortened to 17 h. In the remaining incubation time the cells adhere to surface and do not markedly proliferate.

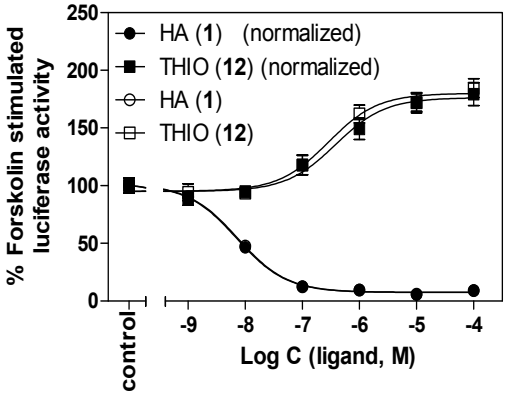

Ligand	hH_4R			
	With normalization		Without normalization	
	pEC_{50}	α	pEC_{50}	α
HA (**1**)	8.55 ± 0.40	1.00	8.45 ± 0.32	1.00
THIO (**12**)	6.69 ± 0.27	-0.87	6.76 ± 0.21	-0.89

Figure 4.9: Representative reporter gene assay using a 96-well plate with histamine (HA, **1**) and thioperamide (THIO, **12**) in HEK293-SF-hH_4R-His_6-CRE-Luc cells. The cells were seeded two days prior to the assay. The luciferase expression was pre-stimulated with 500 nM of forskolin, and the incubation time was 5 h. The response to forskolin was defined as 100 %. The luminescence values were normalized according to section 4.1.2.5 or not before they were analyzed by nonlinear regression and best fitted to sigmoidal concentration-response curves. The pEC_{50} values are the means ± SEM of two independet experiments performed in triplicate.

The volume of the lysis buffer per well was reduced from 100 µL to 40 µL as well as the injection volume of the luciferase assay buffer from 100 µL to 80 µL, which contributes to the lower cell number. By analogy with the measurements unsing a luminometer, the RLUs were measured for 10 s with the microplate reader.

4.1.3.4 Optimization of the period of incubation

In literature, the incubation period for luciferase reporter gene assays ranges from 4 h (Kemp *et al.*, 1999) to 8 h (Li *et al.*, 2007). For optimization, the time course of the luciferase expression in HEK293-SF-hH_4R-His_6-CRE-Luc cells was investigated. Luciferase gene transcription was stimulated with 10 µM of forskolin, and the cells were lysed after various incubation periods as shown in **Figure 4.10**. After a latency period of 0.5 h, expression steeply increased until 5 h. The maximum was reached after a period of 8 h and sustained for a period of 24 h. Therefore, an incubation period of 5 h appeared to be sufficient, particularly as 88 % of the maximum expression was reached. Furthermore, longer incubation periods carry the risk of receptor desensitization by agonists.

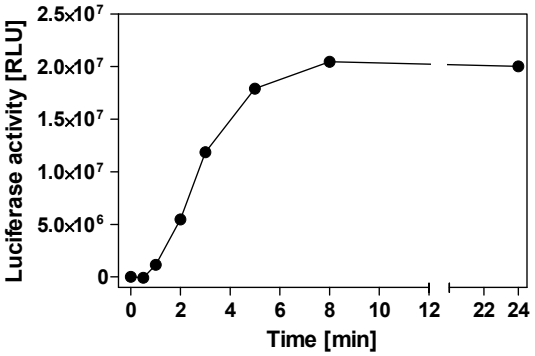

Figure 4.10: Representative time course of luciferase expression in HEK293-hH_4R-His_6-CRE-Luc cells after the stimulation with 10 µM of forskolin. Luciferase activity was determined after the indicated incubation periods (mean values ± SEM; n = 9).

4.1.3.5 Optimization of pre-stimulation with forskolin

In literature, the concentration of forskolin used in reporter gene assays for $G\alpha_{i/o}$ coupled GPCRs ranges from 500 nM (Kemp *et al.*, 1999) to 10 µM (Liu *et al.*, 2001a). To optimize assay performance, the pEC_{50} value of forskolin in the cAMP reporter gene assay system was determined (Rodrigues and McLoughlin, 2009). Furthermore, the use of the universal PDE inhibitor IBMX was evaluated.

HEK293-SF-hH_4R-His_6-CRE-Luc cells were incubated with increasing forskolin concentrations (see **Figure 4.11** A). Forskolin stimulated luciferase expression in a concentration dependent manner up to a concentration of 10 µM. High forskolin concentrations caused a decrease in luciferase expression as already described for several cell types expressing the luciferase gene reporter (George *et al.*, 1997; Kemp *et al.*, 2002; Stroop *et al.*, 1995). To exclude the possibility that the effect arose from limited solubility of forskolin, the dilutions were freshly prepared for every assay. Furthermore, the wells were monitored in terms of the presence of forskolin precipitates during the assay by a light microscope. The cell viability was not apparently affected by forskolin, since the cell layer remained intact during the washing step. Therefore, intracellular mechanisms, like, for example, an alteration of the PDE activity may have caused the downturn. However, the decline of the concentration response curve was not prevented by co-incubation with 50 µM of the PDE inhibitor IBMX (see **Figure 4.11** B). The curve was shifted to the left, so that the maximum was already reached at 3.2 µM, and the downturn started at 10 µM of forskolin. Further investigations by Kemp et al. showed that the activitation of the induceable cAMP early repressor (ICER) was responsible for the negative regulation of luciferase gene expression in CHO cells (Kemp *et al.*, 2002), suggesting that also the activation of endogenous ICER's provoked the downregulation in the present reporter gene assay in HEK293T cells.

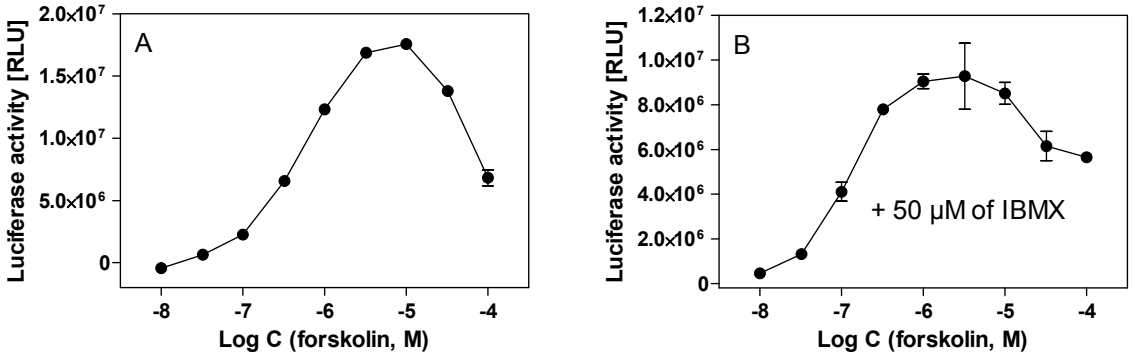

Figure 4.11: Forskolin-stimulated luciferase expression in HEK293-SF-hH_4R-His_6-CRE-Luc cells. Representative "bell-shaped" concentration response curve (A). Representative concentration-response curve in the presence of the PDE inhibitor IBMX, i.e. forskolin solutions were supplemented with 500 µM of IBMX (containing 15 % DMSO) (B). Data points are the mean values ± SEM of one representative experiment performed in triplicate.

As the concentration-response curve shows an optimum, only the ascending part of the curve was considered up to a forskolin concentration of 10 µM (see **Figure 4.12**). The determined EC_{50} value of forskolin was 395 ± 44 nM with a Hill slope of 1.09 ± 0.15. Therefore, a concentration of 400 nM of forskolin was used for pre-stimulating the HEK293-SF-hH_4R-His_6-CRE-Luc cells.

In cAMP assays, the inhibition of the PDE with 50 µM of IBMX was necessary to stabilize the cAMP level (Geßele, 1998). In the presence of IBMX (50 µM) the concentration-response curve of forskolin on HEK293-SF-hH_4R-His_6-CRE-Luc-cells was shifted to the left, resulting in an EC_{50} value of 141 ± 21 nM (N = 3) with a Hill slope of 1.06 ± 0.20 (see **Figure 4.12**). Additionally, IBMX increased the receptor-independent luciferase activity by about a factor of four (data not shown).

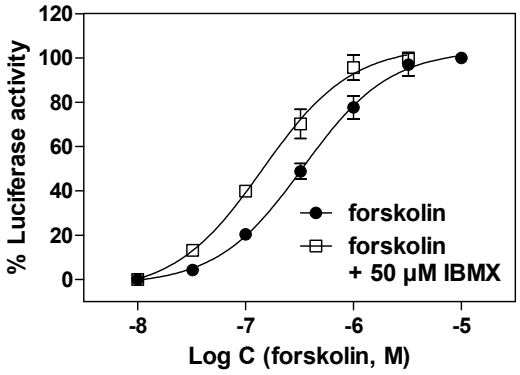

Forskolin		Forskolin + 50 µM IBMX	
EC_{50} [nM]	N	EC_{50} [nM]	N
395 ± 44	6	141 ± 21	3

Figure 4.12: Concentration response curves of forskolin on HEK293-SF-hH_4R-His_6-CRE-Luc cells. Cells were incubated with the indicated concentrations of forskolin alone or in the presence of 50 µM of IBMX. Data were analyzed by nonlinear regression and best fitted to sigmoidal concentration-response curves. Data points shown are the mean ± SEM of N independent experiments performed in triplicate.

In order to investigate the influence of IBMX on the concentration response curve of H_4R ligands, a reporter gene assay was performed with the full hH_4R agonist histamine (**1**) and the hH_4R inverse agonist thioperamide (**12**). HEK293-SF-hH_4R-His_6-CRE-Luc cells were pre-stimulated with 500 nM of forskolin in the absence and presence of 50 µM of IBMX (see **Figure 4.13**). The absolute effects of histamine (**1**) and thioperamide (**12**) and thus the signal-to-noise ratio were clearly reduced in the presence of IBMX. Furthermore, the α value of the inverse agonist thioperamide (**12**), referred to the maximal response of **1**, decreased from -0.89 to -0.54. In the presence of IBMX, the potency of histamine (**1**) was clearly reduced, whereas the potency of thioperamide (**12**) was slightly increased. However, it should be noted that the standard error of the mean (SEM) for the pEC_{50} of thioperamide (**12**) value was very high, probably due to the low signal-to-noise ratio. Hence, IBMX was omitted from all subsequent experiments. However, if the use of a PDE inhibitor is indicated, the changed potency of forskolin must be considered in the respective assay system. In the case of the used HEK293-SF-hH_4R-His_6-CRE-Luc cells, the forskolin concentration could be reduced to 140 nM (cf. **Figure 4.12**).

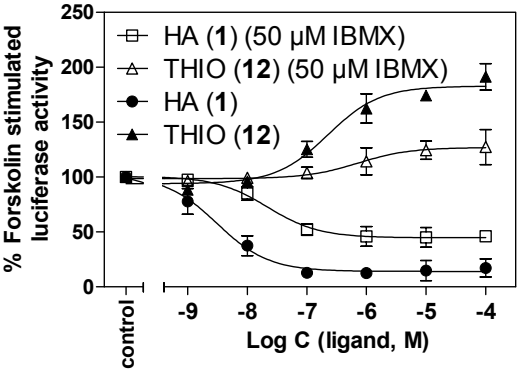

Ligand	hH_4R			
	500 nM forskolin		500 nM forskolin + 50 µM IBMX	
	pEC_{50}	α	pEC_{50}	α
HA (**1**)	8.45 ± 0.32	1.00	7.68 ± 0.13	1.00
THIO (**12**)	6.76 ± 0.21	-0.89	7.03 ± 0.82	-0.54

Figure 4.13: Reporter gene assay with histamine (HA, **1**) and thioperamide (THIO, **12**) in HEK293-SF-hH_4R-His_6-CRE-Luc cells. Reaction mixtures contained ligands at the concentrations indicated on the abscissa to achieve saturated concentration response curves. The cells were pre-stimulated with 500 nM of forskolin alone or in the presence of 50 µM of IBMX. The effect of forskolin or of forskolin plus IBMX was defined as 100 % luciferase activity. Data were analyzed by nonlinear regression and best fitted to sigmoidal concentration-response curves. Data points and pEC_{50} values are the mean ± SEM of two independent experiments performed in triplicate.

To account for positive α values in case of agonism and negative α values in case of inverse agonism, the signs of relative changes in luciferase activity were inverted. A illustraion is given in **Figure 4.14**.

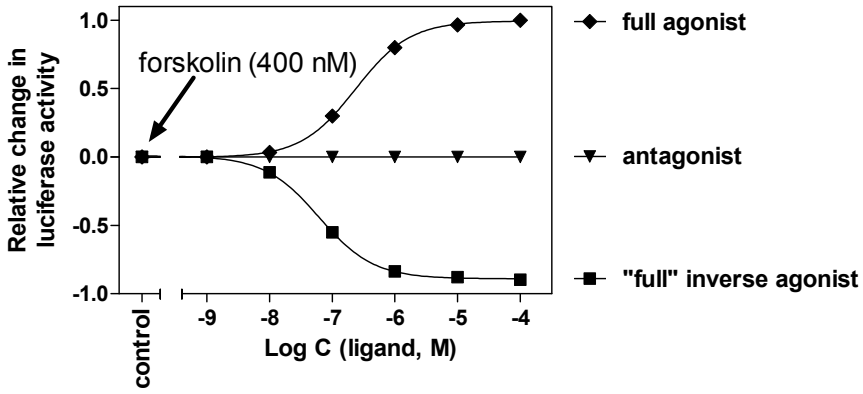

Figure 4.14: Illustration of agonistic and inverse agonistic effects in the cAMP reporter gene assay at the H_4R. As the luminescens signal is an inverse readout, maximum change of 1 indicates full agonism, -1 is defined as "full" inverse agonism, whereas 0 indicates the luminescens signal detected after direct stimulation of adenylyl cyclase by 400 nM forskolin in the absence of H_4R ligands (control).

To conclude, the luciferase gene expression was stimulated by forskolin in a highly sensitive manner (cf. **Figure 4.11** and **Figure 4.12**). As the concentration-response curve shows an optimum, only the ascending part of the curve was considered up to a forskolin concentration of 10 µM for the determination of the EC_{50} value. The decrease in luciferase expression at higher concentrations of forskolin may be interpreted a hint to endogenous cAMP dependent ICER activity in HEK293T cells. Pre-stimulation with 400 nM of forskolin turned out to be suitable to perform the reporter gene assay with HEK293-SF-hH_4R-His_6-CRE-Luc cells (cf. **Figure 4.12**). The use of the PDE inhibitor IBMX in combination with 500 nM of forskolin led to alteration in potencies, efficacies and the signal-to-noise ratio in the luciferase reorter gene assay with histamine (**1**) and thioperamide (**12**). Therefore, IBMX was omitted in subsequent experiments.

4.1.3.6 Selection of the HEK293-CRE-Luc cells

HEK293T cells were stably transfected with pGL4.29[luc2P/CRE/Hygro] using two different ratios of transfection reagent volume (µL) to DNA amount (µg), namely 6:2 and 8:2. For selection of the HEK293-CRE-Luc transfection batches, luciferase expression was induced by 10 µM of forskolin as shown in **Figure 4.15** A. The maximum luciferase activity was satisfactory at both transfection batches. Nevertheless, the 6:2 cells were chosen for further investigations due to a slightly higher maximum. The concentration response curve of forskolin, which was constructed according to section 4.1.2.6.5, offered an EC_{50} value of 3.75 ± 0.96 µM with a Hill slope of 1.33 ± 0.17 in the HEK293-CRE-Luc 6:2 cells (see **Figure 4.15** B). Thus, the potency of forskolin was ten times lower in comparison to the HEK293-SF-hH_4R-His_6-CRE-Luc cells, indicating a lower expression level of the CRE-controlled

luciferase in HEK293-CRE-Luc cells. However, 1 µM of forskolin turned out to be sufficient for the pre-stimulation in HEK293-CRE-Luc cells.

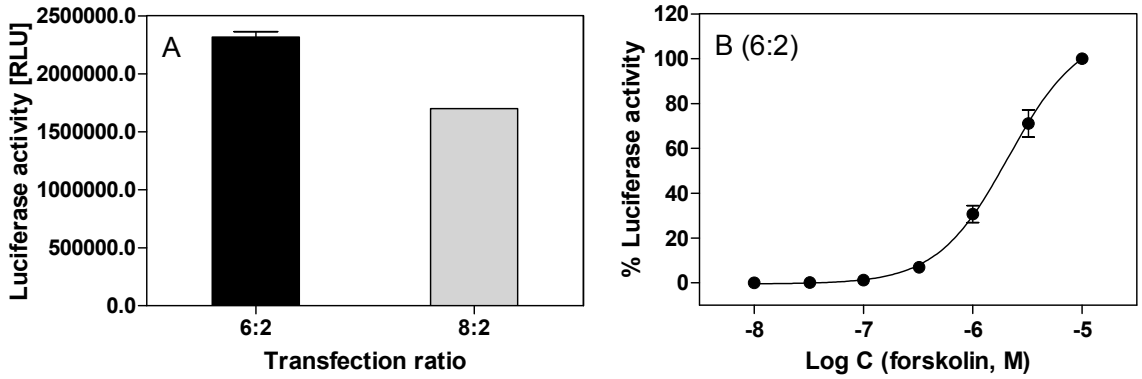

Figure 4.15: Stimulation of the luciferase expression by forskolin in HEK293-CRE-Luc cells. Stimulation of the cells from the 6:2 and 8:2 transfection batches by 10 µM of forskolin (mean values ± SEM; n = 3) (A). Concentration response curve of forskolin in the 6:2 cells. Data were analyzed by nonlinear regression and best fitted to sigmoidal concentration-response curves. Data points shown are the mean ± SEM of six independent experiments performed in triplicate (B).

According to section 4.1.2.6.6, the HEK293-CRE-Luc (6:2) cells were incubated with 10 µM of forskolin for the indicated period of time in order to investigate the time course of luciferase expression (see **Figure 4.16**). The time course was almost identical to that shown in **Figure 4.10** (section 4.1.3.4). After 5 h, 94 % of maximum luciferase expression was detected, whereas after 24 h of incubation luciferase activity was only approx. one third of the maximal value measured at 8 h.

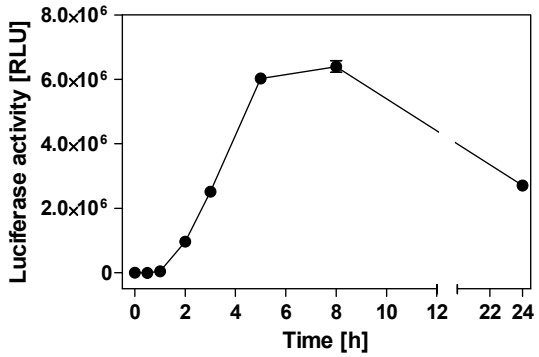

Figure 4.16: Time course of the luciferase expression in HEK293-CRE-Luc cells after stimulation with 10 µM of forskolin. The luciferase activity was determined after the indicated incubation periods (mean values ± SEM; n = 9).

4.1.3.7 Off-target effects

In control experiments, HEK293-CRE-Luc cells devoid of H_4R expression were pre-stimulated with 1 µM forskolin and co-incubated with selected compounds (see **Figure 4.17**). Changes in CRE-controlled luciferase activity result from off-target effects, presumably,

owing to their binding to (unknown) endogenously expressed GPCRs in HEK293T cells (Atwood *et al.*, 2011). Therefore, these unintended activities were considered in the following reporter gene assays to avoid misinterpretation of biological responses at concentrations ≥10 µM.

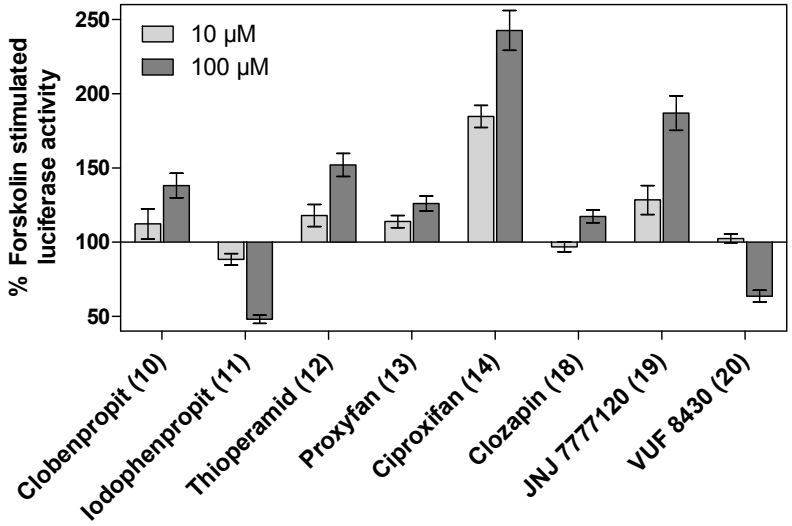

Figure 4.17: Off-target effects of selected ligands in a CRE-controlled luciferase reporter gene assay in HEK293T cells. The effect of (1 µM) forskolin was defined as 100 % luciferase activity. Data are means ± SEM of one representative experiment performed in triplicate.

4.1.3.8 Functional activities of histamine H_4 receptor ligands at the human histamine H_4R

Binding studies were performed with HEK293T cells stably expressing the hH_4R and [^{3}H]UR-PI294 as radioligand (cf. section 3.1.3.3). Additionally, the co-expression of a CRE-controlled luciferase reporter gene enabled the functional analysis of H_4R ligands in HEK293-SF-hH_4R-His_6-CRE-Luc cells. The endogenous H_4R ligand histamine (**1**) inhibited forskolin (400 nM) stimulated luciferase gene transcription in the optimized reporter gene assay to an extent of 79.6 ± 8.6 % (N = 6), promising a sufficient signal-to-noise ratio. Thioperamide (**12**), described as inverse agonist at the hH_4R (Lim *et al.*, 2005; Liu *et al.*, 2001a; Morse *et al.*, 2001; Schnell *et al.*, 2011), increased the forskolin-stimulated CRE activity by 17.0 ± 3.7 % (N = 6), indicating only moderate constitutive activity of the hH_4R in HEK293-SF-hH_4R-His_6-CRE-Luc cells. For the purpose of validation, a set of imidazole and non-imidazole ligands including agonists, inverse agonists and antagonists (cf. section 3.1.2.3, section 3.2.2.4, section 4.1.2.7), were investigated for their ability to change forskolin (400 nM) stimulated luciferase activity in HEK293-SF-hH_4R-His_6-CRE-Luc cells. The determined pEC_{50} values or pK_B values were compared, as far as possible, with ligand activities from a CRE-driven β-

galactosidase reporter gene assay in SK-N-MC-/hH_4R cells (Kitbunnadaj *et al.*, 2003; Lim *et al.*, 2005) and with results from functional studies using more proximal readouts in G-protein mediated signal transduction, namely the functional [^{35}S]GTPγS binding assay (Geyer, 2011; Sander *et al.*, 2009; Wifling, 2012) and the steady-state [^{33}P]GTPase activity assay (Sander *et al.*, 2009; Schnell *et al.*, 2011), which were both performed on a membrane preparation of Sf9 cells expressing the hH_4R. The obtained results as well as the reported data are summarized in **Table 4.3**.

Histamine (**1**) and its methylated analogs (R)-α-methylhistamine (**2**), (S)-α-methylhistamine (**3**), N$^{\alpha}$-methylhistamine (**4**) and 5(4)-methylhistamine (**5**) inhibited forskolin stimulated luciferase activity in a concentration dependent manner in HEK293-SF-hH_4R-His$_6$-CRE-Luc cells and acted, with the exception of (S)-α-methylhistamine (**3**)**,** as full agonists (see **Figure 4.18**).

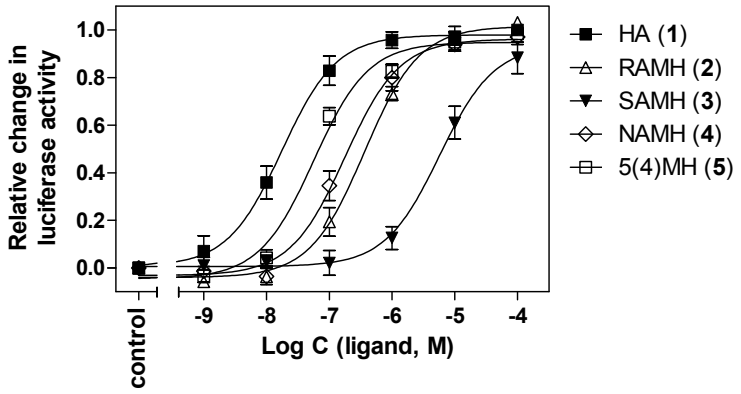

Figure 4.18: Change in forskolin (400 nM) stimulated luciferase activity by HA (**1**), RAMH (**2**), SAMH (**3**), NAMH (**4**) and 5(4)MH (**5**) in HEK293-SF-hH_4R-His$_6$-CRE-Luc cells. Maximum change of 1 is defined as full agonism, whereas 0 indicates the luminescence signal detected after direct stimulation of adenylyl cyclase by forskolin in the absence of H_4R ligands (control). Data were analyzed by nonlinear regression and best fitted to sigmoidal concentration-response curves. Data points shown are mean values ± SEM of at least three independent experiments performed in triplicate.

Except for the potency of N$^{\alpha}$-methylhistamine (**4**), which was higher than reported, both potencies and efficacies of **1**–**3** and **5** were in good agreement with reported data from a β-galactosidase reporter gene assay using SK-N-MC/hH_4R cells. Furthermore, the pEC_{50} value of histamine (**1**) was consistent with results from [^{33}P]GTPase and [^{35}S]GTPγS binding assays. Although, the pEC_{50} values were higher compared to the pK_i values (cf. section 3.1.3.3), the rank order of potencies and affinities (**1** > **5** > **4** > **2** > **3**) was identical, indicating a good correlation of binding and functional data in the hH_4R expressing HEK293T cells.

Contrary to the [^{35}S]GTPγS binding assay, in which immepip (**6**) behaves as strong partial agonist (α = 0.81), **6** was able to fully activate the hH_4R in the luciferase reporter gene assay

(see **Figure 4.19**). Nevertheless, the pEC_{50} value of 7.64 ± 0.12 was in good agreement with reported data. Interestingly, VUF 5681 (**7**), having an extended spacer length compared to immepip (**6**), displayed no functional activity at the hH_4R, which was consistent with functional data from literature (see **Figure 4.19**). In the antagonist mode, VUF 5681 (**7**) antagonized the histamine induced decrease in luciferase activity, resulting in a pK_B value of 6.16 ± 0.20, which was in accordance to its binding affinity (cf. section 3.1.3.3). Immethridine (**8**), the pyridine analog of immepip (**6**), acted only as partial agonist at the hH_4R, which was in agreement with results from a β-galactosidase reporter gene assay (see **Figure 4.19**).

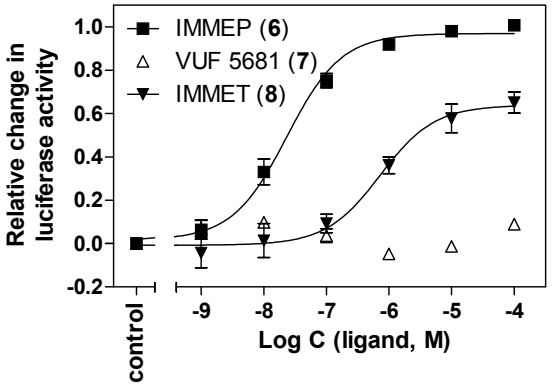

Figure 4.19: Potencies and efficacies of IMMEP (**6**), VUF 5681 (**7**) and IMMET (**8**) at the hH_4R. Maximum change of 1 is defined as full agonism, whereas 0 indicates the luminescence signal detected after direct stimulation of adenylyl cyclase by 400 nM forskolin in the absence of H_4R ligands (control). Data were analyzed by nonlinear regression and best fitted to sigmoidal concentration-response curves. Data points shown are mean values ± SEM of at least three independent experiments performed in triplicate.

Since pronounced non-H_4R mediated effects became obvious at 100 µM of clobenpropit (**10**), iodophenpropit (**11**) and thioperamide (**12**) in forskolin-stimulated HEK293-CRE-Luc cells, the respective RLU values were excluded from the EC_{50} calculations (see **Figure 4.17** and **Figure 4.20** B).

Imetit (**9**), the isothiourea analog of histamine (**1**), was a potent and almost full agonist, which was consistent with recently reported results (see **Figure 4.20** A). Clobenpropit (**10**) and iodophenpropit (**11**) are structurally related and can be considered as analogs of imetit (**9**) with an increased distance between the basic moieties and a large lipophilic group in the side chain. Interestingly, the intrinsic activity of both isothiourea-type compounds was clearly higher than described in literature. Clobenpropit (**10**) exerted almost full instead of partial agonistic activity (α = 0.45) in the [^{35}S]GTPγS binding assay as reported. Most strikingly, iodophenpropit (**11**), described as antagonist (Lim *et al.*, 2005), displayed strong partial agonistic activity with a pEC_{50} value of 7.30 ± 0.14 and an α value of 0.73 ± 0.02 (see **Figure 4.20** A). However, partial agonistic activity was also determined at 10 µM of iodophenpropit (**11**) in a Ca^{2+} mobilization assay in HEK293 cells, co-transfected with the hH_4R and the chimeric G-protein G_{qi5}, which directed the H_4R signaling to the G_q pathway (Zhu *et al.*, 2001). Thioperamide (**12**) revealed inverse agonist activity at the hH_4R, and the pEC_{50} value was in accordance to other functional assays (see **Figure 4.20** A). However, the constitutive

activity of thioperamide (**12**) was rather low compared to functional assays on Sf9 cell membranes. Moreover, the extent of detectable constitutive activity varied seriously between the different assay systems. The α values of thioperamide (**12**), which refer to the intrinsic activity of histamine (**1**) (α = 1), were -1.39, -0.95, -0.52 and -0.32 in the [^{35}S]GTPγS binding assay, the steady state [^{33}P]GTPase assay, the β-galactosidase reporter gene assay (the α value consists of the data for the inhibitory effect of histamine (**1**) (58 %) and the stimulatory effect of thioperamide (**12**) (130 %), c.f. (Lim *et al.*, 2005)) and the present luciferase reporter gene assay, respectively. However, it should be noted that the extent of constitutive activity for thioperamide (**12**) was distinctly higher in initial reporter gene assays compared to later experiments performed after cryo conservation of the HEK293-SF-hH_4R-His_6-CRE-Luc cells in liquid nitrogen (cf. **Figure 4.9** and **Figure 4.13**).

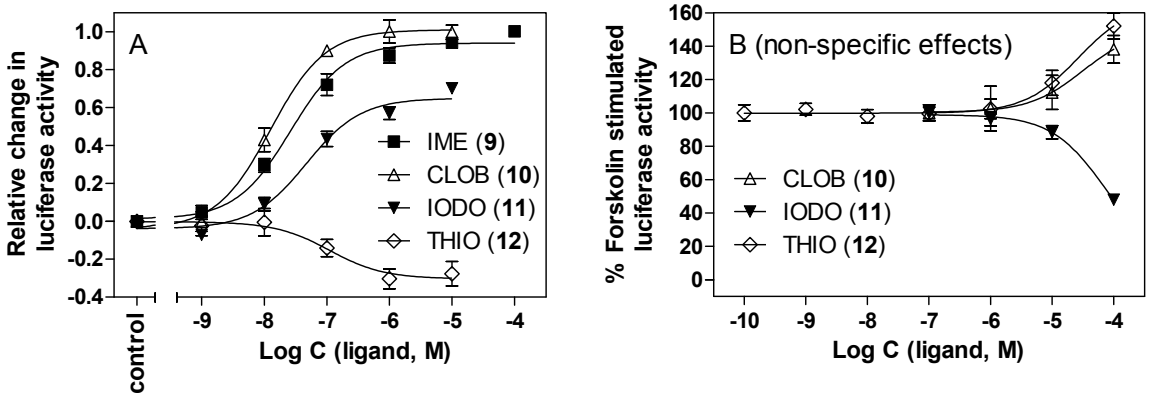

Figure 4.20: CRE-mediated response of IME (**9**), CLOB (**10**), IODO (**11**) and THIO (**12**). Potencies and intrinsic activies at the hH_4R in the luciferase reporter gene assay using HEK293-SF-hH_4R-His_6-CRE-Luc cells. Maximum change of 1 indicates full agonism, -1 is defined as "full" inverse agonism, whereas 0 indicates the luminescence signal detected after direct stimulation of adenylyl cyclase by 400 nM forskolin in the absence of H_4R ligands (control). Data were analyzed by nonlinear regression and best fitted to sigmoidal concentration-response curves. Data points shown are mean values ± SEM of at least three independent experiments performed in triplicate (A). Non-specific effects in the luciferase reporter gene assay using HEK293-CRE-Luc cells. Data are presented as percental change in forskolin (1 μM) stimulated luciferase activity (100 %). Data shown are from one representative experiment performed in triplicate (B).

In accordance with results from a β-galactosidase reporter gene assay in SK-NM-C/hH_4R cells, proxyfan (**13**) showed partial agonistic activity at the hH_4R with a pEC_{50} value of 6.93 ± 0.06 (see **Figure 4.21** A). Whereas H_4R-independent ("off-target") effects of proxyfan (**13**) were negligible at concentrations >10 μM, the structural analog ciproxifan (**14**) induced a strong increase (by up to 250 %) in luciferase activity at concentrations from 1 to 100 μM in HEK293-CRE-Luc cells devoid of H_4R expression (see **Figure 4.17** and **Figure 4.21** B). This seriously hampered the pharmacological characterization of ciproxifan (**14**) in the luciferase reporter gene assay (see **Figure 4.21**). The stimulation of the luciferase activity possibly

resulted from interactions of ciproxifan (**14**) with endogenously expressed GPCRs in HEK293T cells. For example, a moderate affinity of ciproxifan (**14**) at the human α_{2a} and α_{2c} adrenergic receptors was recently demonstrated (Esbenshade *et al.*, 2003b).

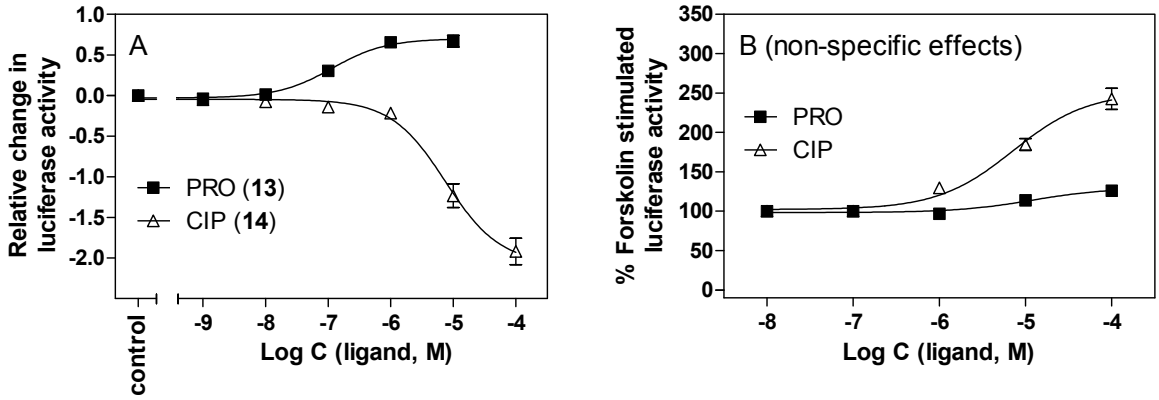

Figure 4.21: Relative change of the CRE-activity by PRO (**13**) and CIP (**14**). Concentration response curves in the luciferase reporter gene assay using HEK293-hH_4R-His_6-CRE-Luc cells. Maximum change of 1 indicates full agonism, -1 is defined as "full" inverse agonism, whereas 0 indicates the luminescence signal detected after direct stimulation of adenylyl cyclase by 400 nM forskolin in the absence of H_4R ligands (control). Data were analyzed by nonlinear regression and best fitted to sigmoidal concentration-response curves. Data points shown are the mean values ± SEM of at least three independent experiments performed in triplicate (A). Non-specific effects in the luciferase reporter gene assay using HEK293-CRE-Luc cells. Data are represented as percentage change in forskolin (1 µM) stimulated luciferase activity (100 %). Data shown are from one representative experiment performed in triplicate (B).

The acylguanidine UR-PI294 (**15**) as well as the cyanoguanidines UR-PI376 (**16**), trans-(+)-(1S,3S)-UR-RG98 (**17**), trans-(-)-(1R,3R)-UR-RG98 (**23**) and trans-(+)-(1S,3S)-UR-RG94 (**27**) changed forskolin induced luciferase gene transcription in HEK293-SF-hH_4R-His_6-CRE-Luc cells (see **Figure 4.22**). In agreement with data from the [^{33}P]GTPase and the [^{35}S]GTPγS binding assay, UR-PI294 (**15**) and UR-PI376 (**16**) proved to be full agonists, equipotent with histamine (**1**) (**16**) and approximately 10 times more potent (**15**) than the reference substance. Interestingly, trans-(+)-(1S,3S)-UR-RG98 (**17**) and trans-(+)-(1S,3S)-UR-RG94 (**27**) were described as strong partial agonists with α values of 0.71 – 0.75 in the [^{35}S]GTPγS binding assay, whereas both fully activated the hH_4R in the luciferase reporter gene assay with pEC_{50} values of 7.65 ± 0.04 and 7.18 ± 0.04, respectively. The increase in intrinsic activity as an agonist became even more obvious in case of trans-(-)-(1R,3R)-UR-RG98 (**23**), which was a weak neutral antagonist in the [^{35}S]GTPγS binding assay and a moderately potent partial agonistic in the reporter gene assay with a pEC_{50} value of 6.26 ± 0.11. Nevertheless, the recently described high agonistic potency of the eutomer trans-(+)-(1S,3S)-UR-RG98 (**17**) and the stereodiscrimination between trans-(+)-(1S,3S)-UR-RG98

(**17**) and trans-(-)-(1R,3R)-UR-RG98 (**23**) (Geyer, 2011) by the receptor was confirmed in the luciferase reporter gene assay.

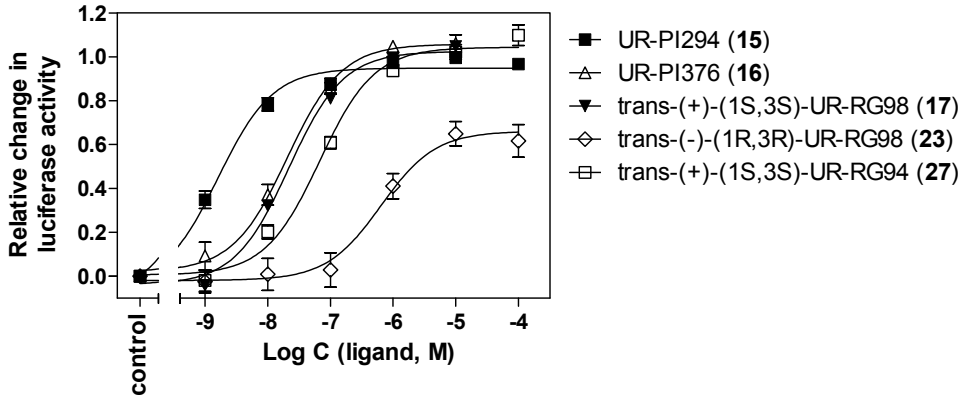

Figure 4.22: Potencies and efficacies of UR-PI294 (**15**), UR-PI376 (**16**), trans-(+)-(1S,3S)-UR-RG98 (**17**), trans-(-)-(1R,3R)-UR-RG98 (**23**) and trans-(+)-(1S,3S)-UR-RG94 (**27**) in HEK293-hH_4R-His_6-CRE-Luc cells. Maximum change of 1 is defined as full agonism, whereas 0 indicates the luminescence signal detected after direct stimulation of adenylyl cyclase by 400 nM forskolin in the absence of H_4R ligands (control). Data were analyzed by nonlinear regression and best fitted to sigmoidal concentration-response curves. Data points shown are the mean values ± SEM of at least four independent experiments performed in triplicate.

Besides the widely used non-imidazole H_4R ligands clozapine (**18**), JNJ 7777120 (**19**) and VUF 8430 (**20**), two recently described aminopyrimidines, ST1006 (**30**) and ST1012 (**31**) (Sander *et al.*, 2009), were investigated in the reporter gene assay as shown in **Figure 4.23** A. With a pEC_{50} value of 6.56 ± 0.09, clozapine (**18**) exhibited only moderate potency at the hH_4R, which was in agreement with reported data. However, there are distinct discrepancies regarding the intrinsic activity of clozapine (**18**) in the different assay systems. While clozapine (**18**) acted as partial agonist in the systems using a proximal readout in G-protein signaling, the [^{33}P]GTPase and the [^{35}S]GTPγS binding assays, the hH_4R was fully activated in the β-galactosidase reporter gene assay in SK-NM-C/hH_4R cells. In the luciferase reporter gene assay, the maximal agonistic response of clozapine (**18**) surpassed that of histamine (**1**) by 40 %. Investigations with respect to non-H_4R mediated effects revealed only a slight increase in CRE-activity at 100 µM (see **Figure 4.17** and **Figure 4.23** B), suggesting that the (super) agonistic effect of clozapine (**18**) was mediated by the hH_4R. However, due to the pleiotropic character of clozapine, effects mediated by targets other than the H_4R must be taken into account. The indole derivative JNJ 7777120 (**19**) has become the standard antagonist in laboratories working in the H_4R field. In line with the reported data, JNJ 7777120 (**19**) antagonized the histamine (**1**) response in HEK293-SF-hH_4R-His_6-CRE-Luc cells with a pK_B value of 7.81 ± 0.19, which was in accordance with the binding data of **19** (cf. section 3.1.3.3). By analogy with ciproxifan, but much less pronounced, JNJ 7777120 (**19**)

produced receptor-independent increases in luciferase activity at concentrations ≥10 µM in control experiments using cells devoid of H_4R expression (see **Figure 4.17** and **Figure 4.23** B). The corresponding values were therefore omitted in the construction of concentration-response curves of JNJ 7777120 (**19**), when studied in the antagonist mode. In the [^{33}P]GTPase and the [^{35}S]GTPγS binding assay, JNJ 7777120 (**19**) showed partial inverse agonistic activity. In agreement with reported data, VUF 8430 (**20**) acted as full agonist at the hH_4R with a pEC_{50} value of 7.04 ± 0.10. Contrary to [^{33}P]GTPase and the [^{35}S]GTPγS assays, surprisingly, ST 1006 (**30**) was an almost full agonist in the luciferase reporter gene assay with a slightly lower pEC_{50} value of 8.05 ± 0.05. The potency and intrinsic activity of ST 1012 (**31**) were consistent with reported data.

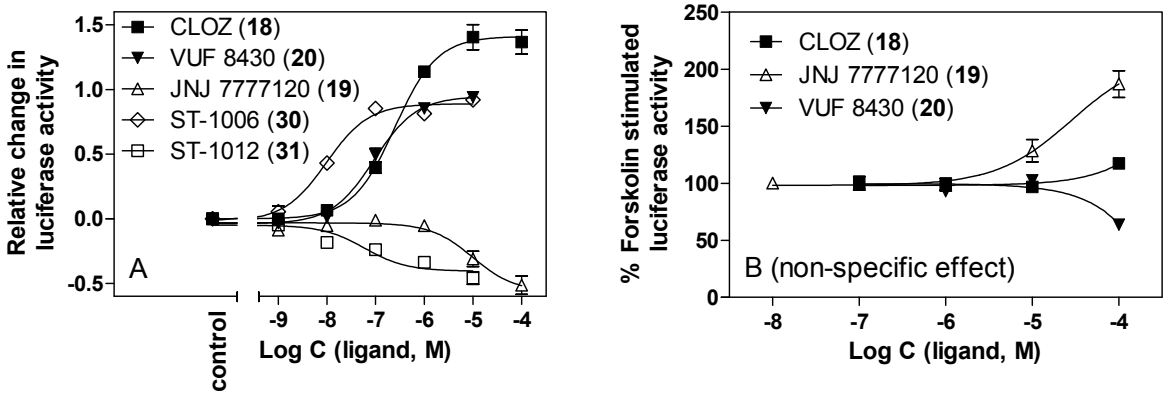

Figure 4.23: CRE-mediated response of CLOZ (**18**), JNJ 7777120 (**19**), VUF 8430 (**20**), ST-1006 (**30**) and ST-1012 (**31**). Potencies and intrinsic activies at the hH_4R in the luciferase reporter gene assay using HEK293-SF-hH_4RHis_6-CRE-Luc cells. Maximum change of 1 indicates full agonism, -1 is defined as "full" inverse agonism, whereas 0 indicates the luminescence signal detected after direct stimulation of adenylyl cyclase by 400 nM forskolin in the absence of H_4R ligands (control). Data were analyzed by nonlinear regression and best fitted to sigmoidal concentration-response curves. Data points shown are the mean values ± SEM of at least three independent experiments performed in triplicate (A). Non-specific effects in the luciferase reporter gene assay using HEK293-CRE-Luc cells. Data are represented as percental change in forskolin (1 µM) stimulated luciferase activity (100 %). Data shown are from one representative experiment performed in triplicate (B).

In summary, agonistic, inverse agonistic and and antagonistic activies at the hH_4R were determined on genetically engineered HEK293 cells (HEK293-SF-hH_4R-His_6-CRE-Luc cells) co-expressing the hH_4R and a CRE controlled luciferase reporter gene. The agonistic and inverse agonistic potencies of the examined H_4R ligands were consistent with data from a β-galactosidase reporter gene assay in SK-NM-C/hH_4R cells as well as with data from [^{33}P]GTPase and the [^{35}S]GTPγS binding assays on hH_4R expressing Sf9 cell membranes. Furthermore, the pK_B values of neutral H_4R antagonist *versus* histamine (**1**) in the reporter gene assay were in good agreement with antagonist affinities from competition binding assays (cf.section 3.1.3.3). However, differences in ligand efficacies became obvious

comparing assays based on proximal and distal readouts. Presumably, due to signal amplification in the second messenger cascade downstream from G-protein activation, several partial agonists turned out to be full agonists in the reporter gene assay. Most strikingly, iodophenpropit (**11**) and trans-(-)-(1R,3R)-UR-RG98 (**23**), which were previously described as neutral hH_4R antagonist, acted as partial agonists in the luciferase reporter gene assay in HEK293-SF-hH_4R-His_6-CRE-Luc cells.

Table 4.3: Potencies and efficacies of H_4R ligands at the hH_4R in the luciferase reporter gene assay in comparison to reported β-galactosidase activity in SK-N-MC/hH_4R cells, reported activity of ligands in functional binding assay with [^{35}S]GTPγS and to reported steady-state GTPase activity on membrane preperations of Sf9 cells expressing the hH_4R. Luciferase reporter gene assay data are the mean values ± SEM of N independent experiments performed in triplicate.

Ligand	**hH_4R**								
	pEC_{50} or (pK_B)	α	N	pEC_{50} or (pA_2)	α	pEC_{50} or (pK_B)	α	pEC_{50}	α
	Luciferase reporter gene assay in HEK293-SF-hH_4R-His_6-CRE-Luc cells			β-galactosidase reporter gene assay (reported)		[^{35}S]GTPγS binding (reported)		Steady-state [^{33}P]GTPase activity (reported)	
Histamine (**1**)	7.77 ± 0.12	1.00 ± 1.00	6	7.7[a]	1	8.13[f]	1.00	7.92[g]	1.00
(R)-α-Methylhistamine (**2**)	6.47 ± 0.09	1.03 ± 0.04	5	6.2[a]	1	-	-	-	-
(S)-α-Methylhistamine (**3**)	5.22 ± 0.09	0.90 ± 0.04	5	4.9[a]	1	-	-	-	-
N^{α}-Methylhistamine (**4**)	6.74 ± 0.12	0.98 ± 0.03	4	6.1[a]	1	-	-	-	-
5(4)-Methylhistamine (**5**)	7.25 ± 0.05	0.97 ± 0.03	3	7.4[a]	1	-	-	7.15[g]	0.90
Immepip (**6**)	7.64 ± 0.12	0.98 ± 0.02	5	7.8[a]	0.9	7.67[f]	0.81	-	-
VUF 5681 (**7**)	(6.16 ± 0.20)	0.09 ± 0.00	3	< 5[b]	-	-	-	-	-
Immethridine (**8**)	6.12 ± 0.20	0.65 ± 0.02	3	6.0[a]	0.5	-	-	-	-
Imetit (**9**)	7.54 ± 0.12	0.94 ± 0.02	5	7.9[a]	0.9	-	-	-	-
Clobenpropit (**10**)	7.87 ± 0.07	0.97 ± 0.03	3	7.7[a]	0.8	7.65[f]	0.45	-	-
Iodophenpropit (**11**)	7.30 ± 0.14	0.73 ± 0.02	4	(8.0)[a]	0	(7.68)[f]	0.00	-	-
Thioperamide (**12**)	6.92 ± 0.10	-0.32 ± 0.04	6	7.0[a]	-1	6.58[f]	-1.39	6.96[g]	-0.95
Proxyfan (**13**)	6.93 ± 0.06	0.68 ± 0.02	4	7.2[a]	0.5	-	-	-	-

Table 4.3 (continued)

Ligand	hH_4R								
	pEC_{50} or (pK_B)	α	N	pEC_{50} or (pA_2)	α	pEC_{50} or (pK_B)	α	pEC_{50}	α
	Luciferase reporter gene assay in HEK293-SF-hH_4R-His_6-CRE-Luc cells			β-galactosidase reporter gene assay (reported)		[^{35}S]GTPγS binding (reported)		Steady-state [^{33}P]GTPase activity (reported)	
UR-PI294 (**15**)	8.74 ± 0.11	0.98 ± 0.02	6	-	-	8.35[f]	1.02	8.52[g]	0.90
UR-PI376 (**16**)	7.70 ± 0.07	1.02 ± 0.02	4	-	-	7.79[f]	1.11	7.47[g]	0.93
Clozapine (**18**)	6.56 ± 0.09	1.40 ± 0.09	4	6.8[a]	1	6.24[f]	0.67	5.78[h]	0.66
JNJ 7777120 (**19**)	(7.81 ± 0.19)	-0.31 ± 0.06	3	(7.8)[a]	0	(7.60)[f]	-0.40	7.50[g]	-0.35
VUF 8430 (**20**)	7.04 ± 0.10	0.97 ± 0.04	3	7.3[c]	1	7.42[f]	0.84	-	-
trans(+)-(1S,3S)-UR-RG98 (**17**)	7.65 ± 0.04	1.03 ± 0.01	4	-	-	7.96[d]	0.75	-	-
trans(-)-(1R,3R)-UR-RG98 (**23**)	6.24 ± 0.11	0.64 ± 0.02	4	-	-	(5.11)[d]	0.02	-	-
trans(+)-(1S,3S)-UR-RG94 (**27**)	7.18 ± 0.04	1.04 ± 0.02	4	-	-	7.00[d]	0.71	-	-
ST-1006 (**30**)	8.05 ± 0.05	0.91 ± 0.01	3	-	-	8.95[e]	0.28	8.85[e]	0.18
ST-1012 (**31**)	7.26 ± 0.05	-0.39 ± 0.03	3	-	-	7.43[e]	-1.11	-	-

pEC_{50} values determined in the luciferase reporter gene assay calculated from the change of forskolin (400 nM) induced luciferase activity in HEK293-SF-hH_4R-His_6-CRE-Luc cells. N gives the number of independent experiment performed in triplicate. Intrinsic activity (α) referred to the maximal response to histamine (α = 1.00). The K_B values of neutral antagonists were determined in the antagonist mode *versus* histamine (100 nM) as the agonist. Data taken from: CRE-β-galactosidase reporter gene assay in SK-N-MC cells stably co-expressing the hH_4R [a] (Lim *et al.*, 2005), [b] (Kitbunnadaj *et al.*, 2003), [c] (Lim *et al.*, 2006); functional [^{35}S]GTPγS-binding assay on Sf9 cell membranes co-expressing the hH_4R + $G_{iα2}$ + $β_{1γ2}$ [d] (Geyer, 2011), [e] (Sander *et al.*, 2009) (α value of ST-1012 referred to thioperamide = -1.0), [f] (Wifling, 2012); steady-state [^{32}P]GTPase assay on Sf9 cell membranes co-expressing: hH_4R-RGS19 + $G_{iα2}$ + $β_{1γ2}$ [g] (Schnell *et al.*, 2011),[h] (Appl *et al.*, 2011), hH_4R + $G_{iα2}$ + $β_{1γ2}$ [e] (Sander *et al.*, 2009).

4.2 Development of a reporter gene assay for the mouse and rat histamine H_4R

4.2.1 Introduction

The H_4R is preferably expressed on cells of hematopoietic origin, such as eosinophils and mast cells, and thus supposed to be involved in inflammatory diseases like allergic asthma and pruritis (de Esch *et al.*, 2005; Leurs *et al.*, 2009; Leurs *et al.*, 2011; Thurmond *et al.*, 2008; Zhang *et al.*, 2007). To investigate the (patho)physiological role of the H_4R, several studies used translational animal models like murine models for allergic asthma and allergic contact dermatitis (Beermann *et al.*, 2012; Deml *et al.*, 2009; Dunford *et al.*, 2006; Morgan *et al.*, 2007; Rossbach *et al.*, 2009) or rat models such as carrageenan induced acute inflammation and conjunctivitis (Coruzzi *et al.*, 2007; Zampeli *et al.*, 2009). Although most of the studies confirmed the pro-inflammatory role of the H_4R by blocking H_4R-mediated response with the standard H_4R antagonist JNJ 7777120, which is reported as equipotent at the human, mouse and rat H_4R (Thurmond *et al.*, 2004), there were also controversial reports: The administration of the selective H_4R agonist 5(4)-methylhistamine was beneficial in a murine asthma model (Morgan *et al.*, 2007), and JNJ 777120 increased the ocular histamine concentration in a rat conjunctivitis model (Zampeli *et al.*, 2009) (for a recent review cf. Neumann et al. (Neumann *et al.*, 2010)). Furthermore, in various *in vitro* assay systems, the recombinantly expressed mouse and rat H_4R revealed substantial species-dependent differences compared to the human receptor concerning affinity, potency and quality of action of pharmacological tools, compromising the predictive value with respect to translational animal models (Esbenshade *et al.*, 2003a; Lim *et al.*, 2010; Liu *et al.*, 2001b; Schnell *et al.*, 2011). For example, in comparison to the human H_4R, the N^G-acetylated imidazolylpropylguanidine UR-PI294 (Igel *et al.*, 2009b) and the cyanoguanidine UR-PI376 (Igel *et al.*, 2009a) displayed considerably lower potencies and efficacies (UR-PI376) in the [^{33}P]GTPase and [^{35}S]GTPγS binding assays on membrane preparations of Sf9 insect cells expressing the mouse or the rat H_4R (Schnell *et al.*, 2011; Wifling, 2012). Most strikingly, JNJ 7777120 exhibited stimulatory effects at the mouse and the rat H_4R in functional assays on Sf9 cell membranes (Schnell *et al.*, 2011). Moreover, the use of JNJ 7777120 as standard antagonist in animal models was questioned due to stimulation of G-protein independent β-arrestin recruitment (Rosethorne and Charlton, 2011). Biased signaling of the hH_4R has also been shown for other H_4R ligands (Nijmeijer *et al.*, 2012).

The aforementioned controversial findings underline the necessity to evaluate pharmacological tools at the H_4R species orthologs of interest using different assay systems. For this purpose, a CRE-controlled luciferase reporter gene assay in HEK293T cells, stably

expressing the mouse or the rat H_4R, was established. For validation, potencies and efficacies of a set of imidazole and non-imidazole H_4R ligands, including agonists, inverse agonists and antagonists, were determined and, if possible, compared to results from the (more proximal) functional assays on Sf9 cell membranes. In order to find new pharmacological tools for the mouse and rat histamine H_4R, the purified stereoisomers of the cyanoguanidines UR-RG98 and UR-RG94 (cf. section 3.1.2.3 and section 3.2.2.4) as well as two selected aminopyrimidines ST-1006 and ST-1012 (cf. section 4.1.2.7) were investigated in the cAMP sensitive reporter gene assay.

4.2.2 Material and Methods

4.2.2.1 Stable transfection of HEK293-SF-mH$_4$R-His$_6$ cells with pGL4.29[luc2P/CRE/Hygro]

HEK293-SF-mH$_4$R-His$_6$ cells were cultured according to section 3.1.2.1 and section 3.2.2.2. The transfection was performed according to section 3.2.2.2 with the exception that the ratios of transfection reagent (µL) to DNA amount (µg) were 6:2 and 8:2. The transfection batches were initially selected as well as maintained with DMEM containing 10 % FCS, 600 µg/mL of G418 and 200 µg/mL of hygromycin B.

4.2.2.2 Preparation of the pcDNA3.1(+)-SF-rH$_4$R-His$_6$ vector and sequencing

The pcDNA3.1(+)-SF-rH$_4$R-His$_6$ vector was kindly provided by Prof. Dr. Seifert (Institute of Pharmacology, Medical School of Hannover, Hannover, Germany). The preparation of media and agar plates were performed as described in section 3.2.2.1.4. The transformation of competent *E. coli* was conducted according to section 3.2.2.1.5. The subsequent glycerol culture and the large scale preparation of plasmid DNA (Maxi-Prep) was performed as described in section 3.2.2.1.6. The DNA concentration was determined according to section 3.2.2.1.2. The sequencing (performed by Entelechon) of the large scale preparation product confirmed the right identity and composition of the SF-rH$_4$R-His$_6$ insert in pcDNA3.1(+).

4.2.2.3 Stable transfection of HEK293-CRE-Luc cells with the pcDNA3.1(+)-SF-rH$_4$R-His$_6$ vector

HEK293-CRE-Luc cells were cultured as described in section 3.1.2.1 and section 4.1.2.4. The transfection was performed according to section 3.2.2.2 with the exception that the ratios of transfection reagent (µL) to DNA amount (µg) were 6:2 and 8:2. The transfectants were initially selected with DMEM containing 10 % FCS, 800 µg/mL of G418 and 200 µg/mL of hygromycin. Subsequently, the HEK293-CRE-Luc-SF-rH$_4$R-His$_6$ cells were maintained in DMEM containing 10 % FCS, 600 µg/mL of G418 and 200 µg/mL of Hygromycin B.

4.2.2.4 Luciferase reporter gene assay

For the implementation see section 4.1.2.6. The K_B values of neutral antagonists / inverse agonists were determined in the antagonist mode at the mH$_4$R and rH$_4$R *versus* histamine (150 and 1000 nM, respectively) as the agonist.

4.2.3 Results and discussion

4.2.3.1 Selection of the HEK293-SF-mH$_4$R-His$_6$-CRE-Luc transfectants

In order to investigate H_4R ligand activity at the mH_4R in the luciferase reporter gene assay, the HEK293-SF-mH_4R-His_6 cells were stably transfected with the pGL4.29[luc2P/CRE/Hygro] vector at two different ratios of transfection reagent (µL) to DNA amount (µg), namely 6:2 and 8:2. For comparison of the two transfection batches, the effect of histamine (**1**) (100 µM) and thioperamide (**12**) (100 µM) on forskolin (1µM) stimulated luciferase activity was determined (see **Figure 4.24**). In the 6:2 and the 8:2 cells the luciferase gene transcription was clearly induced by forskolin, indicating a successful transfection with the CRE controlled luciferase gene. Furthermore, histamine (**1**) gave an appropriate response by the activation of the $G\alpha_{i/o}$-coupled mH_4R. Thioperamide (**12**) acted as inverse agonist at the hH_4R (cf. 4.1.3.8) and increased the forskolin stimulated luciferase activity in the 8:2 transfectants by 24 %. However, off-target effects of thioperamide (**12**) at 100 µM on HEK293-CRE-Luc cells must be taken into account (cf. section 4.1.3.7 and 4.1.3.8). Although both transfection baches gave appropriate cellular systems for performing a luciferase reporter gene assay, the 8:2 cells were chosen for further assays due to the pronounced effect of histamine (**1**) (see **Figure 4.24**).

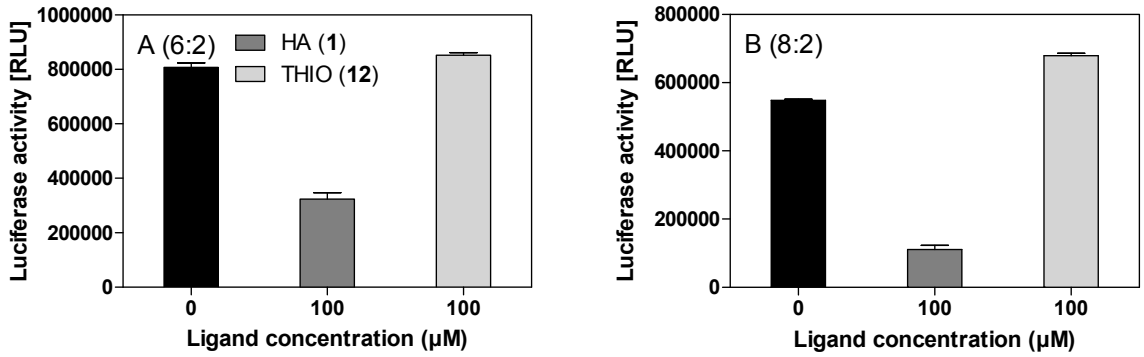

Figure 4.24: Testing of $G\alpha_{i/o}$-mediated mH_4R response. The effect of 100 µM of the agonist HA (**1**) and the inverse agonist THIO (**12**) upon pre-stimulation by 1 µM of forskolin in HEK293-SF-mH_4R-His_6-CRE-Luc cells. 6:2 transfection (A). 8:2 transfection batch (B).

Forskolin concentration dependently increased the luciferase activity in HEK293-SF-mH_4R-His_6-CRE-Luc (6:2). An EC_{50} value of 1.14 ± 0.10 µM with a Hill slope of 1.43 ± 0.16 was determined (see **Figure 4.25**). Therefore, pre-stimulation with 1 µM of forskolin was considered appropriate.

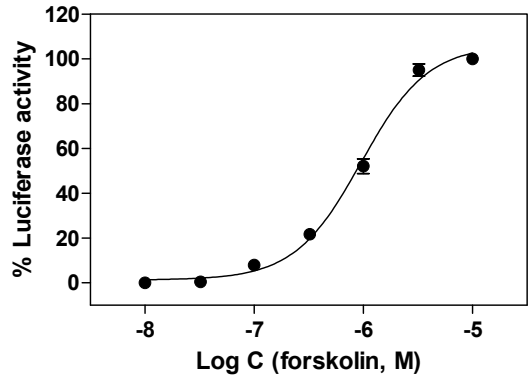

Figure 4.25: Concentration-response curve of forskolin in HEK293-SF-mH_4R-His_6-CRE-Luc (6:2) cells. Data were analyzed by nonlinear regression and best fitted to sigmoidal concentration-response curves. Data points shown are the mean values of three independent experiments performed in triplicate.

Determination of the time course of luciferase expression in HEK293-SF-mH_4R-His_6-CRE-Luc cells (6:2) (data are not shown) revealed no significant differences compared to that depicted in **Figure 4.16**.

4.2.3.2 Selection of the HEK293-CRE-Luc-SF-rH_4R-His_6 cells

For the extension of the luciferase reporter gene assay to the rH_4R, HEK293-CRE-Luc cells (cf. section 4.1.3.6) were stably transfected with the pcDNA3.1(+)-SF-rH_4R-His_6 vector. The inhibition of the forskolin (1 µM) stimulated luciferase activity by 100 µM of histamine (**1**) confirmed the successful expression of the rH_4R in the HEK293-CRE-Luc-SF-rH_4R-His_6 cells (see **Figure 4.26**). There were no significant differences detectable in forskolin stimulation and $G\alpha_{i/o}$-mediated rH_4R response among the 6:2 and 8:2 cells. Since the 6:2 cells were more readily available due to faster growth, these cells were chosen for the investigations of H_4R ligand activity at the rH_4R.

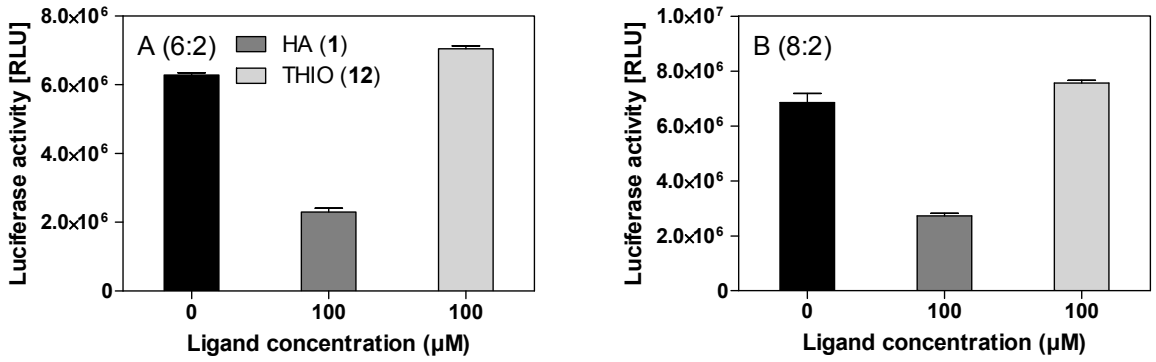

Figure 4.26: Changes in luciferase activity by $G\alpha_{i/o}$-mediated rH_4R responses. The effect of 100 µM of the agonist histamine (**1**) and the inverse agonist thioperamide (**12**) upon pre-stimulation by 1 µM of forskolin in HEK293-CRE-Luc-SF-rH_4R-His_6 cells. 6:2 transfection (A). 8:2 transfection batch (B).

4.2.3.3 Influence of forskolin on the potency of histamine

The EC_{50} value of forskolin in HEK293-CRE-Luc cells, which were used for the transfection with the rH_4R, was 3.75 ± 0.96 µM as shown is section 4.1.3.6. Therefore, a forskolin concentration of 4 µM should be used to enable the determination of both agonistic and inverse agonistic activity of H_4R ligands. To evaluate the dependence of agonist potency on forskolin concentrations, the EC_{50} value of histamine (**1**) was determined in the presence of various forskolin concentration ranging from 0.5 µM to 5 µM in HEK293-CRE-Luc-SF-rH_4R-His_6 cells (see **Figure 4.27**).

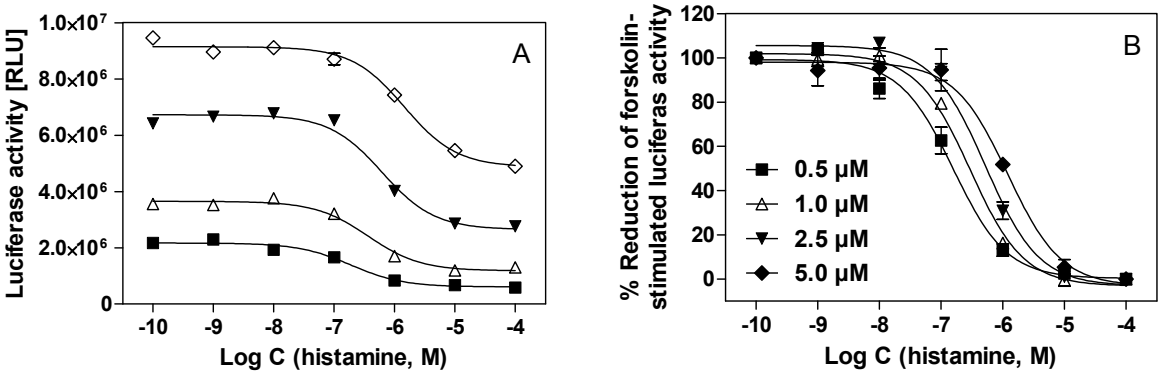

Figure 4.27: Concentration response curves of HA (**1**) in HEK293-CRE-Luc-SF-rH_4R-His_6 cells upon pre-stimulation with various forskolin concentrations (0.5 – 5.0 µM). Representative luciferase reporter gene assay, luciferase activity is presented as RLU values (A). Inhibition of forskolin stimulated luciferase activity (100 %) by increasing histamine (HA, **1**) concentrations; the maximum inhibitory effect of histamine corresponds to 0 % luciferase activity. Data points shown are the mean values ± SEM of at least three independent experiments performed in triplicate (B). Data were analyzed by nonlinear regression and best fitted to sigmoidal concentration-response curves.

Forskolin concentration-dependently increased the luciferase expression, which in turn was inhibited by histamine (**1)** to an extent of 70.2 ± 1.9 % (N = 3), 66.0 ± 1.3 % (N = 6), 56.0 ± 0.72 % (N = 3) and 43.7 ± 2.5 % (N = 3) using 0.5 µM, 1 µM, 2.5 µM and 5 µM of forskolin, respectively, i.e. although the absolute inhibitory effect (RLU values) of histamine (**1**) seemed to be amplified at higher forskolin concentrations (see **Figure 4.27** A), the relative inhibitory effect decreased. Furthermore, the higher the forskolin concentration used for pre-stimulation, the more the concentration-response curve was shifted to the right (see **Figure 4.27** B), resulting in lower pEC_{50} values (see **Table 4.4**). With the exception of 2.5 µM of forskolin, the determined pEC_{50} values were statistically different relative to the pEC_{50} values of histamine (**1**) in the presence of 1 µM of forskolin (see **Table 4.4**). This correlated with a lower pEC_{50} value and signal-to-noise ratio of histamine (**1**) at the hH_4R in the presence of 50 µM IBMX (cf. section 4.1.3.5).

Table 4.4: Histamine potencies determined upon pre-stimulation with various concentrations of forskolin in HEK293-CRE-Luc-SF-rH_4R-His_6 cells. Mean values ± SEM of N independent experiments performed in triplicate. Statistical analysis of significant differences relative to the pEC_{50} value of histamine in the presence of 1 µM of forskolin: one-way ANOVA, Bonferroni's multiple comparison test. (*: $p < 0.05$; ***: $p < 0.001$; confidence intervall 95 %).

C forskolin (µM)	**Histamine (rH_4R)**	
	pEC_{50}	N
0.5	6.81 ± 0.11*	3
1.0	6.53 ± 0.04	6
2.5	6.29 ± 0.07	3
5.0	5.91 ± 0.04***	3

The results revealed a decreasing influence of the activated $G\alpha_{i/o}$-protein on the intracellular cAMP level as well as the signal-to-noise ratio with increasing concentrations of cAMP induced by forskolin or IBMX. The use of 1 µM of forskolin for the HEK293-CRE-Luc-SF-rH_4R-His_6 cells was considered appropriate in terms of pEC_{50} values and signal-to-noise ratio.

4.2.3.4 Functional activity of histamine H_4 receptor ligands at the mouse and rat histamine H_4 receptor

Histamine (**1**) inhibited the forskolin (1 µM) stimulated luciferase reporter gene transcription by 74.2 ± 5.5 % (N = 4) and 66.0 ± 1.3 % (N = 6) in the HEK293-SF-mH_4R-His_6-CRE-Luc and the HEK293-CRE-Luc-SF-rH_4R-His_6 cells, respectively, suggesting that the signal-to-noise ratio was appropriate for performing the luciferase reporter gene assay at the mouse and rat H_4R. Thioperamide (**12**) increased the forskolin stimulated luciferase activity by 34.1 ± 2.8 (N = 4) and 10.3 ± 2.0 (N = 4) in the mH_4R and rH_4R expressing reporter cells, respectively, indicating considerable constitutive activity of the mH_4R and only low constitutive activity of the rH_4R. The H_4R ligands, which were already characterized at the hH_4R, were tested for their ability to change forskolin stimulated (1 µM) luciferase activity in the reporter gene on the mouse and rat H_4R orthologs. The obtained results were compared with data from literature and from functional [^{35}S]GTPγS binding assay on membrane preparations of Sf9 cells expressing the mH_4R or the rH_4R (D. Wifling, personal communication; results of the dissertation project of D.W., to be reported in detail elsewhere) (cf. **Table 4.6**).

In addition to binding studies at the mH_4R (cf. section 3.2.3.3), the separated stereoisomers of the phenylthioethyl-substituted (UR-RG98) and methyl-substituted (UR-RG94) cyano-

guanidines were evaluated in the luciferase reporter gene assay at the mH_4R and in part at the rH_4R. The results are summarized in **Table 4.7**.

Histamine (**1**), (R)-α-methylhistamine (**2**), (S)-α-methylhistamine (**3**), N^{α}-methylhistamine (**4**) and 5(4)-methylhistamine (**5**) changed forskolin stimulated luciferase activity in a concentration-dependent manner in HEK293-SF-mH_4R-His_6-CRE-Luc cells as well as in HEK293-CRE-Luc-SF-rH_4R-His_6 cells as shown **Figure 4.28**. Except for (S)-α-methylhistamine (**3**), histamine (**1**) and its methylated analogs displayed full agonistic activies (α = 1) at the mouse and rat H_4R. The potency of (S)-α-methylhistamine (**3**) was insufficient to fully activate the receptors. In comparison to the hH_4R, only a slight decrease in potency was detected at the mH_4R for compounds **1**-**5**. Species-dependent differences became more obvious at the rH_4R. For example, histamine (**1**) was 6 and 17 times less potent at the mH_4R and the rH_4R, respectively. Despite these species-dependent differences, the preference for the stereoisomer (R)-α-methylhistamine (**2**) over (S)-α-methylhistamine (**3**) was preserved among the three H_4Rs species orthologs (cf. **Figure 4.18**).

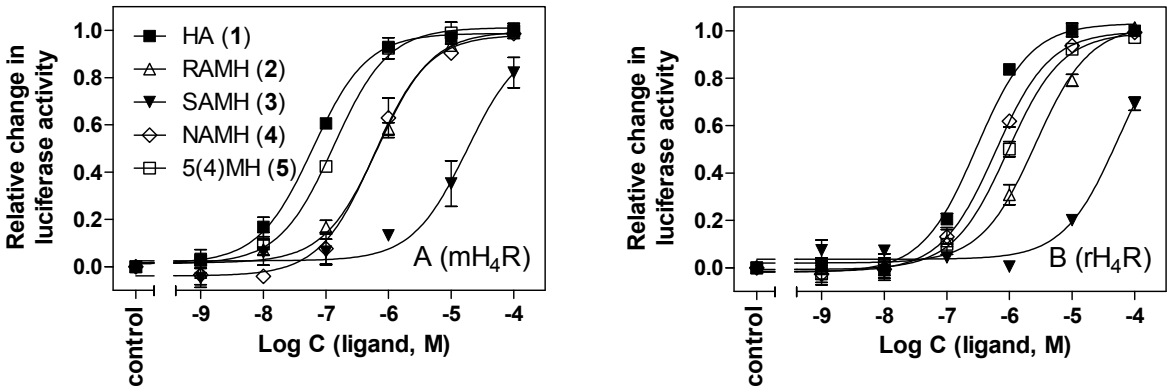

Figure 4.28: Relative change of the luciferase-activity by HA (**1**), RAMH (**2**), SAMH (**3**), NAMH (**4**) and 5-MHA (**5**) in HEK293-SF-mH_4R-His_6-CRE-Luc (A) and HEK293-CRE-Luc-SF-rH_4R-His_6 (B) cells. Maximum change of 1 is defined as full agonism, whereas 0 indicates the luminescence signal detected after direct stimulation of adenylyl cyclase 1 µM forskolin in the absence of H_4R ligands (control). Data were analyzed by nonlinear regression and best fitted to sigmoidal concentration-response curves. Data points shown are the mean values ± SEM of at least three independent experiments performed in triplicate.

The comparison of the determined potency for histamine (**1**) and its methylated analogs at the mouse and rat H_4R with literature, however, yielded controversial findings. Especially, the reported pEC_{50} values for histamine (**1**) differ by two orders of magnitude for both receptors as shown in **Table 4.5**. On the one hand, the pEC_{50} values of histamine (**1**), (R)-α-methylhistamine (**2**) and N^{α}-methylhistamine (**4**) were the same or even lower compared to data from a Ca^{2+} assay using HEK293 cells co-expressing the mouse or the rat H_4R and the

chimeric G-protein $G\alpha_{qi5}$, which directed the H_4R signaling to the G_q pathway (Liu *et al.*, 2001a; Strakhova *et al.*, 2009). On the other hand, the potencies of histamine (**1**) and 5(4)-methylhistamine (**5**) were significantly higher compared to the steady state [^{33}P]GTPase assay (Schnell *et al.*, 2011). Nevertheless, next to more comparable agonist potencies of the aforementioned Ca^{2+} assay, discrepancies regarding efficacies became obvious. Contrary to the luciferase reporter gene assay, (R)-α-methylhistamine (**2**) and N^{α}-methylhistamine (**4**) only reached 80 % and 40 - 50 % of the maximal response of histamine at the mH_4R and the rH_4R, respectively (Liu *et al.*, 2001b).

Table 4.5: Potencies of histamine at the mouse and rat H_4R in various assay systems reported in literature.

Assay	mouse H_4R	rat H_4R
	pEC_{50}	pEC_{50}
CRE controlled β-galactosidase reporter gene assay in SK-NM-C cells	6.47[a]	-
SRE-controlled luciferase reporter gene assay in HEK293 cells (co-expressing chimeric $G\alpha_{qi}$)	5.27[a]	6.77[a]
Ca^{2+} assay in HEK293 cells (co-expressing chimeric $G\alpha_{qi5}$)	7.23[b]	6.49[b]
Ca^{2+} assay in (HEK)293-EBNA cells (co-expressing chimeric $G\alpha_{qi5}$)	7.52[c]	7.10[c]
Steady-state [^{33}P]GTPase activity assay on Sf9 membranes (co-expressing $G\alpha_{i2}$, $\beta_{1\gamma2}$ and R**GS1**9 (regulator of G-protein 19))	5.81[d]	5.23[d]

Data taken from: [a] (Yu *et al.*, 2010); [b] (Strakhova *et al.*, 2009); [c] (Liu *et al.*, 2001a); [d] (Schnell *et al.*, 2011).

Immepip (**6**) fully activated the mouse and the rat H_4R, compared to the hH_4R, with only slightly lower pEC_{50} values of 6.85 ± 0.17 and 7.17 ± 0.06, respectively (see **Figure 4.29**). These results were in disagreement with the [^{35}S]GTPγS binding assay. In the latter immepip (**6**) was a partial agonist with 10- and 100-fold lower potencies at the mH_4R and rH_4R, respectively (see **Table 4.6**). In line with results at the hH_4R, extension of the spacer length in immepip (**6**) by two carbon atoms led to substantial decrease in potency and intrinsic activity at the mH_4R, as shown for VUF 5681 (**7**) in **Figure 4.29** A. Surprisingly, the hH_4R partial agonist immethridine (**8**) exhibited almost full agonist activity at both the mouse and rat H_4R, and the pEC_{50} values (5.95 ± 0.03 and 5.80 ± 0.13, respectively) were comparable to that at the hH_4R (see **Figure 4.29**).

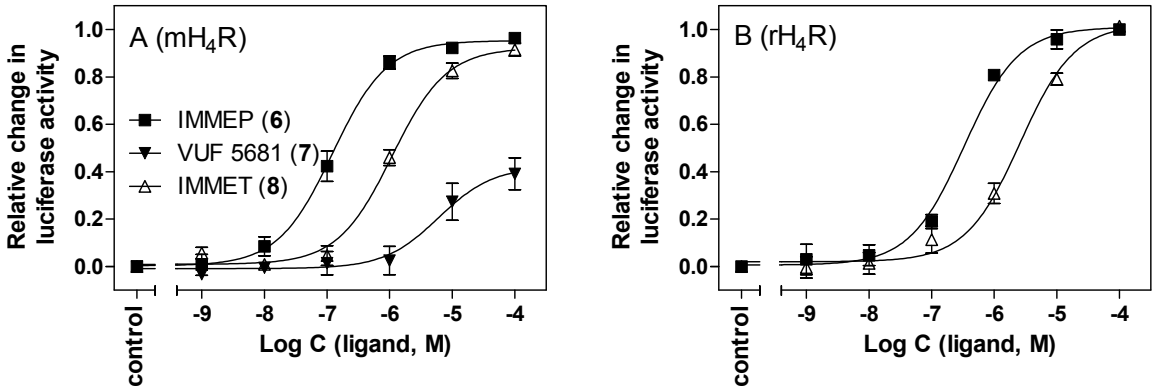

Figure 4.29: Potencies and efficacies of IMMEP (**6**), VUF 5681 (**7**) and IMMET (**8**) at the mH_4R (A) and the rH_4R (B) stably co-expressed with a CRE-controlled luciferase reporter gene in HEK293T cells. Maximum change of 1 is defined as full agonism, whereas 0 indicates the luminescence signal detected after direct stimulation of adenylyl cyclase by 1 µM forskolin in the absence of H_4R ligands (control). Data were analyzed by nonlinear regression and best fitted to sigmoidal concentration-response curves. Data points shown are the mean values ± SEM of at least three independent experiments performed in triplicate.

Furthermore, the isothiourea containing $H_{4/3}R$ ligands imetit (**9**), clobenpropit (**10**) and iodophenpropit (**11**) as well as the $H_{3/4}R$ inverse agonist thioperamide (**12**) were examined (see **Figure 4.30**). Interestingly, at the mouse and the rat H_4R, imetit (**9**) retained almost the same potency (pEC_{50} values: 7.41 ± 0.11 and 7.21 ± 0.12) as at the hH_4R. Moreover, imetit (**9**) acted at all three H_4R species orthologs as nearly full agonist with α values of 0.94 – 0.96. The conserved activity of imetit (**9**) at the species orthologs is in agreement with reported data from Ca^{2+} assays on HEK293 cells at the human, mouse and rat H_4R, however, although imetit (**9**) was more potent and less efficacious at all three receptors (Liu *et al.*, 2001b). By contrast, clobenpropit (**10**) and iodophenpropit (**11**) displayed a clear decrease in potency and efficacy at the mouse and rat H_4R compared to the hH_4R. Whereas clobenpropit (**10**) potently and fully activated the hH_4R**,** this compounds was only a partial agonist with moderate pEC_{50} values at the mouse and rat H_4R in the luciferase reporter gene assay (α = 0.55 ± 0.05 and α = 0.37 ± 0.03, respectively). Potency and efficacy were only slightly higher than in the [^{35}S]GTPγS binding assay (see **Table 4.6**). Iodophenpropit (**11**) exhibited partial agonistic activity at the hH_4R, but was a neutral antagonist at the mouse and the rat H_4R (α values close to zero, pK_B values comparable to data from the [^{35}S]GTPγS binding assay; cf. **Table 4.6**). Surprisingly, thioperamide (**12**) acted as an inverse agonist at the mH_4R achieving a pEC_{50} values of 6.52 ± 0.13. This was unexpected, since neither in the [^{35}S]GTPγS binding assay nor in the [^{33}P]GTPase assay (Schnell *et al.*, 2011) constitutive activity was detectable with thioperamide (**12**) at the mH_4R. Furthermore, thioperamide (**12**) revealed a clear decrease in affinity at the mH_4R in competition binding assays, and proved to be unsuitable for the determination of non-specific binding in saturation binding

experiments with [^{3}H]UR-PI294 and [^{3}H]histamine on HEK293-SF-mH$_4$R-His$_6$ cells (cf. section 3.2.3.2 and 3.2.3.3). Thioperamide (**12**) displayed negligible inverse agonistic activity at the rH$_4$R, but revealed a pK$_B$ value of 6.89 ± 0.14 in the antagonist mode, which was in agreement with results from the [^{35}S]GTPγS binding assay (see **Table 4.6**).

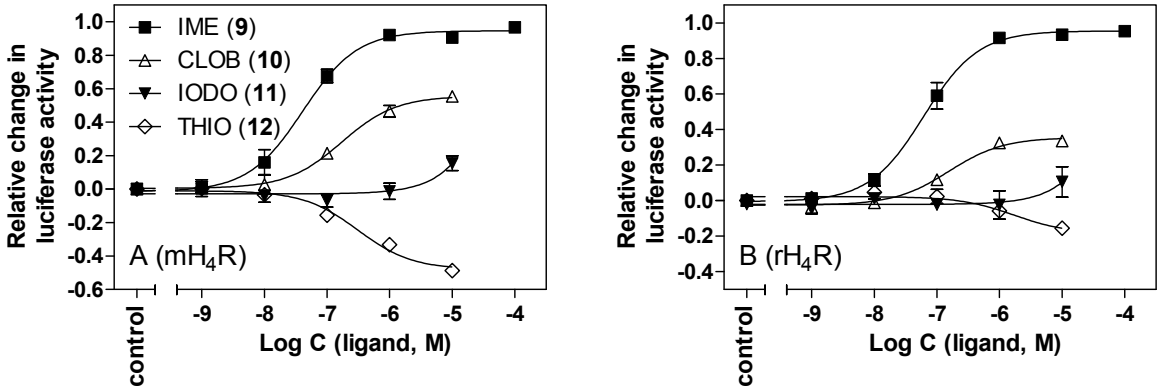

Figure 4.30: Percental change in forskolin (1 µM) stimulated luciferase activity induced by IME (**9**), CLOB (**10**), IODO (**11**) and THIO (**12**) in HEK293-SF-mH$_4$R-His$_6$-CRE-Luc (A) and HEK293-CRE-Luc-SF-rH$_4$R-His$_6$ (B) cells. Maximum change of 1 indicates full agonism, -1 is defined as "full" inverse agonism, whereas 0 indicates the luminescence signal detected after direct stimulation of adenylyl cyclase by 1 µM forskolin in the absence of H$_4$R ligands (control). Data were analyzed by nonlinear regression and best fitted to sigmoidal concentration-response curves. Data points shown are the mean values ± SEM of at least three independent experiments performed in triplicate.

As at the hH$_4$R, proxyfan (**13**) was a partial agonist at the mouse and rat H$_4$R, although with a significantly lower potency. Clozapine (**18**) fully activated both the mouse and the rat H$_4$R with low pEC$_{50}$ values (see **Figure 4.31**). In contrast, **18** did not show any activity at both species orthologs, neither in the agonist mode nor in the antagonist mode, in the [^{35}S]GTPγS binding assay (Wifling, 2012). The standard H$_4$R antagonist JNJ 7777120 (**19**) behaved as neutral antagonist in the luciferase reporter gene assay at the mH$_4$R. The pK$_B$ value of 7.58 ± 0.13 was in good correlation with the pK$_i$ value of 7.40 ± 0.14 (cf. section 3.2.3.3) and did not significantly differ from the pK$_B$ value determined at the hH$_4$R. In contrast, JNJ 7777120 (**19**) acted as partial agonist (α = 0.49 ± 0.05) with a pEC$_{50}$ value of 8.21 ± 0.10 at the rH$_4$R. However, compared to reported functional data gained from other assays, discrepancies became obvious. Antagonist behavior at both receptors was determined in a CRE-driven β-galactosidase reporter gene assay in SK-N-MC cells (Thurmond *et al.*, 2004) and in a Ca^{2+} assay in HEK293 cells (Strakhova *et al.*, 2009). Partial agonistic activity at the mouse and rat receptor was found in the [^{33}P]GTPase (Schnell *et al.*, 2011) and the [^{35}S]GTPγS binding assay (see **Table 4.6**). The determined pK$_B$ value at the mH$_4$R was consistent with the pK$_B$ value in the Ca^{2+} assay (Strakhova *et al.*, 2009), whereas the potency at the rH$_4$R was about

two orders of magnitude higher compared to the [^{33}P]GTPase assay (Schnell *et al.*, 2011). The discrepancies between the activities of JNJ 7777120 (**19**) at the H_4R orthologs in the different assay systems may be caused by different basal equilibria (presence and absence of constitutively active receptors) of the H_4R as described recently (Seifert *et al.*, 2011). Constitutive activity, unmasked by the inverse agonist thioperamide (**12**), was considerable at the mH_4R, but very low at the rH_4R. As suggested by Seifert et al., JNJ 7777120 (**19**) may influence the equilibrium between active and inactive state for all H_4R orthologs in a comparable manner (Seifert *et al.*, 2011). This might appear as neutral antagonistic activity at the mH_4R, i.e. no shift toward the active or inactive state, whereas in case of the rH_4R (only low constitutive activity unmasked by thioperamide (**12**)), JNJ 7777120 (**19**) shifted the equilibrium toward the active state and thus agonistic activity appeared. VUF 8430 (**20**) had about the same potency at both the mH_4R and the hH_4R, whereas the potency at the rH_4R was distinctly lower (see **Figure 4.31**). At both rodent H_4R orthologs, VUF 8430 (**20**) was almost as efficacious as histamine (α = 0.96–0.98). However, VUF 8430 (**20**) exhibited distinctly lower potencies and efficacies at the mouse and rat H_4R in the [^{35}S]GTPγS binding assay compared to the reporter gene assay (see **Table 4.6**).

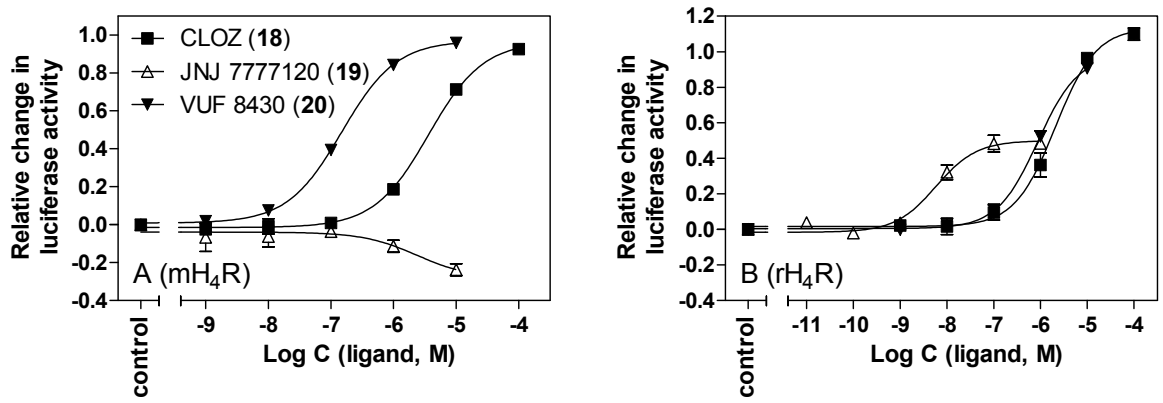

Figure 4.31: Potencies and efficacies of CLOZ (**18**), JNJ 7777120 (**19**) and VUF 8430 (**20**) at the mH_4R (A) and the rH_4R (B) stably co-expressed along with a CRE controlled luciferase reporter gene in HEK293T cells. Maximum change of 1 indicates full agonism, -1 is defined as "full" inverse agonism, whereas 0 indicates the luminescence signal detected after direct stimulation of adenylyl cyclase by 1μM forskolin in the absence of H_4R ligands (control). Data were analyzed by nonlinear regression and best fitted to sigmoidal concentration-response curves. Data points shown are the mean values ± SEM of at least three independent experiments performed in triplicate.

The potency of ST-1006 (**30**) was comparable at the mH_4R (pEC_{50} = 7.76 ± 0.11) and the hH_4R, whereas this compound displayed partial agonistic activity at the mH_4R (α = 0.37 ± 0.04) with lower maximal response than at the hH_4R (α = 0.91 ± 0.01) (see **Figure 4.32** A). Surprisingly, **30** proved to be an inverse agonist at the rH_4R with a pEC_{50} value of 6.08 ± 0.17 and an α value of -0.55 ± 0.12 (see **Figure 4.32** B). This was unexpected, since the standard

inverse agonist thioperamide (**12**) only acted as neutral antagonist at the rH_4R (cf. **Figure 4.30**). ST-1012 (**31**) acted as inverse agonist at the hH_4R, but revealed partial agonistic activity at both the mouse and the rat H_4R with pEC_{50} values of 7.49 ± 0.09 and 8.12 ± 0.08, respectively.

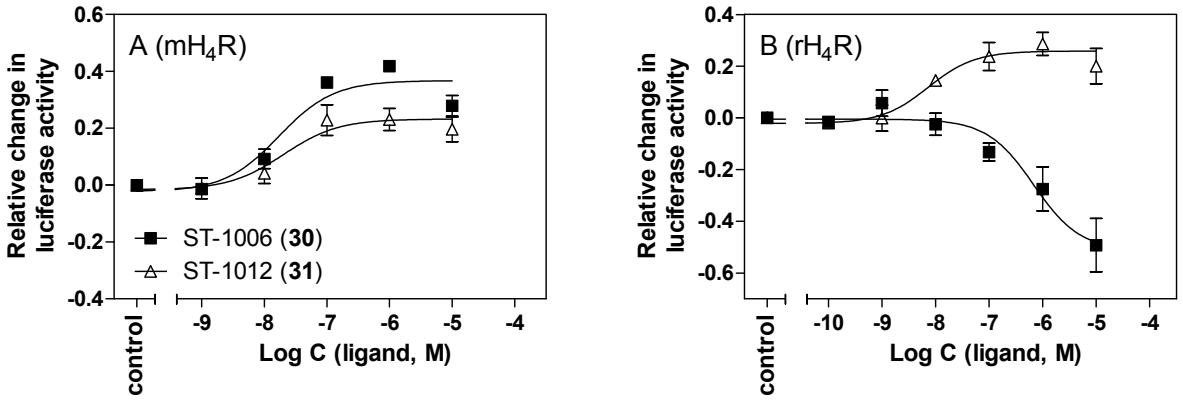

Figure 4.32: Concentration response curves of ST-1006 (**30**) and ST-1012 (**31**) at mH_4R (A) and rH_4R (B) stably co-expressed with a CRE controlled luciferase reporter gene in HEK293T cells. Maximum change of 1 indicates full agonism, -1 is defined as "full" inverse agonism, whereas 0 indicates the luminescence signal detected after direct stimulation of adenylyl cyclase by 1 µM forskolin in the absence of H_4R ligands (control). Data were analyzed by nonlinear regression and best fitted to sigmoidal concentration-response curves. Data points shown are the mean values ± SEM of at least three independent experiments performed in triplicate.

The acylguanidine-type compound UR-PI294 (**15**) fully activated the mH_4R and the rH_4R with pEC_{50} values of 8.29 ± 0.18 and 8.16 ± 0.03 (see **Figure 4.33**) and was the most potent agonist studied at the two rodent H_4R othologs and at the hH_4R. However, these results were not in agreement with data from the [^{35}S]GTPγS binding and the [^{33}P]GTPase assays. Although UR-PI294 (**15**) acted also as full agonist on the Sf9 cell membrane preparations, the pEC_{50} values were about two orders of magnitude lower for the mH_4R and even about three orders of magnitude lower at the rH_4R (see **Table 4.6** and (Schnell *et al.*, 2011)). The cyanoguanidine UR-PI376 (**16**) exhibited only partial agonistic activity at the mH_4R and no agonism at the rH_4R, although full agonistic activity was determined at the hH_4R (see **Figure 4.33**). At the mH_4R, the decrease in intrinsic activity was accompanied with roughly 10-fold lower potency, which was in accordance to data from the [^{33}P]GTPase assay (Schnell *et al.*, 2011). At the rH_4R, UR-PI376 (**16**) only reached a pK_B value of 5.15 ± 0.05, suggesting only very weak binding. In agreement with this result, UR-PI376 (**16**) showed no agonism in the [^{35}S]GTPγS binding assay at the rH_4R, and the determined pK_B value was just as low as in the luciferase reporter gene assay (see **Table 4.6**).

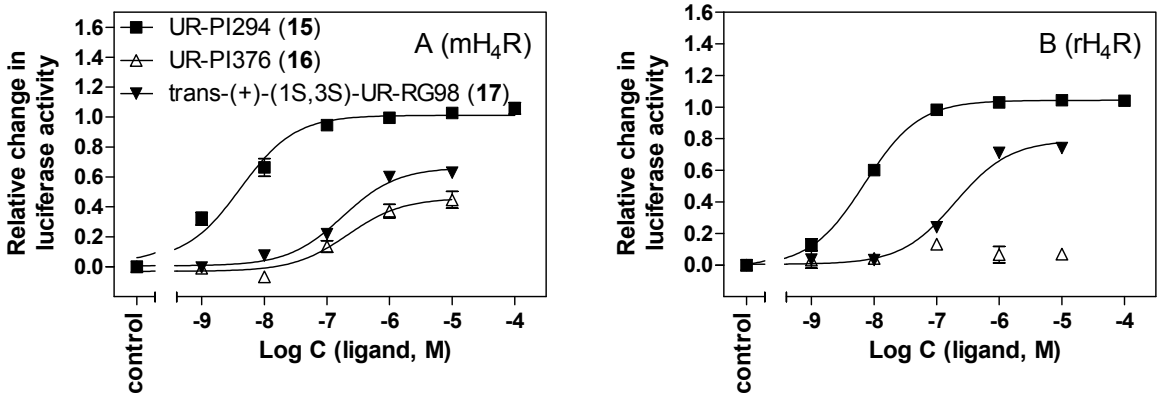

Figure 4.33: Potencies and efficacies of UR-PI294 (**15**), UR-PI376 (**16**) and trans(+)-(1S,3S)-UR-RG98 (**17**) in HEK293-SF-mH_4R-His_6-CRE-Luc(A) and HEK293-CRE-Luc-SF-rH_4R-His_6 (B) cells. Maximum change of 1 is defined as full agonism, whereas 0 indicates the luminescence signal detected after direct stimulation of adenylyl cyclase by 1 µM forskolin in the absence of H_4R ligands (control). Data were analyzed by nonlinear regression and best fitted to sigmoidal concentration-response curves. Data points shown are the mean values ± SEM of at least three independent experiments performed in triplicate.

Table 4.6: Potencies and efficacies of H_4R ligands at the mH_4R and rH_4R in the luciferase reporter gene assay and in functional binding assay with [^{35}S]GTPγS. Data are represented as mean values ± SEM.

Ligand	**mH_4R**					**rH_4R**				
	pEC_{50} or (pK_B)	α	N	pEC_{50} or (pKB)	α	pEC_{50} or (pK_B)	α	N	pEC_{50}	α
	Luciferase reporter gene assay in HEK293-SF-mH_4R-His_6-CRE-Luc cells			[^{35}S]GTPγS binding[a]		Luciferase reporter gene assay in HEK293CRE-Luc-SF-rH_4R-His_6 cells			[^{35}S]GTPγS binding[a]	
Histamine (**1**)	7.06 ± 0.13	1.00 ± 0.00	4	5.17 ± 0.14	1.00 ± 0.00	6.53 ± 0.04	1.00 ± 0.00	6	4.28 ± 0.06	1.00 ± 0.00
(R)-α-Methylhistamine (**2**)	6.16 ± 0.07	0.98 ± 0.01	6	n.d.	n.d.	5.60 ± 0.12	0.96 ± 0.02	3	n.d.	n.d.
(S)-α-Methylhistamine (**3**)	4.72 ± 0.16	0.82 ± 0.07	3	n.d.	n.d.	4.26 ± 0.04	0.69 ± 0.03	3	n.d.	n.d.
N^{α}-Methylhistamine (**4**)	6.24 ± 0.13	0.97 ± 0.02	3	n.d.	n.d.	6.23 ± 0.09	0.98 ± 0.04	3	n.d.	n.d.
5(4)-Methylhistamine (**5**)	6.87 ± 0.05	0.97 ± 0.02	4	n.d.	n.d.	6.03 ± 0.05	1.00 ± 0.03	3	n.d.	n.d.
Immepip (**6**)	6.85 ± 0.17	0.95 ± 0.03	3	5.27 ± 0.06	0.67 ± 0.08	7.17 ± 0.06	0.93 ± 0.05	3	4.95 ± 0.07	0.68 ± 0.10
VUF 5681 (**7**)	5.20 ± 0.15	0.42 ± 0.02	3	n.d.	n.d.	n.d.	n.d.	-	n.d.	n.d.
Immethridine (**8**)	5.95 ± 0.03	0.87 ± 0.02	3	n.d.	n.d.	5.80 ± 0.13	0.94 ± 0.01	3	n.d.	n.d.
Imetit (**9**)	7.41 ± 0.11	0.96 ± 0.02	3	n.d.	n.d.	7.21 ± 0.12	0.95 ± 0.01	4	n.d.	n.d.
Clobenpropit (**10**)	6.73 ± 0.08	0.55 ± 0.05	3	6.07 ± 0.09	0.20 ± 0.02	6.80 ± 0.11	0.37 ± 0.03	3	(6.30 ± 0.07)	0.00 ± 0.00
Iodophenpropit (**11**)	(6.66 ± 0.03)	0.01 ± 0.05	3	(6.41 ± 0.12)	0.00 ± 0.00	(6.49 ± 0.11)	-0.01 ± 0.06	3	(5.98 ± 0.07)	0.00 ± 0.00
Thioperamide (**12**)	6.52 ± 0.13	-0.44 ± 0.02	4	(7.12 ± 0.09)	0.00 ± 0.00	(6.89 ± 0.14)	-0.20 ± 0.02	4	(6.44 ± 0.09)	0.00 ± 0.00
Proxyfan (**13**)	6.10 ± 0.07	0.88 ± 0.04	3	n.d.	n.d.	5.67 ± 0.13	0.76 ± 0.03	3	n.d.	n.d.

Table 4.6 (continued)

Ligand	mH_4R					rH_4R				
	pEC_{50} or (pK_B)	α	N	pEC_{50} or (pKB)	α	pEC_{50} or (pK_B)	α	N	pEC_{50}	α
	Luciferase reporter gene assay in HEK293-SF-mH_4R-His_6-CRE-Luc cells			$[^{35}S]GTP\gamma S$ binding[a]		Luciferase reporter gene assay in HEK293-SF-mH_4R-His_6-CRE-Luc cells			$[^{35}S]GTP\gamma S$ binding[a]	
UR-PI294 (**15**)	8.29 ± 0.18	0.97 ± 0.02	5	6.10 ± 0.11	0.95 ± 0.03	8.16 ± 0.03	1.03 ± 0.02	3	5.48 ± 0.08	1.09 ± 0.03
UR-PI376 (**16**)	6.61 ± 0.25	0.51 ± 0.05	3	(6.06 ± 0.17)	0.00 ± 0.00	(5.15 ± 0.05)	0.08 ± 0.10	3	(5.49 ± 0.06)	0.00 ± 0.00
Clozapine (**18**)	5.44 ± 0.06	0.99 ± 0.01	3	-	0.00 ± 0.00	5.70 ± 0.11	1.12 ± 0.05	4	-	0.00 ± 0.00
JNJ 7777120 (**19**)	(7.58 ± 0.13)	-0.23 ± 0.03	4	6.10 ± 0.07	0.44 ± 0.03	8.21 ± 0.10	0.49 ± 0.05	5	6.13 ± 0.14	0.24 ± 0.01
VUF 8430 (**20**)	6.83 ± 0.03	0.96 ± 0.02	3	5.06 ± 0.14	0.68 ± 0.04	6.06 ± 0.06	0.98 ± 0.02	3	4.47 ± 0.15	0.43 ± 0.05
ST-1006 (**30**)	7.76 ± 0.11	0.37 ± 0.04	4	n.d.	n.d.	6.08 ± 0.17	-0.55 ± 0.12	3	n.d.	n.d.
ST-1012 (**31**)	7.49 ± 0.09	0.24 ± 0.05	4	n.d.	n.d.	8.12 ± 0.08	0.24 ± 0.07	4	n.d.	n.d.

pEC_{50} values determined in the luciferase reporter gene assay show the change of 1 µM forskolin-induced luciferase activity in HEK293-mH_4R-His_6-CRE-Luc and HEK293-CRE-Luc-SF-rH_4R-His_6 cells, respectively. N gives the number of independent experiments performed in triplicate each. The intrinsic activity (α) of histamine was set to 1.00 and α values of other compounds were referred to this value. The K_B values of neutral antaonists were determined in the antagonist mode at the mH_4R and rH_4R *versus* histamine (150 nM and 1µM, respectively) as the agonist. Data taken from: functional $[^{35}S]GTP\gamma S$-binding assay on Sf9 cell membranes co-expressing the mH_4R or rH_4R + $G_{i\alpha 2}$ + $\beta_{1\gamma 2}$ [a] (Wifling, 2012).

Trans-(+)-(1S,3S)-UR-RG98 (**17**), which was the most potent and selective stereoisomer among the conformationally constrained cyanoguanidine-type agonists at the hH_4R (cf. section 4.1.3.8), revealed lower intrinsic activity at the mH_4R ($\alpha = 0.67 \pm 0.04$), but acted, contrary to UR-PI376 (**16**), as potent partial agonist at the rH_4R ($\alpha = 0.81 \pm 0.08$) (see **Figure 4.33**). Nevertheless, a roughly 10-fold decrease in potency was observed at both H_4R species orthologs compared to the hH_4R. trans-(-)-(1R,3R)-UR-RG98 (**23**) (pEC_{50} 6.23 ± 0.14) was equipotent at the mH_4R and hH_4R, but the intrinsic activity at the murine receptor was clearly lower ($\alpha = 0.29 \pm 0.02$) (see **Table 4.7** and cf. **Table 4.3**). Also cis-(-)-(1S,3R)-UR-RG98 (**24**) displayed low intrinsic activity ($\alpha = 0.31 \pm 0.03$) and moderate potency at the mH_4R ($pEC_{50} = 6.45 \pm 0.22$). Surprisingly, cis-(+)-(1R,3S)-UR-RG98 (**25**) seemed to be preferred by the mouse and rat H_4R compared to the hH_4R. In comparison to recently described functional [^{35}S]GTPγS binding data at the hH_4R (Geyer, 2011), cis-(+)-(1R,3S)-UR-RG98 (**25**) acted more potently at the mouse and rat H_4R ($pEC_{50} = 6.97 \pm 0.10$ and $pEC_{50} = 6.98 \pm 0.02$, respectively) and produced higher maximal responses ($\alpha = 0.81 \pm 0.03$ and $\alpha = 1.00 \pm 0.03$, respectively). Interestingly, the methyl-substituted cyanoguanidines (UR-RG94) revealed all strong partial to full agonism at the mH_4R and thus an increased intrinsic activity compared to the [^{35}S]GTPγS binding assay at the hH_4R (Geyer, 2011). Both trans-(-)-(1R,3R)-UR-RG94 (**26**) and trans-(+)-(1S,3S)-UR-RG94 (**27**) fully activated the mH_4R with pEC_{50} values of 5.44 ± 0.15 and 6.27 ± 0.03, respectively, suggesting that the mH_4R, just as the hH_4R, preferred trans-(+)-(1S,3S)-UR-RG94 (**27**) over trans-(-)-(1R,3R)-UR-RG94 (**26**), though at lower potency for both stereoisomers (Geyer, 2011). Stereodiscrimination by the mH_4R was even more pronounced for the cis-configured stereoisomers (-)-(1R,3S)-UR-RG94 (**28**) and (+)-(1R,3S)-UR-RG94 (**29**). Compound **29** was 60 times more potent than **28** at the mH_4R and, with a pEC_{50} values of 6.83 ± 0.08, equipotent with its phenylthioethyl-substituted analog **25**. In summary, the cis-(+) stereoisomers of RG98 (**25**) and RG94 (**29**) were identified as the most potent agonists among the investigated conformationally contrained cyanoguandine-type stereoisomers in the luciferase reporter gene assay at the mH_4R.

Table 4.7: Pharmacological activities of the conformationally constrained cyanoguanidines **17**, **23-29** at the mH_4R and rH_4R in the luciferase reporter gene assay using HEK293-CRE-Luc-SF-mH_4R-His_6 cells and HEK293-CRE-Luc-SF-rH_4R-His_6 cells, respectively. Mean values ± SEM of N independent experiments performed in triplicate.

Ligand	**mH_4R**			**rH_4R**		
	pEC_{50}	α	N	pEC_{50}	α	N
trans-(+)-(1S,3S)-UR-RG98 (**17**)	6.78 ± 0.06	0.67 ± 0.04	3	6.70 ± 0.03	0.81 ± 0.08	3
trans-(-)-(1R,3R)- UR-RG98 (**23**)	6.23 ± 0.14	0.29 ± 0.02	3	n.d.	n.d.	-
cis-(-)-(1S,3R)-UR-RG98 (**24**)	6.45 ± 0.22	0.31 ± 0.03	4	n.d.	n.d.	-
cis-(+)-(1R,3S)-UR-RG98 (**25**)	6.97 ± 0.10	0.81 ± 0.03	4	6.98 ± 0.02	1.00 ± 0.03	3
trans-(-)-(1R,3R)-UR-RG94 (**26**)	5.44 ± 0.15	1.00 ± 0.02	4	n.d.	n.d.	-
trans-(+)-(1S,3S)-UR-RG94 (**27**)	6.27 ± 0.03	0.96 ± 0.02	3	n.d.	n.d.	-
cis-(-)-(1S,3R)-UR-RG94 (**28**)	5.04 ± 0.16	0.87 ± 0.04	4	n.d.	n.d.	-
cis-(+)-(1R,3S)-UR-RG94 (**29**)	6.83 ± 0.08	0.98 ± 0.04	4	n.d.	n.d.	-

n.d.: not determined.

In summary, HEK293T cells co-expressing a CRE-controlled luciferase reporter gene and the mouse or rat H_4R are useful systems to functionally characterized H_4R agonists, inverse agonists and antagonists. However, comparison of the agonist activities at the mouse and rat H_4R revealed striking discrepancies. On the one hand, potencies of the agonists **1**, **5**, **6**, **15**, **18** and **19** (rH_4R) were significantly higher compared to data from the [^{33}P]GTPase and [^{35}S]GTPγS binding assay (Schnell *et al.*, 2011) (cf. **Table 4.6**). On the other hand, agonist potencies of **1**, **2**, **4** and **9** were comparable or lower compared to results from a Ca^{2+} assay using HEK293 cells, co-expressing the mouse or the rat H_4R and $G\alpha_{qi5}$ (Liu *et al.*, 2001a; Strakhova *et al.*, 2009). In contrast to discrepancies regarding agonist pharmacology, the pK_B values of neutral antagonists such as **11** at the mouse and rat H_4R as well as **12** and **16** at the rH_4R were comparable with data from the [^{35}S]GTPγS binding assay (cf. **Table 4.6**). Activation of the mouse and rat H_4R in the luciferase assay resulted in higher potencies compared to functional assays, which exclusively address the proximal hydrolysis of radiolabled GTP ([γ^{33}P]GTP) or the binding of radiolabel GTP ([^{35}S]GTPγS) to the Gα-protein. This may be interpreted as a hint to either signal amplification or to the activation of alternative signaling pathways that potentiate the inhibition of the reporter gene transcription. For instance, H_4R mediated Ca^{2+} signaling via activation of phospholipase C (PLC) (Hofstra *et al.*, 2003) was reported as pathway with the potential to trigger a cross-talk with the cAMP cascade: Ca^{2+} was described as inhibitor of (forskolin) stimulated and Ca^{2+} sensitive adenylate cyclases type V/VI (Fagan *et al.*, 1998; Guillou *et al.*, 1999; Mou *et al.*, 2009), which are endogenously expressed in HEK293T cells (Atwood *et al.*, 2011; Rybin *et al.*,

2000) and interactors of the $G\alpha_{i/o}$ protein (Pavan *et al.*, 2009). Furthermore, the relevance of Ca^{2+} dependent inhibition of the cAMP pathway was demonstrated by the inhibitory effect of the $G\alpha_q$ coupled histamine H_1R on the cAMP level (Wong *et al.*, 2000) in U373 cells and, more importantly, by facilitation of the $G\alpha_{i/o}$ coupled M_2 mACh receptor mediated inhibition of forskolin-stimulated cyclic AMP production by the $G\alpha_q$ coupled M_3 mACh receptor at low agonists concentrations (Hornigold *et al.*, 2003). However, further studies are needed to clarify the influence of Ca^{2+} in general on the present reporter gene assay and whether only the rodent H_4Rs were concerned by this cross-talk, since agonist potencies at the hH_4R were consistent with data from the [^{33}P]GTPase and [^{35}S]GTPγS binding assay (cf. section 4.1.3.8). A hint could be the fact that histamine (**1**) and UR-PI376 (**16**) increased $[Ca^{2+}]_i$ 2.5-fold less effective than the chemokine eotaxin via the CCR3 receptor in human eosinophils (Reher *et al.*, 2012). Unfortunately, such a control experiment was not included in a study reporting on Ca^{2+} mobilization in mouse bone mast cells (Hofstra *et al.*, 2003).

Despite these discrepancies, two new pharmacological tools for the mouse and rat H_4R were identified within this study. The acylguanidine type compound UR-PI294 (**15**) fully and potently activated all three H_4R orthologs, and the aminopyrimidine type compound ST-1012 (**31**) revealed excellent agonistic potency at the rH_4R.

4.3 Concluding Remarks

Using a CRE- controlled luciferase reporter gene assay agonistic, inverse agonistic and antagonistic activity can be determined in HEK293T cells, stably expressing the human, rat and mouse H_4R receptor, respectively. The adaptation to the 96-well format provided high sensitivity and reliability in addition to the potential of higher throughput. Monitoring the time course of the luciferase expression revealed an optimal incubation period of 5 h. The time course was nearly identical for the different tested reporter cells. In contrast, the EC_{50} value of forskolin varied, probably due to different expression levels of the CRE-controlled luciferase within the different HEK293T transfection approaches. Moreover, due to an optimum in luciferase expression, beyond a concentration of 10 µM of forskolin, a downturn of the concentration-response curve became obvious, possibly caused by endogenous ICER activation at high cAMP concentrations in HEK293T cells. The presence of the PDE inhibitor IBMX increased basal luciferase expression and shifted the forskolin concentration response curve to the left, thus lowering the EC_{50} value of forskolin. The influence of the activated $G\alpha_{i/o}$-protein on the intracellular cAMP level as well as the signal-to-noise ratio seemed to be lowered by increasing cAMP levels. This was reflected by lower relative effects and potencies of histamine (**1**). All in all, these findings demonstrated that high forskolin concentration should be avoided.

HEK293-CRE-Luc cells stably expressing the CRE-linked luciferase reporter gene were established for the investigation of non-H_4R mediated effects and successfully used for the transfection with the rH_4R. The determined potencies of the H_4R ligands at the hH_4R were in accordance to reported results, regardless of a tendency toward increased intrinsic activities, presumably, due to signal amplification in the reporter gene assay. Even compounds characterized as neutral antagonists in other assays showed partial agonistic activity in the luciferase reporter gene assay. Surprisingly, differences in agonist potencies between the H_4R othologs were mostly less pronounced compared to [^{33}P]GTPase assay and [^{35}S]GTPγS binding assay. The causes may be multifactorial, including activation/amplification of or crosstalk between different signaling pathways influencing the ultimate readout in the luciferase reporter gene assay. Nevertheless, UR-PI294 (**15**) and ST-1012 (**31**) were identified as potent new pharmacological tools for the mouse and rat H_4R.

4.4 References

Appl, H.; Holzammer, T.; Dove, S.; Haen, E.; Strasser, A.; Seifert, R. Interactions of recombinant human histamine H(1)R, H(2)R, H(3)R, and H(4)R receptors with 34 antidepressants and antipsychotics. *Naunyn-Schmiedeberg's Arch. Pharmacol.* ***2011,*** 385, 145-70.

Atwood, B. K.; Lopez, J.; Wager-Miller, J.; Mackie, K.; Straiker, A. Expression of G protein-coupled receptors and related proteins in HEK293, AtT20, BV2, and N18 cell lines as revealed by microarray analysis. *BMC Genomics* ***2011,*** 12, 14.

Beermann, S.; Glage, S.; Jonigk, D.; Seifert, R.; Neumann, D. Opposite effects of mepyramine on JNJ 7777120-induced amelioration of experimentally induced asthma in mice in sensitization and provocation. *PLoS One* ***2012,*** 7, e30285.

Bronstein, I.; Fortin, J.; Stanley, P. E.; Stewart, G. S.; Kricka, L. J. Chemiluminescent and bioluminescent reporter gene assays. *Anal. Biochem.* ***1994,*** 219, 169-81.

Buckland, K. F.; Williams, T. J.; Conroy, D. M. Histamine induces cytoskeletal changes in human eosinophils via the H_4 receptor. *Br. J. Pharmacol.* ***2003,*** 140, 1117-1127.

Cheng, Y.; Prusoff, W. H. Relationship between the inhibition constant (K1) and the concentration of inhibitor which causes 50 per cent inhibition (I50) of an enzymatic reaction. *Biochem. Pharmacol.* ***1973,*** 22, 3099-108.

Coruzzi, G.; Adami, M.; Guaita, E.; de Esch, I. J. P.; Leurs, R. Antiinflammatory and antinociceptive effects of the selective histamine H_4-receptor antagonists JNJ7777120 and VUF6002 in a rat model of carrageenan-induced acute inflammation. *Eur. J. Pharmacol.* ***2007,*** 563, 240-244.

de Esch, I. J. P.; Thurmond, R. L.; Jongejan, A.; Leurs, R. The histamine H_4 receptor as a new therapeutic target for inflammation. *Trends Pharmacol. Sci.* ***2005,*** 26, 462-469.

Deml, K.-F.; Beermann, S.; Neumann, D.; Strasser, A.; Seifert, R. Interactions of Histamine H_1-Receptor Agonists and Antagonists with the Human Histamine H_4-Receptor. *Mol. Pharmacol.* ***2009,*** 76, 1019-1030.

Dunford, P. J.; O'Donnell, N.; Riley, J. P.; Williams, K. N.; Karlsson, L.; Thurmond, R. L. The histamine H_4 receptor mediates allergic airway inflammation by regulating the activation of CD4+ T cells. *J. Immunol.* ***2006,*** 176, 7062-70.

Eishingdrelo, H.; Cai, J.; Weissensee, P.; Sharma, P.; Tocci, M. J.; Wright, P. S. A cell-based protein-protein interaction method using a permuted luciferase reporter. *Curr. Chem. Genomics* ***2011,*** 5, 122-8.

Esbenshade, T. A.; Kang, C. H.; Krueger, K. M.; Miller, T. R.; Witte, D. G.; Roch, J. M.; Masters, J. N.; Hancock, A. A. Differential activation of dual signaling responses by human H_1 and H_2 histamine receptors. *J. Recept. Signal Transduct. Res.* ***2003a,*** 23, 17-31.

Esbenshade, T. A.; Krueger, K. M.; Miller, T. R.; Kang, C. H.; Denny, L. I.; Witte, D. G.; Yao, B. B.; Fox, G. B.; Faghih, R.; Bennani, Y. L. and others. Two novel and selective nonimidazole histamine H_3 receptor antagonists A-304121 and A-317920: I. In vitro pharmacological effects. *J. Pharmacol. Exp. Ther.* ***2003b,*** 305, 887-96.

Fagan, K. A.; Mons, N.; Cooper, D. M. Dependence of the Ca2+-inhibitable adenylyl cyclase of C6-2B glioma cells on capacitative Ca2+ entry. *J. Biol. Chem.* ***1998,*** 273, 9297-305.

Fitzgerald, L. R.; Mannan, I. J.; Dytko, G. M.; Wu, H. L.; Nambi, P. Measurement of responses from Gi-, Gs-, or Gq-coupled receptors by a multiple response element/cAMP response element-directed reporter assay. *Anal. Biochem.* ***1999,*** 275, 54-61.

George, S. E.; Bungay, P. J.; Naylor, L. H. Evaluation of a CRE-directed luciferase reporter gene assay as an alternative to measuring cAMP accumulation. *J. Biomol. Screen.* ***1997,*** 2, 235-240.

Geßele, K. Zelluläre Testsysteme zur pharmakologischen Charakterisierung neuer Neuropeptid Y-Rezeptorantagonisten: Rezeptor-Bindungsstudien und funktionelle Untersuchungen zur Calciummobilisierung und cAMP-Bildung. PhD thesis, University of Regensburg, Regensburg, Germany, 1998.

Geyer, R. Hetarylalkyl(aryl)cyanoguanidines as histamine H_4 receptor ligands: Synthesis, chiral separation, pharmacological characterization, structure-activity and -selectivity relationships. PhD thesis, University of Regensburg, Regensburg, 2011.

Geyer, R.; Buschauer, A. Synthesis and histamine H(3) and H(4) receptor activity of conformationally restricted cyanoguanidines related to UR-PI376. *Arch. Pharm.* ***2011,*** 344, 775-85.

Guillou, J. L.; Nakata, H.; Cooper, D. M. Inhibition by calcium of mammalian adenylyl cyclases. *J. Biol. Chem.* ***1999,*** 274, 35539-45.

Hill, S. J.; Baker, J. G.; Rees, S. Reporter-gene systems for the study of G-protein-coupled receptors. *Curr. Opin. Pharmacol.* ***2001,*** 1, 526-32.

Hofstra, C. L.; Desai, P. J.; Thurmond, R. L.; Fung-Leung, W.-P. Histamine H_4 Receptor Mediates Chemotaxis and Calcium Mobilization of Mast Cells. *J. Pharmacol. Exp. Ther.* ***2003,*** 305, 1212-1221.

Hornigold, D. C.; Mistry, R.; Raymond, P. D.; Blank, J. L.; Challiss, R. A. Evidence for cross-talk between M2 and M3 muscarinic acetylcholine receptors in the regulation of second messenger and extracellular signal-regulated kinase signalling pathways in Chinese hamster ovary cells. *Br. J. Pharmacol.* ***2003,*** 138, 1340-50.

Igel, P.; Geyer, R.; Strasser, A.; Dove, S.; Seifert, R.; Buschauer, A. Synthesis and structure-activity relationships of cyanoguanidine-type and structurally related histamine H_4 receptor agonists. *J. Med. Chem.* ***2009a,*** 52, 6297-313.

Igel, P.; Schneider, E.; Schnell, D.; Elz, S.; Seifert, R.; Buschauer, A. N(G)-acylated imidazolylpropylguanidines as potent histamine H_4 receptor agonists: selectivity by variation of the N(G)-substituent. *J. Med. Chem.* ***2009b,*** 52, 2623-7.

Jiang, W.; Lim, H. D.; Zhang, M.; Desai, P.; Dai, H.; Colling, P. M.; Leurs, R.; Thurmond, R. L. Cloning and pharmacological characterization of the dog histamine H_4 receptor. *Eur. J. Pharmacol.* ***2008,*** 592, 26-32.

Kemp, D. M.; George, S. E.; Bungay, P. J.; Naylor, L. H. Partial agonism at serotonin 5-HT1B and dopamine D2L receptors using a luciferase reporter gene assay. *Eur. J. Pharmacol.* ***1999,*** 373, 215-22.

Kemp, D. M.; George, S. E.; Kent, T. C.; Bungay, P. J.; Naylor, L. H. The effect of ICER on screening methods involving CRE-mediated reporter gene expression. *J. Biomol. Screen.* ***2002,*** 7, 141-8.

Kitbunnadaj, R.; Zuiderveld, O. P.; De Esch, I. J.; Vollinga, R. C.; Bakker, R.; Lutz, M.; Spek, A. L.; Cavoy, E.; Deltent, M. F.; Menge, W. M. and others. Synthesis and structure-activity relationships of conformationally constrained histamine H(3) receptor agonists. *J. Med. Chem.* ***2003,*** 46, 5445-57.

Kricka, L. J.; De Luca, M. Effect of solvents on the catalytic activity of firefly luciferase. *Arch. Biochem. Biophys.* ***1982,*** 217, 674-681.

Leurs, R.; Chazot, P. L.; Shenton, F. C.; Lim, H. D.; de Esch, I. J. Molecular and biochemical pharmacology of the histamine H_4 receptor. *Br. J. Pharmacol.* ***2009,*** 157, 14-23.

Leurs, R.; Vischer, H. F.; Wijtmans, M.; de Esch, I. J. En route to new blockbuster anti-histamines: surveying the offspring of the expanding histamine receptor family. *Trends Pharmacol. Sci.* ***2011,*** 32, 250-7.

Li, X.; Shen, F.; Zhang, Y.; Zhu, J.; Huang, L.; Shi, Q. Functional characterization of cell lines for high-throughput screening of human neuromedin U receptor subtype 2 specific agonists using a luciferase reporter gene assay. *Eur. J. Pharm. Biopharm.* ***2007,*** 67, 284-92.

Lim, H. D.; de Graaf, C.; Jiang, W.; Sadek, P.; McGovern, P. M.; Istyastono, E. P.; Bakker, R. A.; de Esch, I. J.; Thurmond, R. L.; Leurs, R. Molecular determinants of ligand binding to H_4R species variants. *Mol. Pharmacol.* ***2010,*** 77, 734-43.

Lim, H. D.; Smits, R. A.; Bakker, R. A.; van Dam, C. M.; de Esch, I. J.; Leurs, R. Discovery of S-(2-guanidylethyl)-isothiourea (VUF 8430) as a potent nonimidazole histamine H_4 receptor agonist. *J. Med. Chem.* ***2006,*** 49, 6650-1.

Lim, H. D.; van Rijn, R. M.; Ling, P.; Bakker, R. A.; Thurmond, R. L.; Leurs, R. Evaluation of histamine H_1-, H_2-, and H_3-receptor ligands at the human histamine H_4 receptor: identification of 4-methylhistamine as the first potent and selective H_4 receptor agonist. *J. Pharmacol. Exp. Ther.* ***2005,*** 314, 1310-21.

Ling, P.; Ngo, K.; Nguyen, S.; Thurmond, R. L.; Edwards, J. P.; Karlsson, L.; Fung-Leung, W.-P. Histamine H_4 receptor mediates eosinophil chemotaxis with cell shape change and adhesion molecule upregulation. *Br. J. Pharmacol.* ***2004,*** 142, 161-171.

Liu, C.; Ma, X.; Jiang, X.; Wilson, S. J.; Hofstra, C. L.; Blevitt, J.; Pyati, J.; Li, X.; Chai, W.; Carruthers, N. and others. Cloning and pharmacological characterization of a fourth histamine receptor (H(4)) expressed in bone marrow. *Mol. Pharmacol.* ***2001a,*** 59, 420-6.

Liu, C.; Wilson, S. J.; Kuei, C.; Lovenberg, T. W. Comparison of human, mouse, rat, and guinea pig histamine H4 receptors reveals substantial pharmacological species variation. *J. Pharmacol. Exp. Ther.* ***2001b,*** 299, 121-30.

Ma, Y.; Su, Q.; Tempst, P. Differentiation-stimulated activity binds an ETS-like, essential regulatory element in the human promyelocytic defensin-1 promoter. *J. Biol. Chem.* ***1998,*** 273, 8727-40.

Memminger, M. Synthesis and characterization of subtype-selective estrogen receptor ligands and their application as pharmacological tools - Cross-talk between estrogen

and NPY Y1 receptors in human breast cancer cells. PhD thesis, University of Regensburg, Regensburg, 2009.

Morgan, R. K.; McAllister, B.; Cross, L.; Green, D. S.; Kornfeld, H.; Center, D. M.; Cruikshank, W. W. Histamine 4 receptor activation induces recruitment of FoxP3+ T cells and inhibits allergic asthma in a murine model. *J. Immunol.* ***2007,*** 178, 8081-9.

Morse, K. L.; Behan, J.; Laz, T. M.; West, R. E., Jr.; Greenfeder, S. A.; Anthes, J. C.; Umland, S.; Wan, Y.; Hipkin, R. W.; Gonsiorek, W. and others. Cloning and Characterization of a Novel Human Histamine Receptor. *J. Pharmacol. Exp. Ther.* ***2001,*** 296, 1058-1066.

Mosandl, J. Radiochemical and luminescence-based binding and functional assays for human histamine receptors using genetically engineered cells. PhD thesis, University of Regensburg, Regensburg, Germany, 2009.

Mou, T. C.; Masada, N.; Cooper, D. M.; Sprang, S. R. Structural basis for inhibition of mammalian adenylyl cyclase by calcium. *Biochemistry* ***2009,*** 48, 3387-97.

Neumann, D.; Beermann, S.; Seifert, R. Does the Histamine H(4) Receptor Have a Pro- or Anti-Inflammatory Role in Murine Bronchial Asthma? *Pharmacology* ***2010,*** 85, 217-223.

Nijmeijer, S.; Vischer, H. F.; Rosethorne, E. M.; Charlton, S. J.; Leurs, R. Analysis of Multiple Histamine H_4 Receptor Compound Classes Uncovers Galphai and beta-Arrestin2 Biased Ligands. *Mol. Pharmacol.* ***2012***.

O'Reilly, M.; Alpert, R.; Jenkinson, S.; Gladue, R. P.; Foo, S.; Trim, S.; Peter, B.; Trevethick, M.; Fidock, M. Identification of a histamine H_4 receptor on human eosinophils - Role in eosinophil chemotaxis. *J. Recept. Signal Transduct. Res.* ***2002,*** 22, 431-448.

Pavan, B.; Biondi, C.; Dalpiaz, A. Adenylyl cyclases as innovative therapeutic goals. *Drug Discov. Today* ***2009,*** 14, 982-91.

Reher, T. M.; Neumann, D.; Buschauer, A.; Seifert, R. Incomplete activation of human eosinophils via the histamine H_4-receptor: evidence for ligand-specific receptor conformations. *Biochem. Pharmacol.* ***2012,*** 84, 192-203.

Rodrigues, D. J.; McLoughlin, D. 2009. Using Reporter Gene Technologies to Detect Changes in cAMP as a Result of GPCR Activation. p 319-328.

Rosethorne, E. M.; Charlton, S. J. Agonist-biased signaling at the histamine H_4 receptor: JNJ7777120 recruits beta-arrestin without activating G proteins. *Mol. Pharmacol.* ***2011,*** 79, 749-57.

Rossbach, K.; Wendorff, S.; Sander, K.; Stark, H.; Gutzmer, R.; Werfel, T.; Kietzmann, M.; Baumer, W. Histamine H_4 receptor antagonism reduces hapten-induced scratching behaviour but not inflammation. *Exp. Dermatol.* ***2009,*** 18, 57-63.

Rybin, V. O.; Xu, X.; Lisanti, M. P.; Steinberg, S. F. Differential targeting of beta -adrenergic receptor subtypes and adenylyl cyclase to cardiomyocyte caveolae. A mechanism to functionally regulate the cAMP signaling pathway. *J. Biol. Chem.* ***2000,*** 275, 41447-57.

Sander, K.; Kottke, T.; Tanrikulu, Y.; Proschak, E.; Weizel, L.; Schneider, E. H.; Seifert, R.; Schneider, G.; Stark, H. 2,4-Diaminopyrimidines as histamine H_4 receptor ligands-

Scaffold optimization and pharmacological characterization. *Biorg. Med. Chem.* ***2009,*** 17, 7186-7196.

Schneider, E. H.; Seifert, R. Histamine H(4) receptor-RGS fusion proteins expressed in Sf9 insect cells: a sensitive and reliable approach for the functional characterization of histamine H(4) receptor ligands. *Biochem. Pharmacol.* ***2009,*** 78, 607-16.

Schnell, D.; Brunskole, I.; Ladova, K.; Schneider, E. H.; Igel, P.; Dove, S.; Buschauer, A.; Seifert, R. Expression and functional properties of canine, rat, and murine histamine H(4) receptors in Sf9 insect cells. *Naunyn-Schmiedeberg's Arch. Pharmacol.* ***2011,*** 383, 457-70.

Seamon, K. B.; Padgett, W.; Daly, J. W. Forskolin: unique diterpene activator of adenylate cyclase in membranes and in intact cells. *Proc. Natl. Acad. Sci. U. S. A.* ***1981,*** 78, 3363-7.

Seifert, R.; Schneider, E. H.; Dove, S.; Brunskole, I.; Neumann, D.; Strasser, A.; Buschauer, A. Paradoxical stimulatory effects of the "standard" histamine H_4-receptor antagonist JNJ7777120: The H_4-receptor joins the club of 7TM receptors exhibiting functional selectivity. *Mol. Pharmacol.* ***2011***.

Shinde, R.; Perkins, J.; Contag, C. H. Luciferin derivatives for enhanced in vitro and in vivo bioluminescence assays. *Biochemistry* ***2006,*** 45, 11103-12.

Strakhova, M. I.; Cuff, C. A.; Manelli, A. M.; Carr, T. L.; Witte, D. G.; Baranowski, J. L.; Vortherms, T. A.; Miller, T. R.; Rundell, L.; McPherson, M. J. and others. In vitro and in vivo characterization of A-940894: a potent histamine H_4 receptor antagonist with anti-inflammatory properties. *Br. J. Pharmacol.* ***2009,*** 157, 44-54.

Stroop, S. D.; Kuestner, R. E.; Serwold, T. F.; Chen, L.; Moore, E. E. Chimeric human calcitonin and glucagon receptors reveal two dissociable calcitonin interaction sites. *Biochemistry* ***1995,*** 34, 1050-7.

Tang, Y.; Luo, J.; Fleming, C. R.; Kong, Y.; Olini, G. C., Jr.; Wildey, M. J.; Cavender, D. E.; Demarest, K. T. Development of a sensitive and HTS-compatible reporter gene assay for functional analysis of human adenosine A2a receptors in CHO-K1 cells. *Assay Drug Dev Technol* ***2004,*** 2, 281-9.

Thurmond, R. L.; Desai, P. J.; Dunford, P. J.; Fung-Leung, W. P.; Hofstra, C. L.; Jiang, W.; Nguyen, S.; Riley, J. P.; Sun, S.; Williams, K. N. and others. A potent and selective histamine H_4 receptor antagonist with anti-inflammatory properties. *J. Pharmacol. Exp. Ther.* ***2004,*** 309, 404-13.

Thurmond, R. L.; Gelfand, E. W.; Dunford, P. J. The role of histamine H_1 and H_4 receptors in allergic inflammation: the search for new antihistamines. *Nat. Rev. Drug Discov.* ***2008,*** 7, 41-53.

Werthmann, R. C.; Volpe, S.; Lohse, M. J.; Calebiro, D. Persistent cAMP signaling by internalized TSH receptors occurs in thyroid but not in HEK293 cells. *FASEB J.* ***2012,*** 26, 2043-8.

Wifling, D. 2012. Personal communication. University of Regensburg, Regensburg, Germany.

Williams, C. cAMP detection methods in HTS: selecting the best from the rest. *Nat. Rev. Drug Discov.* ***2004,*** 3, 125-35.

Williams, T. M.; Burlein, J. E.; Ogden, S.; Kricka, L. J.; Kant, J. A. Advantages of firefly luciferase as a reporter gene: Application to the interleukin-2 gene promoter. *Anal. Biochem.* ***1989,*** 176, 28-32.

Wong, M. P.; Cooper, D. M.; Young, K. W.; Young, J. M. Characteristics of the Ca(2+)-dependent inhibition of cyclic AMP accumulation by histamine and thapsigargin in human U373 MG astrocytoma cells. *Br. J. Pharmacol.* ***2000,*** 130, 1021-30.

Yu, F.; Wolin, R. L.; Wei, J.; Desai, P. J.; McGovern, P. M.; Dunford, P. J.; Karlsson, L.; Thurmond, R. L. Pharmacological characterization of oxime agonists of the histamine H_4 receptor. *J. Receptor Ligand Channel Res.* ***2010,*** 3, 37-49.

Zampeli, E.; Thurmond, R. L.; Tiligada, E. The histamine H_4 receptor antagonist JNJ7777120 induces increases in the histamine content of the rat conjunctiva. *Inflammation Res.* ***2009,*** 58, 285-91.

Zhang, M.; Thurmond, R. L.; Dunford, P. J. The histamine H(4) receptor: a novel modulator of inflammatory and immune disorders. *Pharmacol. Ther.* ***2007,*** 113, 594-606.

Zhu, Y.; Michalovich, D.; Wu, H.-L.; Tan, K. B.; Dytko, G. M.; Mannan, I. J.; Boyce, R.; Alston, J.; Tierney, L. A.; Li, X. and others. Cloning, Expression, and Pharmacological Characterization of a Novel Human Histamine Receptor. *Mol. Pharmacol.* ***2001,*** 59, 434-441.

Chapter 5

Development of radioligand binding assays for human and rat histamine H_3 receptors

5.1 Radioligand binding assay for the human histamine H_3 receptor

5.1.1 Introduction

After the first cloning of the H_3R cDNA in the year 1999 by Lovenberg and co-workers (Lovenberg *et al.*, 1999), several binding assays using [^{3}H]N$^\alpha$-methylhistamine ([^{3}H]NAMH) and more rarely [^{3}H](R)-α-methylhistamine ([^{3}H]RAMH) on membrane preparations of the full-length (445 aa) hH_3R expressing rat C6 glioma cells (Lovenberg *et al.*, 1999; Witte *et al.*, 2006), SK-N-MC cells (Barbier *et al.*, 2004; Bongers *et al.*, 2007; Kitbunnadaj *et al.*, 2003; Lovenberg *et al.*, 2000; Wieland *et al.*, 2001) and Sf9 insect cells (Schnell *et al.*, 2010) were established. Furthermore, the antagonistic radioligand [^{125}I]iodoproxyfan was successfully applied on membrane preparations of CHO-K1 (Coge *et al.*, 2001) and HEK293 cells (Wulff *et al.*, 2002). Due to the presence of several introns in the H_3R gene, alternative splicing revealed at least 20 different isoforms of the hH_3R, of which, however, the full length receptor (445 aa) is the best characterized one (Leurs *et al.*, 2005).

In contrast to reported binding assays with broken cell systems, the present work focused on radioligand binding studies with whole HEK293T cells stably expressing the full length hH_3R (HEK293-SF-hH_3R-His_6). As radioactive tracer, the standard agonist [^{3}H]NAMH was utilized. For validation, the affinities of imidazoles and non-imidazoles, comprising agonists, antagonists and inverse agonists, were determined.

5.1.2 Materials and Methods

5.1.2.1 Whole cell radioligand binding assay

The HEK293-SF-hH_3R-His_6 cells, stably expressing the tagged hH_3R, were kindly provided by Dr. Schnell (Department of Pharmacology and Toxicology, University of Regensburg, Germany), and cultured as described in section 3.1.2.1. The preparation of the HEK293-SF-hH_3R-His_6 cells, the separation of bound from free radioligand and data processing were identical to that described in section 3.1.2.4. [^{3}H]N$^\alpha$-methylhistamine ([^{3}H]NAMH) was used as radioligand (85.3 Ci/mmol) (Perkin Elmer).

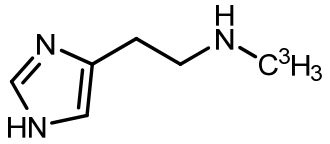

[^{3}H]NAMH

Figure 5.1: Structure of the radioactive tracer [^{3}H]N$^\alpha$-methyl-histamine ([^{3}H]NAMH).

In saturation binding assays with [^{3}H]NAMH, non-specific binding was determined in the presence of JNJ 5207852 at a final concentration of 10 µM. In competition binding assays, displacement of 1 nM of [^{3}H]NAMH by the $H_{3/4}$R ligands listed in section 3.1.2.3 was measured. The K_i values are presented as as the mean ± SEM of at least three independent experiments performed in duplicate (see **Table 5.1**).

5.1.3 Results and discussion

5.1.3.1 Saturation binding assay

The radioligand [^{3}H]NAMH exhibited specific and saturable binding to HEK293-SF-hH_3R-His_6 cells (see **Figure 5.2** A). The non-specific binding was less than 10 % of the total binding within the investigated concentration range using 10 µM of JNJ 5207852 as competitor. Scatchard plot analysis of the specific binding isotherm revealed a linear correlation between the ratio bound/free *versus* bound [^{3}H]NAMH, indicating the presence of a single binding site (see **Figure 5.2** B). The reported K_D values was in the range of 0.5-1.1 nM (Bongers *et al.*, 2007; Lovenberg *et al.*, 2000; Schnell *et al.*, 2010; Witte *et al.*, 2006) and thus slightly lower than the K_D value of 5.09 ± 1.21 nM (N = 3) using whole HEK293-SF-hH_3R-His_6 cells. In studies using [^{3}H]NAMH, a minor nucleotide sensitivity of the high affinity state was demonstrated, wherein the K_D value was 2-5 times higher in the presence of GDP or GTPγS (Schnell *et al.*, 2010; Witte *et al.*, 2006). Therefore, also the slightly increased K_D value in the present study might be attributed to high GTP concentration in whole cells (cf. section 3.1.3.3).

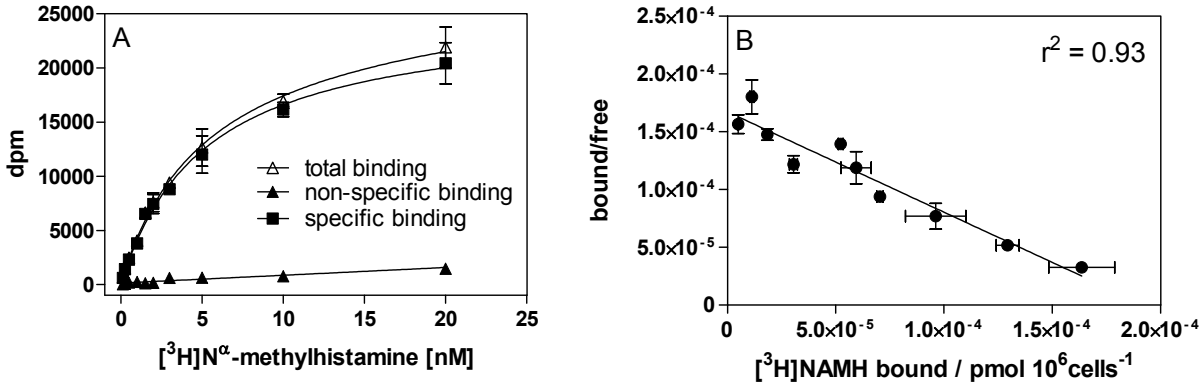

Figure 5.2: Representative [^{3}H]NAMH saturation binding experiment, performed in triplicate, using HEK293-SF-hH_3R-His_6 cells. Non-specific binding was determined in the presence of 10 µM JNJ 5207852. Saturation binding curve was best fitted by nonlinear regression to a one-site model (A). The corresponding Scatchard plot of saturation binding data was best fitted by linear regression (B).

5.1.3.2 Competition binding assay

In competition binding experiments, a large variety of H_3R ligands comprising imidazoles and non-imidazoles (cf. section 3.1.2.3) were investigated for their ability to displace 1 nM of [^{3}H]NAMH on HEK293-SF-hH_3R-His_6 cells. The results were compared with hH_3R ligand binding data reported in literature as well as with ligand affinities determined at the hH_4R

using [^{3}H]UR-PI294 (cf. section 3.1.3.3). Most of the reported studies used [^{3}H]NAMH as radioactive tracer and invariably broken cell systems such as membrane preparations. The results and reported data are summarized in **Table 5.1**.

Histamine (**1**) and its methylated analogs (R)-α-methylhistamine (**2**), (S)-α-methylhistamine (**3**) and N$^{\alpha}$-methylhistamine (**4**) concentration dependently inhibited specific binding of [^{3}H]NAMH on HEK293-SF-hH_3R-His_6 cells (see **Figure 5.3**). In line with reported data, the hH_3R affinities of **2**–**4** were distinctly higher compared to the hH_4R. Nevertheless, a pronounced stereoselectivity in favor of (R)-α-methylhistamine (**2**) (pK_i = 8.60 ± 0.12) compared to (S)-α-methylhistamine (**3**) (pK_i = 7.34 ± 0.08) was also found at the hH_3R. Whereas the affinity of **1** was lower than described in literature, the pK_i values of **2**-**4** were in agreement with reported data.

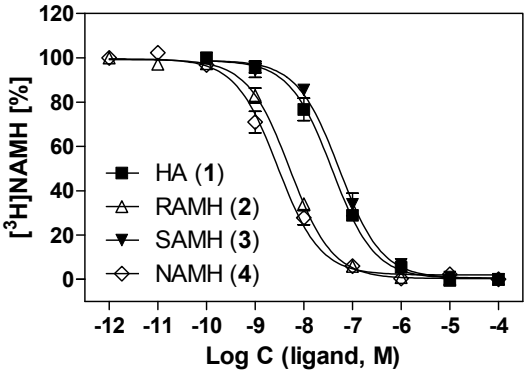

Figure 5.3: Displacement of specifically bound [^{3}H]NAMH by HA (**1**), RAMH (**2**), SAMH (**3**) and NAMH (**4**) on HEK293-SF-hH_3R-His_6 cells. Reaction mixtures contained 1 nM [^{3}H]NAMH and ligand concentrations indicated on the abscissa. Data were analyzed by nonlinear regression and best fitted to one-site (monophasic) competition curves. Data points are the mean of at least three independent experiments performed in duplicate.

Immepip (**6**) and its analogs VUF5681 (**7**) and immethridine (**8**) displayed low nanomolar affinities at the hH_3R, which were consistent with reported data. Interestingly, the ligands showed, regardless of higher affinities, the same rank order as at the hH_4R (**6** > **8** > **7**). Imetit (**9**), derived from **1** by replacement of the amino group with an isothiourea, revealed nanomolar affinity at the hH_3R. The isothiourea-type ligands clobenpropit (**10**) and iodophenpropit (**11**) yielded also comparably high affinities at the hH_3R. The results were in good accordance with reported data, and the rank order was again the same as at the hH_4R (**9** > **10** > **11**). The $H_{3/4}$R inverse agonist thioperamide (**12**) revealed a pK_i value of 6.71 ± 0.09, which is the same as at the hH_4R and marginally lower compared to reported data. The hH_3R affinities of proxyfan (**13**) as well as of the proxyfan-class compound ciproxifan (**14**) were consistent with data described in literature. As for most of the aforementioned compounds which were originally designed as H_3R ligands, the hH_4R affinity of proxyfan (**13)** and ciproxifan (**14)** was clearly lower. In contrast, the acylguanidine-type ligand UR-PI294 reached low nanomolar affinities at both the hH_3R and the hH_4R, as expected from [^{32}P]GTPase assays at both histamine receptor subtypes (Igel *et al.*, 2009a) (see **Figure**

5.4). In line with literature, the affinity at the hH_3R was low for clozapine (**18**) and only moderate for VUF8430 (**20**). The investigated non-imidazoles displayed thus only 4-10-fold selectivity for the hH_4R over the hH_3R (cf. section 3.1.3.3). Whereas the affinity of JNJ 7777120 (**19**) at the hH_3R was slightly lower compared to literature, the selectivity of **19** for the hH_4R was in good agreement (see **Figure 5.4**) (Lim *et al.*, 2005). Although the hH_3R affinities of JNJ 5207852 (**21**) and conessine (**22**) were lower than reported, these non-imidazoles showed 6000- and 1000-fold selectivity, respectively, for the hH_3R over the hH_4R in the present cellular binding system (see **Figure 5.4**).

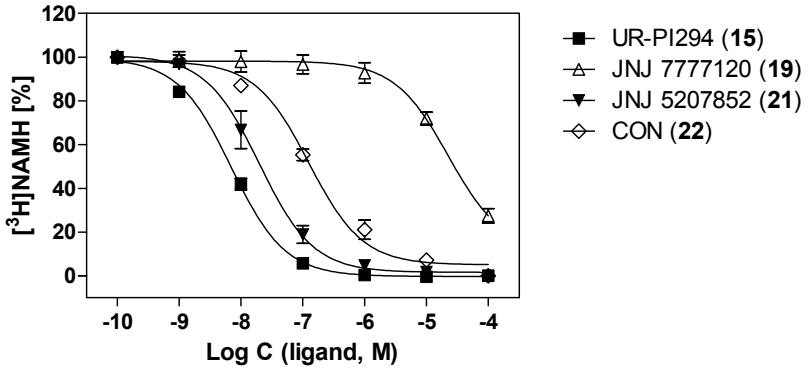

Figure 5.4: Displacement of specifically bound [^{3}H]NAMH binding by UR-PI294 (**15**), JNJ 7777120 (**19**), JNJ 5207852 (**21**) and CON (**22**) on HEK293-SF-hH_3R-His_6 cells. Reaction mixtures contained 1 nM [^{3}H]NAMH and ligand concentrations indicated on the abscissa. Data were analyzed by nonlinear regression and best fitted to one-site (monophasic) competition curves. Data points are the mean of at least three independent experiments performed in duplicate.

In summary, by performing competition binding experiments using whole HEK293-SF-hH_3R-His_6 cells and [^{3}H]NAMH, affinities of H_3R ligands at the hH_3R were determined in a highly reproducible manner. With the exception of histamine (**1**), which displayed a lower pK_i value at the hH_3R as described in literature, the affinities of all agonists (**2**-**4**, **6**-**9**, **13**, **18**, **20**) and antagonists (**10**, **11**, **14**) were comparable with reported data (see **Table 5.1** and **Figure 5.5**). Hence, there was no evidence for a "GTP-shift" as at the hH_4R (cf. section 3.1.3.3). However, it is noticeable that ligands with inverse agonistic activity at the hH_3R (thioperamide (**12**), JNJ 7777120 (**19**), JNJ 5207852 (**21**) and conessine (**22**)) displayed lower affinities at the hH_3R than determined on membranes (see **Table 5.1**).

Table 5.1: pK_i values of reference H_3R ligands determined in competititon binding experiments, using HEK293-SF-hH_3R-His_6 cells and [^{3}H]N^α-methylhistamine, in comparison to pK_i values reported in literature.

Ligand	**hH_3R**		
	pK_i	N	pK_i
	HEK293-SF-hH_3R-His_6		reported
Histamine (**1**)	7.52 ± 0.08	5	7.8-8.6[b, c, e, g, i, j, k, n, o]
(R)-α-Methylhistamine (**2**)	8.60 ± 0.12	6	8.2-9.3[c, e, g, j, m, n, o, k]
(S)-α-Methylhistamine (**3**)	7.34 ± 0.08	3	7.2-7.6[g, n, o]
N^α-Methylhistamine (**4**)	8.85 ± 0.17	6	8.4-9.5[c, g, j, k, n]
Immepip (**6**)	9.28 ± 0.14	5	8.8-9.8[b, c, e, g, l, j, n, o]
VUF 5681 (**7**)	8.20 ± 0.05	3	8.35[e]
Immethridine (**8**)	8.98 ± 0.20	5	9.1[f, g]
Imetit (**9**)	9.19 ± 0.12	8	8.8-9.7[c, g, l, j, k, m, n, o]
Clobenpropit (**10**)	8.81 ± 0.09	6	8.4-9.5[c, d, g, l, j, k, m, n]
Iodophenpropit (**11**)	8.78 ± 0.06	6	8.2-9.1[g, m, n, o]
Thioperamide (**12**)	6.71 ± 0.09	10	6.9-7.7[a, b, c, g, l, j, k, m, n, o, p]
Proxyfan (**13**)	7.80 ± 0.13	3	7.9-8.4[g, k, n, o]
Ciproxyfan (**14**)	6.92 ± 0.26	4	6.7-7.3[c, k, n, o, p]
UR-PI294 (**15**)	8.28 ± 0.07	3	-
Clozapine (**18**)	4.46 ± 0.23	3	> 5[i, j]
JNJ 7777120 (**19**)	4.86 ± 0.13	3	5.3[g, l]
VUF 8430 (**20**)	6.21 ± 0.05	3	6.0[h]
JNJ 5207852 (**21**)	7.79 ± 0.14	3	9.2[a]
Conessine (**22**)	7.00 ± 0.10	3	8.3[p]

Mean values ± SEM. N: number of independent experiments performed in duplicate. Reference data taken from: [^{3}H]NAMH binding on SK-N-MC cell membranes [a] (Barbier *et al.*, 2004), [b] (Bongers *et al.*, 2007), [j] (Lovenberg *et al.*, 2000), [l] (Thurmond *et al.*, 2004); [^{125}I]iodoproxyfan binding on CHO-K1 cell membranes [c] (Coge *et al.*, 2001); [^{3}H]NAMH binding on C6 cell membranes [d] (Esbenshade *et al.*, 2003), [i] (Lovenberg *et al.*, 1999), [n] (Witte *et al.*, 2006), [p] (Zhao *et al.*, 2008); [^{3}H]NAMH binding on SK-N-MC cell homogenates [e] (Kitbunnadaj *et al.*, 2003), [f] (Kitbunnadaj *et al.*, 2004), [g] (Lim *et al.*, 2005), [h] (Lim *et al.*, 2006), [m] (Wieland *et al.*, 2001); [^{3}H]NAMH binding on Sf9 cell membranes [k] (Schnell *et al.*, 2010); [^{125}I]iodoproxyfan binding on HEK293 cell membranes [o] (Wulff *et al.*, 2002).

Witte et al. showed that the tritiated antagonist/inverse agonist [^{3}H]A-349821 detected about 50% more receptors than [^{3}H]NAMH in saturation binding assays at the human H_3R and rH_3R, suggesting that the agonist [^{3}H]NAMH only recognized the active conformation of the H_3R, whereas [^{3}H]A-349821 bound to both receptor states (active and inactive) (Witte *et al.*, 2006). This observation was confirmed in saturation binding studies with [^{3}H]NAMH on rH_3R expressing HEK293-CRE-Luc cells (see section 5.2.3.1). According to theory agonists can distinguish between the inactive (low affinity) and the active (high affinity) conformation of a

receptor, whereas antagonists have the same affinity for both receptor sates (Lefkowitz *et al.*, 1993). The conversion to the active conformation of a receptor can be provoked by an agonist or can occur spontaneously in the absence of an agonist (constitutive activity) (Samama *et al.*, 1993). The agonist-induced active state in whole cells is hampered by the high cytosolic GTP concentration (cf. section 3.1.3.3), but pronounced constitutive activity, i. e. an increased basal activity, of the hH_3R in HEK293-CRE-Luc cells became obvious upon addition of the inverse agonists JNJ 5207852 (**21)** (α = -1.42) and conessine (**22)** (α = -1.33) (see section 6.3.2). Therefore, it can be assumed that [^{3}H]NAMH within the covered concentration range bound to the constitutively active receptor population on HEK293-SF-hH_3R-His_6 cells. Furthermore, the specific binding isotherm revealed one binding site in the Scatchard plot analysis (**Figure 5.2**). Agonists and antagonists presumably displaced [^{3}H]NAMH from the active receptor state resulting in pK_i values comparable with those determined in broken cell systems (see **Figure 5.5**), where the ternary complex can accumulate (cf. section 3.1.3.3).

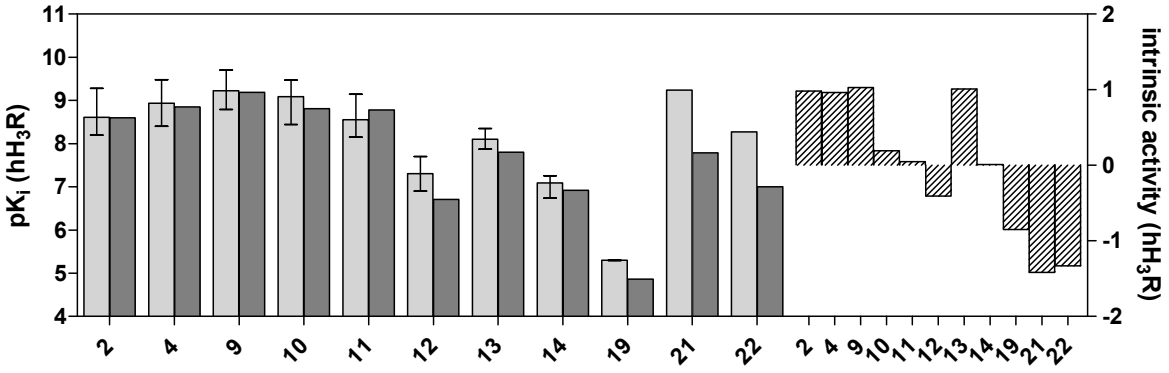

Figure 5.5: Affinities (left) and intrinsic activities (right) of selected agonists, antagonists and inverse agonists at the hH_3R. pK_i values determined on whole cells (dark grey bars) and in broken cell systems reported in literature (bright grey bars). Data are the mean values according to table 5.1. "Error bars" indicate the range covered by reported pK_i values. Intrinsic activities were adopted from section 6.3.2.

Surprisingly, affinities of the inverse agonists thioperamide (**12**), JNJ 7777120 (**19**), JNJ 5207852 (**21**) and conessine (**22**) were lower than those described in literature, and differences in affinity even seemed to correlate with the magnitude of the inverse efficacy (see **Figure 5.5**). In fact, inverse agonists were reported to bind with lower affinity to a constitutively active mutant (CAM) of the β_2 adrenergic receptor (β_2-AR), albeit determined with a radiolabeled antagonist (Samama *et al.*, 1994). Hence, the affinity determined at the wild-type β_2-AR, used as a control with low constitutive activity, was mainly attributable to the inactive states, whereas binding data from the CAM β_2-AR mainly reflected the active state (Samama *et al.*, 1994). In contrast, as in the present study, the reported affinities of JNJ

7777120 (**19**), JNJ 5207852 (**21**) and conessine (**22**) were obtained from [^{3}H]NAMH competition binding assays, which are presumably addressing only the active receptor population. Furthermore, guanine nucleotides were reported to have no effect on the competition binding experiments with an inverse agonist (Samama *et al.*, 1994), suggesting that the whole cell system used in the present study should not have affected the affinity of inverse agonists, too. Therefore, discrepancies regarding binding data of the inverse agonists have to be investigated in more detail in further studies.

5.2 Radioligand binding assay for the rat histamine H_3 receptor

5.2.1 Introduction

The third histamine receptor was discovered by pharmacological investigations on rat brain slices, where the H_3R acts as presynaptic autoreceptor that inhibits histamine release from histaminergic neurons (Arrang *et al.*, 1983). [^{3}H]RAMH was the first radio-labeled H_3R agonist used for binding studies on rat cerebral cortical membranes, at which this radioligand binds with high affinity (K_D = 0.5 nM) to a single binding site (Arrang *et al.*, 1987). Shortly after the hH_3R cDNA (Lovenberg *et al.*, 1999) also the rH_3R cDNA (445 aa) was cloned (Lovenberg *et al.*, 2000) and subsequently expressed in SK-N-MC cells (Barbier *et al.*, 2004; Lovenberg *et al.*, 2000; Wieland *et al.*, 2001), HEK293 cells (Wulff *et al.*, 2002), C6 cells (Witte *et al.*, 2006) or Sf9 cells (Schnell *et al.*, 2010). Radioligand binding assays were usually performed with [^{3}H]NAMH. Although rat and human H_3Rs share 93 % of the amino acid sequence, species-dependent differences, for instance, higher antagonist affinities at the rH_3R, were reported (Lovenberg *et al.*, 2000; Schnell *et al.*, 2010; Yao *et al.*, 2003).

Membrane preparations were used without exception in the reported binding studies. Therefore, the aim of this work was to establish a whole cell radioligand binding assay with HEK293T cells, stably expressing the rH_3R. For this purpose HEK293-CRE-Luc cells, which already expressed the CRE-controlled firefly luciferase (cf. section 4.1.3.6), were transfected with the rH_3R. The resulting HEK293-CRE-Luc-SF-rH_3R-His_6 cells were selected by performing the luciferase reporter gene assay (see section 6.3.1). Thereafter, both binding and functional (see section 6.3.2) assays were performed at the same time. As radioactive tracer the standard radioligand [^{3}H]NAMH as well as the recently described $H_{3/4}R$ radioligand [^{3}H]UR-PI294 (Igel *et al.*, 2009b) were evaluated. In competition binding assays selected agonists, inverse agonists and antagonists were investigated to validate the assay. For comparison only reference data gained from recombinant systems were considered.

5.2.2 Materials and Methods

5.2.2.1 Whole cell radioligand binding assay

Due to new equipment in the radionuclide laboratory allowing a higher throughput, several modifications of the method described in section 3.1.2.4 became necessary. Only one densely grown 75 cm^2 culture flask with HEK293-CRE-Luc-SF-rH_3R-His_6 cells was used for preparing a cell suspension with a lower cell density of 1.7 10^6 cells/mL. Cell-bound radioactivity was separated from free radioactivity by filtration through a 0.3 % (v/v) polyethyleneimine (Sigma) pretreated GF/C glass fiber filter (Whatman, Maidstone, UK) and washed twice with PBS (4 °C) using a 96-sample semi-auto harvester (Brandl, Gaithersburg, USA). Cell-containing filter discs were punched out and transferred to a flexible 24- or 96-well scintillation microplate (Perkin Elmer). Each cavity was filled with 500 µL or 200 µL, respectively, Rotiszint® eco plus (Carl Roth) before the plates were incubated overnight under gentle shaking. On the next day, radioactivity was determined by liquid scintillation counting using a 2450 MicroBeta^{2TM} (Perkin Elmer). Subsequent data processing was performed as described in section 3.1.2.4.

In saturation binding experiments with [^{3}H]NAMH (cf. section 5.1.2.1) and [^{3}H]UR-PI294 (cf. section 3.1.2.4), 10 µM of thioperamide (**12**) were used for determining the non-specific binding. The K_D values were calculated as means of two independent experiments, each performed in triplicate. Competition binding experiments, using [^{3}H]UR-PI294 at a final concentration of 2.5 nM, were conducted in triplicate, too. The number of replicates and independent experiments for the determination of the pK_i value is given in **Table 5.2.**

5.2.3 Results and discussion

5.2.3.1 Saturation binding assay

The transfection of the HEK293-CRE-Luc cells with the rH_3R and the selection of transfectants are described in section 6.3.1. Although [^{3}H]NAMH bound specifically in a saturable manner to a single binding site, the non-specific binding in the presence of 10 µM of thioperamide (**12**) occasionally amounted to about 50 % of the total binding (see **Figure 5.6**). Furthermore, the B_{max} value of the specific binding (maximum amount of specifically bound radioligand) was rather low in two independent saturation binding experiments, suggesting that the expression level of the rH_3R was similarly low in HEK293-CRE-Luc-SF-rH_3R-His_6 cells (see **Figure 5.6**). However, the determined K_D value of 6.05 ± 1.07 nM (N = 2) was comparable with that at the hH_3R and, probably due to the high cytosolic GTP concentration in whole cells, slightly higher compared to the reported range of 0.5 – 1.37 nM (Lovenberg *et al.*, 2000; Schnell *et al.*, 2010; Witte *et al.*, 2006). Nevertheless, the application of [^{3}H]NAMH as radioligand for competition binding experiments at the rH_3R could be exceedingly difficult due to the very low specific binding. Therefore, [^{3}H]UR-PI294 was evaluated as a possible radioligand for the rH_3R.

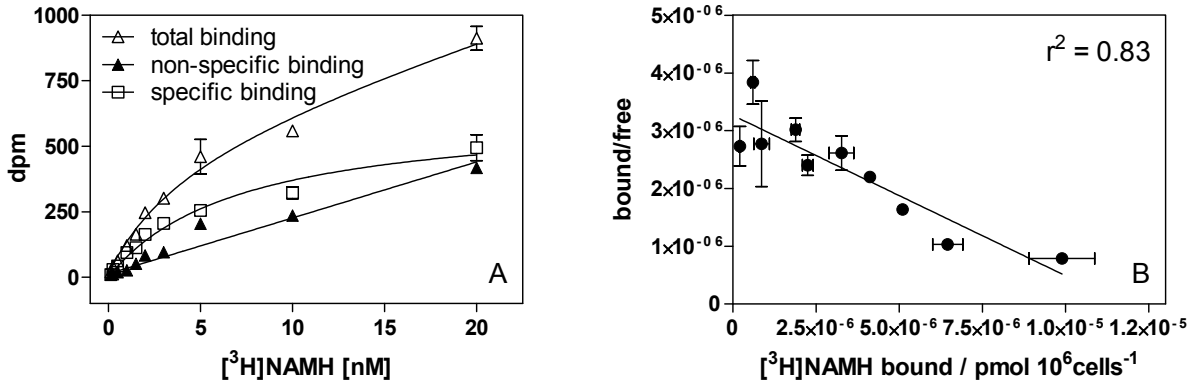

Figure 5.6: Representative [^{3}H]NAMH saturation binding experiment with HEK293-CRE-Luc-SF-rH_3R-His_6 cells. Non-specific binding was determined in the presence of 10 µM of thioperamide (**12**). Saturation binding curve was best fitted by nonlinear regression to a one-site model (A). The corresponding Scatchard Plot was best fitted by linear regression (B).

[^{3}H]UR-PI294 was recently described as non-selective radioligand for the human H_3R and H_4R with a K_D value 1.1 nM at the hH_3R (Igel *et al.*, 2009b). Since [^{3}H]UR-PI294 bound with nearly the same affinity to HEK293-CRE-Luc-SF-rH_3R-His_6 cells (K_D value = 1.93 ± 0.35 (N =2)) the radioligand also proved to be a useful pharmacological tool at the rH_3R (see **Figure**

5.7). Using 10 µM of thioperamide (**12**) non-specific binding was surprisingly low, not exceeding 15 % of the total binding.

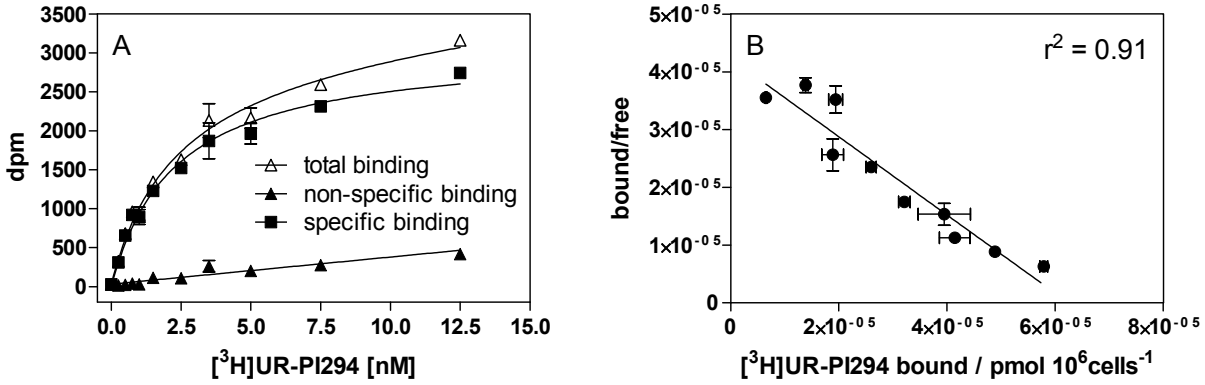

Figure 5.7: Representative [^{3}H]UR-PI294 saturation binding experiment using HEK293-CRE-Luc-SF-rH_3R-His_6 cells. Non-specific binding was determined in the presence of 10 µM thioperamide (**12**). Saturation binding curve was best fitted by non-linear regression to a one-site model (A). The corresponding Scatchard Plot was best fitted by linear regression (B).

The comparison of B_{max} values of [^{3}H]NAMH and [^{3}H]UR-PI294 in HEK293-CRE-Luc-SF-rH_3R-His_6 cells revealed that [^{3}H]NAMH addressed only about 7,000 receptors per cell, whereas [^{3}H]UR-PI294 recognized 34,000 receptors per cell, despite comparable K_D values and specific activities of the radioligands (cf. **Figure 5.6** and **Figure 5.7**). Therefore, it can be assumed that, by analogy to the observations of Witte et al. (Witte *et al.*, 2006), the full rH_3R agonist [^{3}H]NAMH (cf. section 6.3.2) only labeled the constitutively active rH_3Rs. The partial rH_3R agonist [^{3}H]UR-PI294 (cf. section 6.3.2) achieved a 5-fold higher B_{max} value owing to its ability to recognize both receptor states. The constitutive activity of the rH_3R was rather low compared to the hH_3R, as reflected by α values of about -0.3 of the inverse agonists thioperamide (**12**), JNJ 5207852 (**21**) and conessine (**22**) (cf. section 6.3.2). Thus, only a small (active state) portion of the receptor was detected by [^{3}H]NAMH. The affinity of [^{3}H]UR-PI294 to both receptor states seemed to be equal, since the specific binding isotherm was best described by a one-site model (see **Figure 5.7**). Competition binding assays were performed using [^{3}H]UR-PI294.

5.2.3.2 Competition binding assay

In competition binding experiments with HEK293-CRE-Luc-SF-rH_3R-His_6 cells, a selection of H_3R ligands containing agonists, inverse agonists and antagonists were investigated for their ability to inhibit specific binding of 2.5 nM [^{3}H]UR-PI294. The results were compared with

data from literature as well as with the determined affinities at the hH_3R (cf. section 5.1.3.2). The data are summarized in **Table 5.2**.

Histamine (**1**), (R)-α-methylhistamine (**2**), N^{α}-methylhistamine (**4**), imetit (**9**) and proxyfan (**13**) displaced [^{3}H]UR-PI294 in a concentration-dependent manner (see **Figure 5.8** A). However, the affinities of the rH_3R agonists were without exception about one order of magnitude lower compared to binding data at the hH_3R and those reported in literature.

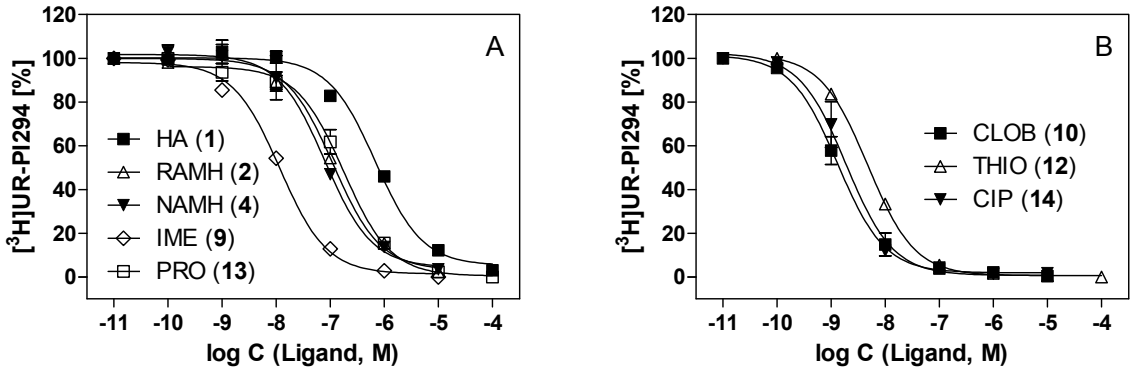

Figure 5.8: Displacement of specifically bound [^{3}H]UR-PI294 by the agonists HA (**1**), RAMH (**2**), NAMH (**4**), IME (**9**) (A) and by the antagonists CLOB (**10**), THIO (**12**), PRO (**13**) and CIP (**14**) (B) on HEK293-CRE-Luc-SF-rH_3R-His_6 cells. Reaction mixtures contained 2.5 nM [^{3}H]UR-PI294 and ligand concentrations indicated on the abscissa. Data were analyzed by nonlinear regression and best fitted to one-site (monophasic) competition curves. Data points are the mean of two independent experiments performed in triplicate.

In contrast, the rH_3R revealed in agreement with literature a 70-120-fold higher affinity to the antagonists thioperamide (**12**) and ciproxifan (**14**) as well as a 2-fold higher affinity to clobenpropit (**10**) compared to the hH_3R (see **Figure 5.8** B). Thus, the recently described species-dependent increased affinity of the rH_3R to antagonists (Lovenberg *et al.*, 2000; Schnell *et al.*, 2010; Yao *et al.*, 2003) was confirmed in this cellular binding study.

Table 5.2: pK_i values of reference H_3R ligands determined in competitive binding experiments using HEK293-CRE-Luc-SF-rH_3R-His_6 cells and [^{3}H]UR-PI294 compared to data reported in literature.

Ligand	**rH_3R**		
	pK_i	N	pK_i
	HEK293-CRE-Luc-SF-rH_3R-His_6		reported
Histamine (**1**)	6.43 ± 0.02	2	7.9-8.6[a, b, d]
(R)-α-Methylhistamine (**2**)	7.20 ± 0.01	2	8.0-9.29[a, b, c, d, e]
N^{α}-Methylhistamine (**4**)	7.35 ± 0.06	2	8.7-9.5[a, b, d]
Imetit (**9**)	8.18 ± 0.02	2	9.0-10.1[a, b, d, e]
Clobenpropit (**10**)	9.12 ± 0.11	3	8.9-9.8[a, b, c, d, e]
Thioperamide (**12**)	8.57 ± 0.02	2	7.9-8.6[a, b, c, d]
Proxyfan (**13**)	7.01 ± 0.10	3	8.0-8.6[b, d, e]
Ciproxifan (**14**)	8.99 ± 0.15	3	8.6-9.4[b, d, e]

Mean values ± SEM. N: number of independent experiments performed in duplicate. Reference data taken from: [^{3}H]NAMH binding on SK-N-MC cell membranes [a] (Lovenberg *et al.*, 2000); ^{3}H]NAMH binding on Sf9 cell membranes [b] (Schnell *et al.*, 2010); [^{3}H]NAMH binding on SK-N-MC cell homogenates [c] (Wieland *et al.*, 2001); [^{3}H]NAMH binding on C6 cell membranes [d] (Witte *et al.*, 2006); [^{125}I]iodoproxyfan binding on HEK293 cell membranes [e] (Wulff *et al.*, 2002).

Figure 5.9 clearly illustrated that the determined affinities of the full agonist histamine (**1**), (R)-α-methylhistamine (**2**), N^{α}-methylhistamine (**4**), imetit (**9**) and the strong partial agonist proxyfan (**13**) were lower compared to broken cell systems even though the rank order of affinity was the same. In contrast, the affinities of the inverse agonist thioperamide (**12**), the antagonist ciproxifan (**14**) and the very weak partial agonist clobenpropit (**10**) were comparable with reference values. These results show again the existence of a "GTP-shift" for agonists as described in section 3.1.3.3 for [^{3}H]UR-PI294 displacement studies at the hH_4R. Similarly, GDP induced a rightward shift of the [^{3}H]A-349821 competition binding curve of histamine (**1**) (Witte *et al.*, 2006). The displacement of the antagonist/inverse agonist [^{3}H]A-349821 by agonists at the H_3R was biphasic, because agonists displaced the radioligand initially from the high affinity binding sites and then from the low affinity sites (Witte *et al.*, 2006). However, no distinct binding sites were detected by displacement of [^{3}H]UR-PI294 with agonists (see **Figure 5.8** A). Maybe there was only a minor portion of receptors in the active state or the number of data points was insufficient to unequivocally discriminate two binding sites.

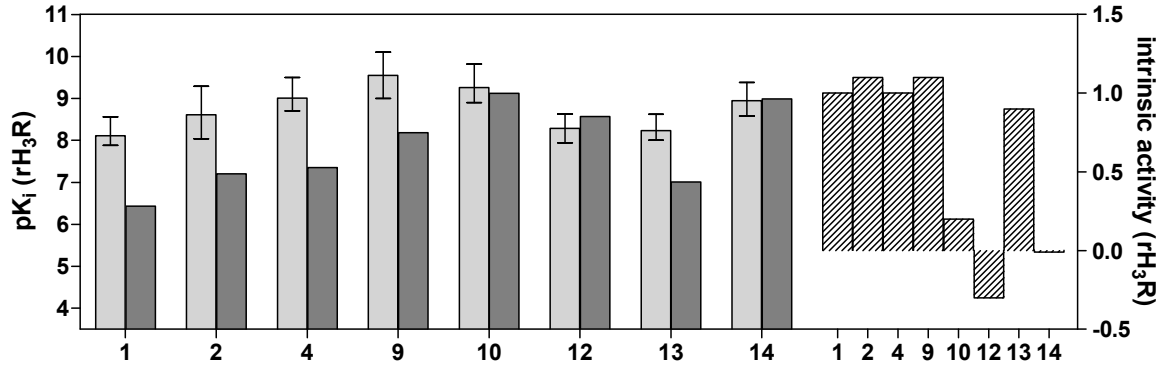

Figure 5.9: Binding data (left) and intrinsic activities in the reporter gene assay (right, cf. section 6.3.2) of compounds **1**, **2**, **4**, **9**, **10**, **12**, **13**, **14** at the rH_3R. Depicted are the determined affinities in whole cells (dark grey bars) and in broken-cell preparations from literature (bright grey bars). Data are the mean values according to table 5.2. “Error bars” indicate the range covered by reported pK_i values.

5.3 Summary

Due to high constitutive activity and the resulting predominance of the active state, [^{3}H]NAMH bound with high affinity to the hH_3R expressed in HEK293T cells. Only minor sensitivity to high cytosolic GTP concentration became apparent, when the K_D values were compared with results from literature. Furthermore, pK_i values determined by displacement of [^{3}H]NAMH with agonists and antagonists were consistent with published data for the hH_3R, whereas, surprisingly, inverse agonists revealed lower affinities.

[^{3}H]UR-PI294 was able to recognize a distinctly higher number of receptors than [^{3}H]NAMH in the rH_3R expressing HEK293-CRE-Luc cells, probably due to binding to the receptor protein in both the active and inactive state. As a consequence, GTP shifted the binding data of agonists toward lower affinities in competition binding experiments. Since antagonists were not affected by this “GTP-shift”, the reported higher affinities of antagonists at the rH_3R compared to the hH_3R could be confirmed with this cellular binding assay.
In the established binding assays, affinities of agonists, inverse agonists and antagonists were determined in a highly reproducible manner.

5.4 References

Arrang, J. M.; Garbarg, M.; Lancelot, J. C.; Lecomte, J. M.; Pollard, H.; Robba, M.; Schunack, W.; Schwartz, J. C. Highly potent and selective ligands for histamine H_3-receptors. *Nature* ***1987,*** 327, 117-23.

Arrang, J. M.; Garbarg, M.; Schwartz, J. C. Auto-inhibition of brain histamine release mediated by a novel class (H_3) of histamine receptor. *Nature* ***1983,*** 302, 832-7.

Barbier, A. J.; Berridge, C.; Dugovic, C.; Laposky, A. D.; Wilson, S. J.; Boggs, J.; Aluisio, L.; Lord, B.; Mazur, C.; Pudiak, C. M. and others. Acute wake-promoting actions of JNJ-5207852, a novel, diamine-based H_3 antagonist. *Br. J. Pharmacol.* ***2004,*** 143, 649-61.

Bongers, G.; Sallmen, T.; Passani, M. B.; Mariottini, C.; Wendelin, D.; Lozada, A.; Marle, A.; Navis, M.; Blandina, P.; Bakker, R. A. and others. The Akt/GSK-3beta axis as a new signaling pathway of the histamine H(3) receptor. *J. Neurochem.* ***2007,*** 103, 248-58.

Coge, F.; Guenin, S. P.; Audinot, V.; Renouard-Try, A.; Beauverger, P.; Macia, C.; Ouvry, C.; Nagel, N.; Rique, H.; Boutin, J. A. and others. Genomic organization and characterization of splice variants of the human histamine H_3 receptor. *Biochem. J* ***2001,*** 355, 279-88.

Esbenshade, T. A.; Krueger, K. M.; Miller, T. R.; Kang, C. H.; Denny, L. I.; Witte, D. G.; Yao, B. B.; Fox, G. B.; Faghih, R.; Bennani, Y. L. and others. Two novel and selective nonimidazole histamine H_3 receptor antagonists A-304121 and A-317920: I. In vitro pharmacological effects. *J. Pharmacol. Exp. Ther.* ***2003,*** 305, 887-96.

Igel, P.; Schneider, E.; Schnell, D.; Elz, S.; Seifert, R.; Buschauer, A. N(G)-acylated imidazolylpropylguanidines as potent histamine H_4 receptor agonists: selectivity by variation of the N(G)-substituent. *J. Med. Chem.* ***2009a,*** 52, 2623-7.

Igel, P.; Schnell, D.; Bernhardt, G.; Seifert, R.; Buschauer, A. Tritium-labeled N(1)-[3-(1H-imidazol-4-yl)propyl]-N(2)-propionylguanidine ([(3)H]UR-PI294), a high-affinity histamine H(3) and H(4) receptor radioligand. *ChemMedChem* ***2009b,*** 4, 225-31.

Kitbunnadaj, R.; Zuiderveld, O. P.; Christophe, B.; Hulscher, S.; Menge, W. M.; Gelens, E.; Snip, E.; Bakker, R. A.; Celanire, S.; Gillard, M. and others. Identification of 4-(1H-imidazol-4(5)-ylmethyl)pyridine (immethridine) as a novel, potent, and highly selective histamine H(3) receptor agonist. *J. Med. Chem.* ***2004,*** 47, 2414-7.

Kitbunnadaj, R.; Zuiderveld, O. P.; De Esch, I. J.; Vollinga, R. C.; Bakker, R.; Lutz, M.; Spek, A. L.; Cavoy, E.; Deltent, M. F.; Menge, W. M. and others. Synthesis and structure-activity relationships of conformationally constrained histamine H(3) receptor agonists. *J. Med. Chem.* ***2003,*** 46, 5445-57.

Lefkowitz, R. J.; Cotecchia, S.; Samama, P.; Costa, T. Constitutive activity of receptors coupled to guanine nucleotide regulatory proteins. *Trends Pharmacol. Sci.* ***1993,*** 14, 303-7.

Leurs, R.; Bakker, R. A.; Timmerman, H.; de Esch, I. J. P. The histamine H_3 receptor: From gene cloning to H_3 receptor drugs. *Nat. Rev. Drug Discov.* ***2005,*** 4, 107-120.

Lim, H. D.; Smits, R. A.; Bakker, R. A.; van Dam, C. M.; de Esch, I. J.; Leurs, R. Discovery of S-(2-guanidylethyl)-isothiourea (VUF 8430) as a potent nonimidazole histamine H_4 receptor agonist. *J. Med. Chem.* ***2006,*** 49, 6650-1.

Lim, H. D.; van Rijn, R. M.; Ling, P.; Bakker, R. A.; Thurmond, R. L.; Leurs, R. Evaluation of histamine H_1-, H_2-, and H_3-receptor ligands at the human histamine H_4 receptor: identification of 4-methylhistamine as the first potent and selective H_4 receptor agonist. *J. Pharmacol. Exp. Ther.* ***2005,*** 314, 1310-21.

Lovenberg, T. W.; Pyati, J.; Chang, H.; Wilson, S. J.; Erlander, M. G. Cloning of Rat Histamine H_3 Receptor Reveals Distinct Species Pharmacological Profiles. *J. Pharmacol. Exp. Ther.* ***2000,*** 293, 771-778

Lovenberg, T. W.; Roland, B. L.; Wilson, S. J.; Jiang, X.; Pyati, J.; Huvar, A.; Jackson, M. R.; Erlander, M. G. Cloning and functional expression of the human histamine H_3 receptor. *Mol. Pharmacol.* ***1999,*** 55, 1101-7.

Samama, P.; Cotecchia, S.; Costa, T.; Lefkowitz, R. J. A mutation-induced activated state of the beta 2-adrenergic receptor. Extending the ternary complex model. *J. Biol. Chem.* ***1993,*** 268, 4625-36.

Samama, P.; Pei, G.; Costa, T.; Cotecchia, S.; Lefkowitz, R. J. Negative antagonists promote an inactive conformation of the beta 2-adrenergic receptor. *Mol. Pharmacol.* ***1994,*** 45, 390-4.

Schnell, D.; Strasser, A.; Seifert, R. Comparison of the pharmacological properties of human and rat histamine H(3)-receptors. *Biochem. Pharmacol.* ***2010,*** 80, 1437-49.

Thurmond, R. L.; Desai, P. J.; Dunford, P. J.; Fung-Leung, W. P.; Hofstra, C. L.; Jiang, W.; Nguyen, S.; Riley, J. P.; Sun, S.; Williams, K. N. and others. A potent and selective histamine H_4 receptor antagonist with anti-inflammatory properties. *J. Pharmacol. Exp. Ther.* ***2004,*** 309, 404-13.

Wieland, K.; Bongers, G.; Yamamoto, Y.; Hashimoto, T.; Yamatodani, A.; Menge, W. M. B. P.; Timmerman, H.; Lovenberg, T. W.; Leurs, R. Constitutive Activity of Histamine H_3 Receptors Stably Expressed in SK-N-MC Cells: Display of Agonism and Inverse Agonism by H_3 Antagonists. *J. Pharmacol. Exp. Ther.* ***2001,*** 299, 908-914.

Witte, D. G.; Yao, B. B.; Miller, T. R.; Carr, T. L.; Cassar, S.; Sharma, R.; Faghih, R.; Surber, B. W.; Esbenshade, T. A.; Hancock, A. A. and others. Detection of multiple H_3 receptor affinity states utilizing [3H]A-349821, a novel, selective, non-imidazole histamine H_3 receptor inverse agonist radioligand. *Br. J. Pharmacol.* ***2006,*** 148, 657-70.

Wulff, B. S.; Hastrup, S.; Rimvall, K. Characteristics of recombinantly expressed rat and human histamine H_3 receptors. *Eur. J. Pharmacol.* ***2002,*** 453, 33-41.

Yao, B. B.; Hutchins, C. W.; Carr, T. L.; Cassar, S.; Masters, J. N.; Bennani, Y. L.; Esbenshade, T. A.; Hancock, A. A. Molecular modeling and pharmacological analysis of species-related histamine H(3) receptor heterogeneity. *Neuropharmacology* ***2003,*** 44, 773-86.

Zhao, C.; Sun, M.; Bennani, Y. L.; Gopalakrishnan, S. M.; Witte, D. G.; Miller, T. R.; Krueger, K. M.; Browman, K. E.; Thiffault, C.; Wetter, J. and others. The alkaloid conessine and analogues as potent histamine H_3 receptor antagonists. *J. Med. Chem.* ***2008,*** 51, 5423-30.

Chapter 6

Reporter gene assay for the investigation of human and rat histamine H_3 receptor ligands

6.1 Introduction

The histamine H_3R couples to $G\alpha_{i/o}$ proteins (Clark and Hill, 1996) and can functionally be investigated, for instance, in cAMP accumulation (Wieland *et al.*, 2001), steady state [^{32}P]GTPase (Schnell *et al.*, 2010a) or in [^{35}S]GTPγS assays (Coge *et al.*, 2001). A major characteristic of the H_3R is to display constitutive activity in both, recombinant (Wieland *et al.*, 2001) and native *ex-vivo* systems (Morisset *et al.*, 2000). Regardless of a high degree of similarity among the human and rat H_3R, species-related pharmacological heterogeneity was described, which becomes especially evident from increased affinities of antagonists (cf. section 5.2.3.2) and higher potencies of inverse agonists at the rH_3R (Schnell *et al.*, 2010b; Wulff *et al.*, 2002).

The aim of this study was to develop a CRE-controlled reporter gene assay for the human and rat H_3Rs in HEK293T cells. For this purpose, the CRE-luciferase expressing HEK293-CRE-Luc cells were stably co-transfected with either the full length (445 aa) human or rat H_3R. The use of the same host cells for the expression of H_3R orthologs enabled comparism of the transfectants in terms of basal receptor activity, which is increased in the presence of constitutive active receptors (Samama *et al.*, 1993). For validation, a variety of imidazoles and non-imidazoles, comprising H_3R agonists, inverse agonists and antagonists was examined.

6.2 Material and methods

6.2.1 Preparation of the pcDNA3.1(+)-SF-rH$_3$R-His$_6$ vector and sequencing

The pcDNA3.1(+)-SF-rH$_3$R-His$_6$ vector was kindly provided by Prof. Dr. Seifert (Institute of Pharmacology, Medical School of Hannover, Hannover, Germany). Media and agar plates were prepared as described in section 3.2.2.1.4. The transformation of competent *E. coli* cells was performed according to section 3.2.2.1.5. The resulting glycerol culture and the large scale preparation of plasmid DNA (Maxi-Prep) were performed as described in section 3.2.2.1.6. The DNA concentration was determined according to section 3.2.2.1.2. Sequencing (performed by Entelechon) confirmed the identity and correctness of the SF-rH$_3$R-His$_6$ insert in pcDNA3.1(+).

6.2.2 Stable transfection of HEK293-CRE-Luc with the human and rat H$_3$R

HEK293-CRE-Luc cells were cultured as described in section 3.1.2.1 and section 4.1.2.4. Cells were transfected with pcDNA3.1(+)-SF-hH$_3$R-His$_6$ (kindly provided by Dr. Schnell, Institute of Pharmacology and Toxicology, University of Regensburg, Germany) and pcDNA3.1(+)-SF-rH$_3$R-His$_6$ according to section 3.2.2.2 with the exception that the ratios of transfection reagent (µL) to DNA amount (µg) were 6:2 and 8:2. The transfection batches were initially selected with DMEM containing 10 % FCS, 800 µg/mL of G418 and 200 µg/mL of hygromycin B. Subsequently, HEK293-CRE-Luc-SF-hH$_3$R-His$_6$ and HEK293-CRE-Luc-SF-rH$_3$R-His$_6$ cells were maintained with DMEM containing 10 % FCS, 600 µg/mL of G418 and 200 µg/mL of hygromycin B.

6.2.3 Luciferase reporter gene assay

For implementation see section 4.1.2.6. The K_B values of neutral antagonists/inverse agonists were determined in the antagonist mode at the hH$_3$R and rH$_3$R *versus* histamine (10 and 15 nM, respectively) as the agonist.

6.3 Results and discussion

6.3.1 Selection of the HEK293-CRE-Luc-SF-h/rH$_3$R-His$_6$ cells

In order to investigate H_3R ligand activity at the human and rat H_3R in the luciferase reporter gene assay, HEK293-CRE-Luc cells were stably transfected with human and rat H_3Rs, respectively. To select in each case the best transfection batch, the cells were incubated with 1 µM of forskolin and either 100 µM of the full agonist histamine (**1**) or the inverse agonist thioperamide (**12**).

Although the luciferase expression evoked by 1 µM of forskolin was comparable among the hH_3R transfectants, the ligand induced effects of histamine (**1**) and thioperamide (**12**) were clearly higher in the 8:2 cells (see **Figure 6.1**). Therefore, the 8:2 cells were chosen for further reporter gene assays at the hH_3R. In both transfection batches, the inverse agonistic effect of thioperamide (**12**) was more pronounced than the effect of histamine (**1**), indicating a high constitutive activity of the hH_3R expressed in HEK293-CRE-Luc cells (see **Figure 6.1**).

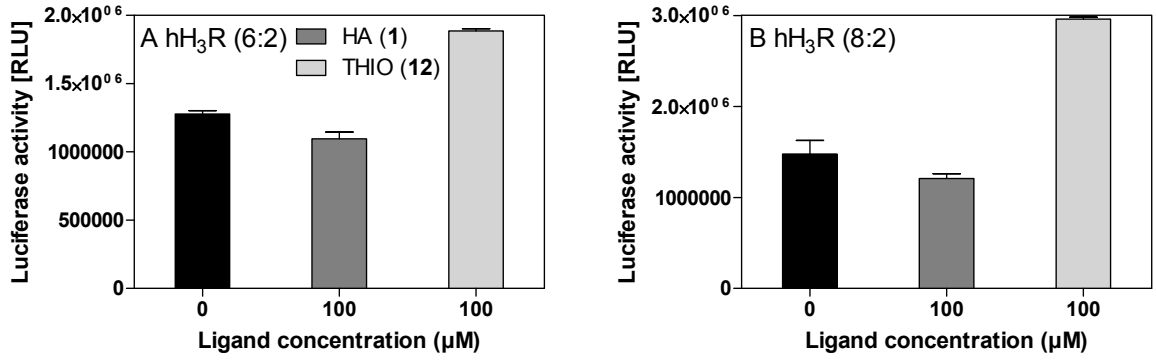

Figure 6.1: $hH_3R/G\alpha_{i/o}$ mediated effect of HA (**1**) and THIO (**12**) upon stimulation with 1 µM forskolin in HEK293-CRE-Luc-SF-hH_3R-His_6 cells. 6:2 transfection batch (A). 8:2 transfection batch (B).

The 8:2 transfection batch of the rH_3R expressing cells was also selected for subsequent reporter gene assays at the rH_3R, since the effect of 100 µM of histamine (**1**) and thioperamide (**12**) were clearly higher compared to the 6:2 cells (see **Figure 6.2**). The EC_{50} values of forskolin in the HEK293-CRE-Luc-SF-hH_3R-His_6 (8:2) and the HEK293-CRE-Luc-SF-rH_3R-His_6 (8:2) cells were 6.06 ± 0.47 (N = 3) and 5.59 (N = 1), respectively, and thus comparable with HEK293-CRE-Luc cells devoid of H_3R (cf. section 4.1.3.6). By analogy with the HEK293-CRE-Luc (cf. section 4.1.3.6) and HEK293-CRE-Luc-SF-rH_4R-His_6 cells (cf. 4.2.3.3), 1 µM of forskolin was used for pre-stimulation in subsequent reporter gene assays.

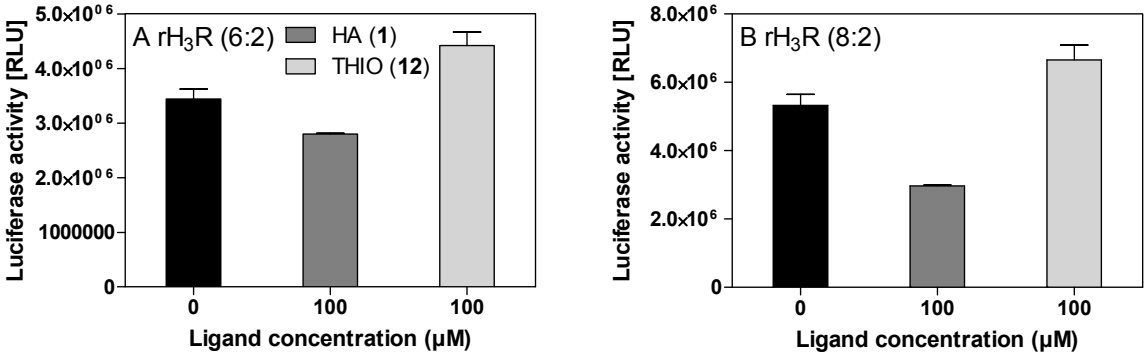

Figure 6.2: Change of the luciferase activity by $G\alpha_{i/o}$-mediated rH_3R response. The effect of 100 µM of the agonist histamine (**1**) and the inverse agonist thioperamide (**12**) upon pre-stimulation with 1 µM of forskolin in HEK293-CRE-Luc-SF-rH_3R-His_6 cells. 6:2 transfection batch (A). 8:2 transfection batch (B).

6.3.2 Functional characterization of ligands at the human and rat histamine H_3R

Histamine (**1**) decreased forskolin (1 µM) stimulated luciferase activity by 58.0 ± 4.2 % (N = 5) and 72.3 ± 3.3 % (N = 4) in HEK293-CRE-Luc-SF-hH_3R-His_6 and HEK293-CRE-Luc-SF-rH_3R-His_6 cells, respectively, which was sufficient for the conduction of the luciferase reporter gene assay at both receptor orthologs. A variety of 23 H_3R ligands comprising agonists, inverse agonists and antagonists was investigated in the luciferase assay at the human and rat H_3R (cf. section 3.1.2.3). These results and data reported in the literature are summarized in **Tabelle 6.1**.

Histamine (**1**), (R)-α-methylhistamine (**2**), (S)-α-methylhistamine (**3**), N^{α}-methylhistamine (**4**) and 5(4)-methylhistamine (**5**) changed the luciferase activity in a concentration-dependent manner via activation of the human and rat H_3R in HEK293-CRE-luc cells (see **Figure 6.3**). At the rH_3R the concentration response curves of **1**-**5** were slightly rightward-shifted compared to the hH_3R, but the rank order was same for histamine (**1**) and its methylated analogs (**2** = **4** > **3** > **1** > **5**). Interestingly, methylation at position 5(4) of the imidazole ring (**5**) resulted in a dramatic decrease in potency of about 1000-fold as shown by and 5(4)-methylhistamine (**5**). This was in accordance with the low binding affinity of **5** at the hH_3R (Lim *et al.*, 2005). By contrast, the introduction of a methyl substituent in the side chain, whether at the α-carbon (**2** and **3**) or at the α-nitrogen (**4**), increased the potency at the H_3R. As at the H_4R (cf. section 4.1.3.8 and 4.2.3.4), the human and rat H_3R preferred (R)-α-methylhistamine (**2**) over (S)-α-methylhistamine (**3**). Whereas the potencies of (S)-α-methylhistamine (**3**) and N^{α}-methylhistamine (**4**) were higher than reference data at the hH_3R,

the pEC_{50} values of histamine (**1**) and (R)-α-methylhistamine (**2**) were comparable. At the rH_3R functional data of **1**-**4** were without exception consistent with literature.

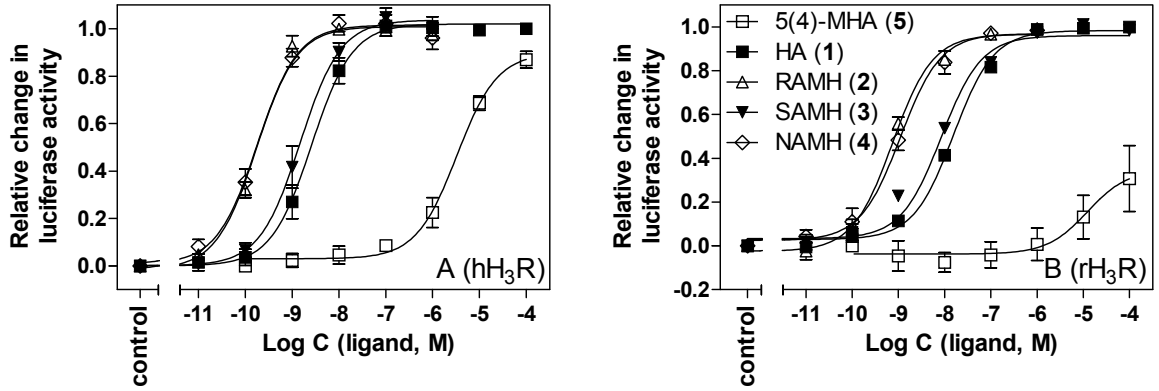

Figure 6.3: Relative change of luciferase activity by HA (**1**), RAMH (**2**), SAMH (**3**), NAMH (**4**) and 5(4)-MHA (**5**) in HEK293-CRE-Luc-SF-hH_3R-His_6 (A) and HEK293-CRE-Luc-SF-rH_3R-His_6 (B) cells. Maximum change of 1 is defined as full agonism, whereas 0 indicates the luminescence signal detected after direct stimulation of adenylyl cyclase by 1 µM forskolin in the absence of H_3R ligands (control). Data were analyzed by nonlinear regression and best fitted to sigmoidal concentration-response curves. Data points shown are mean ± SEM of at least three independent experiments performed in triplicate.

Immepip (**6**) and immethridine (**8**) fully activated both H_3R orthologs with pEC_{50} values >10 at the hH_3R and >9 at the rH_3R, respectively (see **Figure 6.4**). The hH_3R potency of immethridine (**8**) was 10-fold higher than reported, whereas the results for Immepip (**6**) were in good agreement with literature regarding both H_3R orthologs. As already shown for the human and mouse H_4R (cf. section 4.1.3.7 and 4.2.3.4), VUF 5681 (**7**) displayed a clear decrease in terms of potency and intrinsic activity at the H_3R compared to its analog immepip (**6**) (see **Figure 6.4**). Surprisingly, VUF 5681 (**7**) acted as partial agonist at the hH_3R, whereas no intrinsic activity was detected in a CRE-β-galactosidase assay in SK-N-MC/hH_3R cells (Kitbunnadaj *et al.*, 2003). Inversely, at the rH_3R VUF 5681 (**7**) displayed no intrinsic activity, and the pK_B value of 6.74 ± 0.23 was about two log units lower compared to the pEC_{50} value at the hH_3R.

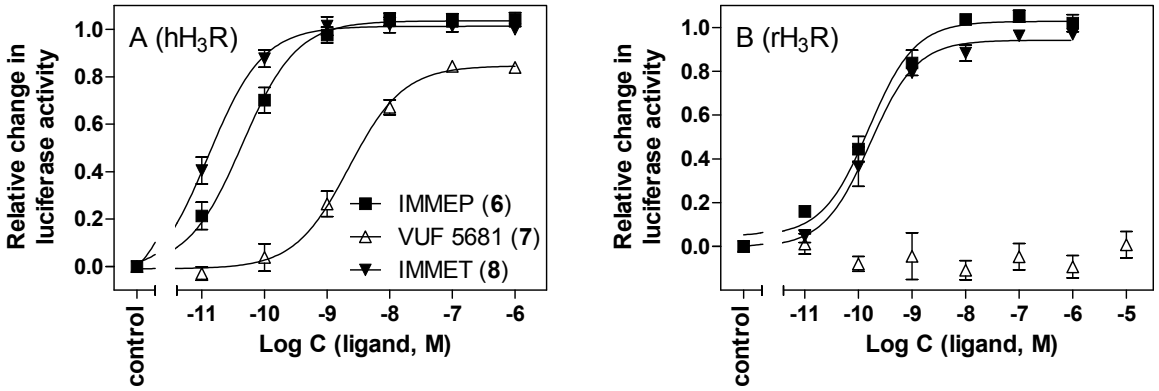

Figure 6.4: Potencies and efficacies of IMMEP (**6**), VUF 5681 (**7**) and IMMET (**8**) at the hH_3R (A) and the rH_3R (B) stably co-expressed with a CRE-controlled luciferase reporter gene in HEK293T cells. Maximum change of 1 is defined as full agonism, whereas 0 indicates the luminescence signal detected after direct stimulation of adenylyl cyclase by 1 µM forskolin in the absence of H_3R ligands (control). Data were analyzed by nonlinear regression and best fitted to sigmoidal concentration-response curves. Data points shown are mean ± SEM of at least three independent experiments performed in triplicate.

The isothiourea analog of histamine (**1**), imetit (**9**), was 30 times more potent than **1** at the human and rat H_3R (see **Figure 6.5** A, B). The pEC_{50} value at the hH_3R was in agreement with the β-galactosidase reporter gene assay (Lim *et al.*, 2005), but higher than data obtained in [^{32}P]GTPase (Schnell *et al.*, 2010a) and [^{35}S]GTPγS assays (Coge *et al.*, 2001). In contrast, at the rH_3R the potency of imetit (**9**) was lower compared to the [^{32}P]GTPase assay (Schnell *et al.*, 2010b). Clobenpropit (**10**) and iodophenpropit (**11**) were mostly described as inverse agonist at both receptor orthologs (see **Tabelle 6.1**). Surprisingly, clobenpropit (**10**) acted as a potent partial agonist with low intrinsic activity and iodophenpropit (**11**) as neutral antagonist at both H_3R receptor orthologs (see **Figure 6.5** A, B). Both ligands showed also tendency toward increased agonist intrinsic activity at the hH_4R (cf. section 4.1.3.8), suggesting a special signal amplification for these structurally related compounds in the luciferase assay. At the hH_3R the pK_B values of Clobenpropit (**10**) and iodophenpropit (**11**) were consistent with their binding affinity (cf. section 5.1.3.2) as well as with data from literature. By contrast, at the rH_3R the pK_B values were lower compared to reported data and in the case of clobenpropit (**10**) distinctly lower than the binding affinity (see **Figure 6.5** C, D) (cf. section 5.2.3.2).

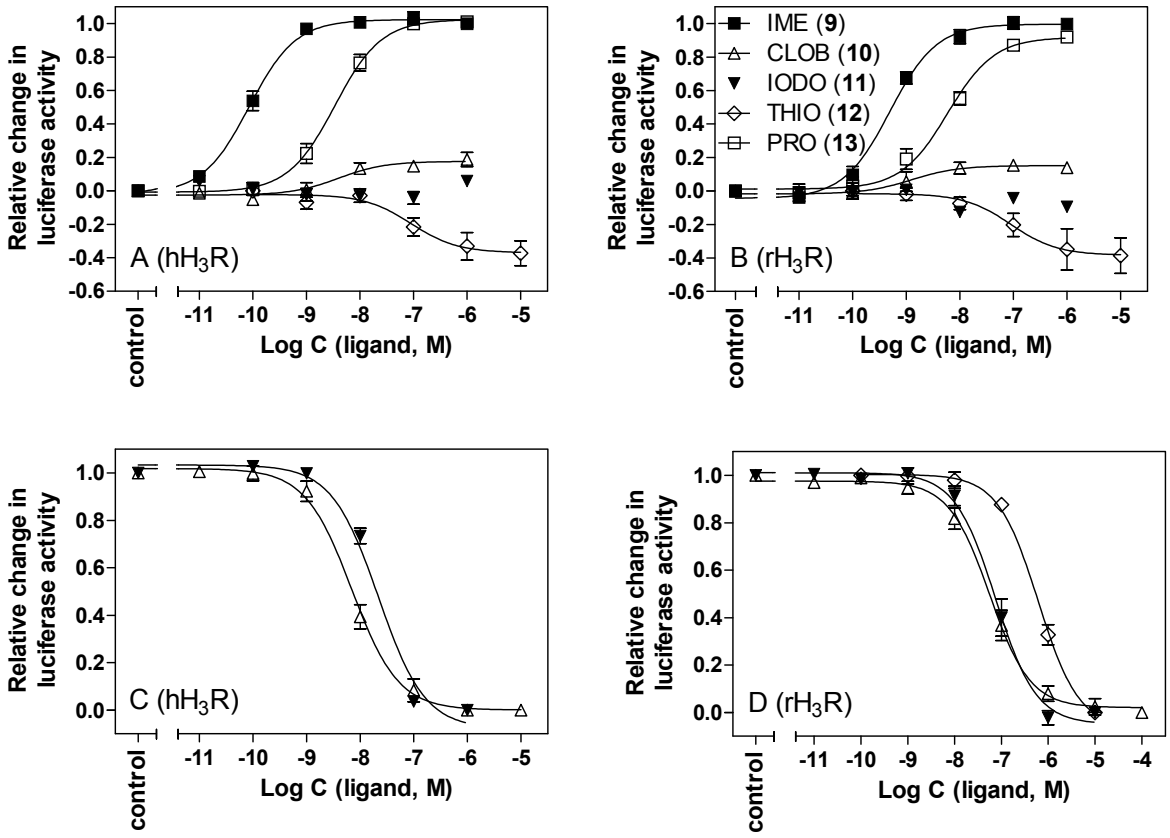

Figure 6.5: Effects of several standard ligands on H_3R orthologs in the luciferase reporter gene assay in HEK293T cells. Maximum change of 1 indicates full agonism, -1 is defined as "full" inverse agonism, whereas 0 indicates the luminescence signal detected after direct stimulation of adenylyl cyclase by 1 µM forskolin in the absence of H_3R ligands (control). Potencies and efficacies of IME (**9**), CLOB (**10**), IODO (**11**), THIO (**12**) and PRO (**13**) at the hH_3R (A) and the rH_3R (B) (agonists mode). Reversal of the HA (**1**) (10 – 15 nM) mediated inhibition of the forskolin-stimulated luciferase activity by CLOB (**10**) and IODO (**11**) at the hH_3R (C) and by CLOB (**10**), IODO (**11**) and THIO (**12**) at the rH_3R (D) (antagonist mode). Data were analyzed by nonlinear regression and best fitted to sigmoidal concentration-response curves. Data points shown are the mean ± SEM of at least three independent experiments performed in triplicate.

In line with literature, thioperamide (**12**) behaved as inverse agonist at the H_3R (see **Figure 6.5** A, B). The potency at the hH_3R was in accordance with reported data and in the same order of magnitude as at the hH_4R (cf section 4.1.3.8). Inversely, at the rH_3R the potency of thioperamide (**12**) was distinctly lower as determined, for example, in the [^{33}P]GTPase assay (Schnell *et al.*, 2010b). Surprisingly, the pK_B value of thioperamide (**12**) was 30 times lower than its binding affinity at the rH_3R in section 5.2.3.2 (see **Figure 6.5** D). Proxyfan (**13**) was a potent and almost full agonist at the human and rat H_3R, which was in accordance to data from literature (see **Figure 6.5** A, B). UR-PI294 (**15**) reached pEC_{50} values >9 at both H_3R orthologs (see **Figure 6.6**). Moreover, UR-PI294 (**15**) was able to fully activate the hH_3R in the reporter gene assay. In contrast, the potency in the [^{32}P]GTPase assay was slightly lower and only partial agonistic activity (α = 0.39) was detected (Igel *et al.*, 2009b). At the rH_3R, UR-PI294 (**15**) was a strong partial agonist. The reported H_4R-selectivity of UR-PI376 (**16**),

trans-(+)-(1S,3S)-UR-RG98 (**17**), JNJ 7777120 (**19**) and the amino-pyrimidine ST-1006 (**30**) could be confirmed in the luciferase assay. Interestingly, with the exception of trans-(+)-(1S,3S)-UR-RG98 (**17**), all of the aforementioned selective H_4R ligands displayed weak inverse agonistic activity. trans-(+)-(1S,3S)-UR-RG98 (**17**) was ~40-fold less potent at the hH_3R compared to the hH_4R, but in contrast to the [^{35}S]GTPγS binding assay (Geyer, 2011), residual intrinsic activity was measured. For the first time also for ST-1012 (**31**) a ~30-fold selectivity for the hH_4R over the hH_3R was found in the present luciferase reporter gene assay. As at the hH_4R, ST-1012 (**31**) showed inverse agonistic activity at the hH_3R. Clozapine (**18**) and VUF8430 (**20**) fully activated the hH_3R. The potencies were only moderate and consistent with literature.

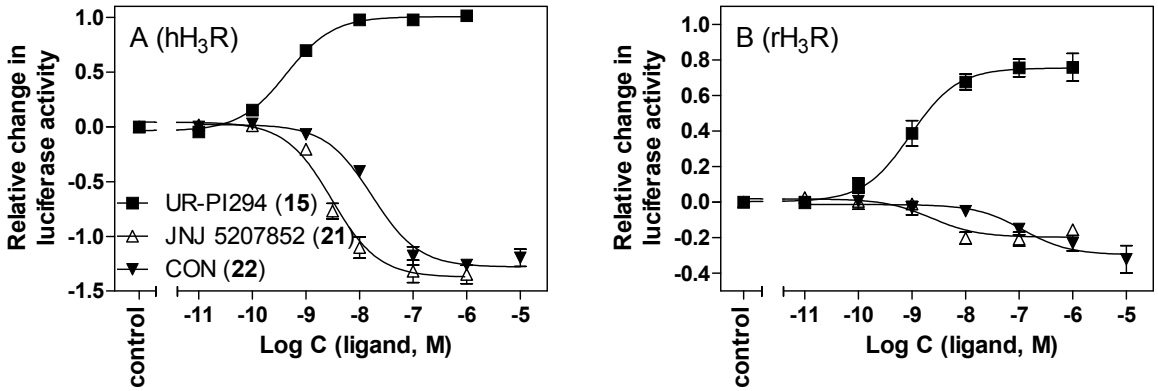

Figure 6.6: Potencies and efficacies of UR-PI294 (**15**), JNJ 5207852 (**21**) and CON (**22**) at the hH_3R (A) and the rH_3R (B) stably co-expressed with a CRE-controlled luciferase reporter gene in HEK293T cells. Maximum change of 1 indicates full agonism, -1 is defined as "full" inverse agonism, whereas 0 indicates the luminescence signal detected after direct stimulation of adenylyl cyclase by 1 µM forskolin in the absence of H_3R ligands (control). Data were analyzed by nonlinear regression and best fitted to sigmoidal concentration-response curves. Data points shown are mean ± SEM of at least three independent experiments performed in triplicate.

Surprisingly, JNJ 5207852 (**21**) and the alkaloid conessine (**22**) displayed exceptionally high inverse agonistic activity at the hH_3R, whereas both compounds were described as neutral antagonists (see **Figure 6.6** A) in assay systems devoid of pronounced constitutive activity (Barbier *et al.*, 2004; Zhao *et al.*, 2008). Obviously, the exceptionally high constitutive activity of the hH_3R in HEK293-CRE-Luc cells is a prerequisite for the detection of inverse agonism in case of reported neutral antagonists (Kenakin, 2004). Control experiments with HEK293-CRE-Luc cells did not reveal a non-specific, off-target mediated increase in luciferase activity, indicating that the inverse agonistic activity of JNJ 5207852 (**21**) and conessine (**22**) was actually hH_3R-dependent (data not shown). At the rH_3R both ligands acted also as inverse agonists, but the intrinsic activities were clearly lower than at the hH_3R and in the same range as that of thioperamide (**12**). However, pK_B values determined in the antagonist

mode at the rH_3R were lower than the pEC_{50} values and also lower than the reported pA_2 (JNJ 5207852 (**21**)) and pK_B values (conessine (**22**)).

The constitutive activity of the rH_3R seemed to be considerably lower compared to the hH_3R. A major hallmark of constitutive activity is increased basal activity of the receptor (Samama *et al.*, 1993; Wieland and Seifert, 2006). Since HEK293-CRE-Luc-SF-hH_3R-His_6 and HEK293-CRE-Luc-SF-rH_3R-His_6 cells were both derived from the HEK293-CRE-Luc cells (cf. section 6.2.2), comparison of the forskolin (1 µM) stimulated activity in the presence and absence of the H_3R was possible. The basal activity of HEK293-CRE-Luc cells served as control and HEK293-CRE-Luc-SF-rH_4R-His_6 cells were additionally considered for comparison. Rat H_4R and H_3R expressing cells displayed almost the same level of luciferase activity as the control (see **Figure 6.7**). This was expected due to moderate constitutive activity of inverse agonists at both rat histamine receptor subtypes (cf. section. 4.2.3.4 and **Figure 6.6**). In contrast, the hH_3R expressing cells showed clearly decreased luciferase activity compared to the HEK293-CRE-Luc cells, reflecting high constitutive activity of the $G\alpha_{i/o}$ coupled hH_3R (see **Figure 6.7**).

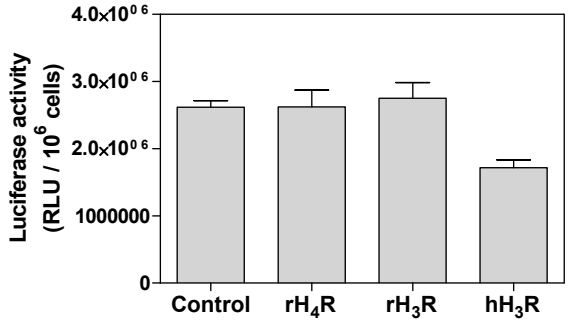

Figure 6.7: Luciferase activity stimulated by 1 µM forskolin in HEK293-CRE-Luc cells devoid of H_xR (control) (N = 2) and expressing the rH_4R (N = 12), the rH_3R (N = 18) or the hH_3R (N = 13). RLU values were normalized to the cell number. Data are mean values ± SEM of N independent experiments.

Investigating a small series ligands at the human and rat H_3R, Schnell et al. detected neither difference in the constitutive activities of these receptor orthologs nor in the potencies of the respective full agonists in the GTPase assay (Schnell *et al.*, 2010b). At a constitutively active mutant (CAM) of the β_2-AR, (full) agonists showed higher binding affinities in concert with higher potencies compared with the wild-type receptor (cf. section 5.1.3.2) (Samama *et al.*, 1993). Likewise, in the luciferase assay, agonists (**1**, **2**, **3**, **4**, **6**, **7**, **8**) revealed higher potencies at the highly constitutively active hH_3R compared to the rH_3R.

In the luciferase assay, increased intrinsic activities were found for the partial agonists proxyfan (**13**) and UR-PI294 (**15**) at the hH_3R compared to the [^{32}P]GTPase assay (Schnell *et al.*, 2010a). This could be due to constitutive activity (Samama *et al.*, 1993) or to signal amplification as a result of the very distal readout in the reporter gene assay (cf. sections 4.1.3.8 and 4.2.3.4). The increased intrinsic activity of VUF 5681 (**7**), reported as a neutral

hH_3R antagonist (Kitbunnadaj *et al.*, 2004), presumably reflects the pronounced constitutive activity of the hH_3R in HEK293-CRE-Luc cells. Interestingly, no partial agonism was observed at the rH_3R, characterized by relatively low constitutive activity in reporter gene assay.

The pK_B values of clobenpropit (**10**) and iodophenpropit (**11**) were in agreement with binding affinities at the hH_3R (cf. section 5.1.3.2) as well as with reported data. In contrast, at the rH_3R pK_B values of clobenpropit (**10**), iodophenpropit (**11**), thioperamide (**12**), JNJ 5207852 (**21**) and conessine (**22**) were lower than reported and distinctly lower than the respective binding affinities (**10**, **12**) (cf. section 5.2.3.2). This was unexpected, since antagonist affinity should be independent from the system (Kenakin, 2009).

Distinctly higher potencies of inverse agonists at the rH_3R in comparison to the hH_3R were reported in the literature (Schnell *et al.*, 2010b; Wulff *et al.*, 2002; Yao *et al.*, 2003). By contrast, the potencies were only slightly higher for thioperamide (**12**) and JNJ 5207852 (**21**) and even lower for conessine (**22)**. Thus, distinctly higher potency of inverse agonists could not be confirmed in this luciferase reporter gene assay.

Tabelle 6.1: Potencies and efficacies of H_3R ligands at the hH_3R and rH_3R in the luciferase reporter gene assay (mean values ± SEM) in comparison to reported data.

Ligand	**hH_3R**			**rH_3R**			**hH_3R**		**rH_3R**	
	Luciferase reporter gene assay in HEK293-CRE-Luc-SF-hH_3R-His_6- cells			Luciferase reporter gene assay in HEK293-CRE-Luc-SF-rH_3R-His6 cells			Reference data		Reference data	
	pEC_{50} or (pK_B)	α	N	pEC_{50} or (pKB)	α	N	pEC_{50} or (pK_B)	α	pEC_{50} or (pK_B)	α
Histamine (**1**)	8.61 ± 0.11	1.00 ± 0.00	5	7.81 ± 0.05	1.00 ± 0.00	4	7.5-8.7[c,h,j,l,p]	1.0	7.9-8.7[m,p]	1.0
(R)-α-Methylhistamine (**2**)	9.76 ± 0.05	0.98 ± 0.04	4	9.12 ± 0.07	1.07 ± 0.03	4	8.6-9.5[c,h,j,l,o,p]	1.0-1.2	8.5-9.4[m,o,p]	0.9-1.0
(S)-α-Methylhistamine (**3**)	8.85 ± 0.10	1.01 ± 0.05	4	8.08 ± 0.02	0.95 ± 0.04	4	8.0-8.2[j,p]	1.0	7.8[p]	1.0
N^{α}-Methylhistamine (**4**)	9.75 ± 0.07	0.96 ± 0.01	4	8.97 ± 0.07	0.99 ± 0.02	4	8.7-9.4[c,j,l]	1.0	9.0[m]	1.1
5(4)-Methylhistamine (**5**)	5.50 ± 0.12	0.80 ± 0.07	3	< 4	0.32 ± 0.14	4	-	-	-	-
Immepip (**6**)	10.46 ± 0.10	1.03 ± 0.03	4	9.83 ± 0.15	0.98 0.02	5	9.3-10.4[b,c,h,j,p]	1.0	9.9[p]	1.0
VUF 5681 (**7**)	8.66 ± 0.01	0.87 ± 0.05	3	(6.74 ± 0.23)	-0.15 ± 0.03	4	8.1 (pA_2)[h]	0.0	-	-
Immethridine (**8**)	10.89 ± 0.14	1.03 ± 0.05	3	9.80 ± 0.16	0.99 ± 0.02	6	9.7-9.8[i,j]	0.90	-	-
Imetit (**9**)	10.06 ± 0.12	0.94 ± 0.03	3	9.31 ± 0.04	1.07 ± 0.05	4	8.8-9.9[c,j,l,o,p]	0.9-1.0	9.8-9.9[m,p]	0.9-1.0
Clobenpropit (**10**)	8.41 ± 0.32 (9.04 ± 0.06)	0.19 ± 0.02	4 4	8.35 ± 0.24 (8.32 ± 0.21)	0.17 ± 0.01	3 5	8.1-9.4[d,j,l,o,p] (8.2-9.3)[c,d,p]	-1.37[l]	8.5-9.0[m,o,p] (9.0-9.3)[d,p]	-0.44[m]
Iodophenpropit (**11**)	(8.50 ± 0.06)	0.05 ± 0.02	3	(8.00 ± 0.13)	-0.13 ± 0.00	6	7.6-8.5[j,o,p] (8.9)[p]	-1.0[j,o]	8.0-8.7[o,p] (8.8)[p]	-1.0[o]
Thioperamide (**12**)	6.92 ± 0.13	-0.27 ± 0.02	3	7.19 ± 0.21 (7.07 ± 0.08)	-0.31 ± 0.08	5 4	6.7-7.8[b,d,j,l,o,p] (6.1-8.1)[c,d,p]	-1.02[l]	7.7-8.6[m,o,p] (7.6-9.0)[d,p]	-0.6[m]
Proxyfan (**13**)	8.47 ± 0.08	1.01 ± 0.02	3	8.27 ± 0.15	0.90 ± 0.03	4	8.2-8.5[j,l,p]	0.9-1.0	8.4-8.5[m,p]	0.7-1.0

Table 6.1 (continued)

Ligand	hH_3R			rH_3R			hH_3R		rH_3R	
	Luciferase reporter gene assay in HEK293-CRE-Luc-SF-hH_3R-His_6- cells			Luciferase reporter gene assay in HEK293-CRE-Luc-SF-rH_3R-His6 cells			Reference data		Reference data	
	pEC_{50} or (pK_B)	α	N	pEC_{50} or (pK_B)	α	N	pEC_{50} or (pK_B)	α	pEC_{50} or (pK_B)	α
UR-PI294 (**15**)	9.36 ± 0.06	1.04 ± 0.03	3	9.10 ± 0.12	0.77 ± 0.05	4	8.80[f]	0.39	-	-
UR-PI376 (**16**)	< 4	-1.55 ± 0.51	2	n.d.	n.d.	-	(6.00)[g]	-0.28	-	-
trans-(+)-(1S,3S)-UR-RG98 (**17**)	6.07 ± 0.19	0.69 ± 0.06	4	n.d.	n.d.	-	(5.9)[e]	-0.01	-	-
Clozapine (**18**)	5.57 ± 0.09	0.99 ± 0.05	3	n.d.	n.d.	-	-	-	-	-
JNJ 7777120 (**19**)	5.09 ± 0.08	-0.85 ± 0.09	2	n.d.	n.d.	-	< 6[j], 6.0 (pA_2)[n]	-0.7[j]	< 6 (pA_2)[n]	-
VUF 8430 (**20**)	6.27 ± 0.10	0.99 ± 0.02	4	n.d.	n.d.	-	6.5[j]	1.00	-	-
JNJ 5207852 (**21**)	8.53 ± 0.07	-1.42 ± 0.06	4	8.63 ± 0.08 (7.56 ± 0.10)	-0.32 ± 0.12	3 3	9.8 (pA_2)[a]	-	8.9 (pA_2)[a]	-
Conessine (**22**)	7.70 ± 0.04	-1.33 ± 0.08	4	7.20 ± 0.24 (6.44± 0.23)	-0.24 ± 0.05	3 6	(6.1-8.1)[q]	-	(6.99)[q]	-
ST-1006 (**30**)	5.77 ± 0.11	-1.14 ± 0.29	3	n.d.	n.d.	-	-	-	-	-
ST-1012 (**31**)	5.78 ± 0.14	-0.75 ± 0.06	3	n.d.	n.d.	-	-	-	-	-

pEC_{50} values determined in the luciferase reporter gene assay show the change of 1 µM forskolin-induced luciferase activity in HEK293-CRE-Luc-SF-hH_3R-His_6 and in HEK293-CRE-Luc-SF-rH_3R-His_6 cells. N gives the number of independent experiment performed in triplicate. The intrinsic activity (α) of histamine was set to 1.00 and α values of other compounds were referred to this value. The K_B values of neutral antaonists were determined in the antagonist mode at the hH_3R and rH_3R versus histamine (10 and 15 nM, respectively) as the agonist. Data taken from: CRE-βgalactosidase reporter gene assay in SK-N-MC cells stably expressing the hH_3R [a,h,l,j,k,n] (Barbier *et al.*, 2004; Kitbunnadaj *et al.*, 2004; Kitbunnadaj *et al.*, 2003; Lim *et al.*, 2006; Lim *et al.*, 2005; Thurmond *et al.*, 2004) or the rH_3R [a,n] (Barbier *et al.*, 2004; Thurmond *et al.*, 2004) with the CRE-βgalactosidase reporter gene; steady-state GTPase activity in Sf9 membranes co-expressing the hH_3R [f,g,l] (Igel *et al.*, 2009a; Igel *et al.*, 2009b; Schnell *et al.*, 2010a; Schnell *et al.*, 2010b) or the rH_3R [m] (Schnell *et al.*, 2010b) with $G\alpha_{i2}$ and $G\beta_{1\gamma2}$; functional [^{35}S]GTPγS binding: with Sf9 membranes co-expressing hH_3R with $G\alpha_{i2}$ and $G\beta_{1\gamma2}$ [e] (Geyer, 2011), with CHO-K1 membranes expressing the hH_3R (445 aa) [c] (Coge *et al.*, 2001) or with HEK293 membranes expressing the hH_3R (445 aa) [d] (Esbenshade *et al.*, 2003); [d] calcium mobilization assay in HEK293 cells co-expressing the hH_3R (445 aa) with $G\alpha_{q/i5}$ [d] (Esbenshade *et al.*, 2003; Yao *et al.*, 2003); cAMP assay: with C6, HEK293 or SK-NM-C cells stably expressing the hH_3R (445 aa) [b,d,p,o] (Bongers *et al.*, 2007; Esbenshade *et al.*, 2003; Wieland *et al.*, 2001; Wulff *et al.*, 2002) or rH_3R (445 aa) [d,o] (Esbenshade *et al.*, 2003; Wieland *et al.*, 2001).

6.4 Summary and conclusion

HEK293-CRE-Luc cells were stably co-transfected with full length (445 aa) human and rat H_3Rs. The established luciferase assays were successfully used for the quantification of agonist, inverse agonist and antagonist activities in a highly sensitive and reliable manner. In contrast to the rH_3R, the hH_3R displayed exceptionally high constitutive activity in the luciferase assay. This became obvious by increased basal activity of the hH_3R in HEK293-CRE-Luc cells and was confirmed by means of inverse agonists. The presence of high constitutive activity led to increased potency of full agonists. Ligands with lower intrinsic activities such as partial agonists were less affected. Although radioligand binding experiments confirmed higher affinities of antagonists and inverse agonists at the rH_3R (cf. section 5.2.3.2), pK_B values and pEC_{50} values were lower than reported. Thus, the reported distinctly increased potencies of inverse agonists at the rH_3R compared to the hH_3R were not confirmed in the present luciferase reporter gene assay.

6.5 References

Barbier, A. J.; Berridge, C.; Dugovic, C.; Laposky, A. D.; Wilson, S. J.; Boggs, J.; Aluisio, L.; Lord, B.; Mazur, C.; Pudiak, C. M. and others. Acute wake-promoting actions of JNJ-5207852, a novel, diamine-based H_3 antagonist. *Br. J. Pharmacol.* ***2004,*** 143, 649-61.

Bongers, G.; Sallmen, T.; Passani, M. B.; Mariottini, C.; Wendelin, D.; Lozada, A.; Marle, A.; Navis, M.; Blandina, P.; Bakker, R. A. and others. The Akt/GSK-3beta axis as a new signaling pathway of the histamine H(3) receptor. *J. Neurochem.* ***2007,*** 103, 248-58.

Clark, E. A.; Hill, S. J. Sensitivity of histamine H_3 receptor agonist-stimulated [^{35}S]GTP γ[S] binding to pertussis toxin. *Eur. J. Pharmacol.* ***1996,*** 296, 223-225.

Coge, F.; Guenin, S. P.; Audinot, V.; Renouard-Try, A.; Beauverger, P.; Macia, C.; Ouvry, C.; Nagel, N.; Rique, H.; Boutin, J. A. and others. Genomic organization and characterization of splice variants of the human histamine H_3 receptor. *Biochem. J* ***2001,*** 355, 279-88.

Esbenshade, T. A.; Krueger, K. M.; Miller, T. R.; Kang, C. H.; Denny, L. I.; Witte, D. G.; Yao, B. B.; Fox, G. B.; Faghih, R.; Bennani, Y. L. and others. Two novel and selective nonimidazole histamine H_3 receptor antagonists A-304121 and A-317920: I. In vitro pharmacological effects. *J. Pharmacol. Exp. Ther.* ***2003,*** 305, 887-96.

Geyer, R. Hetarylalkyl(aryl)cyanoguanidines as histamine H_4 receptor ligands: Synthesis, chiral separation, pharmacological characterization, structure-activity and -selectivity relationships. PhD thesis, University of Regensburg, Regensburg, 2011.

Igel, P.; Geyer, R.; Strasser, A.; Dove, S.; Seifert, R.; Buschauer, A. Synthesis and structure-activity relationships of cyanoguanidine-type and structurally related histamine H_4 receptor agonists. *J. Med. Chem.* ***2009a,*** 52, 6297-313.

Igel, P.; Schneider, E.; Schnell, D.; Elz, S.; Seifert, R.; Buschauer, A. N(G)-acylated imidazolylpropylguanidines as potent histamine H_4 receptor agonists: selectivity by variation of the N(G)-substituent. *J. Med. Chem.* ***2009b,*** 52, 2623-7.

Kenakin, T. Efficacy as a vector: the relative prevalence and paucity of inverse agonism. *Mol. Pharmacol.* ***2004,*** 65, 2-11.

Kenakin, T. P. 2009. A pharmacology primer : theory, applications, and methods. Amsterdam ; Boston: Academic Press/Elsevier. xix, 389 p. p.

Kitbunnadaj, R.; Zuiderveld, O. P.; Christophe, B.; Hulscher, S.; Menge, W. M.; Gelens, E.; Snip, E.; Bakker, R. A.; Celanire, S.; Gillard, M. and others. Identification of 4-(1H-imidazol-4(5)-ylmethyl)pyridine (immethridine) as a novel, potent, and highly selective histamine H(3) receptor agonist. *J. Med. Chem.* ***2004,*** 47, 2414-7.

Kitbunnadaj, R.; Zuiderveld, O. P.; De Esch, I. J.; Vollinga, R. C.; Bakker, R.; Lutz, M.; Spek, A. L.; Cavoy, E.; Deltent, M. F.; Menge, W. M. and others. Synthesis and structure-activity relationships of conformationally constrained histamine H(3) receptor agonists. *J. Med. Chem.* ***2003,*** 46, 5445-57.

Lim, H. D.; Smits, R. A.; Bakker, R. A.; van Dam, C. M.; de Esch, I. J.; Leurs, R. Discovery of S-(2-guanidylethyl)-isothiourea (VUF 8430) as a potent nonimidazole histamine H_4 receptor agonist. *J. Med. Chem.* ***2006,*** 49, 6650-1.

Lim, H. D.; van Rijn, R. M.; Ling, P.; Bakker, R. A.; Thurmond, R. L.; Leurs, R. Evaluation of histamine H_1-, H_2-, and H_3-receptor ligands at the human histamine H_4 receptor: identification of 4-methylhistamine as the first potent and selective H_4 receptor agonist. *J. Pharmacol. Exp. Ther.* ***2005,*** 314, 1310-21.

Morisset, S.; Rouleau, A.; Ligneau, X.; Gbahou, F.; Tardivel-Lacombe, J.; Stark, H.; Schunack, W.; Ganellin, C. R.; Schwartz, J. C.; Arrang, J. M. High constitutive activity of native H_3 receptors regulates histamine neurons in brain. *Nature* ***2000,*** 408, 860-4.

Samama, P.; Cotecchia, S.; Costa, T.; Lefkowitz, R. J. A mutation-induced activated state of the beta 2-adrenergic receptor. Extending the ternary complex model. *J. Biol. Chem.* ***1993,*** 268, 4625-36.

Schnell, D.; Burleigh, K.; Trick, J.; Seifert, R. No evidence for functional selectivity of proxyfan at the human histamine H_3 receptor coupled to defined Gi/Go protein heterotrimers. *J. Pharmacol. Exp. Ther.* ***2010a,*** 332, 996-1005.

Schnell, D.; Strasser, A.; Seifert, R. Comparison of the pharmacological properties of human and rat histamine H(3)-receptors. *Biochem. Pharmacol.* ***2010b,*** 80, 1437-49.

Thurmond, R. L.; Desai, P. J.; Dunford, P. J.; Fung-Leung, W. P.; Hofstra, C. L.; Jiang, W.; Nguyen, S.; Riley, J. P.; Sun, S.; Williams, K. N. and others. A potent and selective histamine H_4 receptor antagonist with anti-inflammatory properties. *J. Pharmacol. Exp. Ther.* ***2004,*** 309, 404-13.

Wieland, K.; Bongers, G.; Yamamoto, Y.; Hashimoto, T.; Yamatodani, A.; Menge, W. M. B. P.; Timmerman, H.; Lovenberg, T. W.; Leurs, R. Constitutive Activity of Histamine H_3 Receptors Stably Expressed in SK-N-MC Cells: Display of Agonism and Inverse Agonism by H_3 Antagonists. *J. Pharmacol. Exp. Ther.* ***2001,*** 299, 908-914.

Wieland, T.; Seifert, R. 2006. Methodological Approaches. G Protein-Coupled Receptors as Drug Targets: Wiley-VCH Verlag GmbH & Co. KGaA. p 81-120.

Wulff, B. S.; Hastrup, S.; Rimvall, K. Characteristics of recombinantly expressed rat and human histamine H_3 receptors. *Eur. J. Pharmacol.* ***2002,*** 453, 33-41.

Yao, B. B.; Hutchins, C. W.; Carr, T. L.; Cassar, S.; Masters, J. N.; Bennani, Y. L.; Esbenshade, T. A.; Hancock, A. A. Molecular modeling and pharmacological analysis of species-related histamine H(3) receptor heterogeneity. *Neuropharmacology* ***2003,*** 44, 773-86.

Zhao, C.; Sun, M.; Bennani, Y. L.; Gopalakrishnan, S. M.; Witte, D. G.; Miller, T. R.; Krueger, K. M.; Browman, K. E.; Thiffault, C.; Wetter, J. and others. The alkaloid conessine and analogues as potent histamine H_3 receptor antagonists. *J. Med. Chem.* ***2008,*** 51, 5423-30.

Chapter 7

Summary

G-protein coupled receptors (GPCRs) represent the most important class of drug targets for the currently available pharmacotherapeutics. In the histamine receptor (HR) field, antagonists of H_1 and H_2 receptors are well established drugs for many decades, whereas the more recently identified H_3 (H_3R) and H_4 receptors (H_4R) are considered promising biological targets for drug discovery programs. Translational animal models are indispensable for investigations on the (patho)physiological role of novel receptors as well as for preclinical studies of potential drug candidates. Thus, with respect to the predictivity of such studies, pharmacological differences between H_3R and H_4R species orthologs should be identified as early as possible, both in binding and functional assays, in particular on human (h) compared to rodent (m, r) HR subtypes. This thesis aimed at the development of cellular binding and functional assays for the hH_4R, mH_4R, rH_4R, hH_3R and rH_3R.

In a whole-cell radioligand binding assay, saturation binding experiments on HEK293T cells, stably expressing the hH_4R, the $H_{3,4}R$ ligand [^{3}H]UR-PI294 was bound with high affinity. Competition binding experiments revealed affinities of reference ligands in a highly reproducible manner. Affinities of agonists were lower than reported data from binding assays using broken cell preparations, probably due to high GTP concentrations in intact cells. Regarding the mH_4R, saturation binding experiments on HEK293T cells stably transfected with the mH_4R gene revealed substantially lower affinities of [^{3}H]UR-PI294 and [^{3}H]histamine compared to the hH_4R. Therefore, it turned out to be exceedingly difficult to obtain valid and robust mH_4R binding data for reference ligands.

To establish functional assays for the hH_4R and mH_4R, using a more distal and non-radioactive readout, compared to [^{32}P]GTPase or [^{35}S]GTPγS assays, the aforementioned transfectants were stably co-transfected with a vector encoding the firefly luciferase (Luc), the transcription of which is under the control of the cAMP responsive element (CRE). Assay parameters were optimized, and a luciferase reporter gene assay was established in the 96-well format of a luminescence plate reader. Moreover, HEK293T cells lacking the H_4R were stably transfected with the CRE-linked luciferase gene (HEK293-CRE-Luc) and established to uncover off-target effects in control experiments. To develop a reporter gene assay for the rH_4R, HEK293-CRE-Luc cells were stably co-transfected with the rH_4R gene. For validation, functional data of agonists, antagonists and inverse agonists were determined. In case of agonism at the hH_4R, the data correlated well with data gained from [^{32}P]GTPase or [^{35}S]GTPγS assays. This also held for the rank order of agonists at the mH_4R and rH_4R, however, the potencies were up to 100-fold higher in the luciferase assay. Obviously, there was a positive effect on the distal readout by activation/amplification of or cross-talk between different signaling pathways in the established reporter gene assay.

Saturation binding experiments on whole HEK293T cells, stably expressing the hH_3R, revealed high-affinity binding of [^{3}H]N(alpha)methylhistamine ([^{3}H]NAMH). This is consistent with recognition of the active receptor population, which was predominantly present due to high constitutive activity of the hH_3R expressed in HEK293T cells. Whereas affinities of agonists and antagonists determined in competition binding experiments were in agreement with published data, inverse agonists achieved lower affinities. In studies at the rH_3R stably expressed in HEK293-CRE-Luc cells, [^{3}H]UR-PI294 was able to label a distinctly higher number of rH_3Rs than [^{3}H]NAMH, presumably, due to binding to the receptor protein in both, the active and inactive state. Consequently, in competition binding experiments with [^{3}H]UR-PI294, cytosolic GTP shifted the binding data of agonists toward lower affinities, whereas affinities of antagonists and inverse agonists were consistent with reported data from broken cell systems.

For the functional characterization of H_3R ligands at the human and rat H_3 receptors, a luciferase assay was established. HEK293-CRE-Luc cells were stably co-transfected with a vector encoding for the hH_3R. In case of the rH_3R the aforementioned rH_3R expressing transfectant was used. In contrast to the rH_3R, the hH_3R displayed exceptionally high constitutive activity. This became obvious by increased basal activity of the hH_3R and was confirmed by means of inverse agonists.

The established reporter gene (luciferase) assays allowed for the quantification of agonistic, inverse agonistic and antagonistic activity in a highly sensitive and reliable manner. In summary, the developed cell-based methods will improve the predictability of in vivo results by characterizing compounds on H_3R and H_4R species orthologs regarding affinity, subtype selectivity, quality of action and potency.

Eidesstattliche Erklärung

Ich erkläre hiermit an Eides statt, dass ich die vorliegende Arbeit ohne unzulässige Hilfe Dritter und ohne Benutzung anderer als der angegebenen Hilfsmittel angefertigt habe; die aus anderen Quellen direkt übernommenen Daten und Konzepte sind unter Angabe des Literaturzitats gekennzeichnet.

Weitere Personen waren an der inhaltlich-materiellen Herstellung der vorliegenden Arbeit nicht beteiligt. Insbesondere habe ich hierfür nicht die entgeltliche Hilfe eines Promotionsberaters oder anderer Personen in Anspruch genommen. Niemand hat von mir, weder unmittelbar noch mittelbar, geldwerte Leistungen fur Arbeiten erhalten, die im Zusammenhang mit dem Inhalt der vorgelegten Dissertation stehen.

Die Arbeit wurde bisher weder im In- noch im Ausland in gleicher oder ähnlicher Form einer anderen Prüfungsbehörde vorgelegt.

Regensburg, _____ _____

Uwe Nordemann